Hydrodynamic lubrication and coating of wire using a polymer melt during drawing process.

CRAMPTON, Richard.

COUNCIL FOR NATIONAL ACADEMIC AWARDS

HYDRODYNAMIC LUBRICATION AND COATING OF WIRE USING A POLYMER MELT DURING DRAWING PROCESS

A thesis submitted for the partial, fulfilment

of the degree of

DOCTOR OF PHILOSOPHY

by

Richard Crampton BSc«

September 1SSO

Department of Mechanical and Production Engineering, Sheffield City Polytechnic, (Sponsoring Estahlishrnent)

Arthur Lee and Sons Ltd, (Collaborating Establishment)

f P v T f

79 24 3 10 -Ol

CONTENTS page

LIST OF FIGURES

LIST OF PLATES Facing page no.

Acknowledgements

The author gratefully acknowledges the valuable suggestions and friendly advice given by Dr. G.R.Symmons under whose supervision this work was carried out. Thanks are expressed to Mr. P.J.Thompson, whose suggestions were received with gratitude.

Dr. M.S.J.Hashmi is thanked for giving advice when it was needed the most.

The technical assistance offered by Mr. R.Teasdale and his staff was much appreciated and particular thanks go to Mr. D. McKay, Mr J.Walton, Mr. R.Wallis and Mr. R.Wilkinson for their assistance in manufacturing and setting up the experimental equipment.

The author also wishes to thank the Collaborating Establishment, Arthur Lee and Sons Ltd., Sheffield, for supplying the wire and the dies and to Dr. A.O.Jakubovic, the Technical Director, for his helpful comments.

Declaration.

No part of this work has been submitted in support of an application for another degree or qualification to this or any other establishment. The author further declares that he has not been a registered candidate for any other awards of the CNAA or of a University during the duration of the research programme.

R. Crampton.

SUMMARY

A device based on an adaptation of the Christopherson tube is investigated for the lubrication and other effects of employing a polymer melt as the lubricant during the wire drawing process. The device is heated to convert the polymer feed into a viscous melt and the pressure required is generated by a hydrodynamic action produced by the motion of the wire.

On the basis of experimental evidence, it is apparent that deformation commences before the wire reaches the die, in the Christopherson tube itself, with the die effectively acting only as a seal. Under these conditions, the die geometry becomes of secondary importance and the deformation actually takes place as if an effective die of continuously changing die angle is being used. To take this aspect of the process into account, a mathematically described effective die shape is used in the present analysis. The plastic strain hardening properties and the strain rate sensitivity of the wire material are also incorporated into the analysis.

The study utilises an empirical expression relating shear stress and rate of shear together with an experimentally derived pressure coefficient of viscosity, in determining the coat thickness possible on the wire. The theory contains the effect of a limiting value to the shear stress, which exhibits itself as slip in the polymer. An alternative theory is also presented which assumes that shear stress is zero at the polymer/tube interface. This much simplified analysis allows the length of the deformation zone to be determined.

An extensive series of experimental studies have shown that the coat thickness reduces both as speed increases and as the wire material strength increases. Predictions of coat thickness from the analysis tend to be lower than those obtained experimentally. At low drawing speeds a coat defect was observed which gave the coated wire a "bamboo" shape. It is probable that this defect is caused by the slip-stick nature of the polymer melt in the Christopherson tube. The assumed die shape and predicted pressure distributions are verified by experiment.

NOTATION

$a, b, c, A, B, C_1 - C_7$	.....	Constants
C_F	.....	Fraction of Christopherson tube at which deformation commences measured from the die
D	.....	Wire diameter at any point during deformation
h	.....	Radial gap between wire and Christopherson tube
h_d	.....	Polymer coat thickness
k	.....	Polymer constant of shear
K	.....	Strain hardening constant
L	.....	Length of Christopherson tube and die unit
L_{CT}	.....	Length of Christopherson tube in which wire remains undeformed
n	.....	Strain hardening index
N	.....	Material constant
p	.....	Pressure
Q	.....	Volumetric flow rate of polymer melt per unit length of circumference of wire
S	.....	Dynamic/static stress ratio
T	.....	Material constant
U	.....	Wire speed ahead of die
U_d	.....	Wire speed after drawing
U_s	.....	Wire speed at commencement of slip

v	.....	Fluid velocity
x,y,z	.....	Rectangular coordinates
Y	.....	Yield stress of wire
Y_o	.....	Initial yield stress of wire
α	.....	Die semi angle
$\dot{\gamma}$	.....	Shear rate
ε	.....	Natural strain
η_o	.....	Viscosity of polymer melt at zero shear
η_a	.....	Viscosity of polymer melt at ambient pressure
σ	.....	Stress in wire
τ	.....	Shear stress in polymer melt
τ_c	.....	Shear stress at wire-polymer interface
τ_a	.....	Critical shear stress

Subscripts:-

1	.....	Before deformation
2	.....	After deformation
r	.....	Denotes radial direction
x	.....	Denotes x direction

Note: Wire reduction is given by; $\frac{D_1^2 - D_2^2}{D_1^2}$

CHAPTER 1. INTRODUCTION.

1.1 The Wire Drawing Process.

The wire drawing process involves pulling a length of metal wire (usually circular in cross section) through a tapered die, in order to obtain a reduced wire diameter of a specific size whilst improving surface quality, obtaining the desired metallurgical properties and maintaining a high reproducibility of the product. These are generally achieved with the wire unheated (cold drawn) and hence deformation loads are high, making efficient lubrication essential. Traditionally, there are two basic methods of lubrication in wire drawing; wet and dry, which differ as regards preparation of wire, lubrication and design of machine. Wet wire drawing is generally conducted on wires of diameter less than 0.46mm (26 s.w.g.). The dies are totally submerged in a solution of soap in water. Boundary lubrication is the operating regime, producing a highly polished drawn wire. Dry drawing is used on wires and rods of diameter above 0.46mm. Here the lubricant is usually a powdered calcium or sodium stearate soap. The dry soap compound is placed in a box, through which the wire passes immediately before entry to the die. To assist pick-up of soap from these boxes, the wire is often coat with either lime or borax in a treatment prior to drawing. The lubrication regime in this case has been termed "quasi-hydrodynamic"[1]*, since the soap film

---

* Numbers as superscripts refer to references which may be found in Chapter 10.

thickness produced on the drawn wire is greater than that which would be expected from boundary lubrication, but less than those for hydrodynamic lubrication.

These methods have been used almost exclusively for many years, but evidence is growing that they may be reaching the limit of their development, and consequently, other ways of lubricating the wire are being investigated.

1.2 Historical Background of the Christopherson Tube.

The wire drawing process, although basically a simple forming operation, needs to achieve many objectives if it is to be used efficiently in production. These may be summarised as follows:-

a) High drawing speeds whilst maintaining wire quality

b) High reductions in area per pass

c) Improved dissipation of heat from the wire and hence low wire temperature

d) An improved surface finish and clean wire

e) Reduction in cost by;

   i) Reduced drawing times

   ii) Elimination of pre-drawing treatments

   iii) Reduction of the number of interpass heat treatments

   iv) Reduction of down time due to changing dies because of excessive wear.

In the past, the wire drawing process had been regarded as an art where die angles and reductions and the lubricant specification were arrived at mainly through trial and error. More recently, however, attempts have been made to introduce a more theoretical background to the process. This deeper understanding makes it possible to introduce new techniques which, hopefully, allow the aims of increased production to be met. Wistreich[2] had established that an increase in wire drawing speed should be possible if the die friction could be reduced. One way of achieving this would be to increase the die angle, but this would cause an increase in redundant deformation, increasing the rise in temperature of the drawn wire. The surface temperature of the wire is required to be kept to a minimum in order to prevent a deterioration in the surface quality and metallurgical properties of the wire.

In 1955, Christopherson and Naylor[3] presented a paper which showed a method of reducing friction in wire drawing by hydrodynamic lubrication. It had been assumed that friction in conventional wire drawing was of a boundary nature and that a change of mode to hydrodynamic lubrication should greatly reduce friction. The device used by Christopherson and Naylor was based upon an idea suggested in 1943 by Maclellan and Cameron[4]. This device, now called the Christopherson tube, consisted of a long tube filled with lubricant, through which the wire passed before entry to the die, and sealed to the approach side of the die. Early efforts were aimed at producing hydrodynamic lubrication using oil, since the rheology of oil was well known, but it

was quickly realised that many problems were inherent in its use. These were the necessity to have long inlet tubes (up to 0.8m) and very small wire clearances (0.04 - 0.05mm on radius). It was also necessary to provide a "leader" to the full size wire to encourage flow to start (see Fig 1). Even then a finite length of wire would remain unlubricated at start up, before sufficient pressure was generated to promote hydrodynamic lubrication. Since oil is a poor boundary lubricant, die wear and seizure were inherent problems at start up. These problems were largely overcome by returning to the traditional dry soap lubrication. This enabled the Christopherson tube to be shortened and since soap is a very good boundary lubricant, start up was no longer a problem. These ideas led to the design of the BISRA dry soap nozzles[5] (Fig 2). The main limitation of these designs seemed to be the deterioration of the lubricating properties of soap when its moisture content is high. Other ideas have stemmed from the desire to have a thick film lubricated die. The most notable of these are the hydrostatic die unit and the double die system. In the hydrostatic die, the lubricant (usually oil) is externally pressurised and fed to the wire in a chamber between an "ironing" die which acts as a seal and the die proper[6] (Fig 3). Subsequently it was found that the ironing die produced more problems of die wear than the simple single die system. This was because the ironing die reduced the wire by a small amount (around 5%) under poorly lubricated conditions. This system also required the use of a pump capable of producing very high pressures. The double die system seemed to offer a better solution. Here two dies with a sealed chamber

between them are used[7]. The approach die has a diameter the same as the nominal size of the undrawn wire (Fig 4). Soap compounds are used as the lubricant. This system has received much favour in the USSR where it is claimed that one of these units increased die life by 500% and mill output by up to 53%, while electric power consumption was reduced by 48%[8].

1.3 Polymer Melt as a Lubricant.

The use of solid polymers as a lubricant is not a new concept; it has been used successfully in cold deep drawing for many years. However, the use of polymer melts as a lubricant has not been exploited to the same extent.

There are many important differences in the rheology of molten polymers when compared to conventional lubricants such as oil. The most obvious of these is the very high viscosity of polymer melts at temperatures which would preclude the use of oil as a lubricant. It is also well known that the viscosity of polymer melts is reduced when the melt is subjected to shear stress (ie. it is shear thinning). Above a certain level of shear stress a discontinuity in flow has been observed for certain polymers[9]. An increase in hydrostatic pressure increases the viscosity of the polymer melt[10]. These rheological effects and their consequences are discussed in detail in Chapter 2.

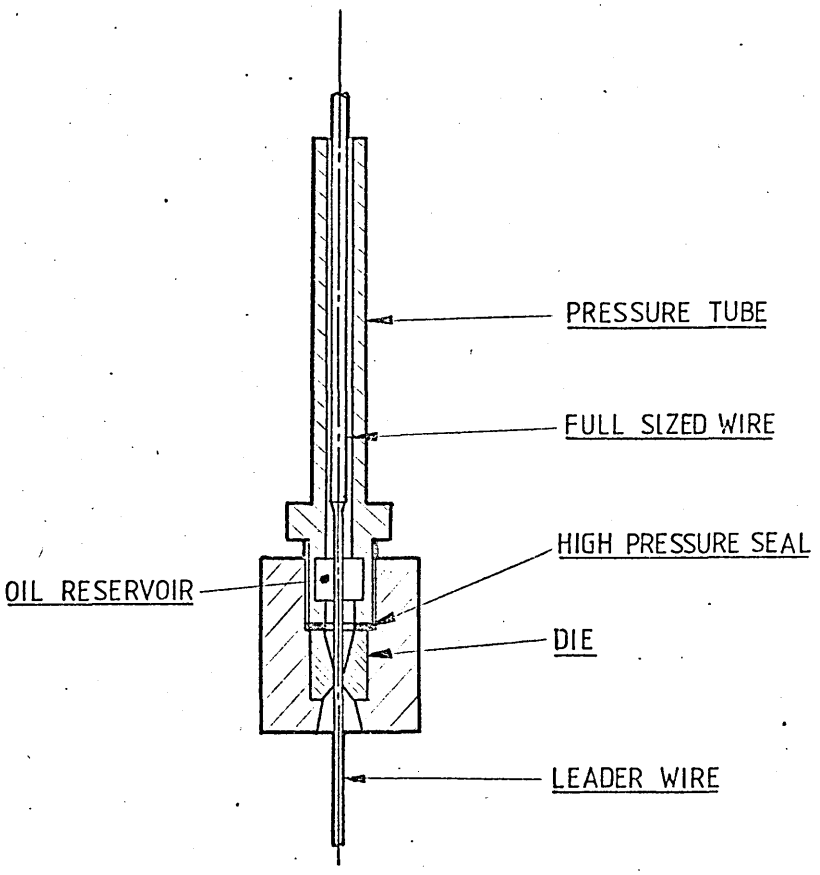

FIG 1 TYPICAL INLET TUBE AND DIE

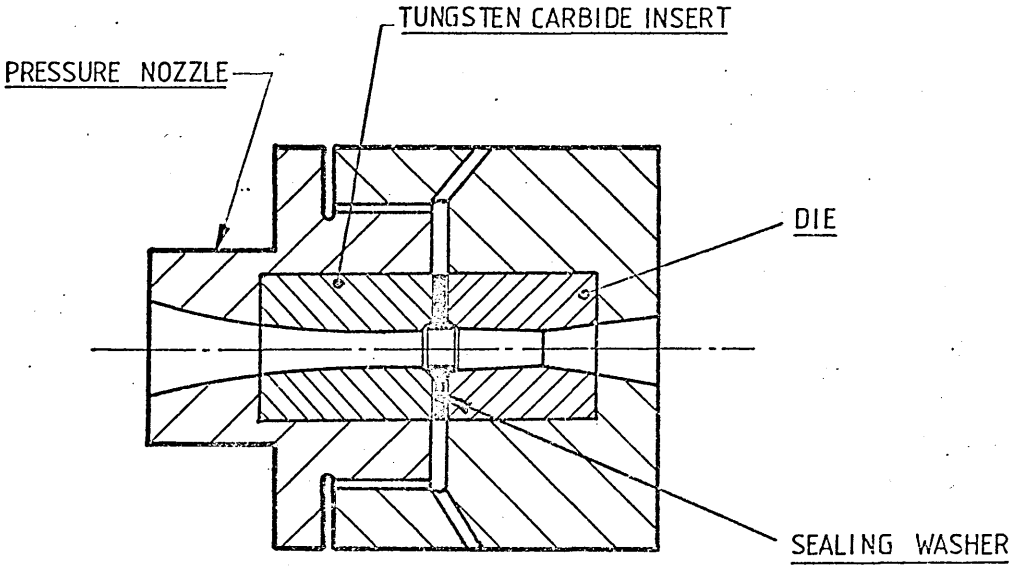

FIG 2 B.I.S.R.A. NOZZLE-DIE UNIT

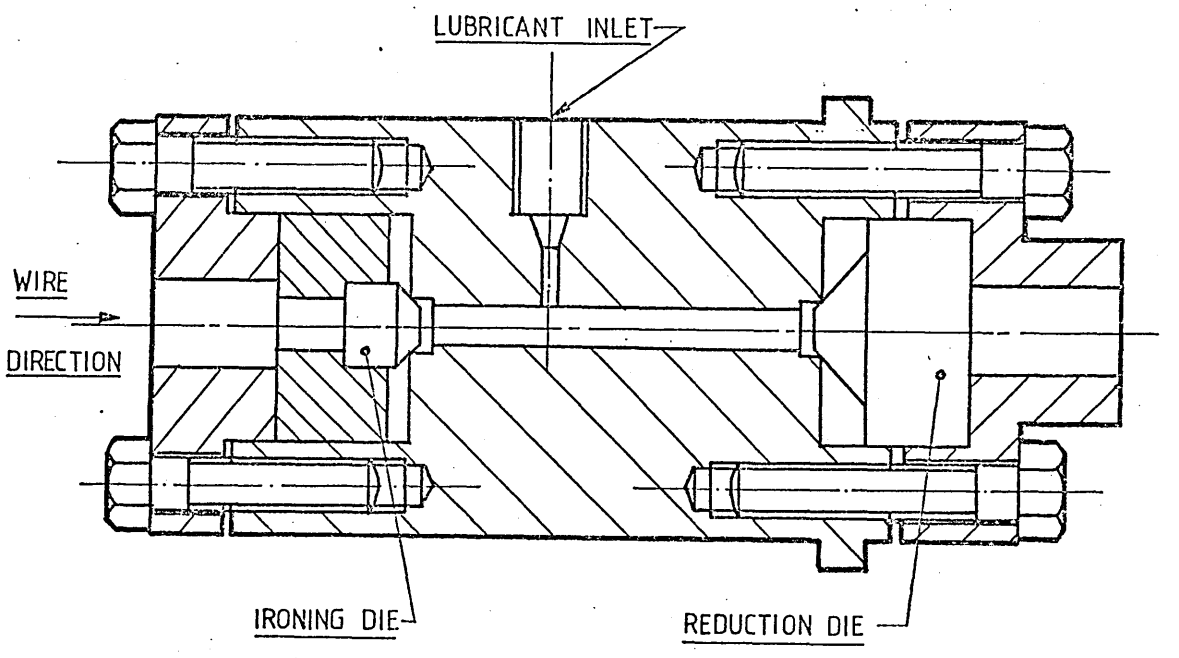

FIG 3 HIGH PRESSURE DIE UNIT

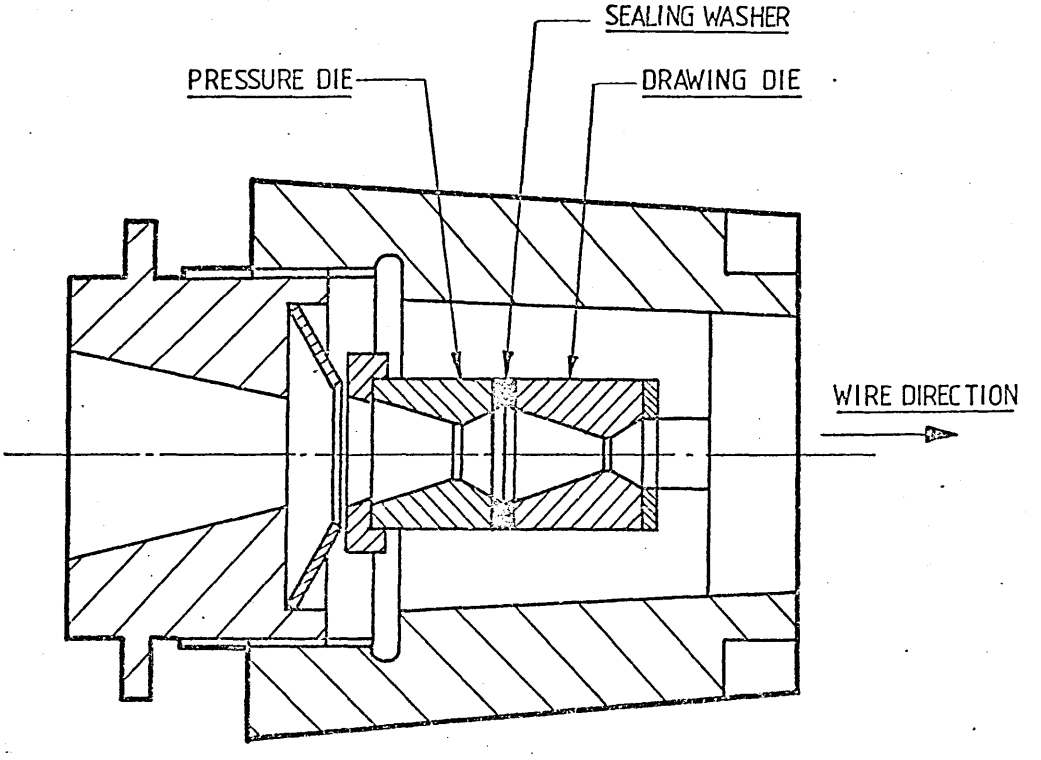

FIG 4 DOUBLE DIE

1.4 Scope of the Present Work.

The application of the Christopherson tube in the present work was originally conceived in order to overcome the difficulties associated with using soap or oil as the lubricant and to provide an alternative lubricating system which would have very different characteristics to those currently in use. It was thought that since the viscosity of polymer melts appeared to be considerably greater than that of oil, and that they did not suffer from moisture absorption as did soap, they would provide an ideal and novel solution to the problem. In addition, if the polymer could be made to bond successfully to the wire, it could be used to protect the wire against corrosion in storage and to lubricate subsequent forming operations such as bending or cold heading. Initial research[11,30,31] showed that certain limitations were present:-

a) At very low drawing speeds the coated surface of the wire exhibited a "bamboo" effect causing the wire itself to be of varying diameter.

b) The coating adhesion was not as good as was hoped but this was improved by increasing the wire temperature relative to the polymer temperature. This unfortunately led to a decrease in coat thickness and increased the bulk temperature of the wire.

c) As drawing speed was increased, the coat thickness was reduced.

d) The dimensional and operating restrictions on the

Christopherson tube were not reduced as much as was thought possible.

e) The wire was ineffectively lubricated at start up causing wire fracture in realistic operating conditions.

Stevens[11] produced a computer aided solution for the design of a Christopherson tube-die unit for specified operating conditions. He used a simplified theory based on the assumption that the polymer melt viscosity remained constant with respect to pressure and shear stress, employing the concept of apparent viscosity.

The principal objectives of the present study are:-

a) To improve the analytical solutions presented earlier by including both pressure and shear components of viscosity.

b) To consider in detail the deformation process and to include into the analysis the effects of strain hardening and strain rate sensitivity of the wire material.

c) To verify, or otherwise, any theory with extensive practical tests.

d) To investigate the performance of a hydrostatic/hydrodynamic system of lubrication and other means of improving the process in order to make it more acceptable to industry.

CHAPTER 2. THE RHEOLOGY OF POLYMER MELTS.

2.1 Introduction.

Polymers are unlike most materials in that they are composed of very long molecular chains. Bonding between the chains is either by cross-linking, as in thermosetting polymers, or by molecular attraction (Van der Waals forces) between the chains, as in thermoplastic polymers. Normally, the chains are randomly orientated, but if stress is applied, the chains would firstly straighten out and then, as further stress is applied, the bonds between the chains would be broken. The straightening out of the chains is partially recoverable, causing the polymer to act elastically. The breaking of the bonds enable flow to occur. The flow characteristics of polymer melts are very different to those of conventional lubricants such as oil. In this chapter, discussions are made of these characteristics and their effects in relation to the present application.

2.2 The Effect of Temperature on Viscosity.

An increase in the temperature of a molten polymer decreases viscosity by varying extents, dependant upon the type of polymer, as shown in Fig 5. The slope of the curve is equivalent to the activation energy for viscous flow. Increases of temperature have a more drastic effect on polymers having a higher activation energy than those with

lower activation energies. Polyethylene, which is the most non-polar of the materials shown, has a very low activation energy because the forces between the chains are very small. If the curves of viscosity versus the reciprocal of the absolute temperature are plotted over a wider range of absolute temperature than shown, there would be a pronounced curvature to the straight line relationship. Dienes[12] believed that this is caused by a decrease in the order of the molecules as the temperature is raised (ie. the molecular structure becomes more random). Viscous flow involves configurational change of the molecules, so that the more random they are, the easier it is to change this configuration. Hence, the energy required for a viscosity change will be less at high temperatures than at low temperatures.

The polymer used for most of the experimental test in the present study was Alkathene WVG 23 - a low density polyethylene of 0.913 specific density. Results of temperature versus viscosity from an extrusion rheometer for this polymer are shown in Fig 6. This curve by itself is not a complete picture since the viscosity measurements refer to zero shear stress. It is necessary with polymer melts to include the effects of shear stress on viscosity together with the effects of changes in temperature.

2.3 The Effects of Shear Stress and Strain on Viscosity.

It is widely accepted that polymer melts exhibit very non-Newtonian flow characteristics. As increasing shear stress is applied, the viscosity of most polymers is reduced.

This is best illustrated in graphical form as shown in Fig 7. This graph shows the results obtained for Alkathene WVG 23 from a capillary rheometer. A non-linear relationship is seen to exist between shear stress and shear rate (a Newtonian fluid would be a straight line passing through zero). The viscosity of the melt can be obtained from the tangent to the curve at any point. Fig 8 shows the same data drawn in another form, where viscosity may be read off directly from known temperature and shear stress or shear rate values. (For a Newtonian fluid this curve would be a horizontal straight line).

Certain polymer melts are known to have flow discontinuities at high shear rates and shear stress values. A critical shear stress value for a polymer may be defined as the one after which flow tends to be irregular.

2.3.1 Critical Shear Stress.

In polymer extrusion, melt flow instability exhibits itself in many forms such as; a regular helix of wavelength comparable with the diameter, a zig-zag in one plane or irregular convolutions and may finally become fragmented. The terms melt fracture, elastic turbulence and distortion have been used to describe this effect, however, the mechanism is not similar either to fracture in a solid or to Reynolds turbulence.

This phenomenon has been investigated by a number of workers[13-18] and there is general agreement on the following

points:-

a) The instability sets in at a critical value of shear stress (τ_a) calculated at the die wall; this value is independant of the die length, radius etc.

b) τ_a has a value in the region of 10^5-10^6 Nm^{-2} for most commercial polymers.

c) τ_a does not vary widely with temperature.

d) Many workers[13, 15, 16, 18] found a discontinuity in the slope of the viscosity-shear stress curve at the critical shear stress, though this has been disputed.

e) The flow defect is often associated with the die inlet although some workers[16] have witnessed the occurrence of the same defect during extrusion from a long cylindrical tube - that is without a die entry.

Several theories have been proposed to account for this defect. First in the field was Nason[19] followed by Westover and Maxwell[20], all of whom ascribed the effects to conventional turbulence. However, Tordella[15] demonstrated that the Reynolds number at the inception of the irregularities were many orders of magnitude lower than the value of 2000 which has been found generally applicable even to non-Newtonian systems. Spencer and Dillon[14] pointed out that the melt, highly orientated in the die capillary, must relax to a distorted state at the die exit and suggested that this caused the buckling of the extrudate. However, cine films of the die entry by Tordella[15], Clegg[13] and Bagley and Birks[21] have shown that extrudate distortion is closely associated

with a disturbance in the flow pattern at the die entry. Later studies by Benbow and Lamb[16] showed that the locus of origin of disturbance was at the die wall, where the shear stresses are the highest. They concluded that the melt fracture was caused by the slip-stick action of the melt against the metal die. To date, no conclusive evidence has been submitted to fully identify the mechanism involved and very little theoretical work has been published on the phenomenon.

2.3.2 Sharkskin.

Another defect, often mistakenly called melt fracture, is the surface irregularity called "Sharkskin" or "Mattness". This is characterised by a series of ridges perpendicular to the flow direction and has been distinguished from melt fracture for the following reasons:-

a) Sharkskin has a perpendicular distortion whereas melt fracture is often helical or irregular.

b) Sharkskin can occur at lower extrusion rates.

c) Sharkskin appears unaffected by die entry and L/D ratio of the die or material of the die. Clegg[13] has reported that there was a slight improvement with shorter die lands.

Sharkskin appears to be a surface effect, one explanation being offered by reference to Fig 9 (after Brydson[22]). On emerging from the die, the velocity distri-

bution changes in nature so that acceleration of the outer layers occur. For a viscous material, this is not difficult, but where a substantial elastic component is present, tensile forces are built up at or near the surface. Eventually, these forces exceed the tensile strength of the melt and the surface tears to release the stresses.

2.4 The Effect of Pressure on Viscosity.

The effect of hydrostatic pressure on the apparent viscosity and other flow properties of polymer melts is not as well understood as the effects of temperature and shear rate. Maxwell and Jung[23] demonstrated that the effects of hydrostatic pressure on the apparent viscosity of branched polyethylene and polystyrene at constant shear stress and temperature are appreciable and should not be neglected. Westover[10] was able to measure the apparent viscosity of several polymeric materials between atmospheric pressure and that of 172 MNm^{-2} at fixed temperature and shear stress. He showed, for example, that the apparent viscosity of a polyethylene increased by a factor of five when the hydrostatic pressure was changed from 13 MNm^{-2} to 172 MNm^{-2}. His apparatus was specially designed and was rather complicated and expensive, but Choi[24] attempted to measure the effects of pressure on viscosity with much simplified apparatus. His results were comparable with those obtained by other workers. Cogswell[25] suggested that the effect of an increase in pressure may be likened to that due to a drop in temperature. He observed that for low density polyethylene, an increase

in pressure of 1000 bar had the same effect on viscosity as that due to a drop in temperature of 53°C within the melt range.

It had been noted that at very high pressures (above 140 MNm^{-2}) the melt tended to recrystallise and in consequence, the melt acted like a solid plug[23]. For this reason, pressure-viscosity measurements are often conducted at relatively high temperatures.

Since the work carried out by Westover appears to be the most comprehensive, his results are used in the present work to determine the pressure coefficient of viscosity. Fig 10 shows the effects of pressure alone on viscosity. Fig 11 shows how pressure affects viscosity together with changing shear stress and shear rate.

2.5 The Effects of the Polymer Flow Characteristics.

In the present application the polymer is subjected to very high shear stresses and pressures which are much greater than those capable of being investigated in any existing rheometer. It is believed that the critical shear stress is reached at very low drawing speeds giving a reduction in coat thickness as speed is increased. The melt flow instability and sharkskin are believed to be possible causes for the bamboo effect present at low drawing speeds. The high pressures generated are believed to have the effect of increasing the melt viscosity in the Christopherson tube. Temperature was maintained at a steady value when the tests

were conducted, minimising the effects inherent with changing temperature. Tests at different temperatures were conducted to show the effects of such changes. All of the above effects are discussed in detail in Chapter 8.

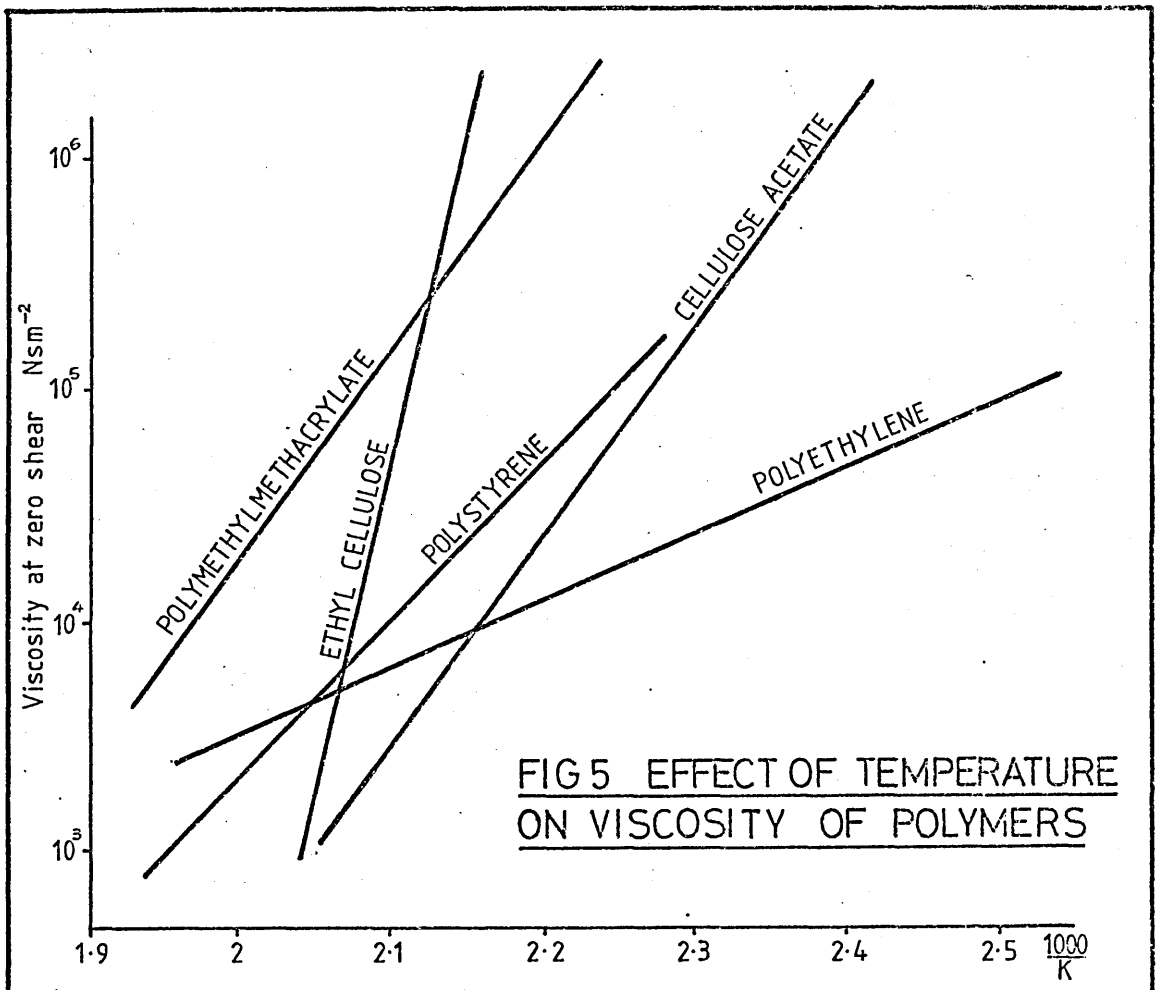

FIG 5 EFFECT OF TEMPERATURE ON VISCOSITY OF POLYMERS

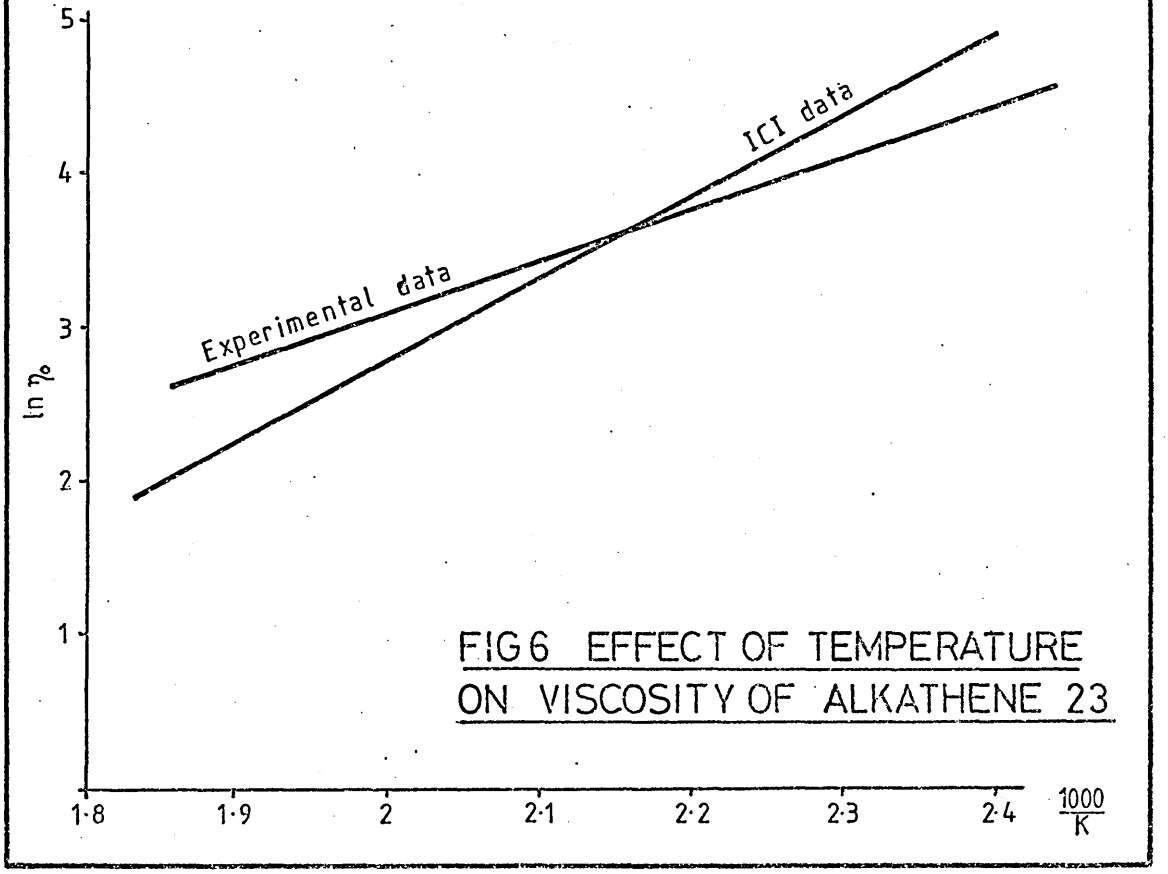

FIG 6 EFFECT OF TEMPERATURE ON VISCOSITY OF ALKATHENE 23

FIG 7 FLOW CURVES FOR ALKATHENE TYPE WVG 23

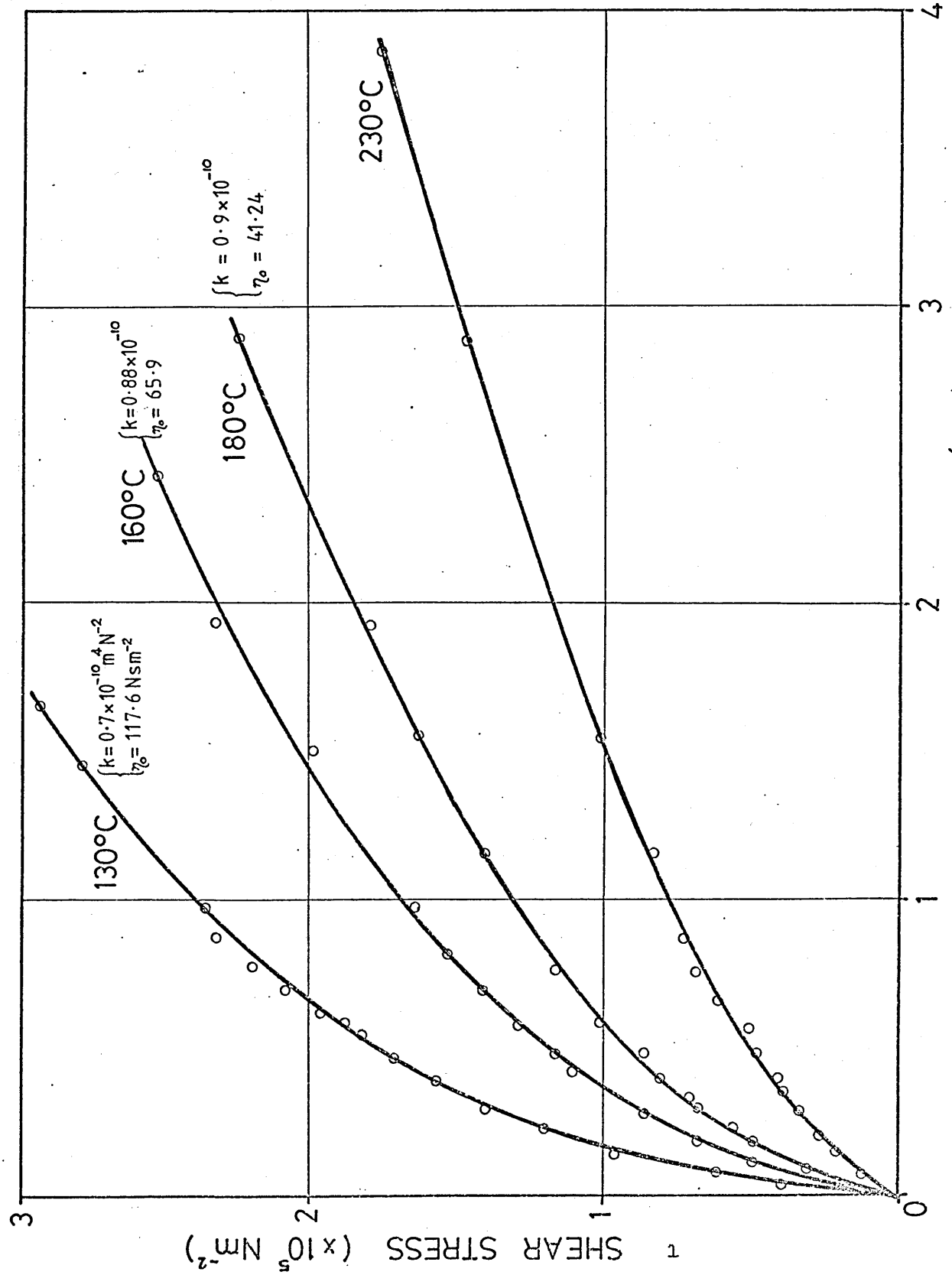

FIG 8 VISCOSITY VERSUS SHEAR STRESS FOR ALKATHENE WVG 23

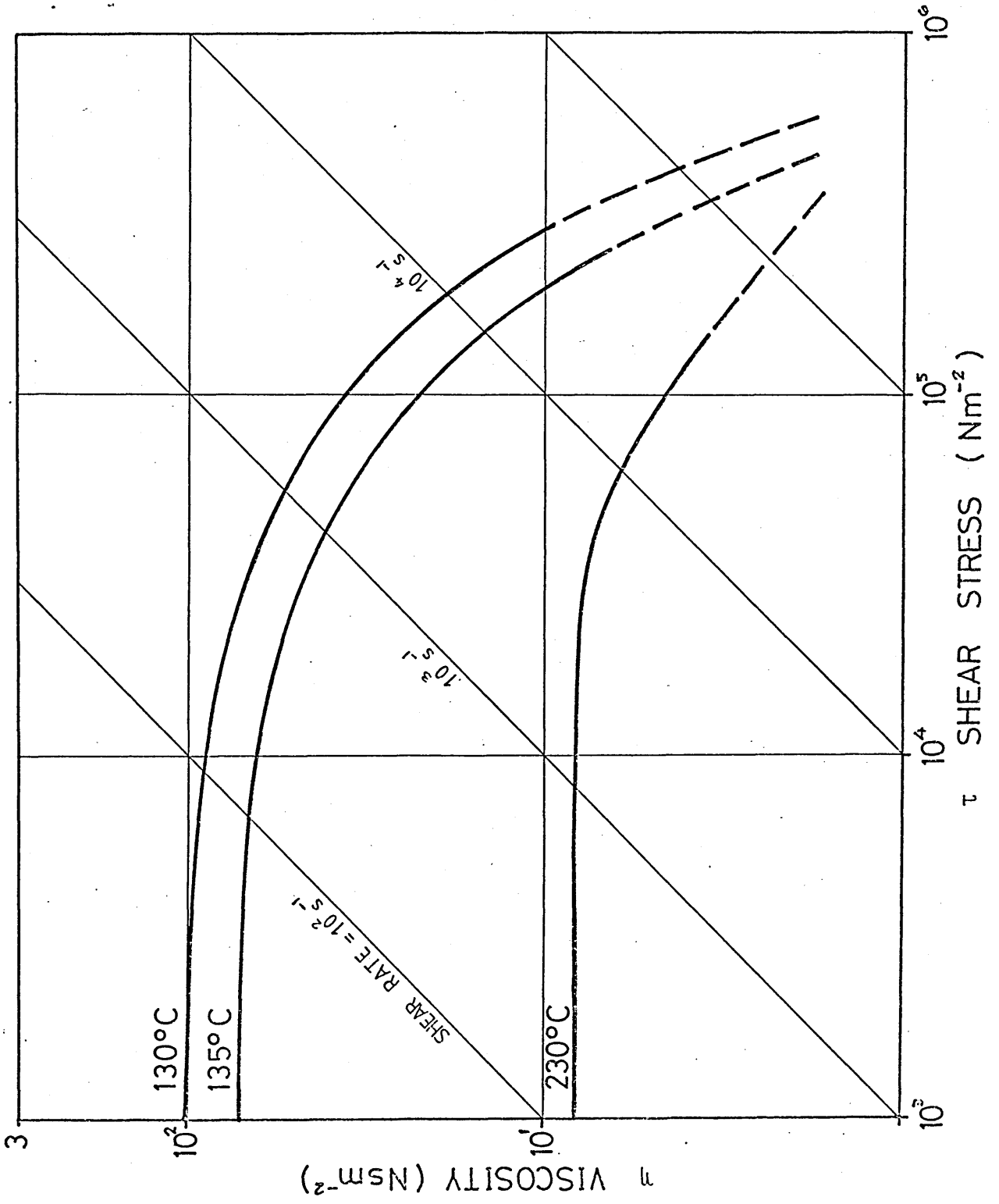

FIG 9 A POSSIBLE MECHANISM OF SHARKSKIN AFTER BRYDSON [22]

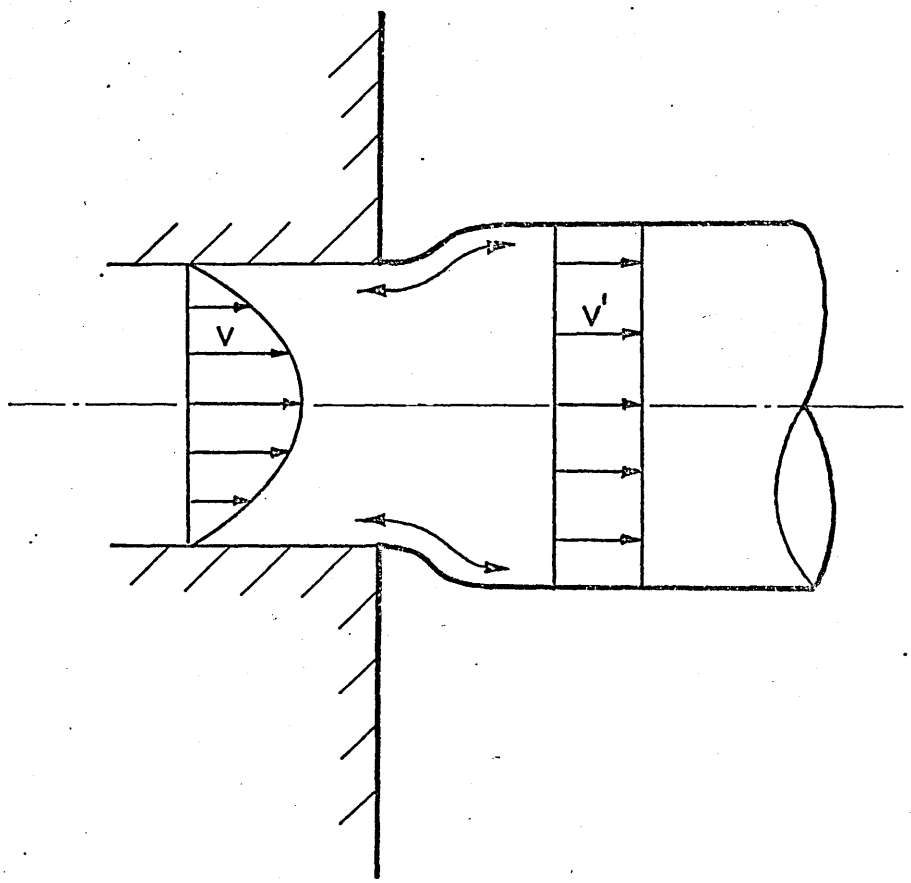

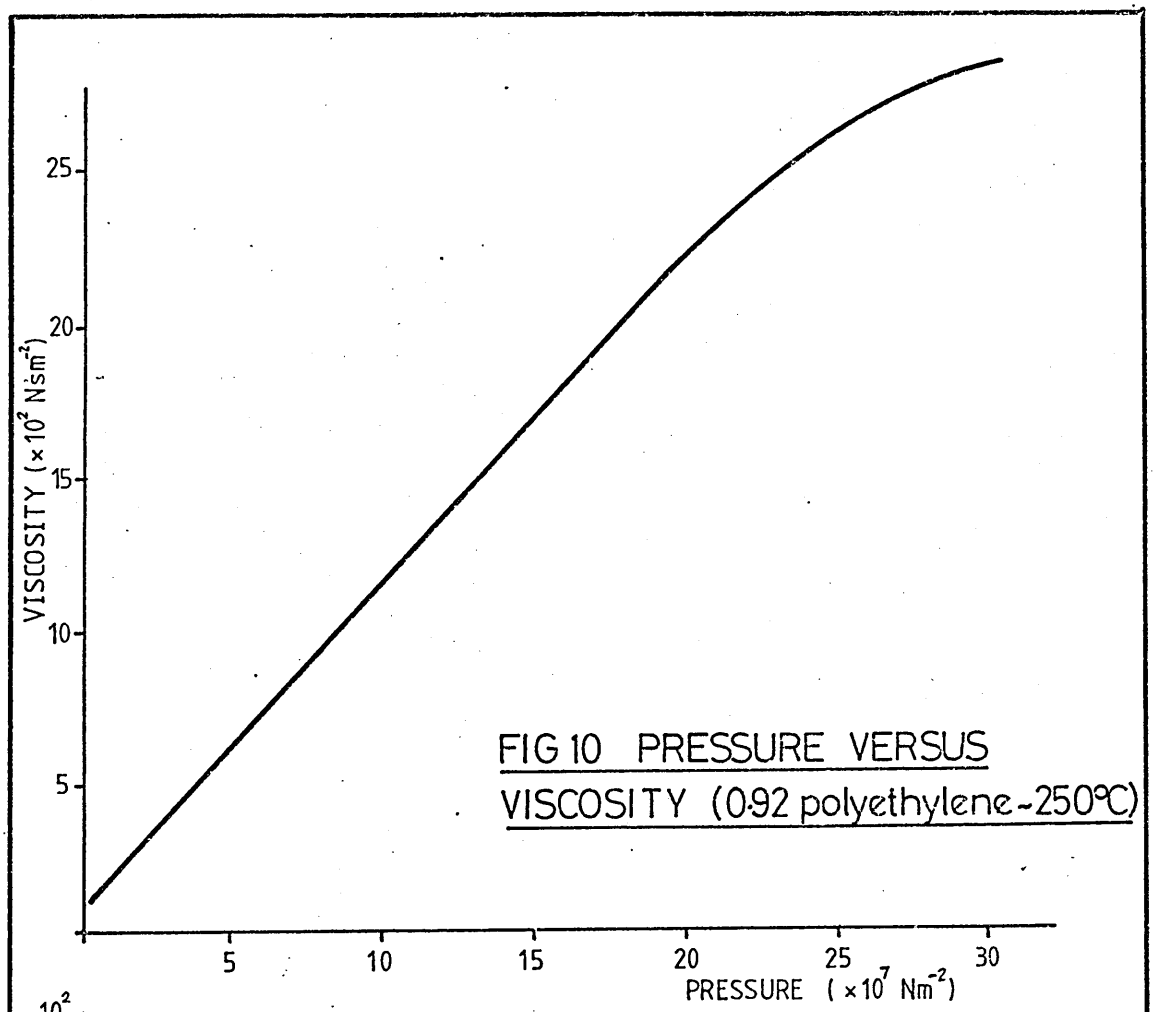

FIG 10 PRESSURE VERSUS VISCOSITY (0·92 polyethylene-250°C)

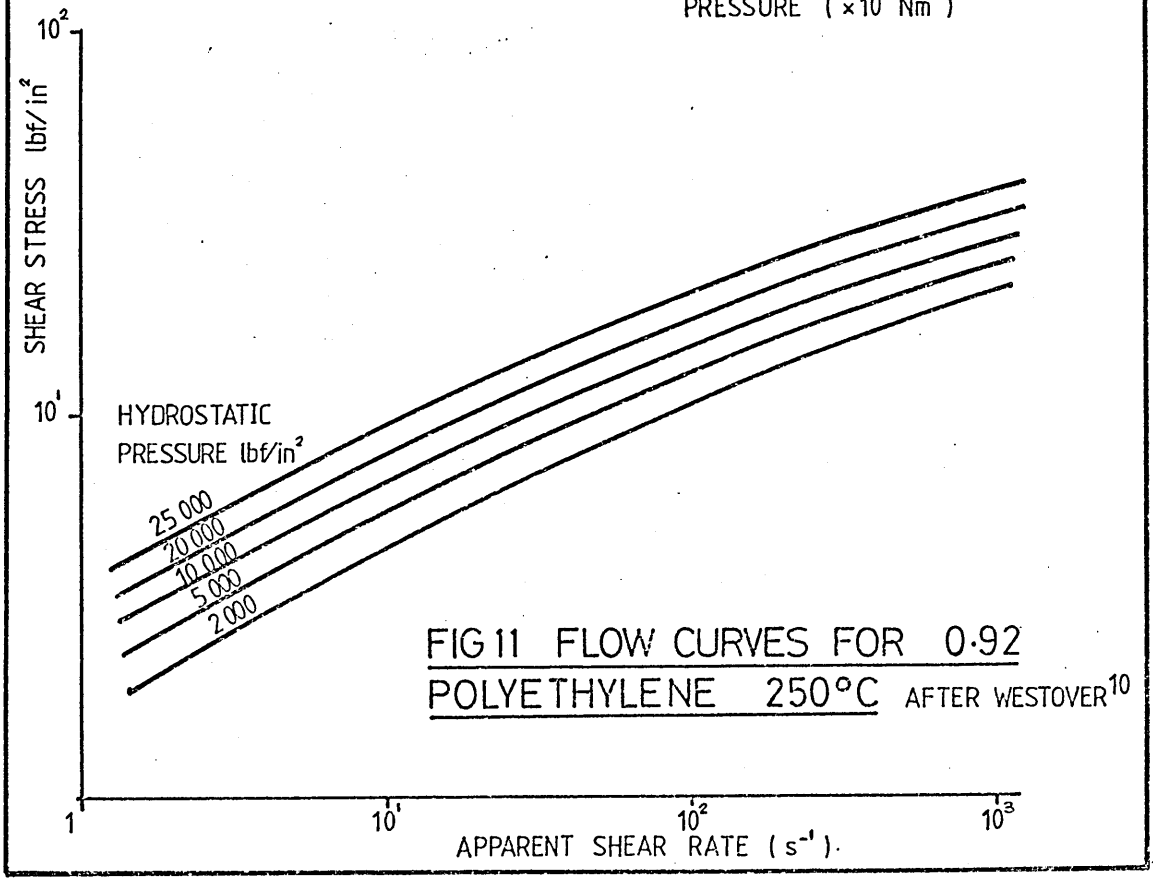

FIG 11 FLOW CURVES FOR 0·92 POLYETHYLENE 250°C AFTER WESTOVER[10]

CHAPTER 3. DESIGN, DEVELOPMENT AND CONSTRUCTION OF THE TEST EQUIPMENT.

The apparatus used in the initial tests was the same one as used by Stevens[11]. In the light of increasing experience on this apparatus, various modifications were undertaken to improve both the ease at which readings could be taken and the safety aspect of the draw bench. Further modifications were planned and executed at a later stage in order to investigate the different parameters in more detail. Final modifications to the rig were designed to improve the process itself.

3.1 Description of the Existing Equipment.

The apparatus used for the initial tests was the one designed by Stevens[11] for a previous investigation. A full description of this equipment is given below.

The drawing bench, of the bull block type, was powered by a Shraga 3-phase electric motor (type BTH 18/4.5hp VSC.) capable of running at speeds infinitely variable between 550 and 2200 revolutions per minute. The power was passed from the motor to the bull block via a flexible tyre coupling (Fenner F80), a 10:1 reduction worm gear (Croft type 41/551/05) and a coupling clutch (Broadbent type DP25) which enabled the bull block to be engaged when the motor was running at the required speed and so enabled a quick build up to full speed. Two interchangable bull blocks, of sizes 305mm

diameter and 100mm diameter, were used, giving a speed range infinitely variable between 0.25 ms^{-1} to 3.5 ms^{-1}.

The drawing speed was measured using a tachogenerator (servo products type SA 740A/7) connected to a digital voltmeter. The drawing load was measured by attaching strain gauges on to the die retaining plate which was designed to flex during drawing. This system was calibrated in situ using static loads to give a direct readout on a Sangmo direct reading transducer meter (type C52). The polymer was heated by an electric band heater and the temperature controlled thermostatically to within $\pm 3^{o}C$ of the set temperature and measured using a thermocouple connected to a digital meter.

The Christopherson tube/die unit was designed to allow it to be heated or cooled as experiments dictated. The heater and the controller used were the same as for the polymer. When cooling was required, a water jacket could be fitted and water circulated from a large tank using a standard washing machine pump. This enabled the Christopherson tube to be kept as low as $10^{o}C$ above ambient temperature when separated from the polymer reservoir by a 6mm asbestos disc.

The components described above were mounted on a suitably stiffened bench of welded steel construction, and all moving parts were adequately guarded.

The Christopherson tube/die unit consisted of a polymer melt reservoir, Christopherson tube and die, held together with three socket headed cap screws as shown in Fig 12. A copper seal was incorporated between the die and the Christopherson tube to prevent leakage. This assembly

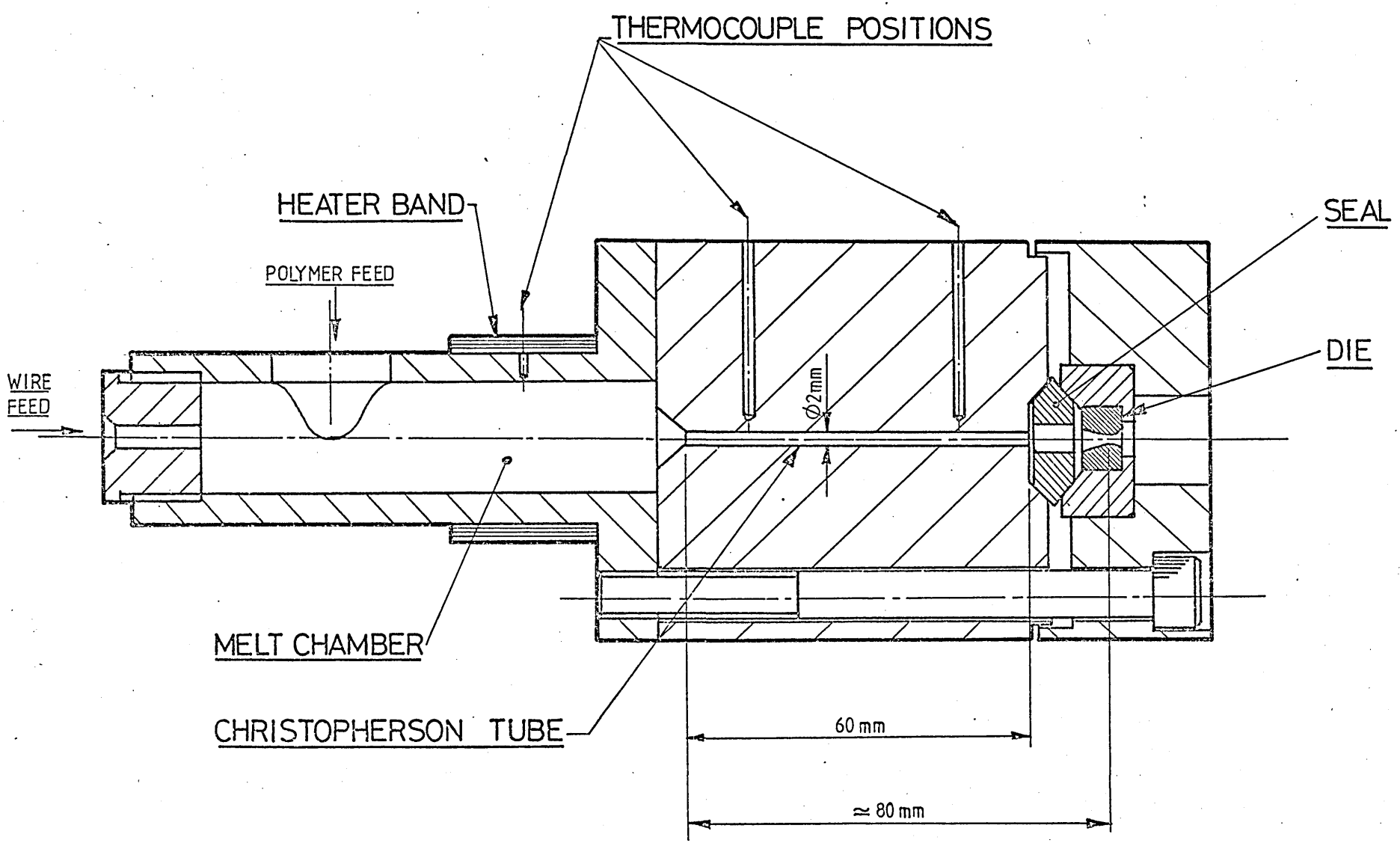

FIG 12 CHRISTOPHERSON TUBE ~ DIE ASSEMBLY

was located in a vee on the drawing bench, being retained in the direction of drawing by means of the load plate described previously.

This rig allowed readings of drawing speed, load and temperature to be taken. It was quickly realised that certain modifications were necessary to improve experimental procedure.

3.2 Modifications to the Experimental rig.

It was impractical with the existing rig to conduct tests on wire longer than four metres since no feed mechanism was present (the wire was simply laid out on the laboratory floor). The laboratory door had to be kept locked during drawing to stop people inadvertently stepping onto the fast moving wire. Visits to local wire manufacturers and reference to wire journals assisted the design of the feed mechanism.

The objectives of the design were:-

a) To be simple in operation.
b) To be inexpensive.
c) To operate at wire speeds of up to 3.5 ms^{-1}.
d) To take up little floor space.

Various types of mechanism were considered. The resulting design appeared to meet all of the objectives at the minimum cost. The wire coil would be placed at the side of the drawing bench, thus using little floor space. A

weighted ring placed over the coil would straighten out and restrain the wire enough to prevent it becoming entangled. Guides and a pulley wheel would turn the wire through a right angle so that a horizontal feed to the Christopherson tube could be achieved. Fig 13 and Plates 1 and 2 show the final form of the feed mechanism which worked faultlessly for the majority of the tests.

The addition of an ultra-violet recorder (UV) to the load cell allowed detailed investigations of the variations in drawing load to be undertaken. An extensive series of tests were conducted with the rig in this modified form.

Further modifications became necessary as the tests proceeded. It was decided that the pressure inside the Christopherson tube must be measured. This was originally attempted by using a spring loaded plunger which would be raised by the melt pressure as shown in Fig 14. This unit was manufactured, but the fit between the piston and its bore could not be made accurately enough to ensure a perfect seal without having frictional losses. This method was abandoned in preference to others. The most promising of these appeared to be in the use of commercially available piezo-electric pressure transducers. The maximum pressure that these transducers could measure (5000 bar) precluded the drawing of high strength wires, but since most of the tests had been conducted on copper, it was decided to incorporate this method. A Christopherson tube was designed and manufactured to incorporate three pressure transducers (Kistler type 6203) as shown in Fig 15 and Plate 3. This method was successful, although the measured pressures were

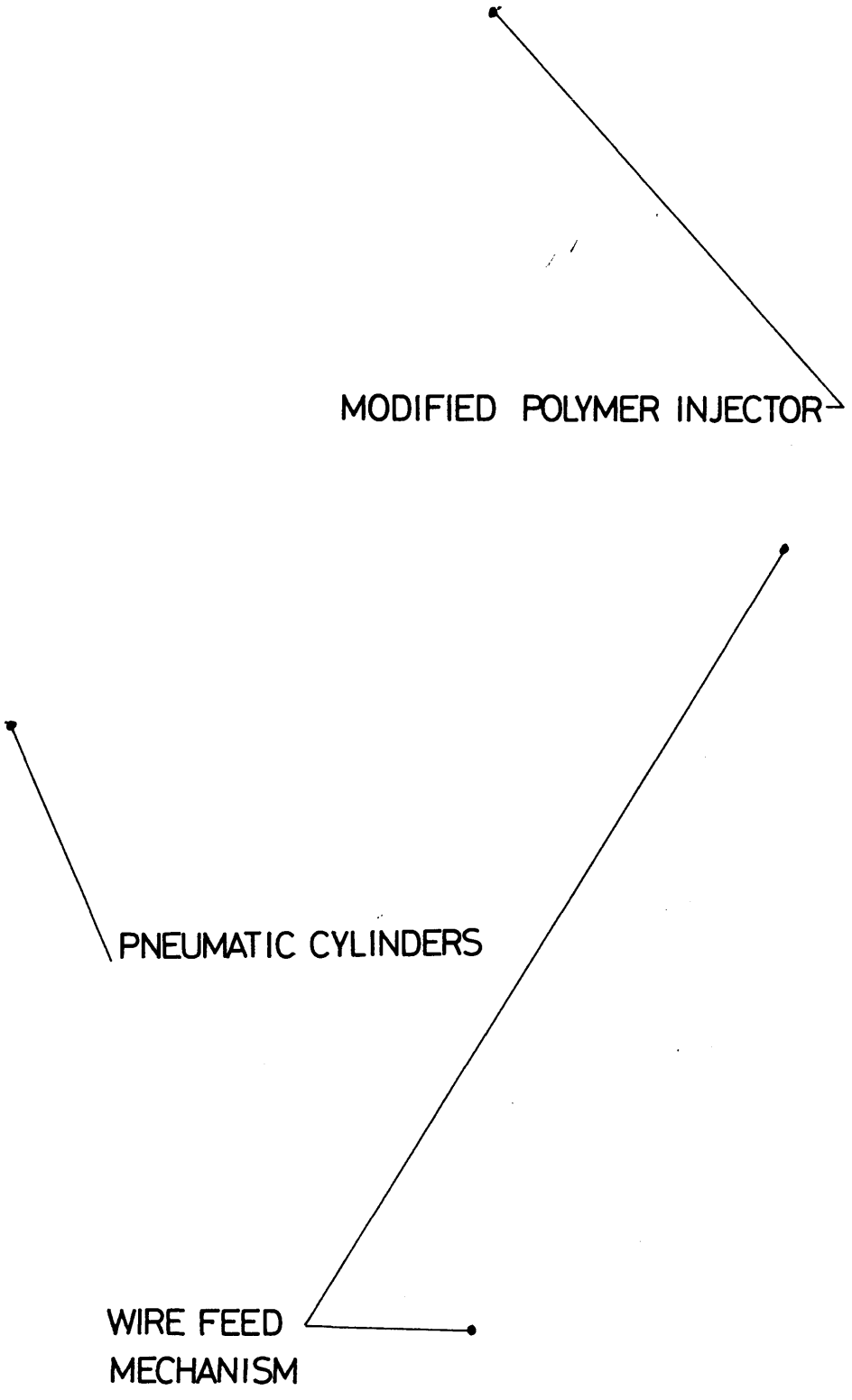
MODIFIED POLYMER INJECTOR
PNEUMATIC CYLINDERS
WIRE FEED
MECHANISM

PLATE 1

■■R0TD3LHI R3MYJOT Q3HIQOM

8R3GMJYD DITAMU3HS

• 0333 3P1W
M2IMAH33M

r BiAjq

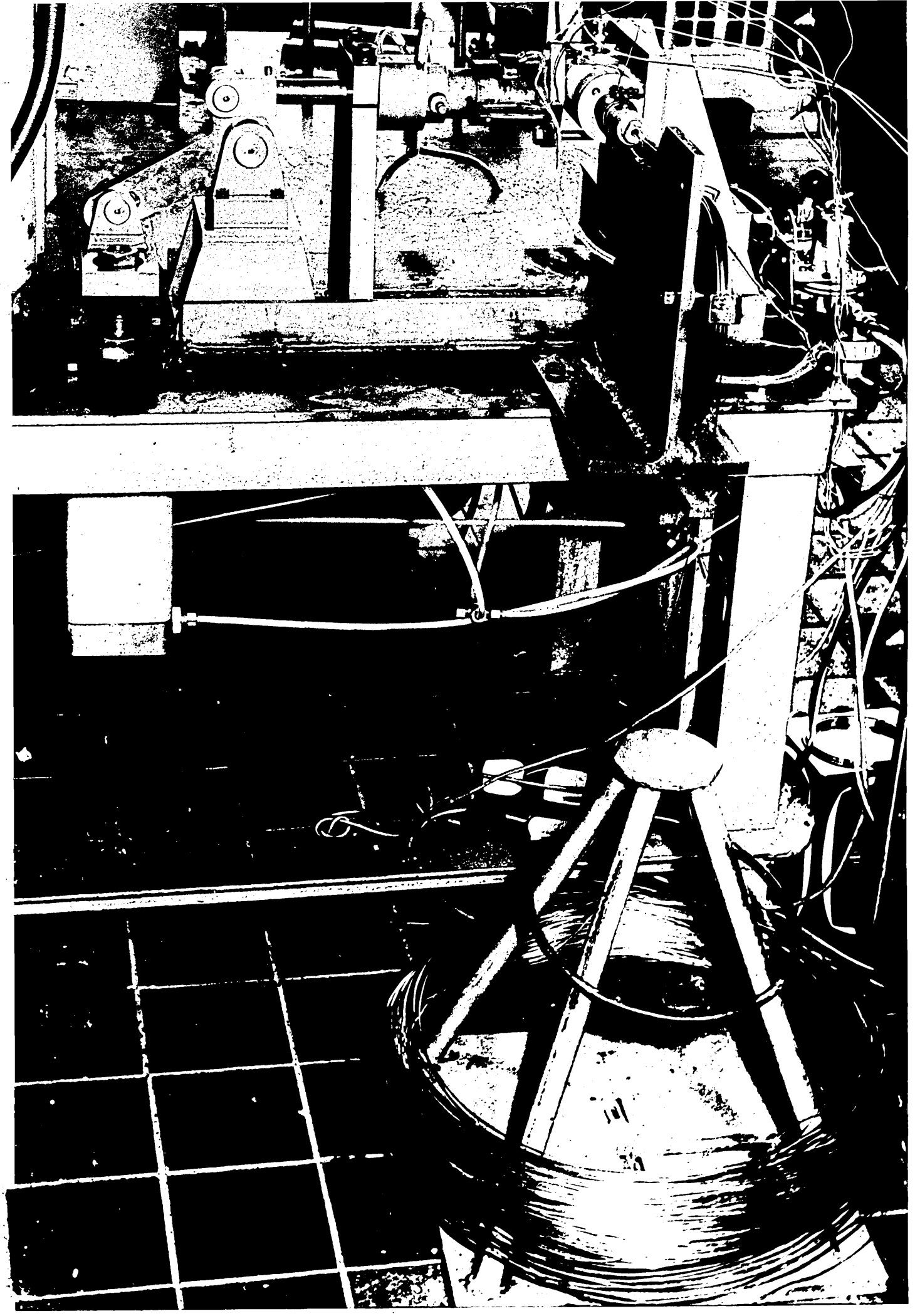

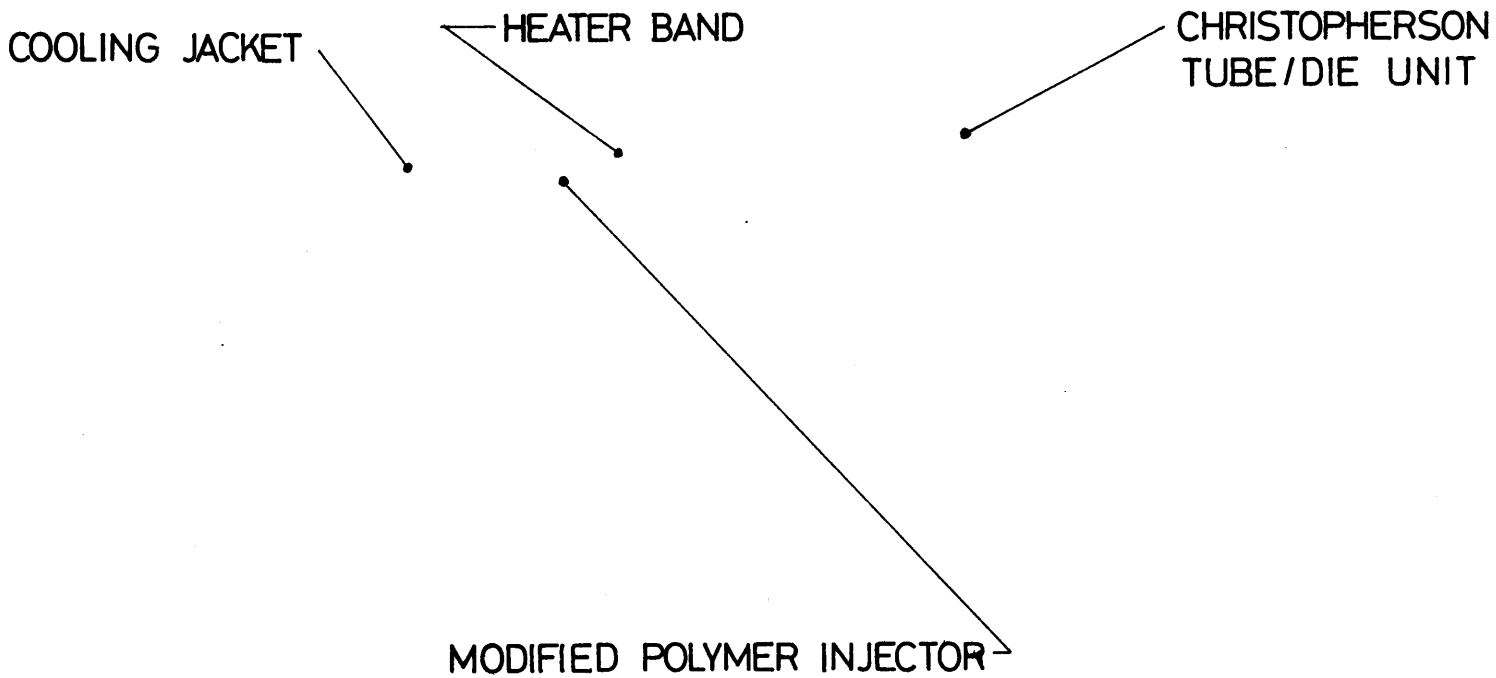
COOLING JACKET
HEATER BAND
CHRISTOPHERSON
TUBE/DIE UNIT
MODIFIED POLYMER INJECTOR

PLATE 2

LO

LU

I

JD

/

2

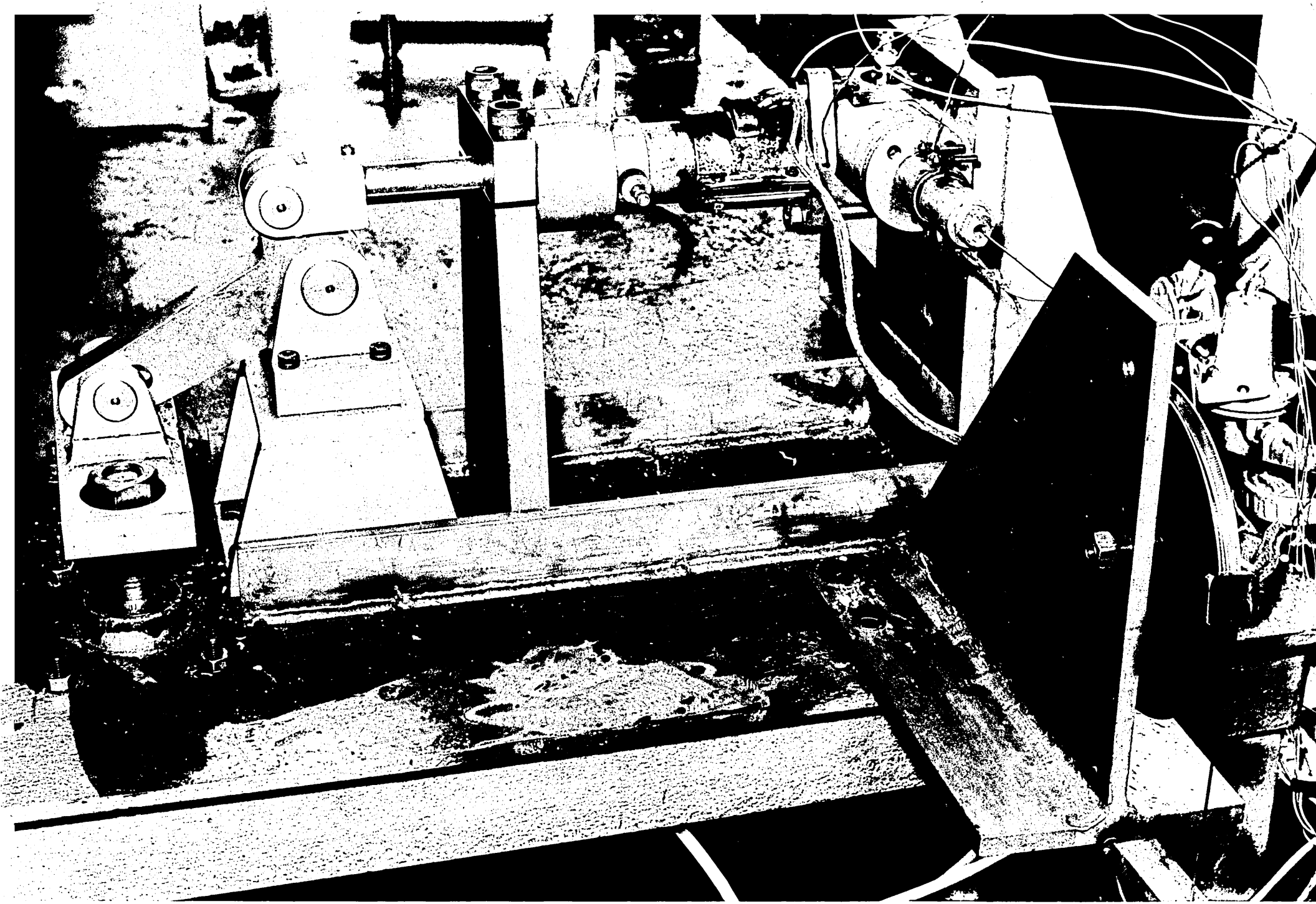

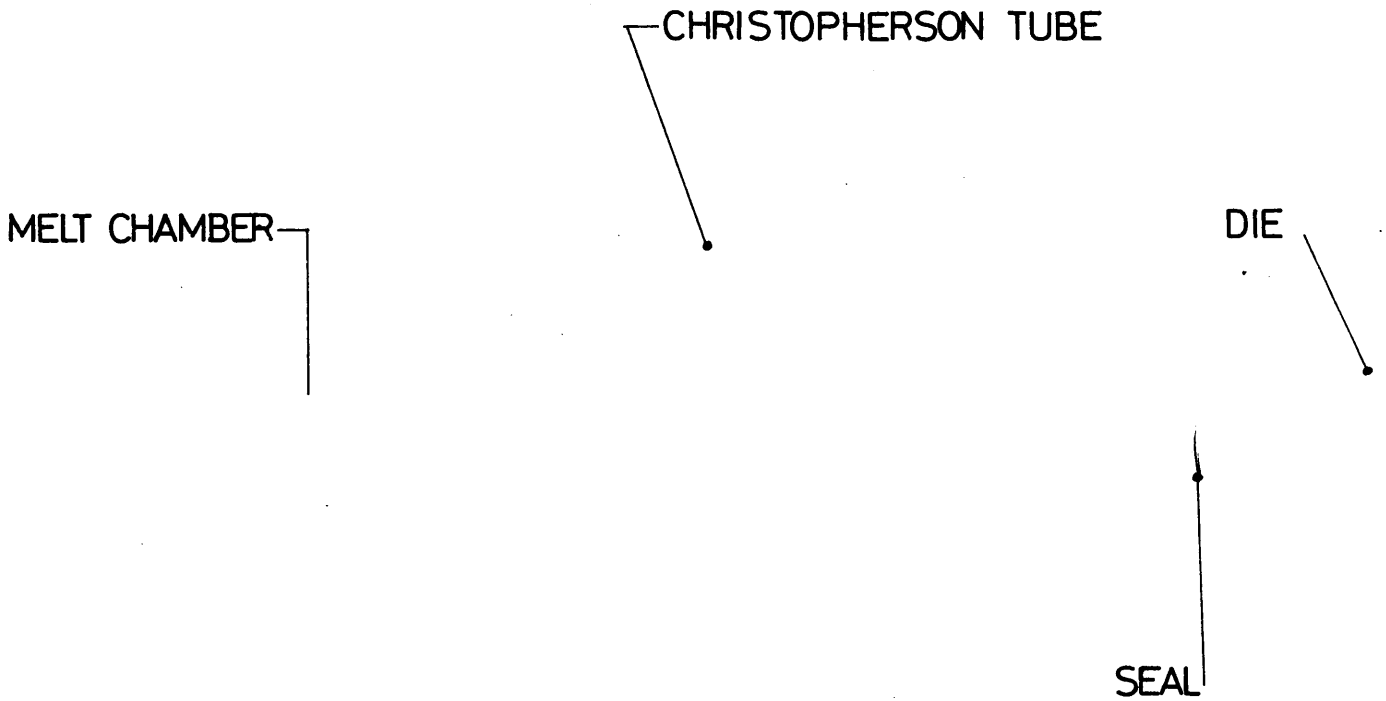

PLATE 3

bfViE 3

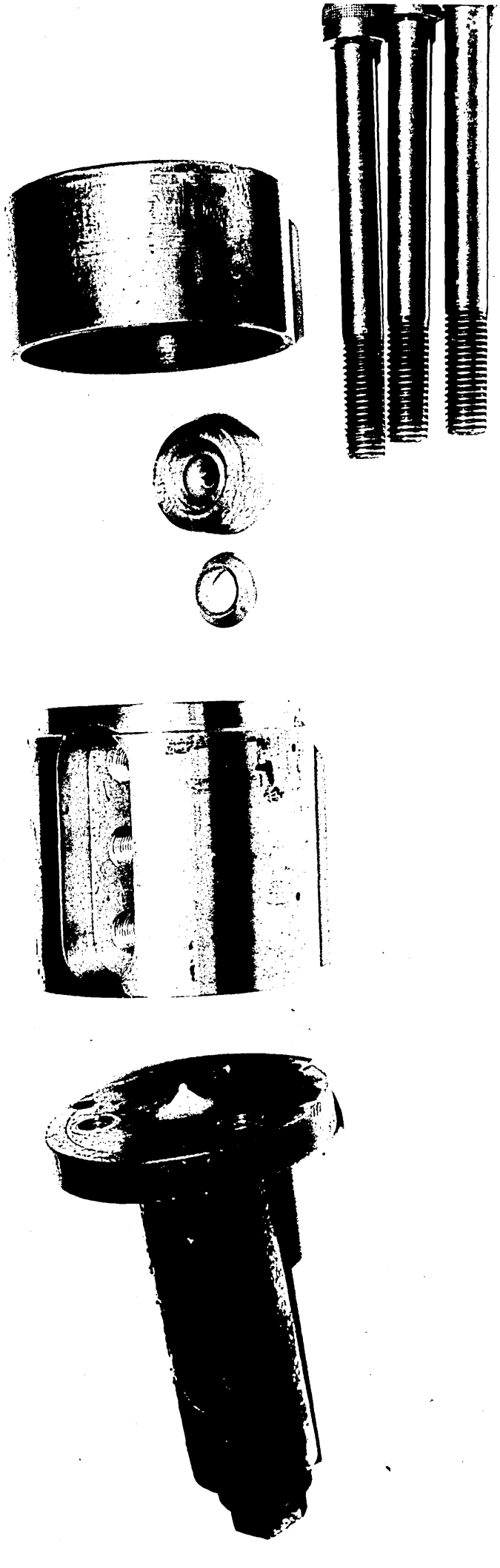

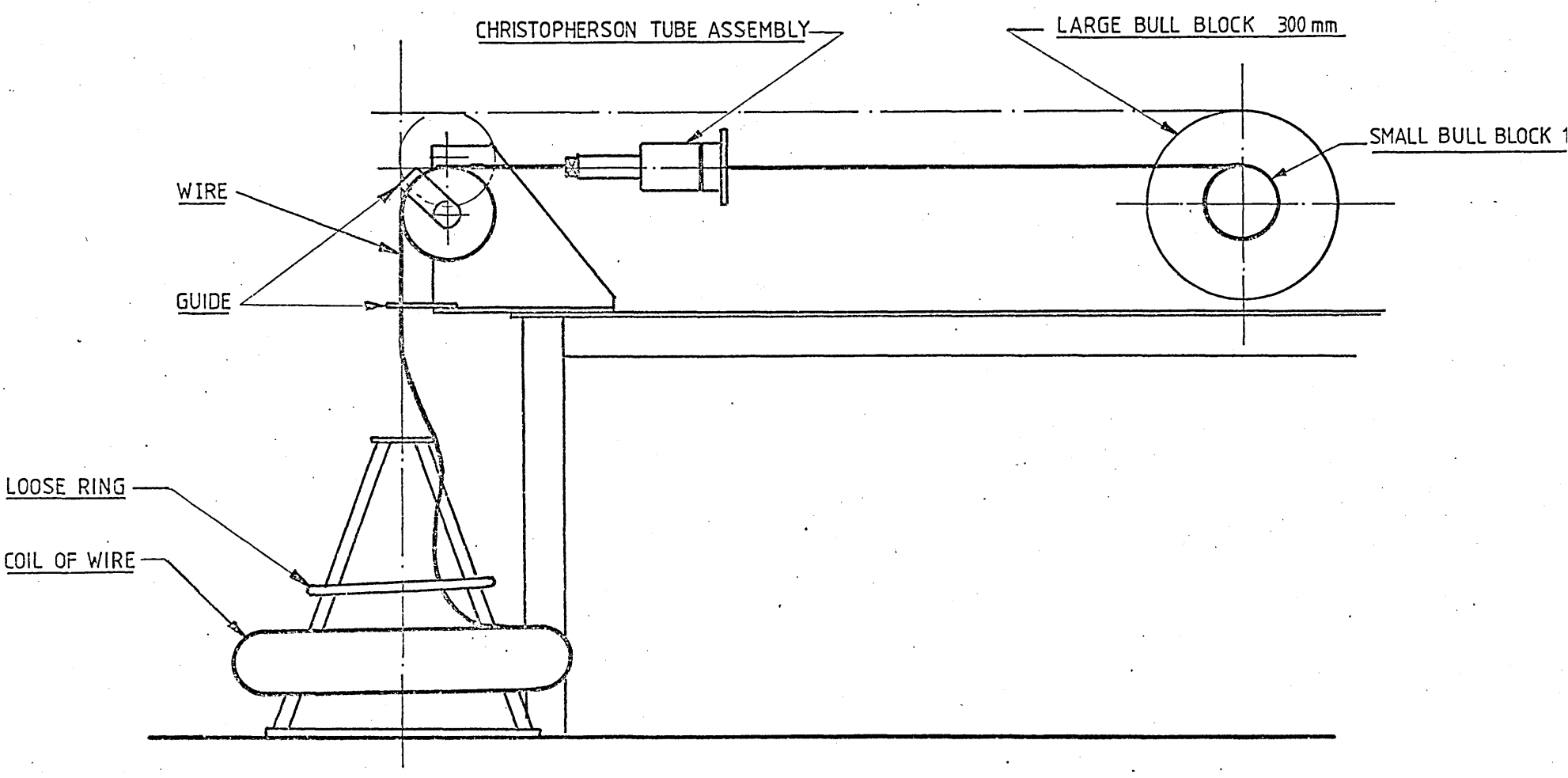

FIG 13 WIRE FEED MECHANISM

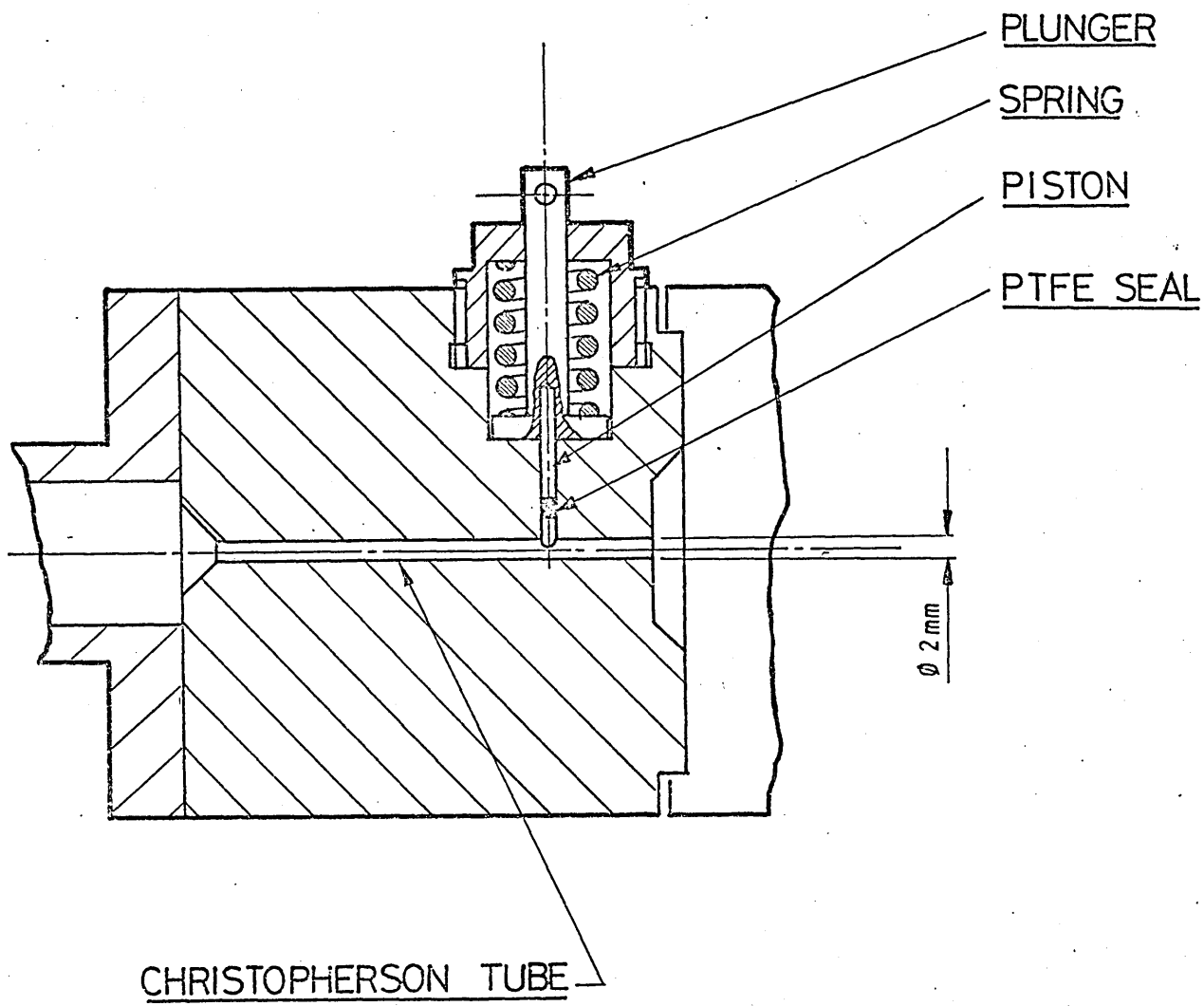

FIG 14 PROPOSED METHOD OF MEASURING PRESSURE

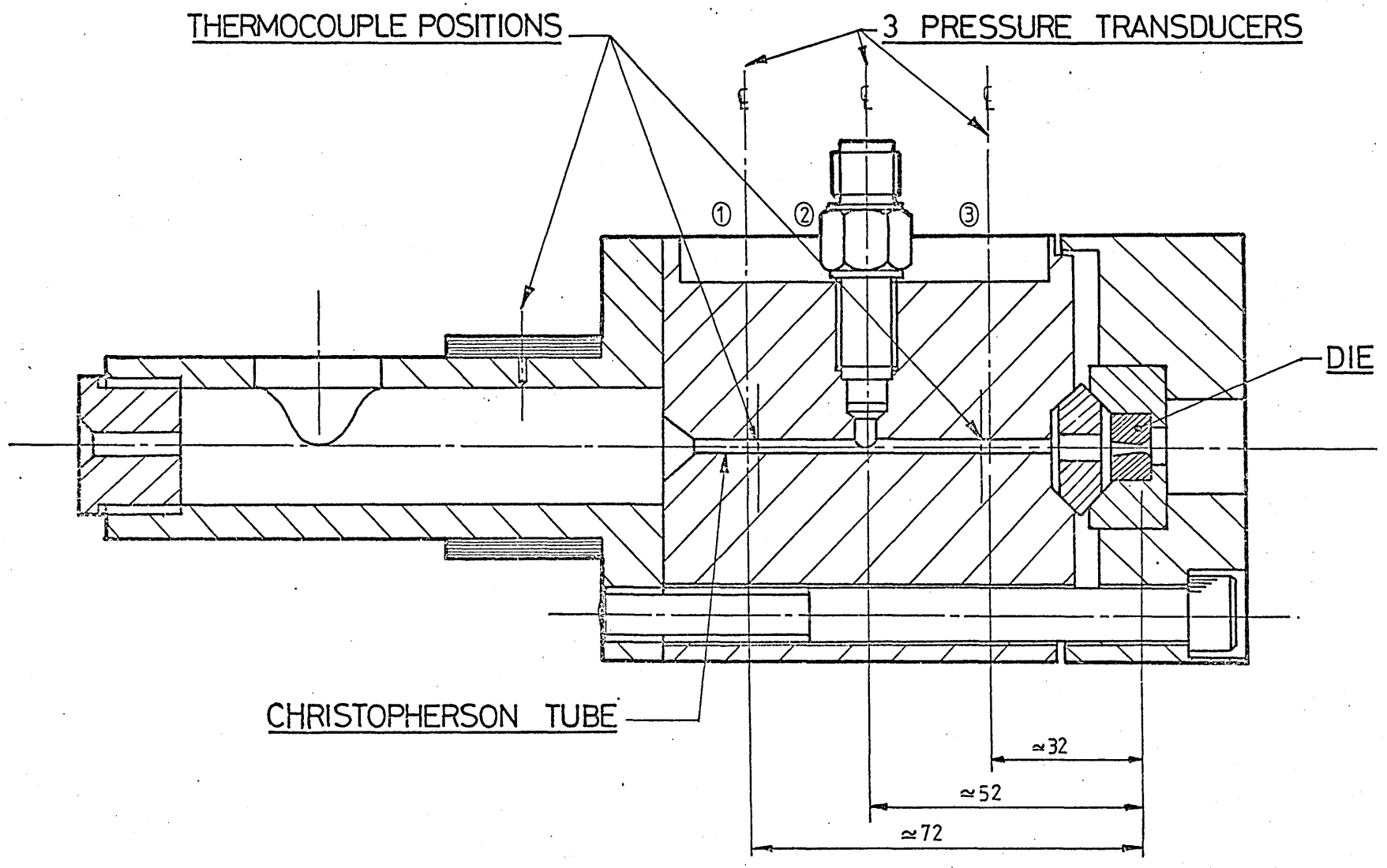

FIG 15 CHRISTOPHERSON TUBE WITH PRESSURE TRANSDUCERS

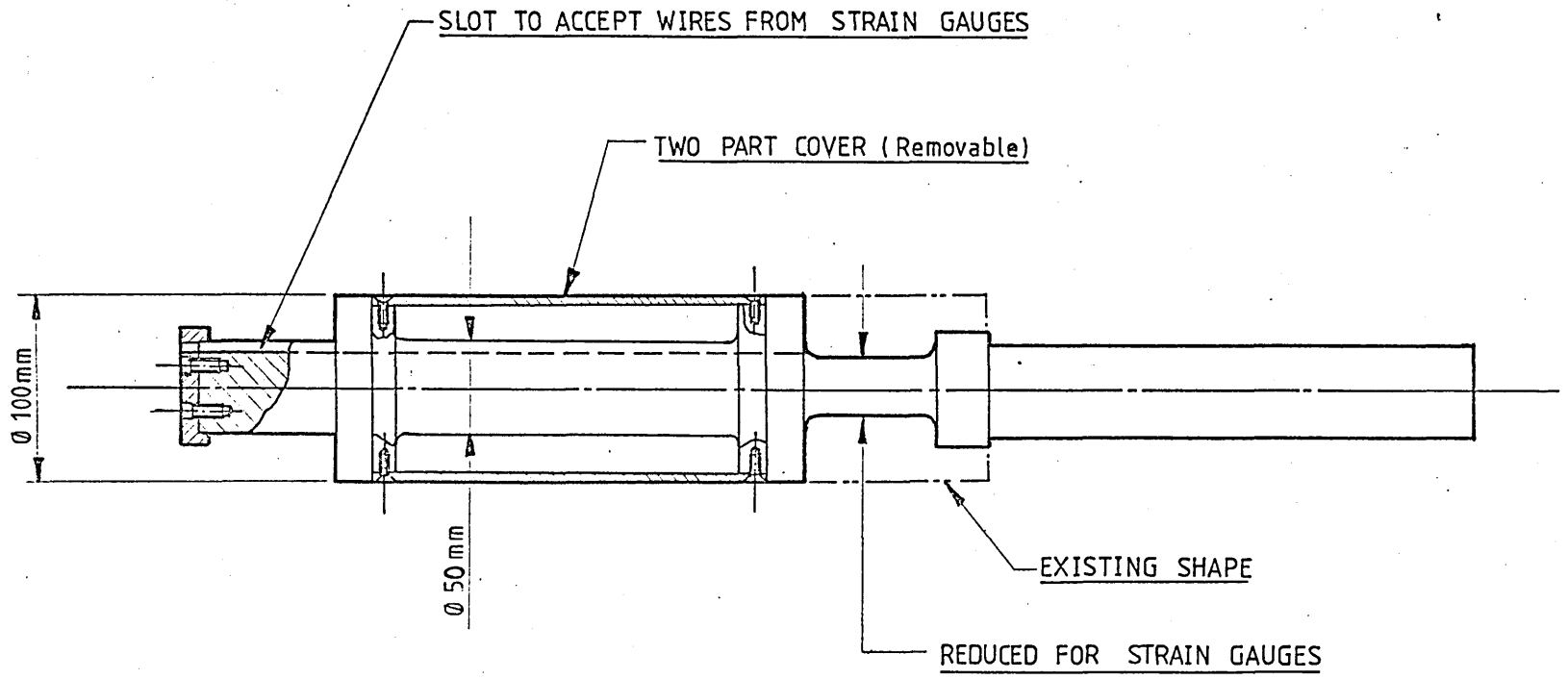

FIG 16 MODIFIED BULL BLOCK

not as high as was assumed. At this stage of development it was decided to run tests at very slow speeds to investigate further the "bamboo" effect which occurred at the lower drawing speeds. The small bull block was reduced in size to 50mm diameter and using an adaptor 100mm diameter, the original size was retained (see Fig 16 and Plates 4 and 5).

3.3 Hydrostatic Rig.

When tests had been performed under industrial conditions, the wire was unlubricated at start up causing die wear and fracture. It had been assumed that these were a result of the lack of lubrication before the hydrodynamic pressure had been generated. To overcome this, it was decided to attempt to pressurise the polymer outside the Christopherson tube and feed it into the tube at a pressure sufficient to cause immediate yielding of the wire at the die. This was to be achieved whilst retaining the hydrodynamic capabilities of the Christopherson tube. Measurements of pressure had shown the pressure gradient in the tube and estimates of the equipment required could be made. Various considerations were examined:-

a) Would a seal be necessary on the inlet side?
b) How would the polymer be pressurised?
c) What would prevent the polymer from being forced into the compressor once the hydrodynamic pressure had been developed?
d) How would the drawing load be measured?

100 mm DIAMETER BULL
BLOCK ADAPTER

PLATE 4

>

a
m

XI
uj Y

>0 W
Q >
> Q

X 3
U 3

2 o
m o

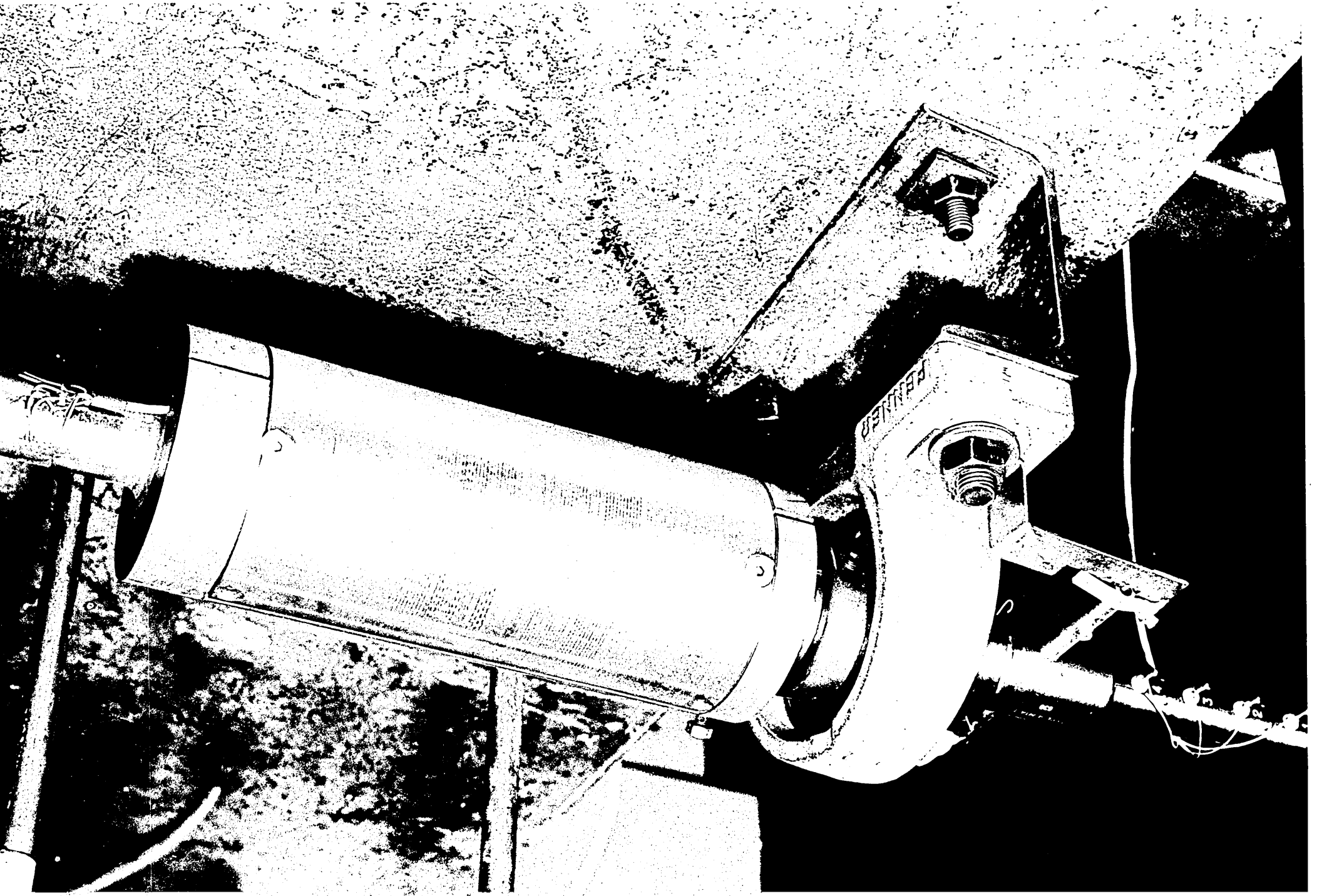

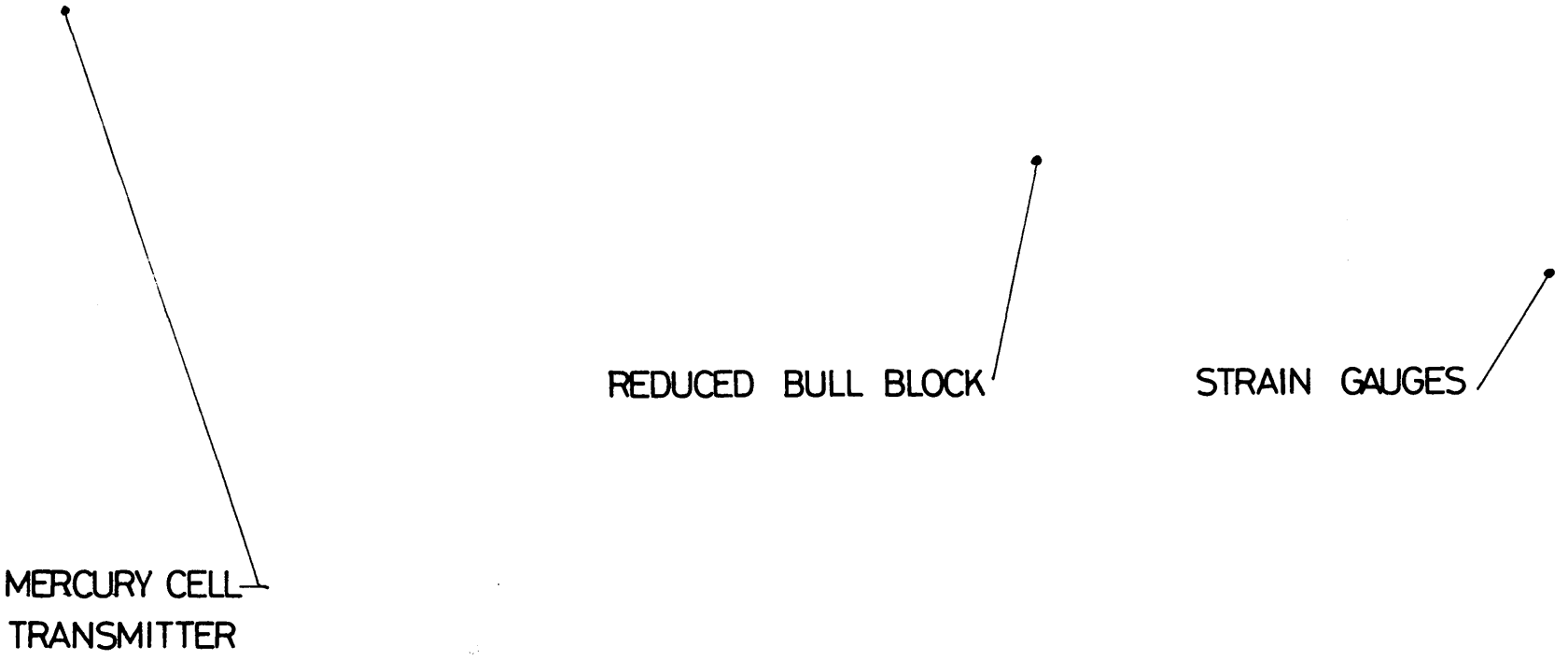
REDUCED BULL BLOCK
STRAIN GAUGES
MERCURY CELL
TRANSMITTER

PLATE 5

00
UJ
o
§
X
>
--I
ru

X:
U
e
CD
L
L
c
m

o
LU
O
C
Q
UJ
20

bfViE

X tz
y UJ
y O
5= Y
nj c
CJ
> a
2

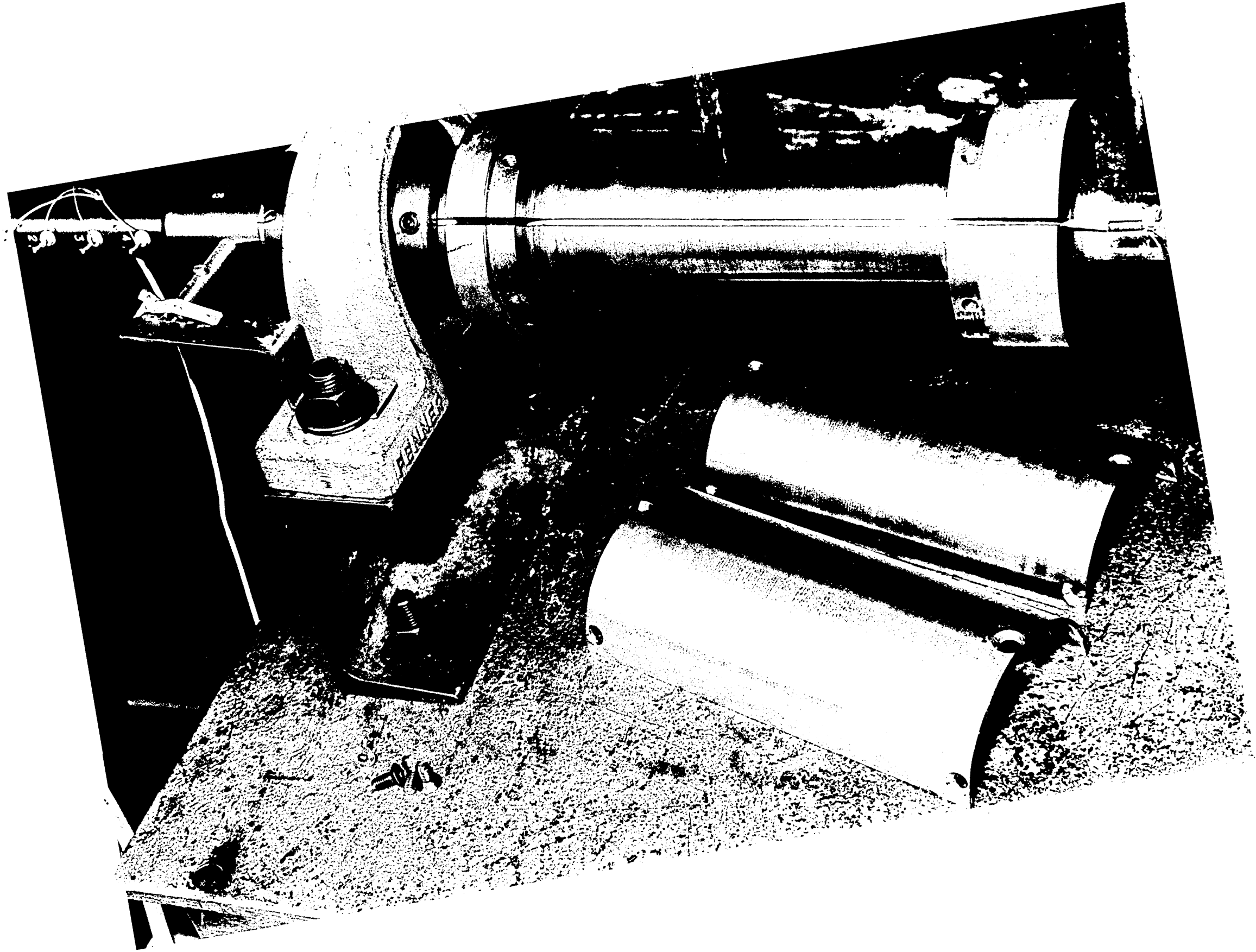
PENNER

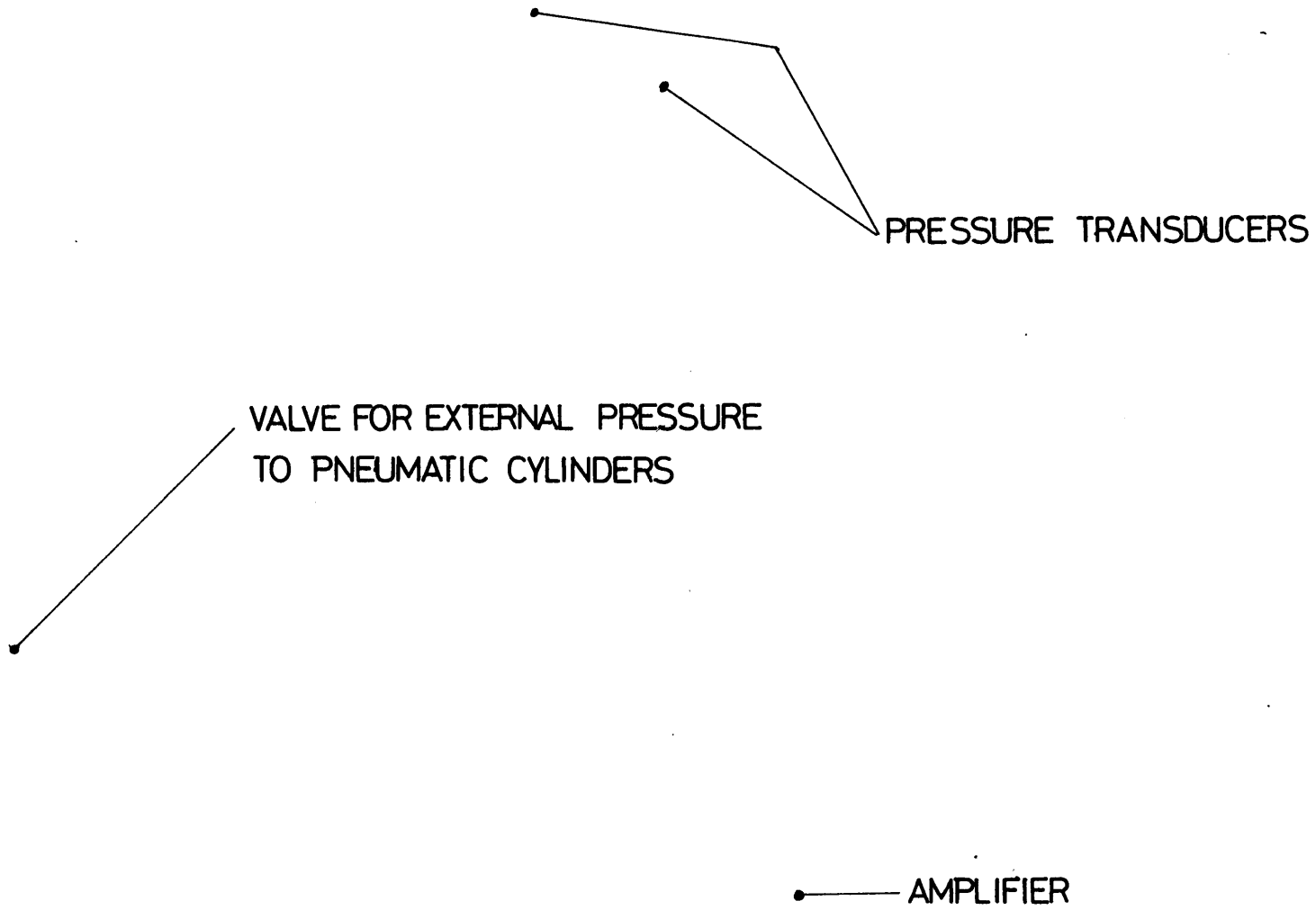
PRESSURE TRANSDUCERS
VALVE FOR EXTERNAL PRESSURE
TO PNEUMATIC CYLINDERS
AMPLIFIER

PLATE 6

Qy

Jd

VNbHblEB

JO UJ LU X)

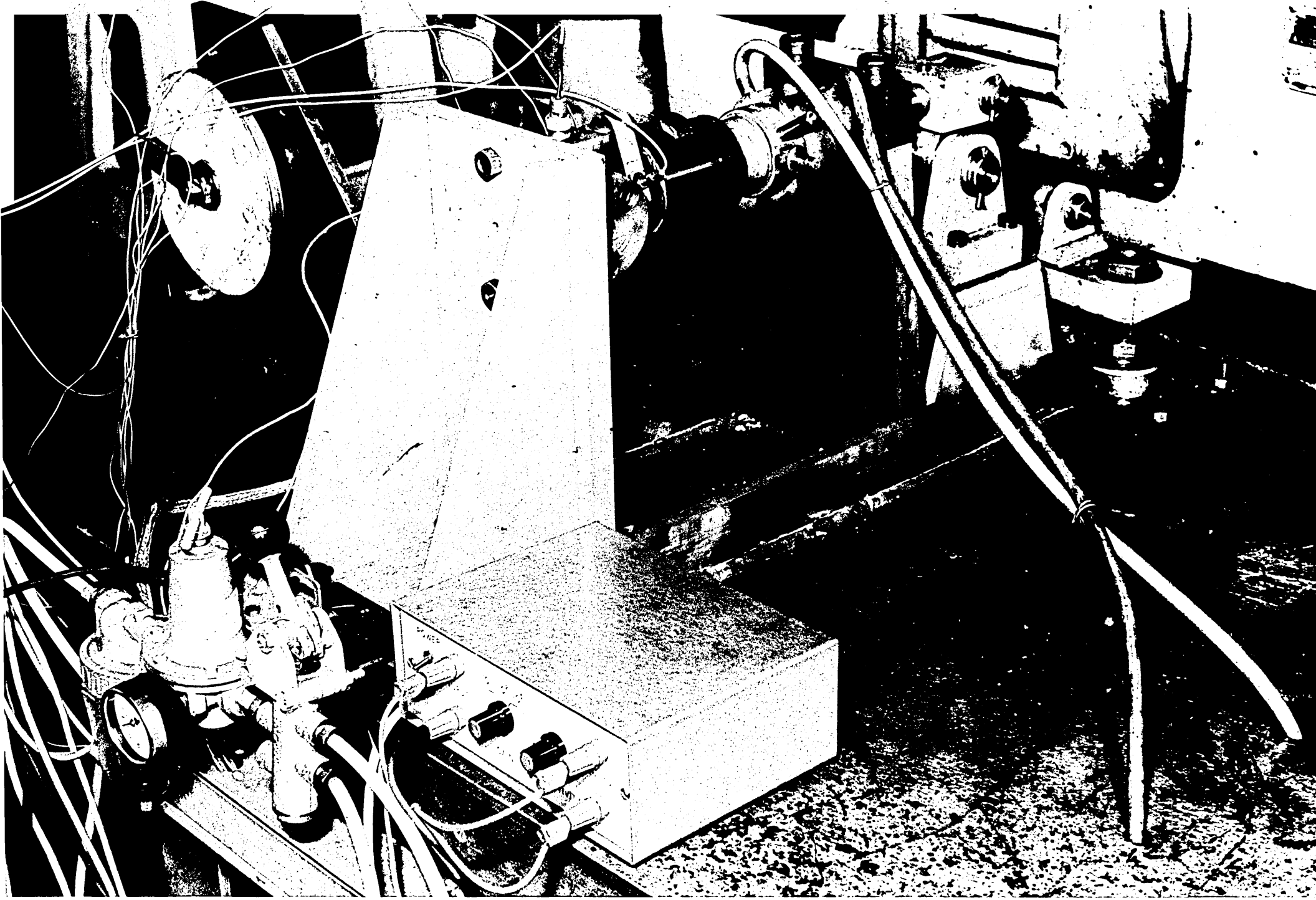

A simple calculation showed that a pressure of around 1000 bar could be maintained before significant leakage could occur through the inlet side of the Christopherson tube and so a seal would not be required.

There are two basic methods of pressurising polymer in use in injectors; screw injectors and straightforward compression injectors. A screw injector would require a motorised drive to cause a rotation of the screw and also some form of direct force to cause it to be driven into the cylinder. A simple injector would only require a direct force. A few enquiries revealed that a simple injector was available in the department for no cost and so it was decided to incorporate this unit into the design. Some method of forcing the piston into the injector cylinder was required. The best way appeared to be either pneumatic or hydraulic, and since compressed air was available, pneumatic power was chosen. A choice of air cylinder was now required. This necessitated a knowledge of the pressure required to be developed by the polymer. It was considered that a pressure of 500 bar injected at a suitable entry point in the Christopherson tube should be sufficient for the purposes. Since only5.5bar (80 psi) was available on line, a fairly large pneumatic cylinder was required if 500 bar was to generated directly. (The injector was 25.4mm diameter and would therefore require a direct force of approximately 2.54×10^4 N or a cylinder of 254mm diameter (10") for this to be achieved). There were also problems of where to put such a large cylinder, since the space on the drawing bench was very restricted. Two 100mm diameter (4") pneumatic cylinders became available, so the design proceeded using these as motive power. The

the cylinders had a 150mm (6") stroke and in consequence, were too long to be mounted next to the Christopherson tube. The logical place for these appeared to be below the bench. A simple crank arrangement allowed the injector to be mounted horizontally. Since the two 100mm diameter cylinders were not equivalent to a single 254mm diameter one, a mechanical advantage of three was required on the crank. This allowed a movement of 50mm at the piston. A few simple calculations were performed to find the required thickness of the crank and the diameter of the pivot pins.

It was realised that the pressure developed hydrostatically would be less than that developed hydrodynamically and that some form of non-return valve would be required to prevent leakage of pressure from the Christopherson tube to the injector, once drawing had commenced. A simple ball valve was designed to be fitted into the Christopherson tube at the injection point.

It was not feasible with this new equipment to measure the drawing load by means of the load plate as before since it was necessary to clamp the Christopherson tube. Therefore, a strain gauge bridge was constructed on a specially reduced part of the bull block shaft. This necessitated the use of mercury cell transmitters from the gauges on the rotating shaft to the recording instruments. The transmitter used was a Vibro-meter Sa type 4MTA/T. This unit allowed the speed of rotation of the bull block to be measured by the use of a magnetic sensor fitted into the body of the transmitter. The output from the gauges was fed, via the transmitter, to the UV recorder and the output from the magnetic sensor passed through an amplifier and then to a digital counter which,

when calibrated, gave a visual indication of the drawing speed.

A detail drawing of each component was produced and the equipment was manufactured. No special manufacturing techniques were necessary. A general arrangement drawing of the equipment is shown in Fig 18. Fig 16 shows the modified bull block and Fig 17 shows the new Christopherson tube unit with non-return valve. Plates 2, 4, 6 and 7 show the final form of the equipment.

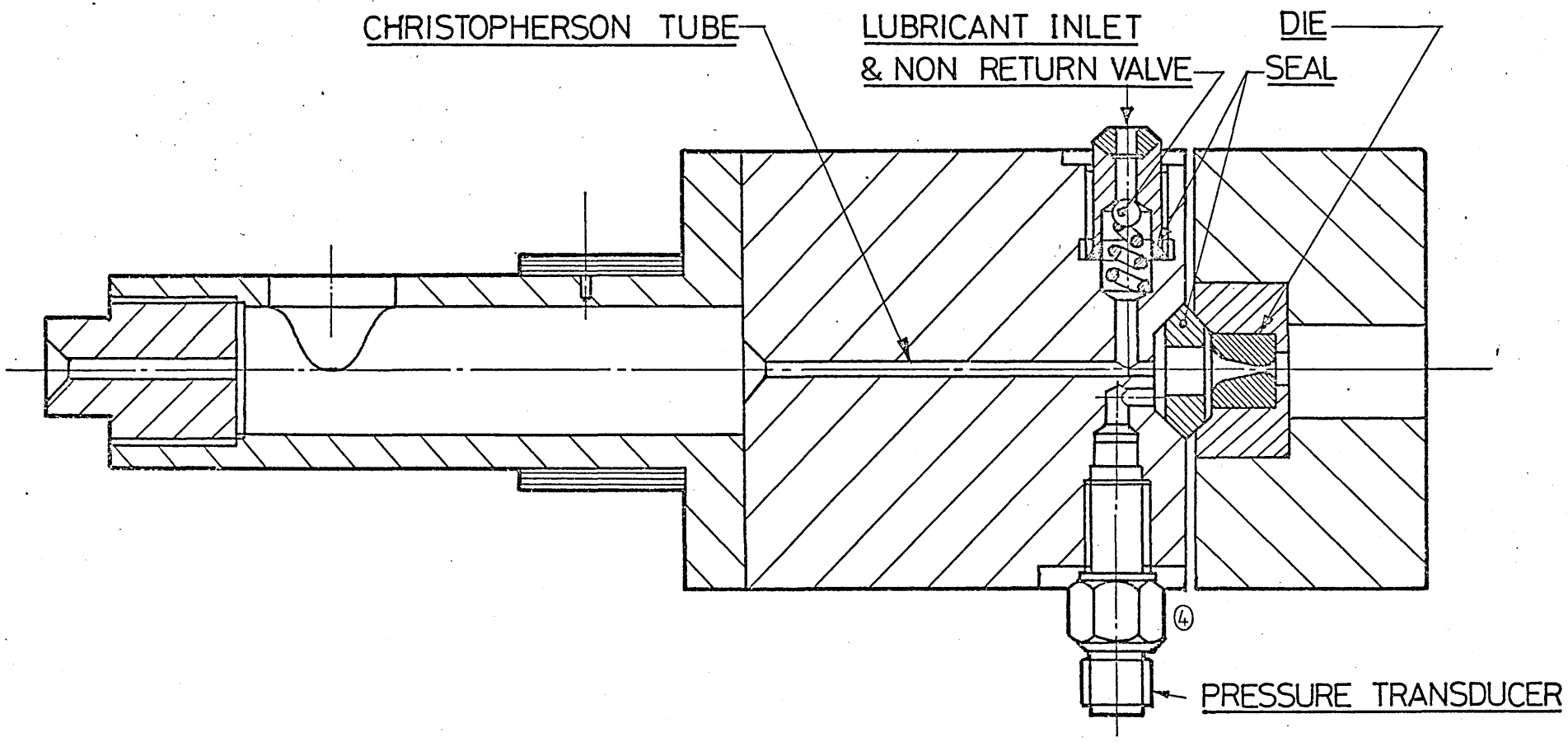

FIG 17 HYDROSTATIC-HYDRODYNAMIC CHRISTOPHERSON TUBE

31	AIR CYLINDER 4" x 6" STROKE	—	2	—	EXISTING
30	NUT – M10	—	8	—	
29	DRAW BENCH	—	—	—	EXISTING
28	BOLT – M10 x 85 LONG	—	8	—	
27	SCKT. HD. CAP SCREW M12 x 25 LG	—	4	—	
26	DOWEL – Ø6 x 30 LONG	—	1	—	
25	BRACKET	M.S.	1	12	
24	CHRISTOPHERSON TUBE ASSEMBLY	—	1	11	
23	SKT. HD. CAPSCREW 2BA x 20 LONG	—	3	—	
22	TIE ROD	M.S.	2	23	
21	PRESSURE PLATE	MS.	1	13	
20	NUT – M10	—	2	—	
19	HEATER BAND	—	1	—	EXISTING
18	INJECTOR CYLINDER	—	1	—	EXISTING
17	COOLING JACKET	BRASS	1	16	
16	SCKT. HD. CAP SCREW M10 x 25	—	4	—	
15	PISTON	EN24	1	14	
14	BRACKET	M.S.	1	21	
13	SCKT. HD. CAP SCREW M8 x 25 LG	—	4	—	
12	BRACKET	MS.	1	20	
11	SOCKET HD. CAP SCREW M5 x 40 LG	—	1	—	
10	CLEVIS	M.S.	1	15	
9	WASHER (20.1 ID)	M.S	2	19	
8	LEVER	EN8	1	17	
7	PIN	EN8	2	18	
6	CYLINDER CONNECTOR	M.S	1	22	
5	NUT – 1" BSF	—	4	—	
4	SPLIT PIN – Ø4	—	3	—	
3	WASHER	M.S	1	19	
2	WASHER (28.1 ID)	M.S.	2	19	
1	PIN	EN8	1	18	
N°	DESCRIPTION	MATL	N° OFF	DRG #	

FIGURE 18 (continued)

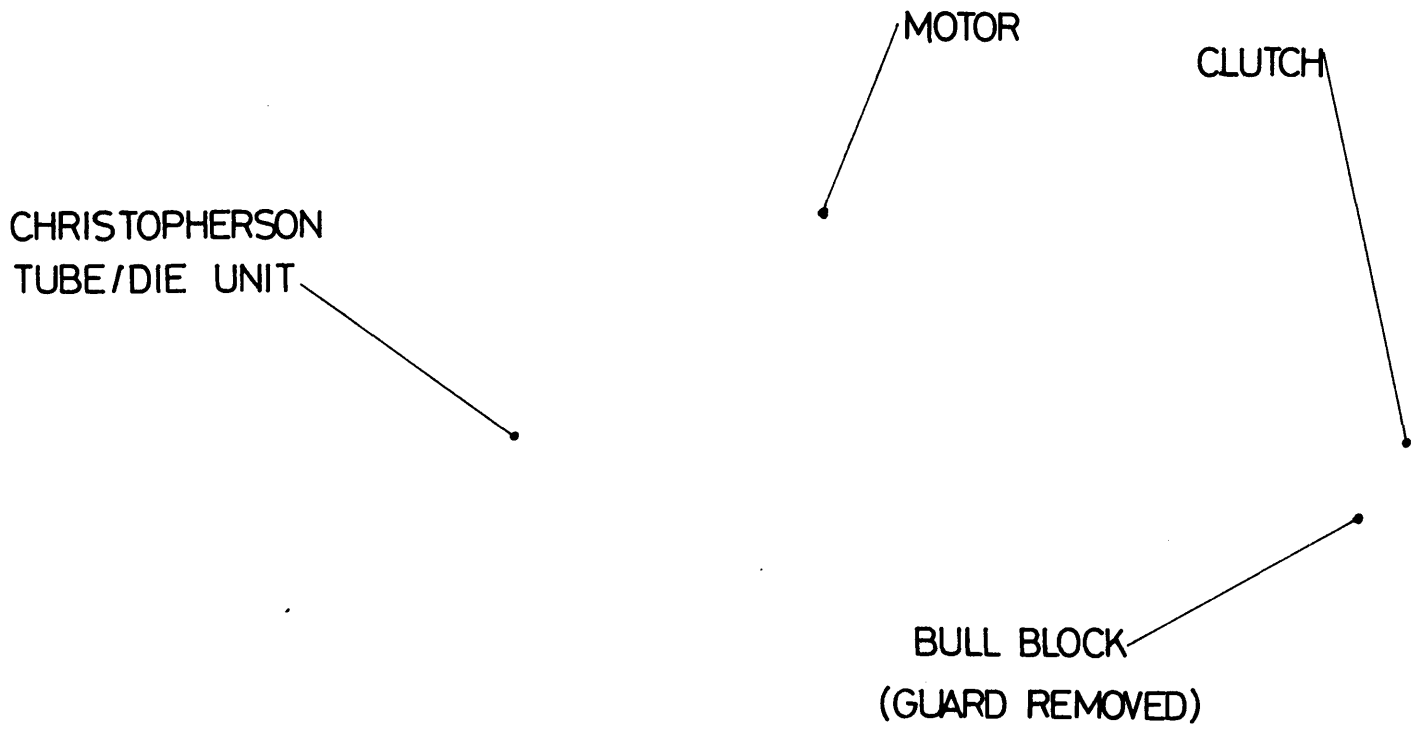
MOTOR
CLUTCH
CHRISTOPHERSON
TUBE/DIE UNIT
BULL BLOCK
(GUARD REMOVED)

PLATE 7

bfVlE A

~ 8
c 3
UJ 3
9 9
LIJ 0^
CD :o
Q

Q LLJ 6 K LLJ 3D QD O

y u 2 CD

c: CD

*

± y c u u

■H010B

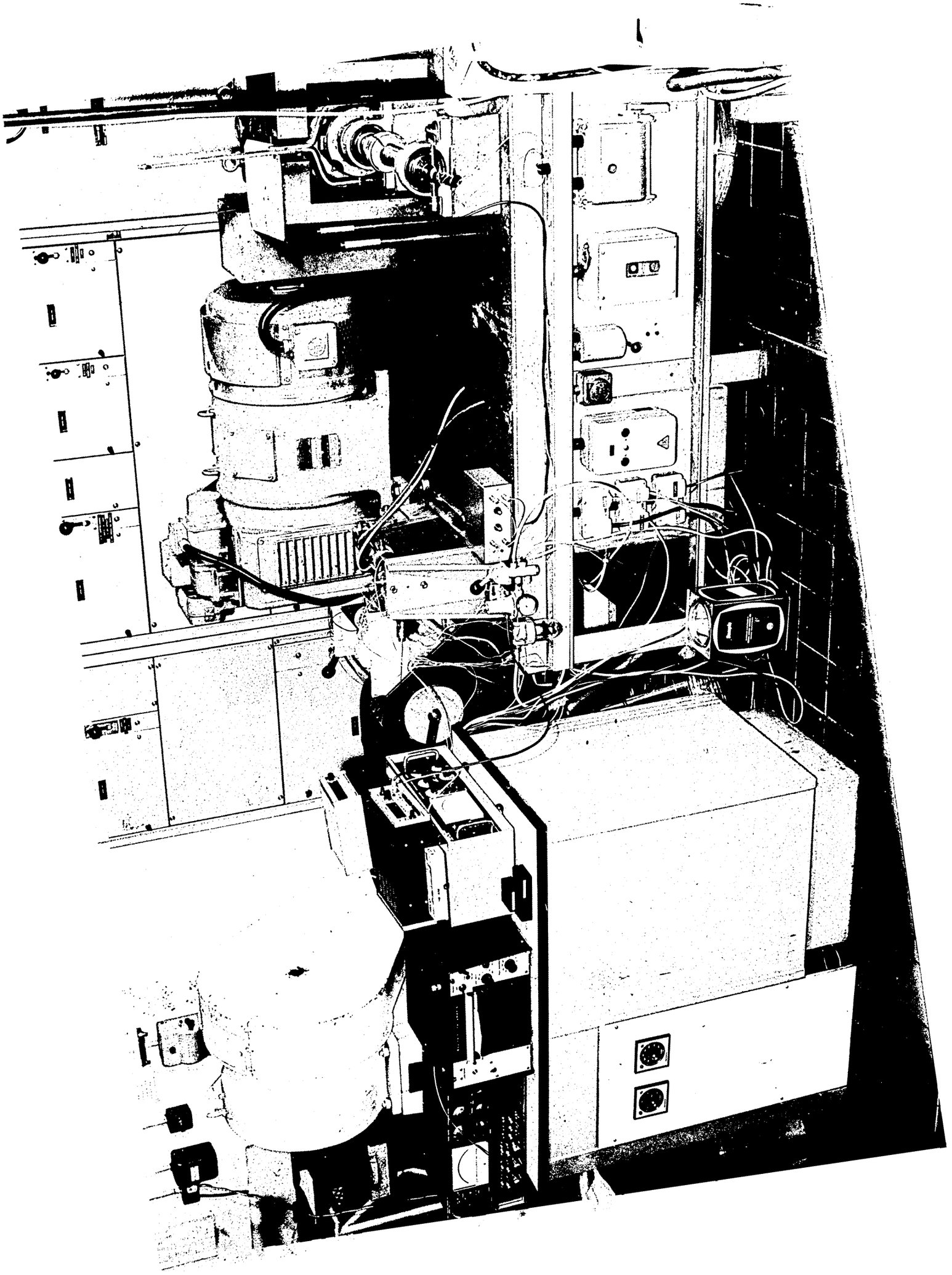

METER FOR STRAIN GAUGES

UV RECORDER

CHARGE AMPLIFIERS FOR PRESSURE TRANSDUCERS

THERMOSTAT CONTROLS

PLATE 8

CO
LU
>!
L_
-Q

X
LD
Q
X
8
LU
X
<
c

a'
LO
X

8

Co
O
K
X
L||
X
– !

LU
X
c
ru
CO
x
X
X
X
3
a>
X
yj
JJ
L_
X
>
y
>
X
(j

$
UJ
u
C:
|
>
X
H

WEiEB KOB EIBVM GVEIGE

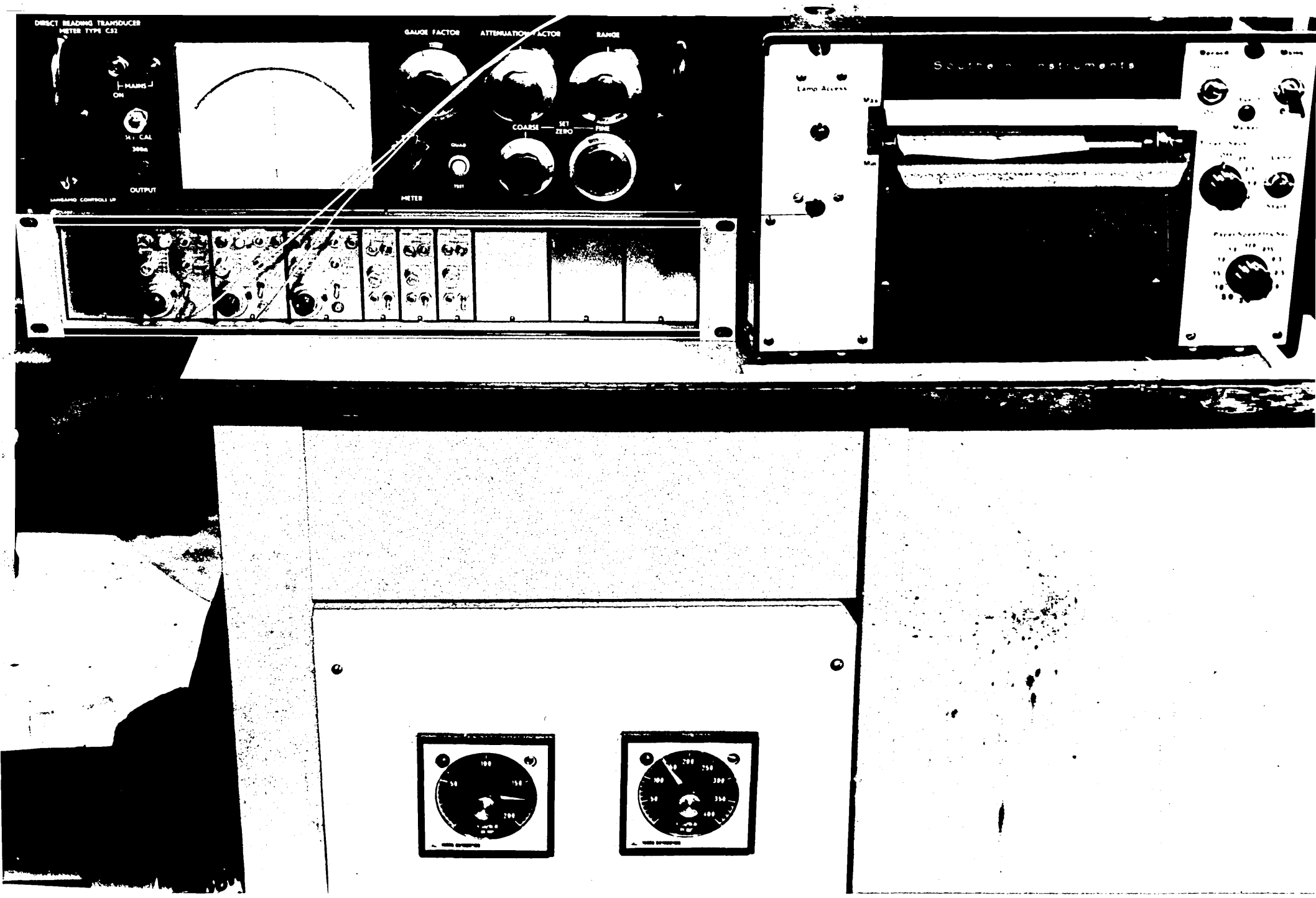
DIRECT READING TRANSDUCER
METER TYPE C32
MAINS
ON
CAL
OUTPUT
GAUGE FACTOR
ATTENUATION FACTOR
RANGE
COARSE
SET ZERO
FINE
METER
TEST
Lamp Access

THERMOMETER (COUPLES)

DIGITAL COUNTER (TACHOMETER)

DIGITAL VOLTMETER
(TACHOGENERATOR)

METER FOR STRAIN GAUGES

PLATE 9

(23JSU03) H3T3M0MR3HT

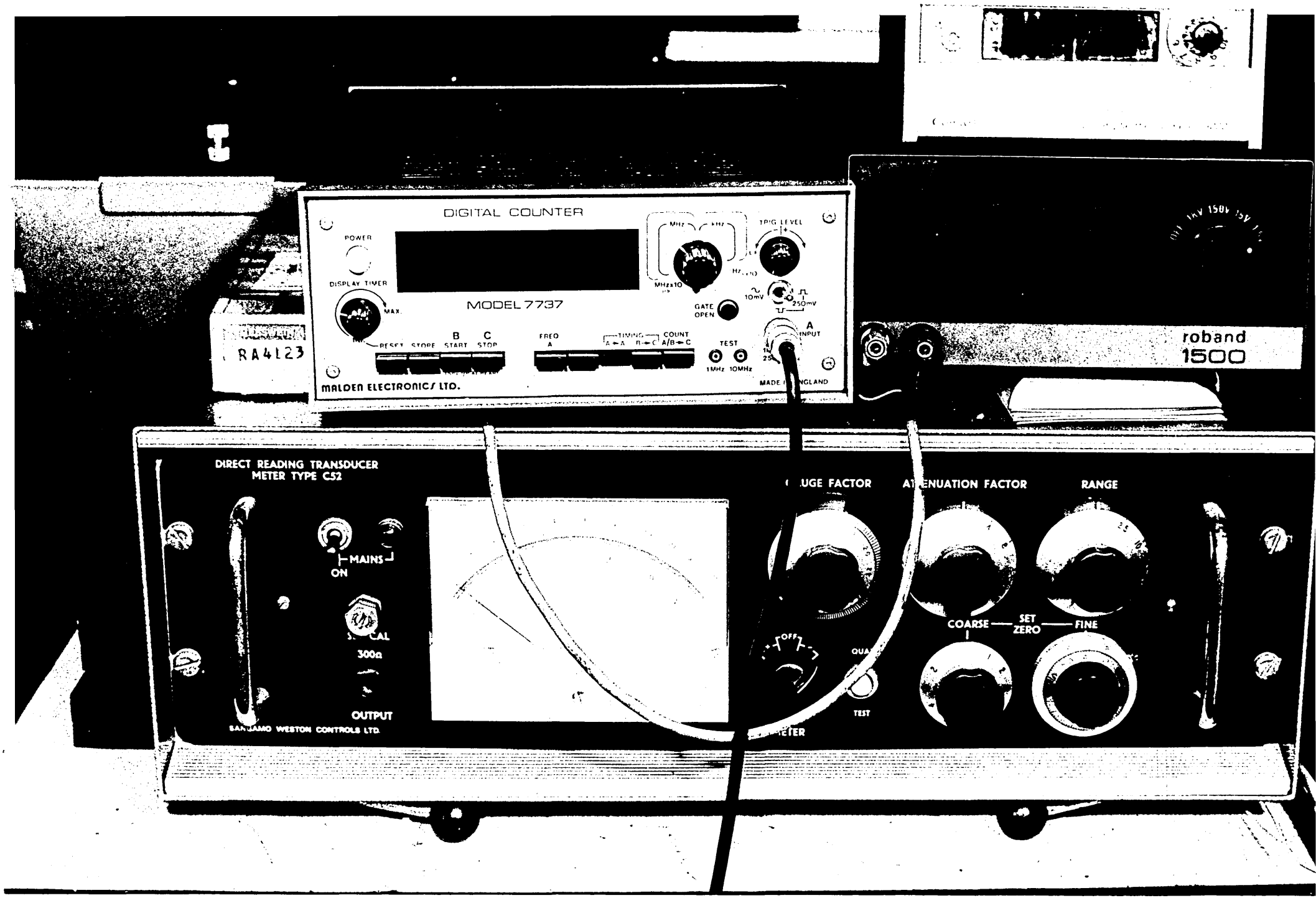
DIGITAL COUNTER
POWER
DISPLAY TIMER
MAX.
MODEL 7737
MHz
KHz
MHzx10
TRIG LEVEL
GATE OPEN
10mV
250mV
RESET
STORE
B START
C STOP
FREQ A
TIMING
COUNT A/B→C
TEST
1MHz 10MHz
A INPUT
MALDEN ELECTRONICS LTD.
RA4123
roband
1500
DIRECT READING TRANSDUCER
METER TYPE C52
MAINS
ON
CAL
300Ω
OUTPUT
SAN JAMO WESTON CONTROLS LTD.
GAUGE FACTOR
ATTENUATION FACTOR
RANGE
COARSE
SET ZERO
FINE
OFF
TEST

CHAPTER 4. TEST PROCEDURE AND RESULTS FROM THE TESTS.

The following chapter explains the experimental procedure used in the tests and highlights any areas which created unusual problems. The results from the tests are presented here in graphical form for convenience. Appendix V contains a catalogue of the most important results in tabular form.

4.1 Test Procedures.

The test procedure varied as the experimental equipment was modified. Two sets of test procedure were adopted; one for the basic hydrodynamic rig and the other when an externally pressure aided equipment was used. These will be described in detail.

4.1.1 Test Procedure Adopted for the Hydrodynamic Rig.

Before test runs could be conducted, a short length of wire needed to be swaged down to below the diameter of the die so that it could be pushed through the die and attached to the bull block. Having done this, the coil of wire was placed in the feed mechanism and fed through as described. The guards were placed in position. The polymer melt chamber was filled with the appropriate amount of

polymer and the temperature set on the thermostat. The heater band, thermostat and instrumentation were switched on. The polymer was quickly melted, but the Christopherson tube required at least one hour to reach a steady temperature (two thermocouples gave the temperature gradient in the Christopherson tube). After the one hour soaking period, temperature stability was achieved and tests were allowed to proceed. The motor was started and set running at the desired speed (the motor speed was adjustable by altering the position of the commutator brushes). The ultra-violet recorder paper was set in motion and the clutch engaged. The load and pressure readings were recorded by the UV recorder, which left only drawing speed and temperature to be noted. Several metres of wire were drawn. The speed was then changed and the test procedure repeated until all the tests had been conducted, or the wire coil had been expended. (several very long runs were conducted to investigate any changes in the measured parameters as time progressed). It was now necessary to measure the coat thickness (if any) produced on the wire. This was done by the weight loss method. The drawn wire was removed from the bull block and separated into individual runs. Four samples of wire (about 200mm long) were removed from the length of wire and placed in marked envelopes. Each of these were later cut in half, one piece being weighed, stripped of polymer and reweighed. The remaining piece could be used for subsequent tests if necessary and provided evidence of the coat present. Since the density of the polymer was known and the length and diameter of the piece of wire could be easily measured, the thickness of the polymer coat could be calculated. The average thickness was calculated from the four samples taken

and used in the results. A qualitative assessment of coating adhesion and coat quality was made whilst removing the coat during weighing. The UV recorder gave values of pressure at three points along the Christopherson tube as the drawing progressed, together with the variations in drawing load. The average value of each was taken and noted with the other information on the test sheet. A typical trace from the UV recorder is included as Fig 19. Experiments were conducted as above on three types of wire; copper, 18/8 stainless steel and 60/65 carbon steel. The wire used was 1.62mm diameter in all cases. A change in reduction of area was achieved by using different die sizes. Three sizes were investigated; 1.58, 1.49 and 1.37mm diameter giving 5%, 15% and 30% reductions in area respectively. A 12^{o} inclusive die angle was used on all dies. Several polymers were tried but Alkathene WVG 23 was used for most of the tests.

4.1.2 Problems Encountered with the Hydrodynamic Rig.

Few problems were met during operation of the apparatus after initial modifications had been undertaken. The most significant problem was that of the die seal. After a long series of tests on 60/65 carbon steel wire, the copper seal became extruded through the gap formed by the die and the Christopherson tube, causing leakage of pressure. Several new seals of varying hardness and size were made and tried, but the problem still remained. A change from copper to aluminium alloy for the seal proved to be successful. After

FIG 19 TYPICAL UV TRACE

Copper ~ 30 % reduction ;
150 °C ; 0·205 ms^{-1}

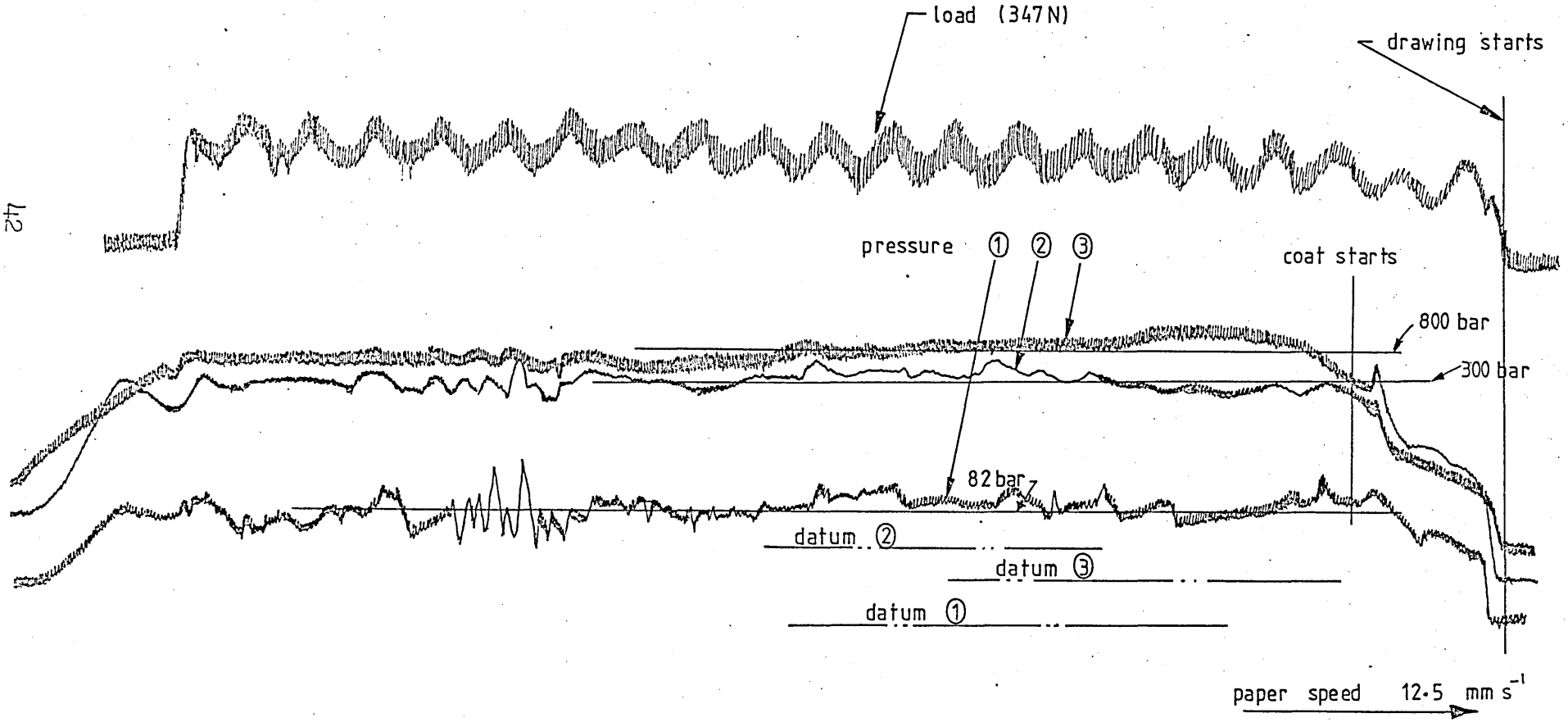

initial runs the aluminium seal had bedded down and become work hardened. Extrusion of the seal no longer occurred.

Problems were encountered using the pressure transducers. It was thought that the readings were much lower than was actually occurring. An estimate of pressure had been made assuming the pressure at the die end was close to the yield stress of the wire. Several efforts to improve the validity of the results were tried. The transducers were placed as close as possible to the bore of the Christopherson tube, but the results were still the same. (This was done to reduce the effects of compressibility of the melt around the transducer). Results were taken with the Christopherson tube in this condition. Later theoretical work showed that the pressure was not as high as was first thought.

The first two metres of wire from the first run after cleaning out the die were uncoated. This was because the Christopherson tube and seal area were not filled with polymer after cleaning and required a finite length of time to be filled with polymer by means of the incoming wire. Subsequent runs required about 300mm of wire to build up enough pressure to encourage hydrodynamic action. It was this lack of coat and the subsequent lack of lubrication that had caused problems when full scale plant trials had been undertaken previously. In order to improve the start up, it was decided to attempt to pressurise the polymer melt externally and feed this pressurised polymer into the Christopherson tube at a suitable entry point, prior to drawing. As mentioned in Chapter 3, modifications to the apparatus were undertaken. This new rig required a different test procedure.

4.1.3 Test Procedure Adopted for the Pressure Assisted Apparatus.

The wire was fed through the Christopherson tube and the die to the bull block as previously described. Water was supplied to the cooling band around the feed cylinder. The feed cylinder and polymer melt chamber were filled with polymer and the heater bands were switched on. All recording instruments were switched on. One hour was allowed for the apparatus to reach a steady temperature. The temperature of the feed cylinder thermostat was set at 20°C above that of the melt chamber to allow for the heat losses that may have occurred between the feed cylinder and the Christopherson tube. When a steady temperature had been achieved, the motor was started and set running at the desired speed. The UV recorder paper was set in motion and compressed air supplied to the feed cylinder arrangement. A short period was allowed for the pressure to become fully developed and the clutch was then engaged. The air pressure to the feed cylinder was then removed and the tests proceeded as before.

Pressure was measured at only one position in the Christopherson tube in the area around the seal (position 4 in Fig 17). The pressure generated by the feed cylinder was also monitored. The load reading was taken from strain gauges attached to the bull block shaft having been transmitted to the display instruments by the mercury cells fastened to the end of the bull block shaft as described in Chapter 3.

4.1.4 Problems Encountered with the Pressure Assisted Rig.

The pressure assisted Christopherson tube had the desired effect of reducing the uncoated length of the wire at start up, however, it is felt that this reduction could have been greater than was achieved. The polymer feed cylinder was calculated to give a pressure of 50 MNm^{-2} at the Christopherson tube. The losses were much higher than anticipated. A pressure of 20 MNm^{-2} was measured by the pressure transducer placed in the end plate of the cylinder.

The bench required stiffening in highly stressed areas to prevent the whole bedplate from bending. Before stiffening, the top of the mounting bracket to which the Christopherson tube was attached moved visibly by 10mm as the pressure was applied.

It was found that insulation was required between the Christopherson tube and the retaining bracket to which it was attached. Without the insulation, heat was conducted from the Christopherson tube to the bracket, causing the temperature of the Christopherson tube to be too low for the polymer to remain molten. A 3mm thick asbestos plate sandwiched between the Christopherson tube and the bracket cured this problem.

The load readings from the strain gauges on the bull block shaft were not as accurate as was hoped, since an oscillation in the readings was present. The pitch of an oscillation corresponded to one revolution of the bull block.

All efforts were made to alleviate this effect but these were unsuccessful, and consequently, only readings of average drawing load were possible with this apparatus.

4.2 Determination of the Yield Characteristics of the Wire.

Compression tests were conducted on the wires using a Hounsfield Tensometer. Very small samples (1.5 diameters long) were cut from the wire coil and subjected to compression. The platens of the compression tester were lubricated in an attempt to obtain homogeneous compression. Readings of load and extension were obtained at close interval throughout the tests. These readings were converted to true stress and natural strain values knowing the initial length and diameter of the wire and assuming constant volume and no "barrelling" of the sample had occurred during compression. ie:-

$$\text{True Stress } \sigma = \frac{4W}{\pi do^2} \cdot \frac{h}{ho}$$

where W = load

do = original diameter

ho = original height

h = height when load is W

$$\text{Natural Strain } \epsilon = \ln\left(\frac{ho}{h}\right)$$

The results from the compression tests on copper wire were obtained on the basis of several tests and the results

are shown as Fig 20. A number of simple tensile tests showed that the initial yield point of the copper wire was around 100 MNm^{-2}, so an average stress-strain curve was drawn through this point as shown in Fig 20.

The compression tests for 18/8 stainless steel and 60/65 carbon steel produced the curves as shown in Figs 21 and 22 respectively.

The stress-strain characteristics were assumed to take the form:-

$$Y = Yo + K\epsilon^{n}$$

where Yo = initial yield stress

ϵ = natural strain

n = strain index

K = constant

These were shown to be:-

For copper wire - $Y = (1 \times 10^{8}) + (3.41 \times 10^{8})\epsilon^{0.25}$

For 18/8 stainless steel wire -

$$Y = (3.4 \times 10^{8}) + (16.3 \times 10^{8})\epsilon^{0.75}$$

For 60/65 carbon steel wire -

$$Y = (12 \times 10^{8}) + (7.2 \times 10^{8})\epsilon^{0.35}$$

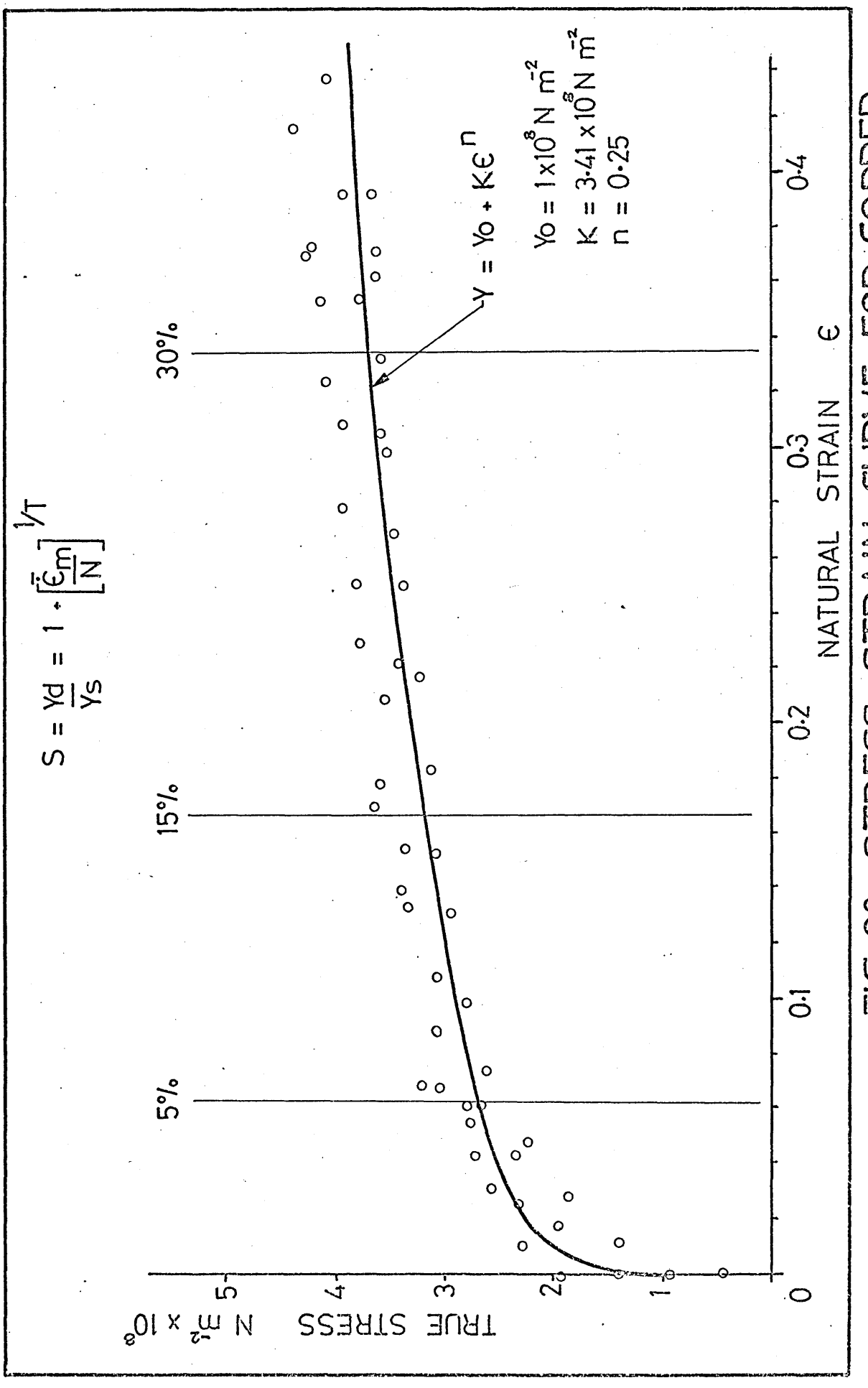

FIG 20 STRESS~STRAIN CURVE FOR COPPER

FIG 21 STRESS~STRAIN CURVE FOR 18/8 STAINLESS

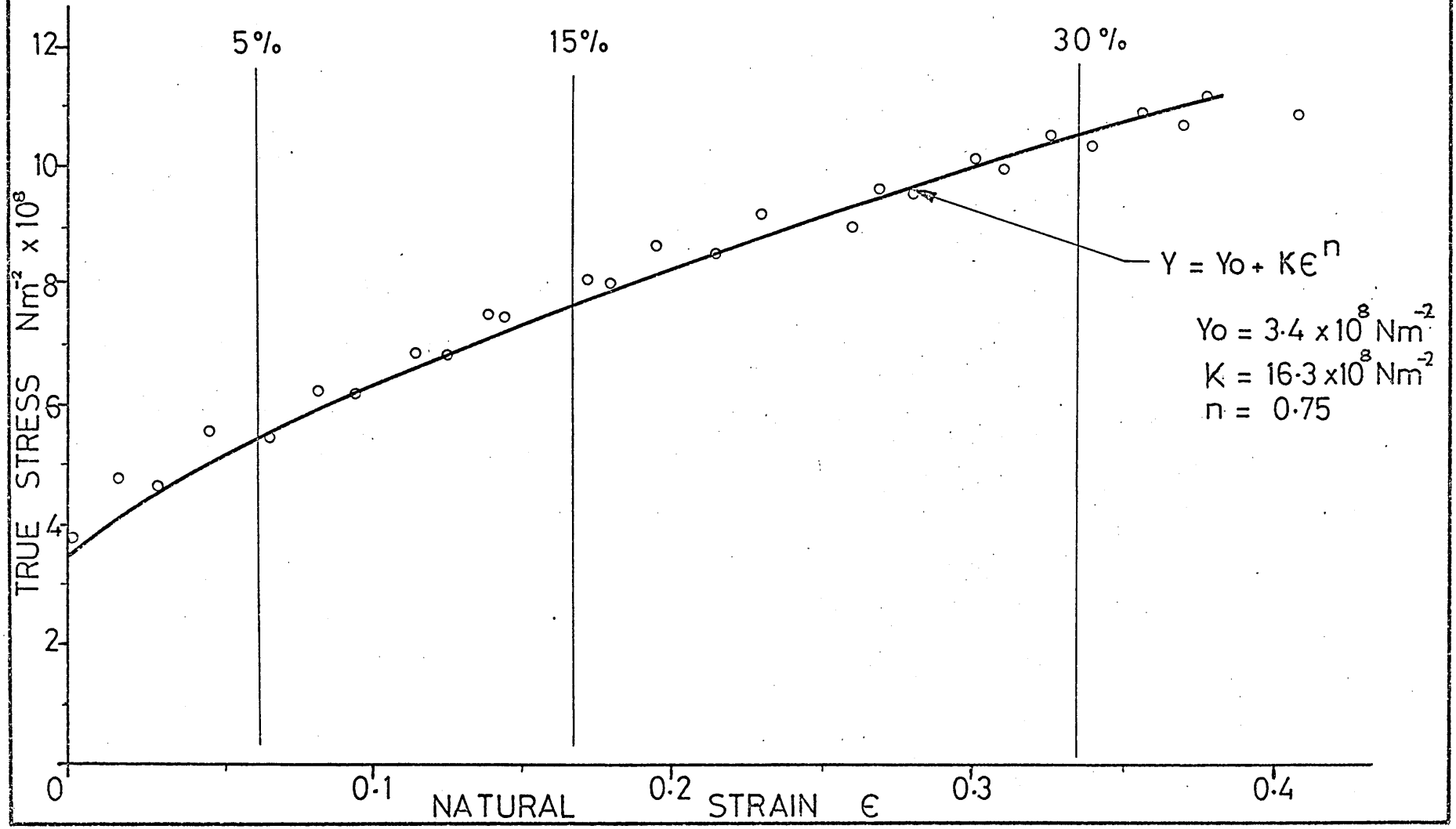

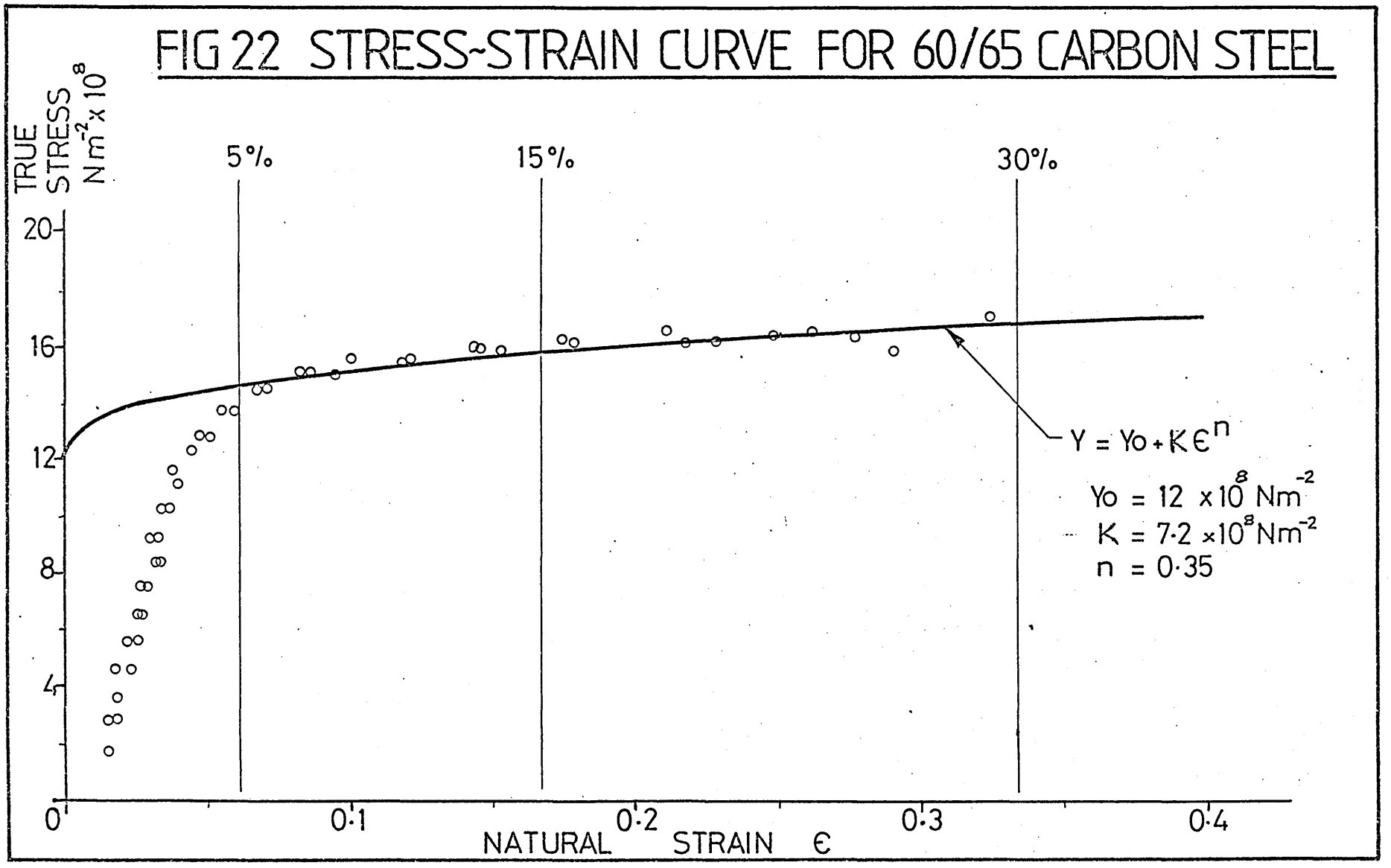
FIG 22 STRESS-STRAIN CURVE FOR 60/65 CARBON STEEL
TRUE STRESS $Nm^{-2} \times 10^8$
5%
15%
30%
20
16
12
8
4
0
0·1
0·2
0·3
0·4
NATURAL STRAIN ϵ
$Y = Yo + K\epsilon^n$
$Yo = 12 \times 10^8 Nm^{-2}$
$K = 7{\cdot}2 \times 10^8 Nm^{-2}$
$n = 0{\cdot}35$

4.3 Result from the Tests.

The results are presented here in graphical form for convenience. The following test conditions may be assumed to be standard unless otherwise stated:-

Christopherson tube length	60mm
Christopherson tube diameter	2mm
Wire diameter	1.62mm
Die angle	12°

The polymer used was Alkathene WVG 23.

4.3.1 Results of Coat Thickness v Drawing Speed.

Fig 23 shows the coat thickness produced on copper wire using a 30% reduction die at varying speeds and temperatures. There was a marked difference between the polymer temperature of 180°C and the other two temperatures. The curves for 135°C and 150°C were not significantly different but varied with respect to the bamboo transitions. At a polymer temperature of 135°C the copper wire fractured at and below 0.37 ms^{-1} but breakage did not occur at the other two temperatures. (The fracture is believed to have been caused by an excessive reduction in cross-sectional area due to the bamboo effect and is discussed later).

Several observations were made from the results of copper:-

a) Bamboo occurred at low drawing speeds
b) Below a certain speed bamboo always occurred and above another, never occurred. Between these two speeds, bamboo occurred randomly (often one run contained both smooth and bamboo coated wire).
c) Hydrodynamic action always occurred (except for start up, when a short length of wire was poorly lubricated until the pressure was sufficient to cause hydrodynamic lubrication, and for the initial run after the Christopherson tube had been cleaned out, when about 2m of wire remained uncoated at start up).
d) Polymer adhesion was better at slower speeds (especially when bamboo was present) and was not improved by higher polymer temperatures.
e) The quality of polymer coating was reduced as drawing speed was increased.
f) When bamboo occurred, mechanical vibrations from the machine were noticed.

Fig 24 shows the coat thickness produced on 60/65 carbon steel wire when using a 30% reduction die at varying speeds and temperatures. These results show the same general trends as those for copper wire although the various conditions were not as well defined, with the graphs produced being less uniform (coat thicknesses at 135°C were almost random). (Coat thicknesses were much lower than those on copper at all speeds and bamboo was generally more severe.) Wire breakage occurred

at all temperatures (0.76 ms^{-1} at 135°C, 0.92 ms^{-1} at 150°C and 0.36 ms^{-1} at 180°C).

At low temperatures, hydrodynamic lubrication did not always occur for steel wire. The higher polymer temperatures improved this. It was noted that for steel wire, the lower the temperature, the greater the speed at which bamboo ceased to exist.

Fig 25 shows the coat thickness produced on copper wire for various wire reductions at 150°C and varying speeds. It can be seen that a 5% reduction die gave greater thicknesses than the other two reductions at very low speeds, but the differential was reduced as the speed was increased. A 30% reduction die gave marginally greater coat thicknesses at speeds above about 1 ms^{-1}. The bamboo transitions were shorter and bamboo ceased to exist at lower speeds for smaller wire reductions. A qualitative assessment of coat quality and adhesion showed that quality was improved with smaller reductions but adhesion was not affected by reduction.

Fig 26 shows the coat thickness obtained on 18/8 stainless steel for different wire reductions at a constant temperature of 150°C for varying speeds. The general trends were the same as those for copper and carbon steel with coat thicknesses between the two. At very low speeds, the 5% reduction die gave much greater thicknesses than the higher reductions, but as the speed was increased, the die size made little difference. The adhesion was improved with a greater wire reduction but the coat quality remained unaffected by the die size.

Fig 27 and Plates 10, 11 and 12 give an illustration of the bamboo defect which occurred at the lower drawing speeds. Note that the wire itself was deformed where bamboo had occurred.

4.3.2 Results of Pressure and Load.

Fig 28 shows the pressures measured in the Christopherson tube for copper using a 30% reduction die at a polymer temperature of 150°C.

The number on each curve refers to the position of the pressure transducer in the Christopherson tube (see Fig 15). The curves show that pressure was essentially constant at high speeds, but at very low speeds (below about 0.3 ms^{-1}) the pressure increased as speed was reduced for position 1, 2 and 3, but pressure at position 4 reduced (close to the die).

Fig 29 shows the same curves for copper using a 5% reduction die. Similar values were obtained, but the "dip" in the curve was more pronounced.

Fig 30 gives pressure curves for 18/8 stainless steel at a polymer temperature of 150°C. The rise in pressure as speed was reduced is clearly shown, pressures at low speeds being around two times greater than the average pressure at higher speeds. The pressure at position 4 in this case follows the trends as in the other positions.

Fig 31 shows the same curves for 18/8 stainless steel using a 5% reduction die. Similar overall values were obtained, although the pressure at low speeds was not as high

as that obtained using a 30% reduction die.

Fig 32 shows the drawing load measured for all materials at varying speeds and wire reductions and at a constant temperature of 150°C. The drawing load was greater at low speeds and reduced in a similar manner to the pressure curves as the speed was increased. The curves for 60/65 carbon steel and 18/8 stainless steel at 30% reduction were of the same order. A 5% reduction die gave lower drawing loads for 18/8 stainless steel but for copper wire the die size seemed to make little difference to load. These trends follow directly those of the pressure in the Christopherson tube.

4.3.3 Miscellaneous Results.

A number of runs were cut short by deliberately severing the wire between the die and the bull block. The wire was then pulled out backwards through the die and closely inspected to investigate the deformation in the die. Fig 33 shows the experimental readings taken compared to an assumed die profile. The figure clearly shows that deformation occurred well before the die and did not follow the shape of the die itself. Close correlation was achieved between the assumed die profile and the points obtained experimentally.

The inclusion of pressure feed to the Christopherson tube had the effect of reducing the uncoated length of wire at start up. Figs 34a and 34b show the traces obtained from the UV recorder of pressure in the seal area both with and

without the pressure assisted feed. The effect was to increase the starting pressure, so reducing the time required to reach full pressure. Fig 34c shows a trace of pressure at start up after cleaning and refilling the Christopherson tube. It is evident that the pressure was not developed until the whole system was full of polymer, and a large amount of wire had been pulled through. Fig 34d shows the system under the same conditions as Fig 34c but with the addition of external pressure. The time required to reach full pressure was greatly reduced, showing the effectiveness of the system.

Fig 35a shows a trace of load as time progressed. It can be seen that the load was constant after about 30 seconds. This is interpreted as the time required to reach temperature stability. Fig 35b shows the hydrodynamic build up, which may be related to the pressure curves, Figs 34. When bamboo was present the traces of load with the time scale greatly expanded, produced a sine wave which had the same pitch as the bamboo and an amplitude of approximately 10% of the load. It is interesting to note that the pressure curves indicate the presence of bamboo, since a fluctuating line was recorded when bamboo was present. This suggests that bamboo was initiated in the Christopherson tube.

Many different types of polymer/wire combinations were tried in the investigations, with varying amounts of success. A summary of the results is included here:-

Polypropylene; Coat thicknesses were almost random. Required temperatures above 250°C to obtain a coat, since the polymer was not fluid enough below this temperature to allow flow to take place. Wire fracture occurred

at and below a greater drawing speed than for WVG 23. Generally the coat on the wire was good but adhesion was poor.

Polyvinylbutyral; A coating was very difficult to obtain. A coat could be achieved at very low speeds, but bamboo was very severe. Adhesion was excellent.

Nylon; The melt temperature of the polymer was too high for the equipment (the highest temperature possible for the rig was 260°C).

Rigidex; Again a coating was difficult to obtain. The wire continually fractured due to high viscous drag in the Christopherson tube.

Polystyrene; Same comments as Rigidex.

Diakon; Same comments as Rigidex.

From the above statements it is clear that only certain polymers are applicable under the conditions and geometry used. The main problem was one of wire fracture due to high viscous drag in the Christopherson tube. (The drawing force was higher than the strength of the wire). A further common problem was the deterioration of the polymer at high temperatures and a nauseating smell given off by some of the polymers as they deteriorated.

Steel wire was used with polyvinylbutyral, but the results were not encouraging. The carbide die pellet became subjected to undue stress, causing it to fracture.

A full discussion of the results is presented in Chapter 8.

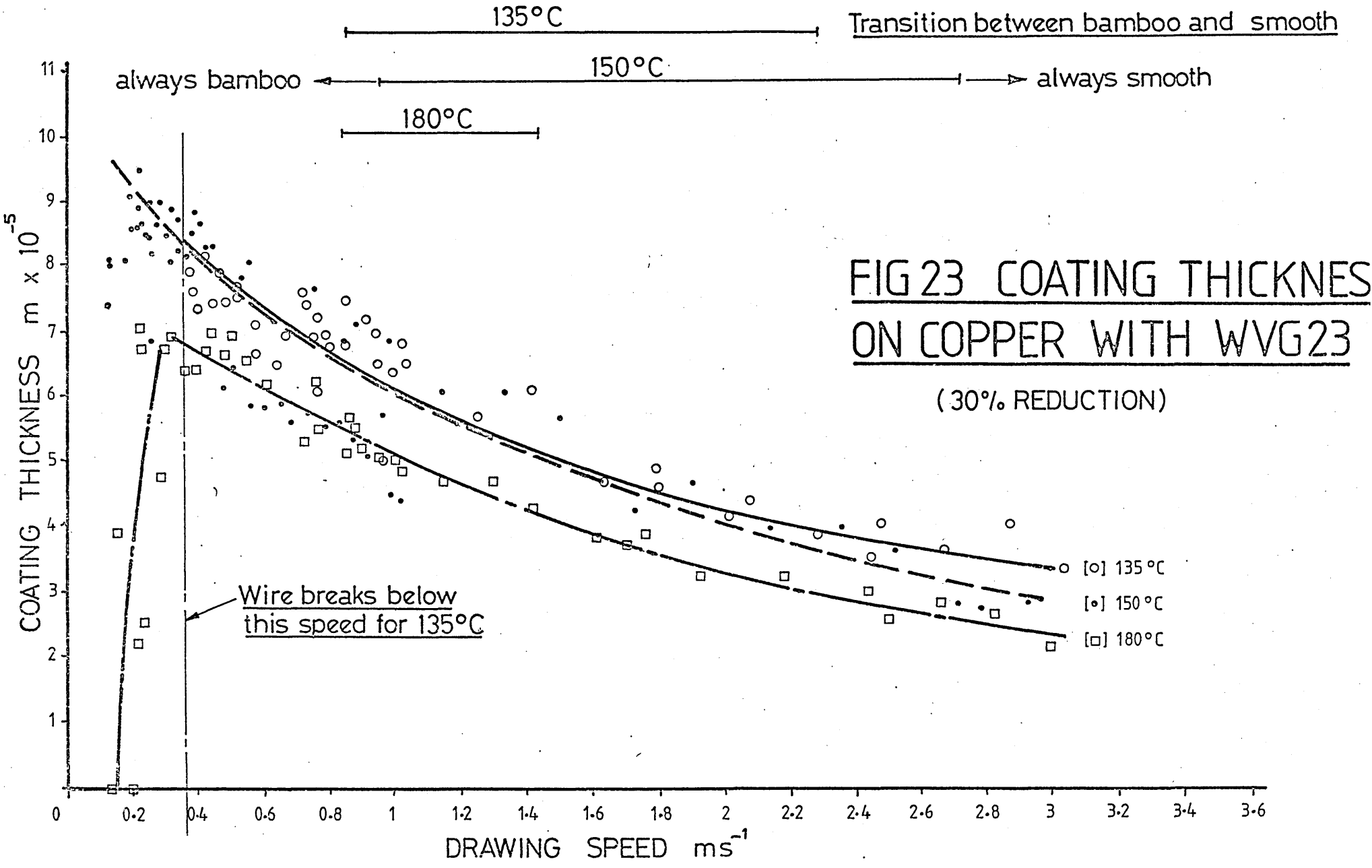

FIG 23 COATING THICKNESS ON COPPER WITH WVG23

(30% REDUCTION)

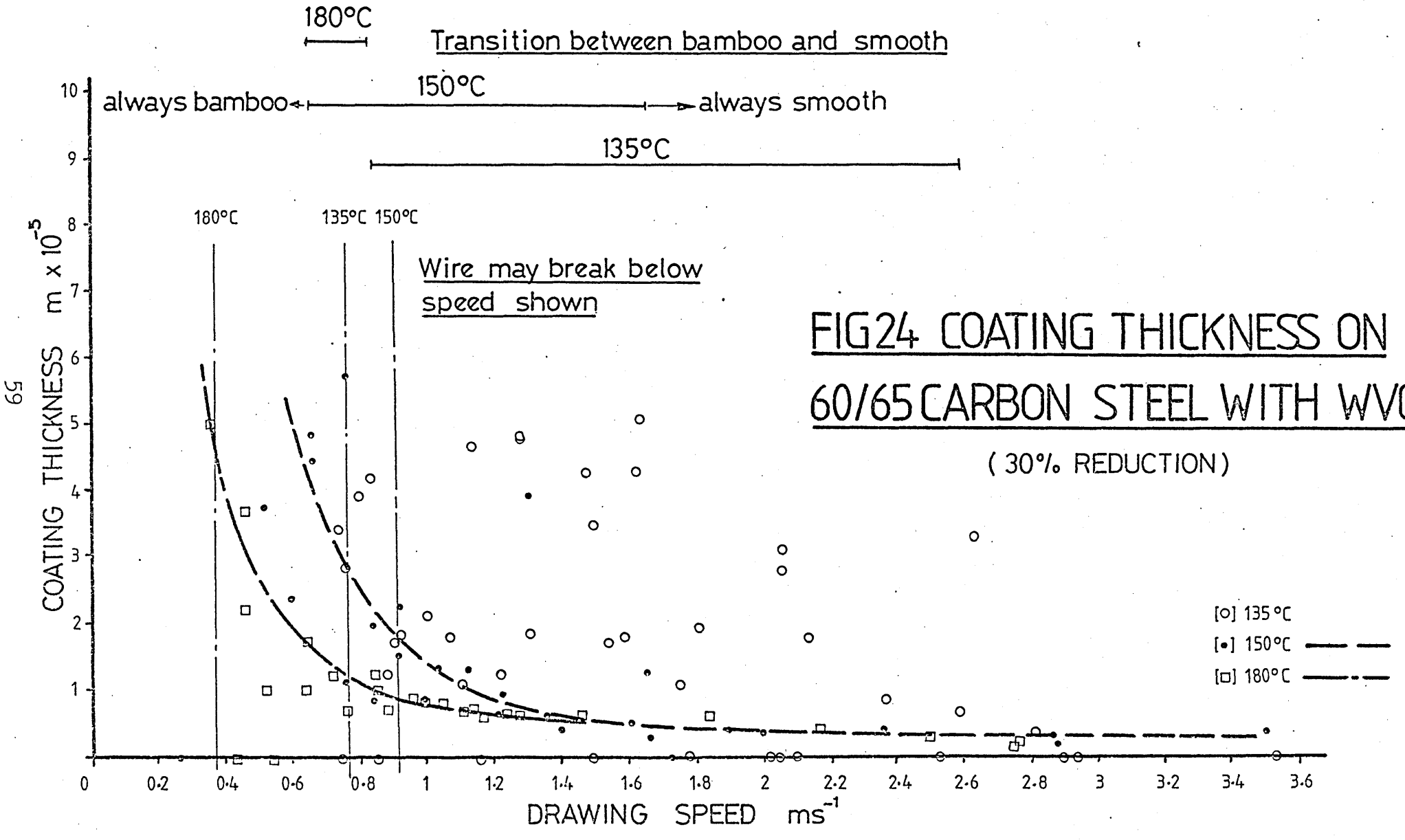

FIG24 COATING THICKNESS ON 60/65 CARBON STEEL WITH WVG

(30% REDUCTION)

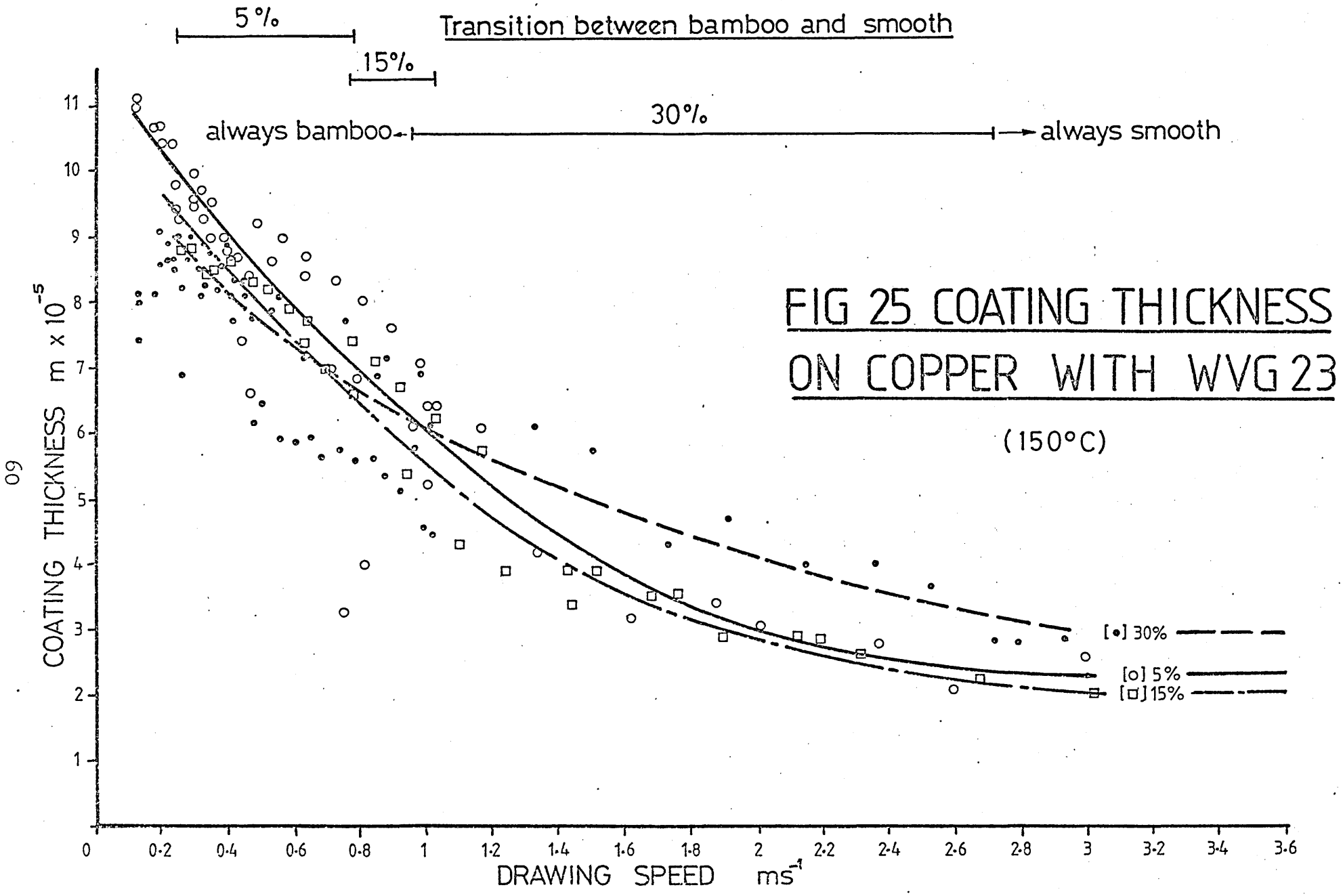

FIG 25 COATING THICKNESS ON COPPER WITH WVG 23

(150°C)

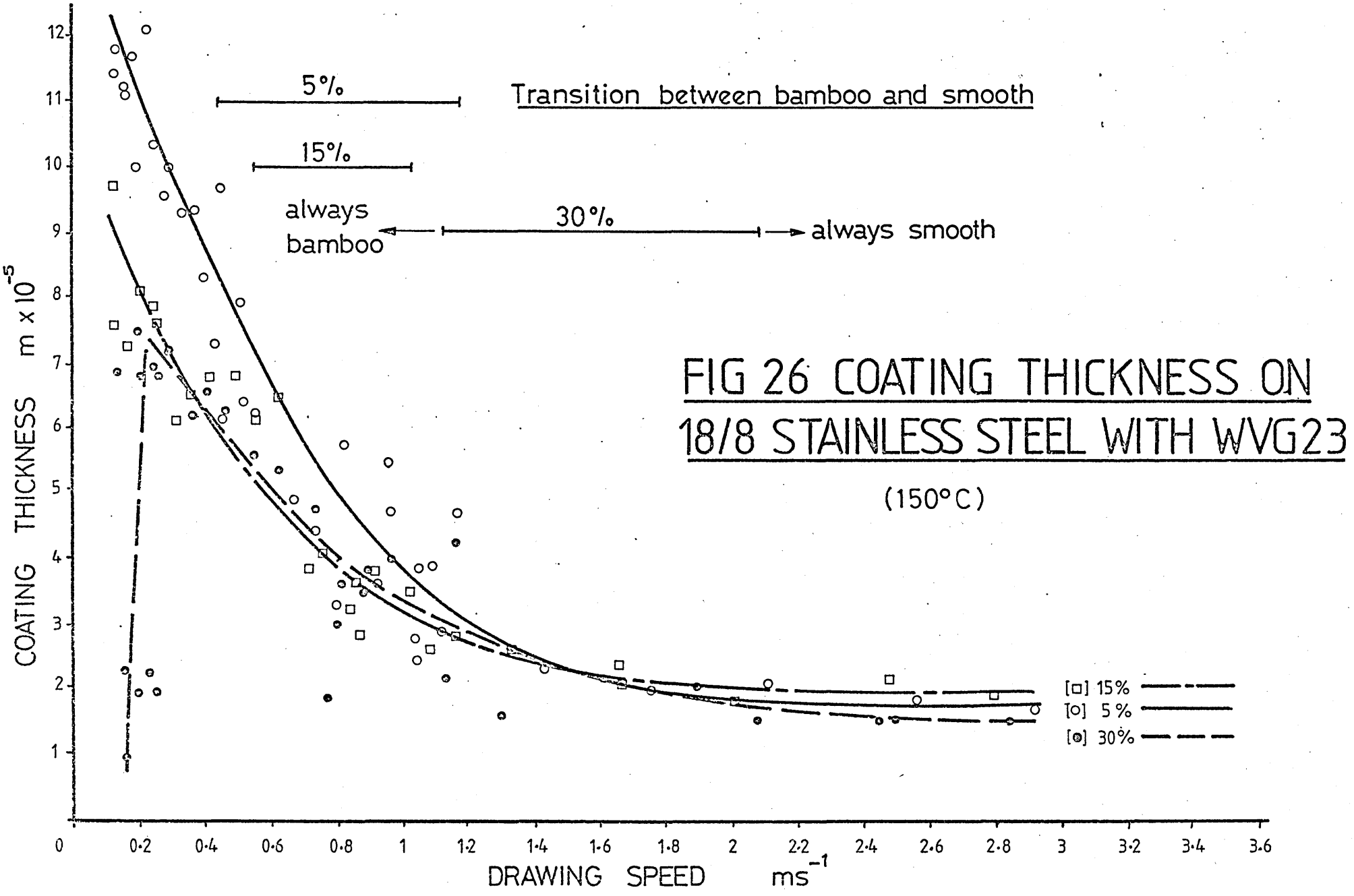

FIG 26 COATING THICKNESS ON 18/8 STAINLESS STEEL WITH WVG23

(150°C)

FIG 27 DIAGRAMMATICAL REPRESENTATION OF BAMBOO

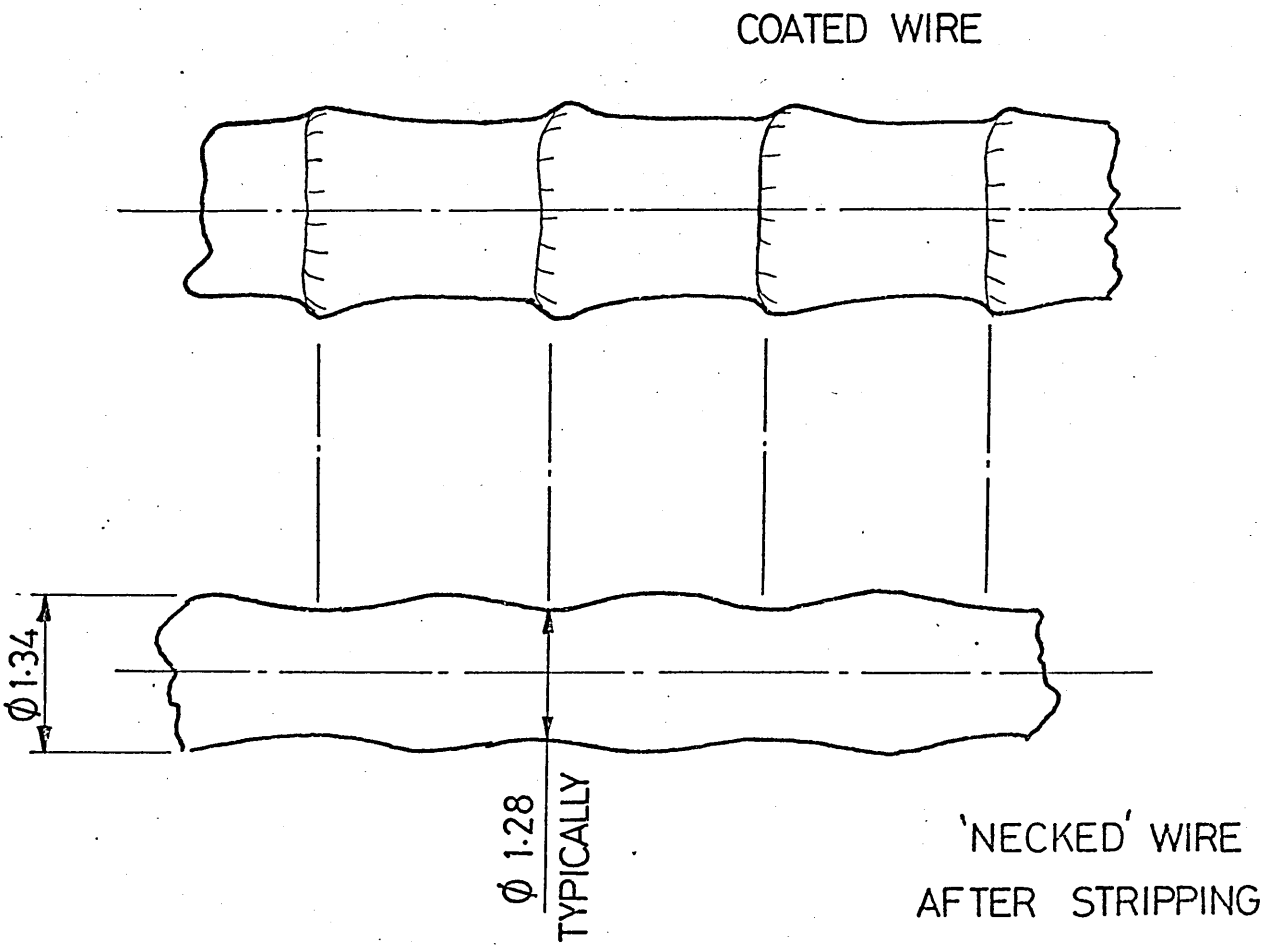

(DIE~1·34 DIA)

PLATE 10 SAMPLE OP COPPER WIRE SHOWING BAMBOO AND NECKING (**0.302** ms”1, 30%, **1**50°Ce Coat thickness **0**.083mm)

PLATE 11 (COPPER, 0.4 ms"1, 150°C Coat thickness 0.09mm

PLATE 12 (1**8/8** 0.41 ms***1 5 30**/, 150°C Coat thickness **0 0 66**mm

FIG 28 PRESSURE DISTRIBUTIONS FOR COPPER ~ 30% REDUCTION, 150°C

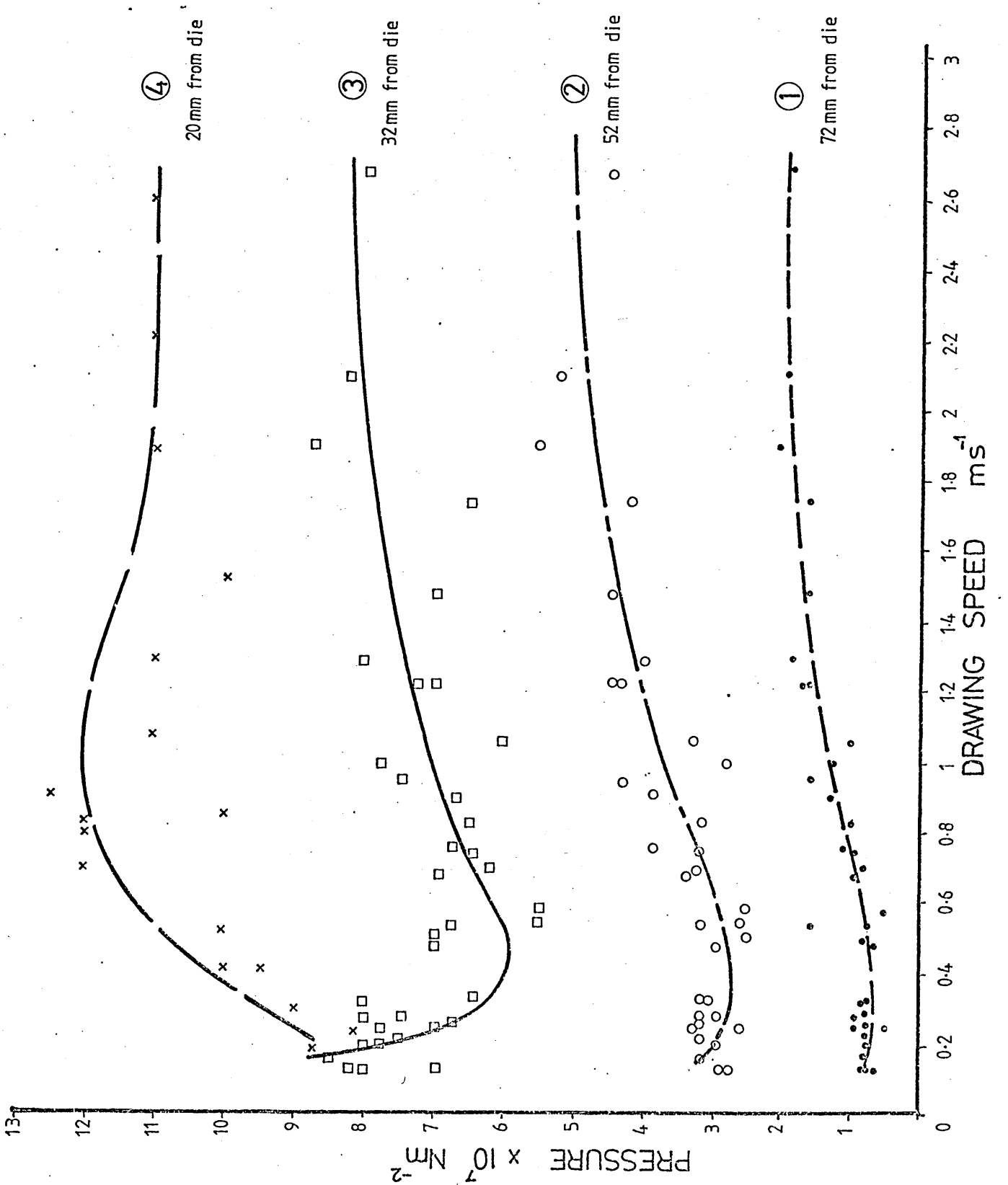

FIG 29 PRESSURE DISTRIBUTIONS FOR COPPER ~ 5% REDUCTION, 150°C

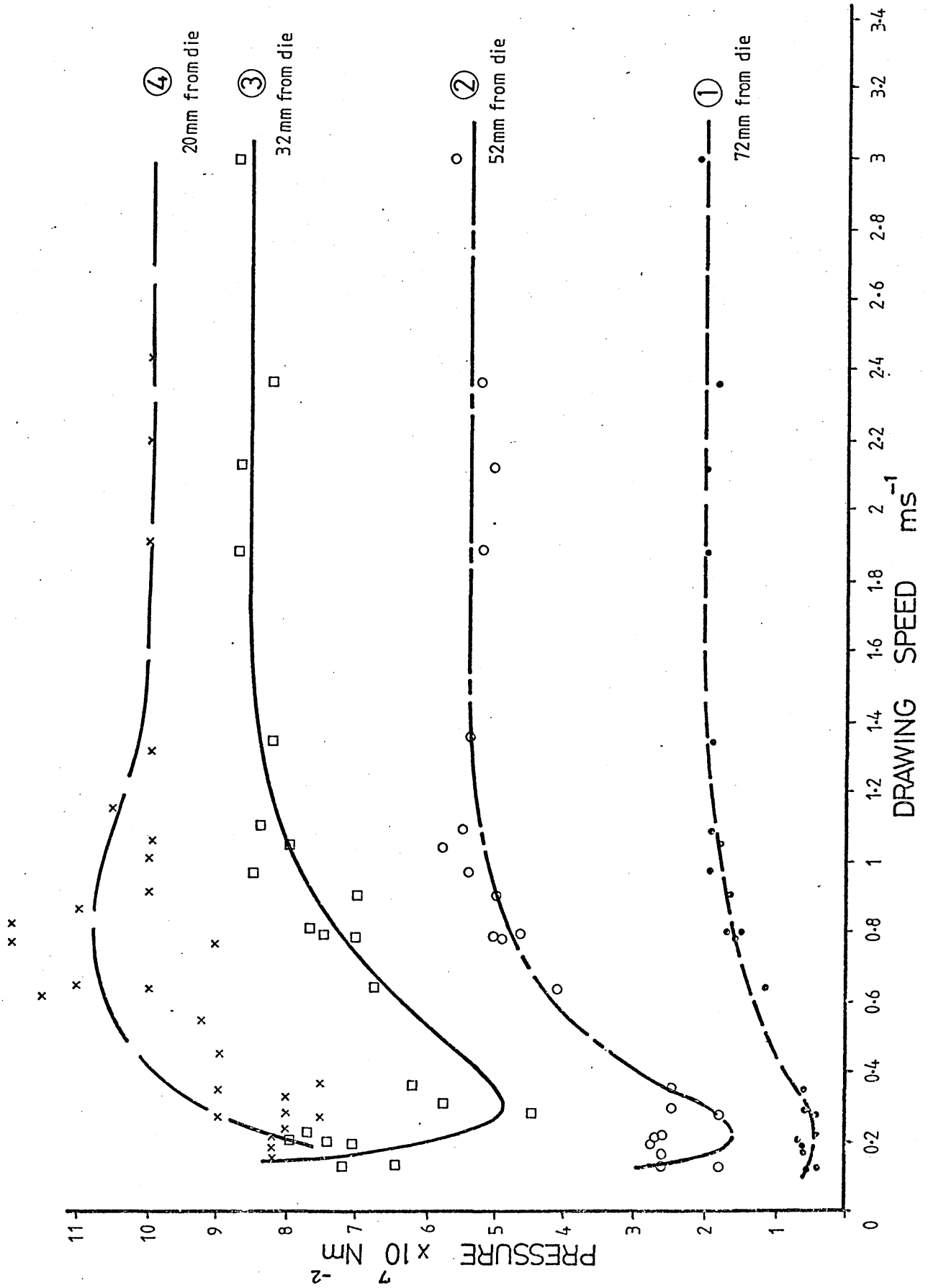

FIG 30 PRESSURE DISTRIBUTIONS FOR 18/8 ~ 30% REDUCTION, 150°C

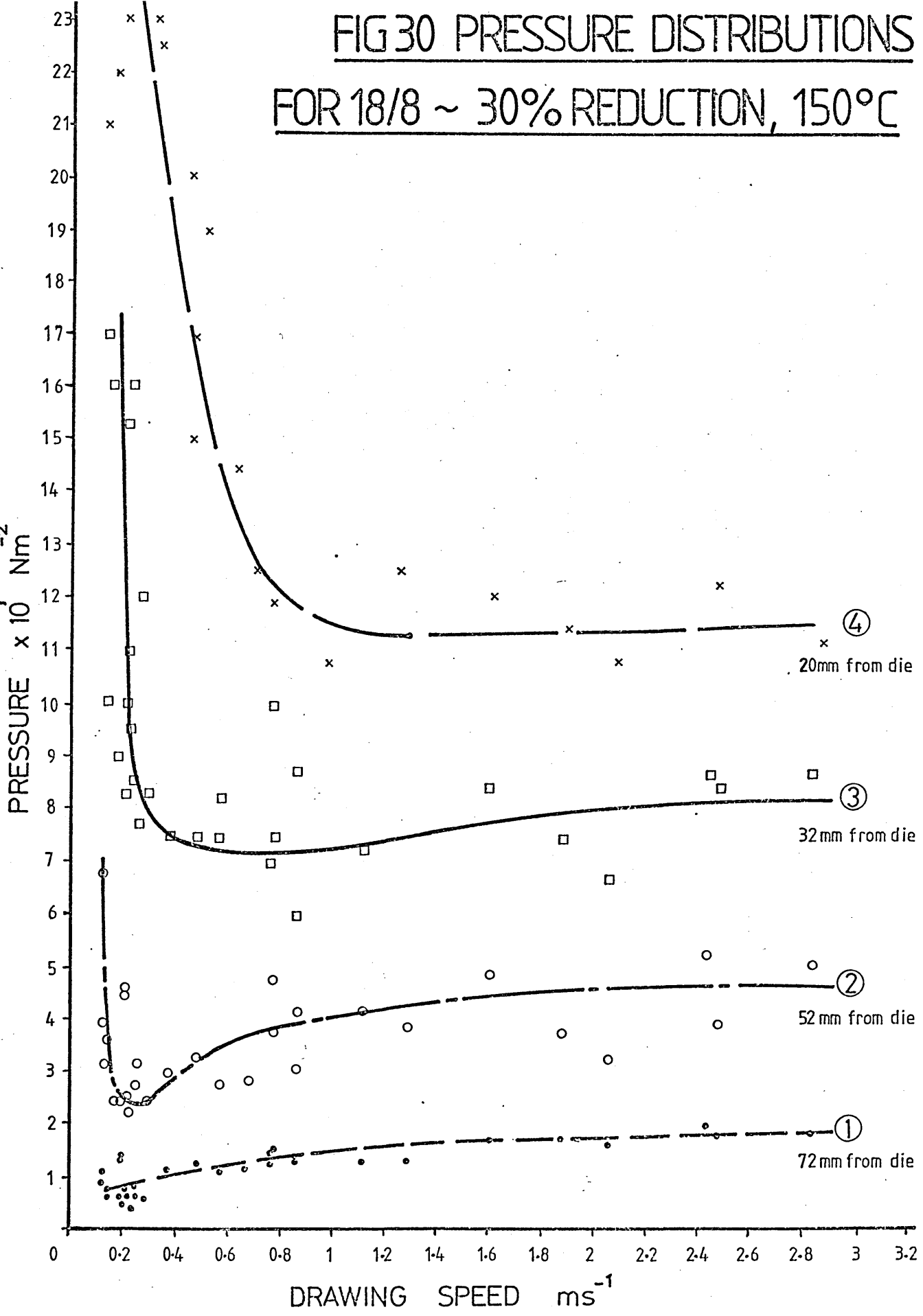

FIG 31 PRESSURE DISTRIBUTIONS FOR 18/8 ~ 5% REDUCTION, 150°C

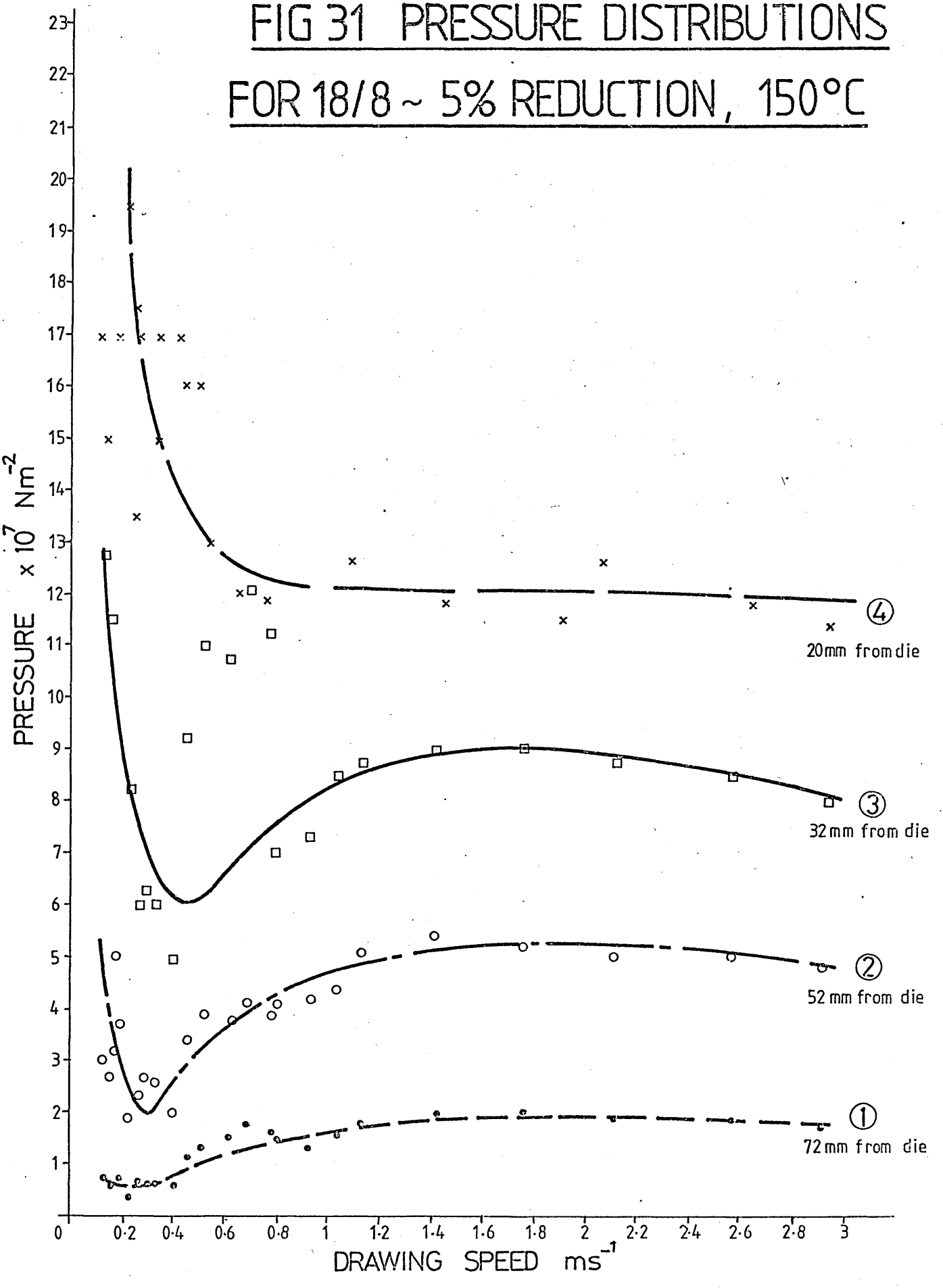

FIG 32 DRAWING LOADS

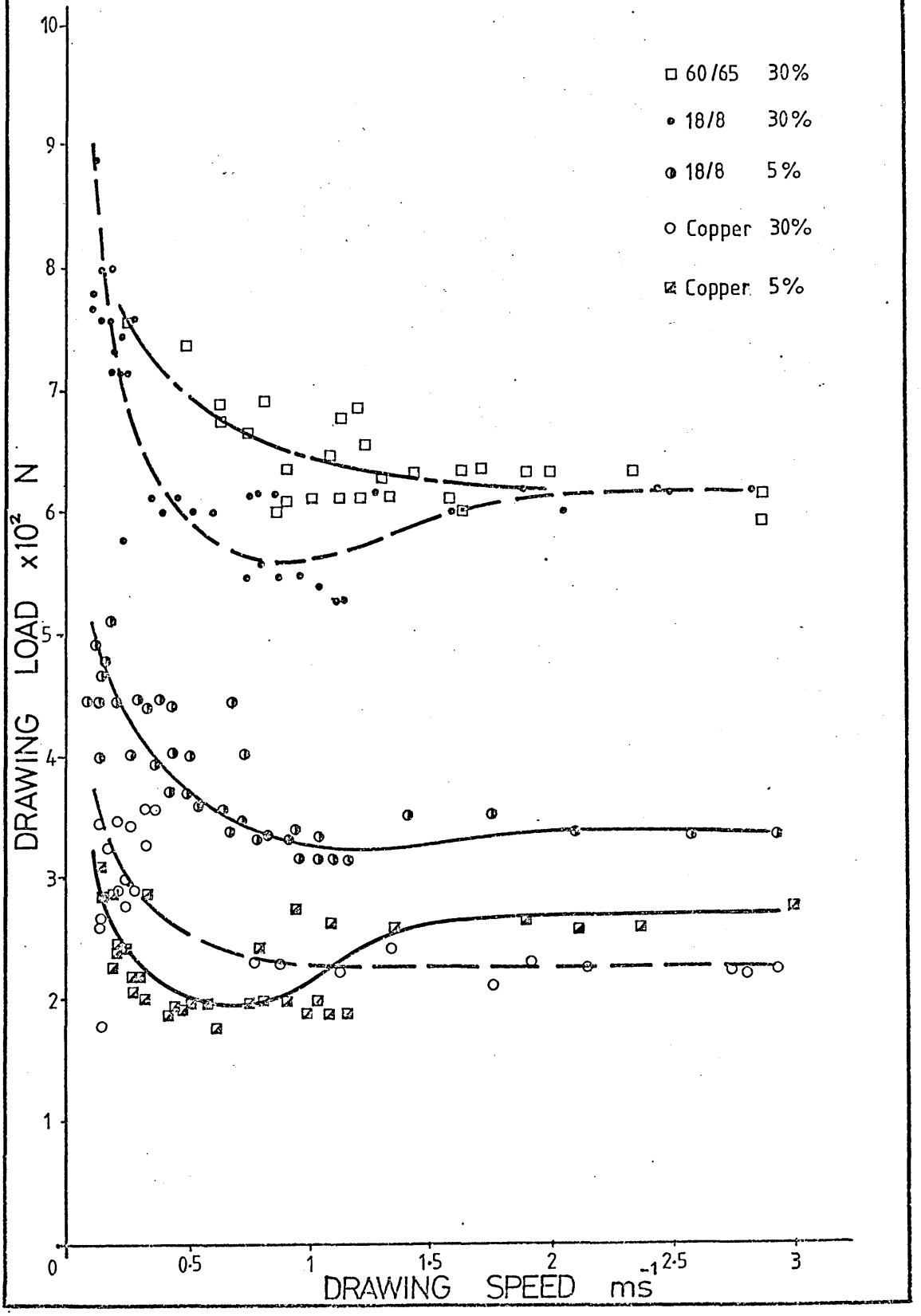

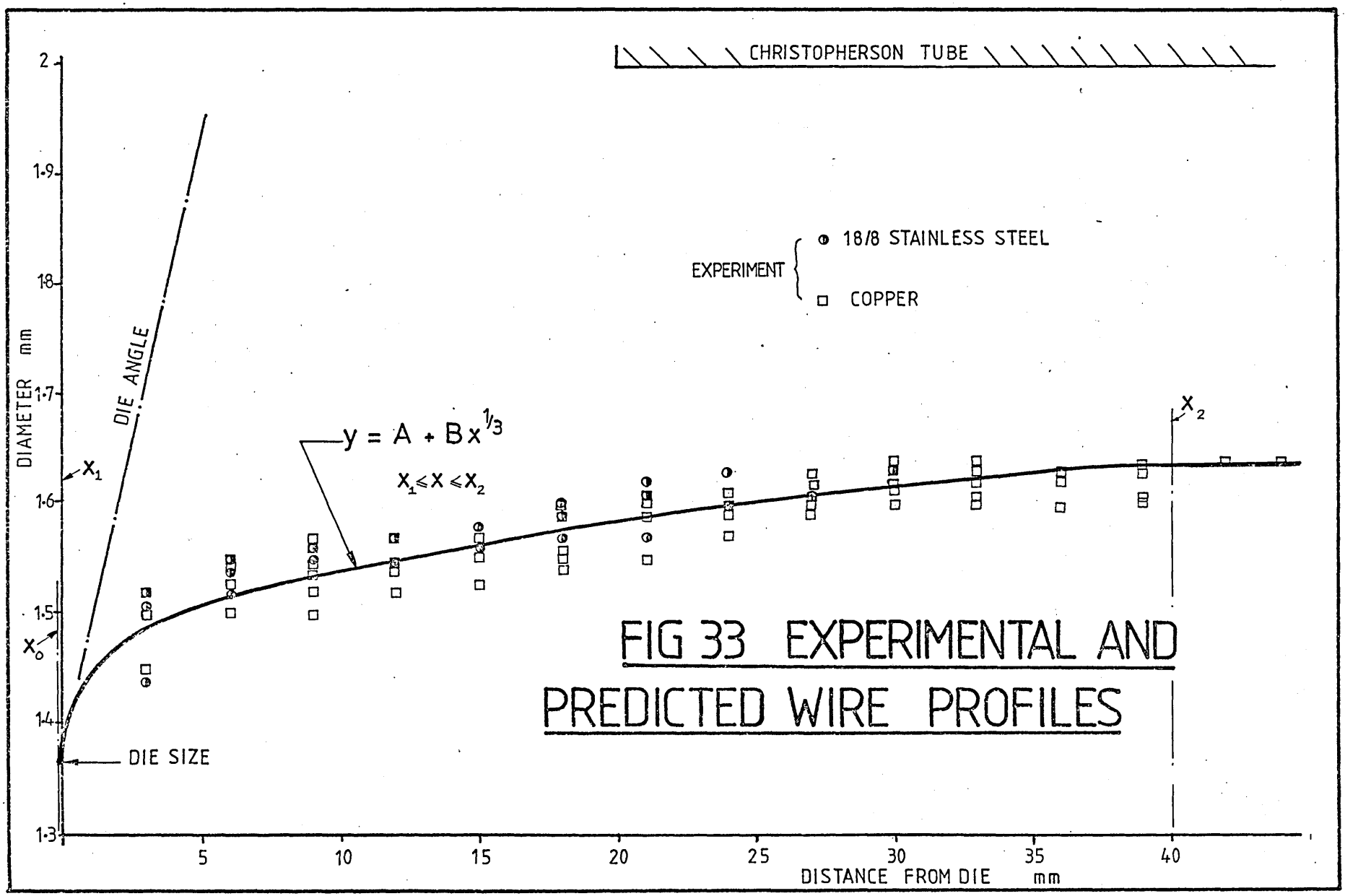

FIG 33 EXPERIMENTAL AND PREDICTED WIRE PROFILES

FIG 34a UV TRACE WITH HYDROSTATIC PRESSURE

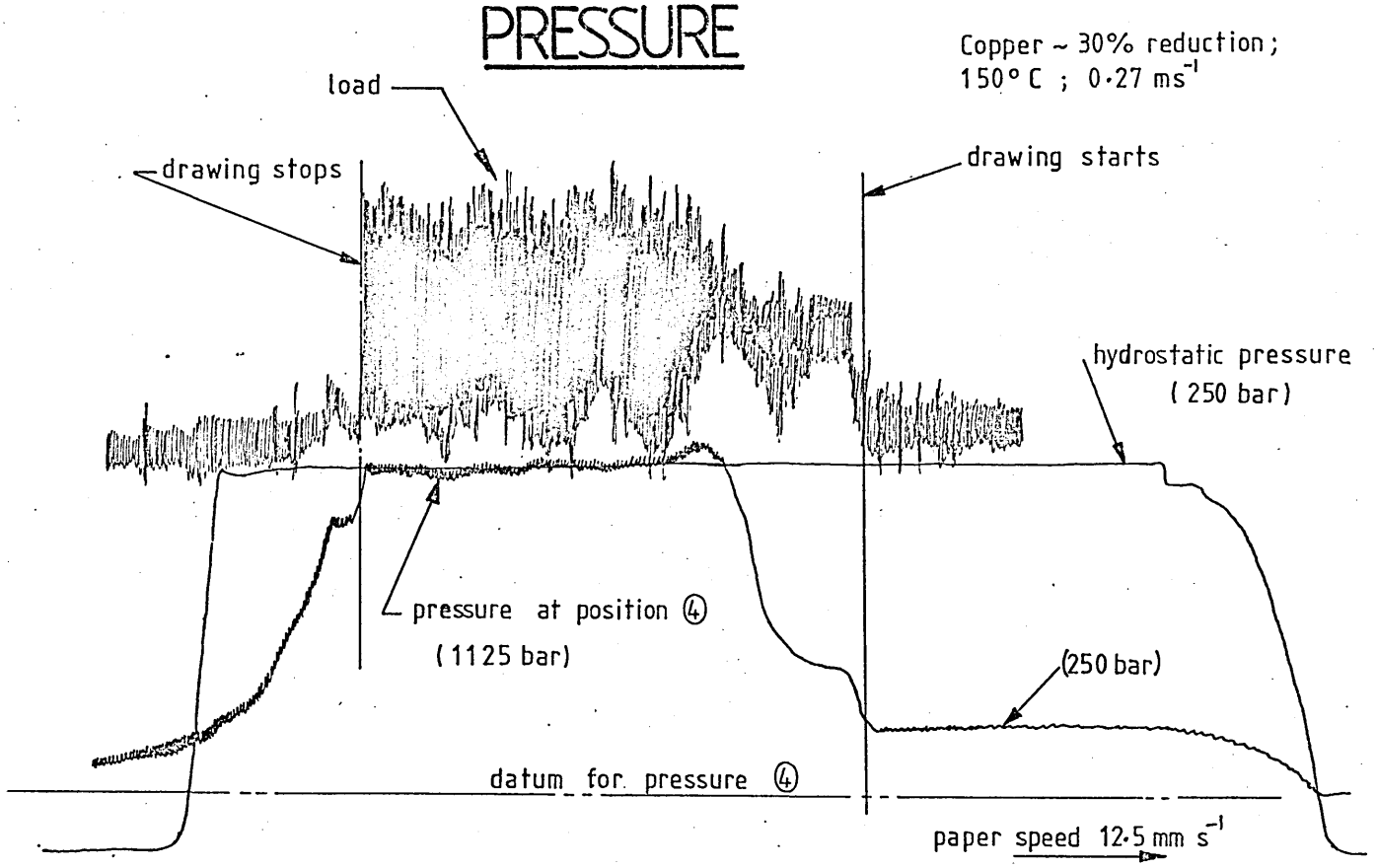

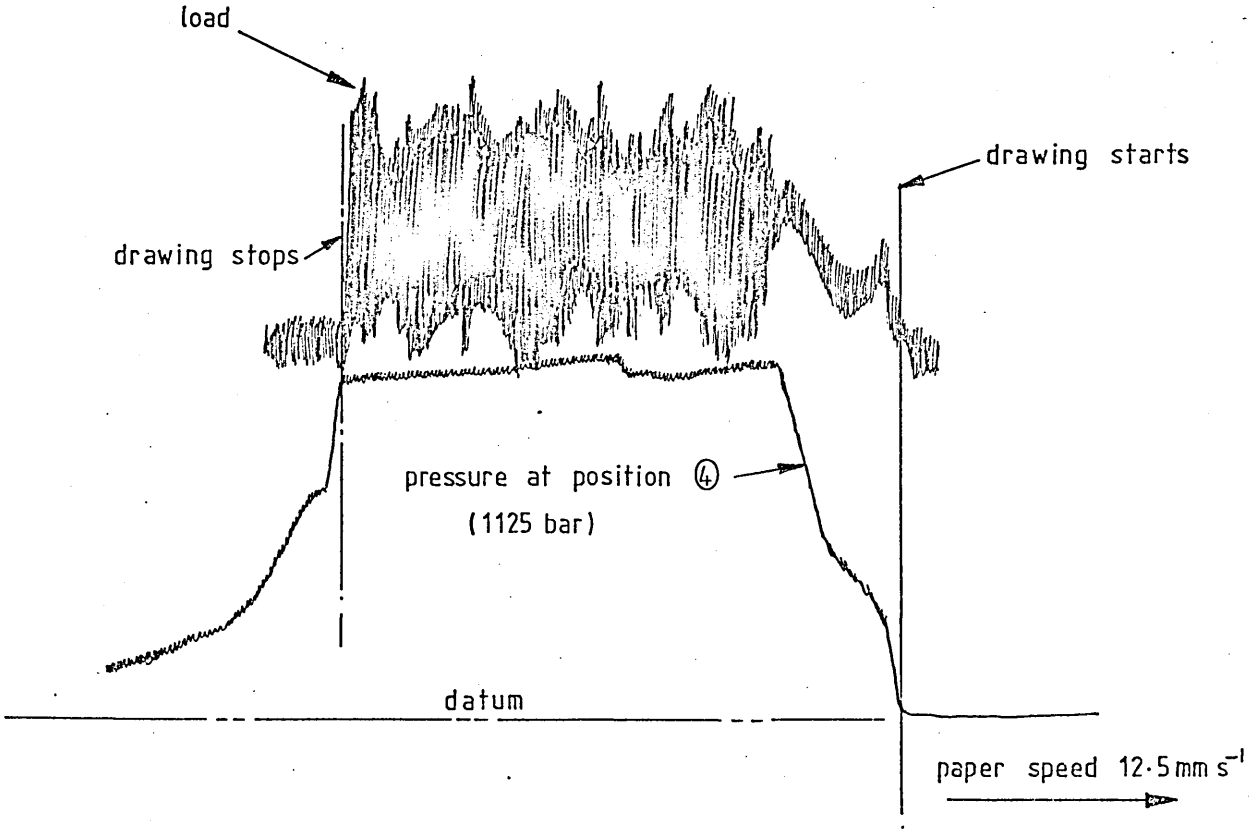

FIG 34b UV TRACE WITHOUT HYDROSTATIC PRESSURE

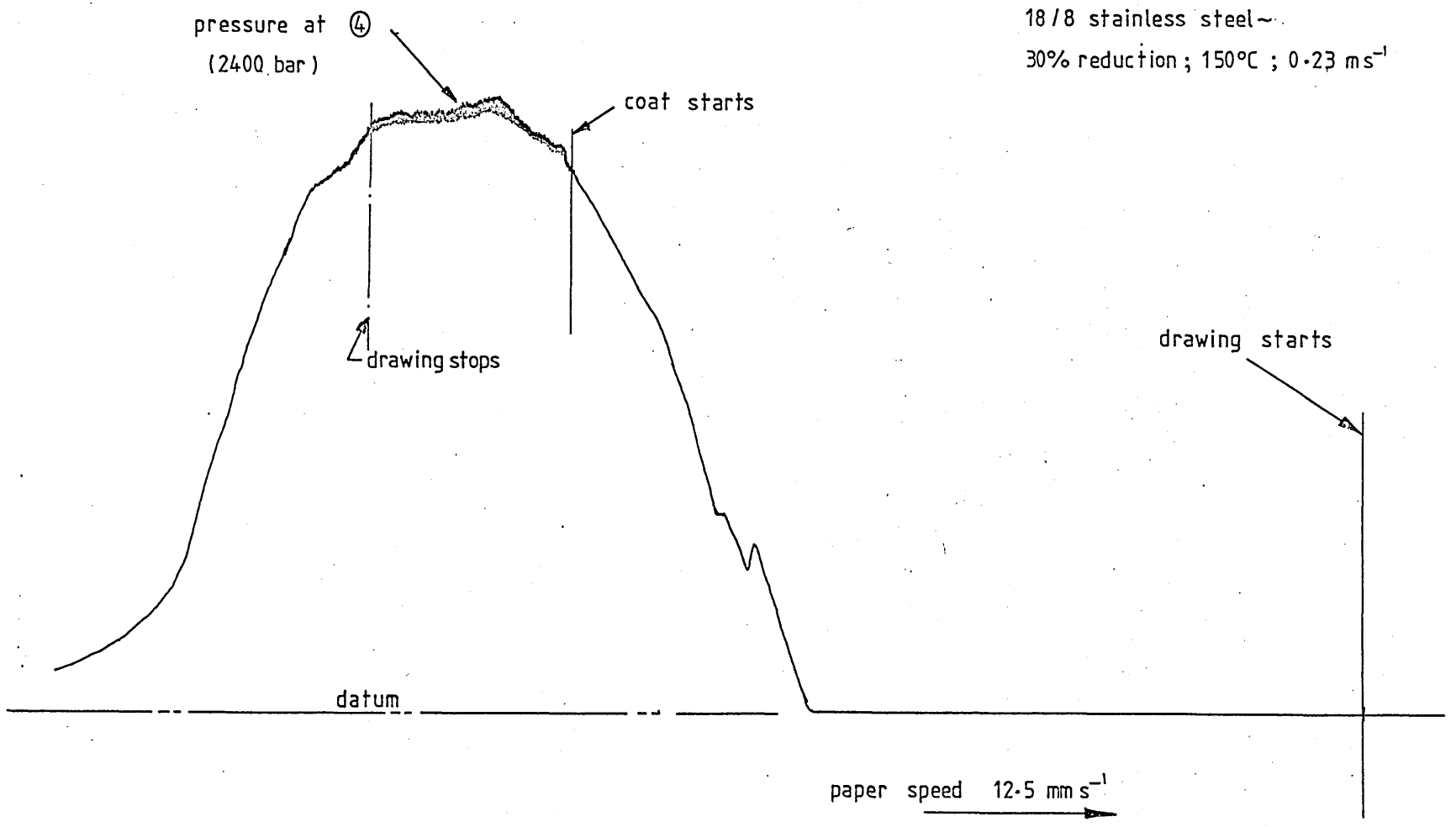

FIG 34c UV TRACE OF PRESSURE FOR INITIAL RUN ~ NO HYDROSTATIC PRESSURE

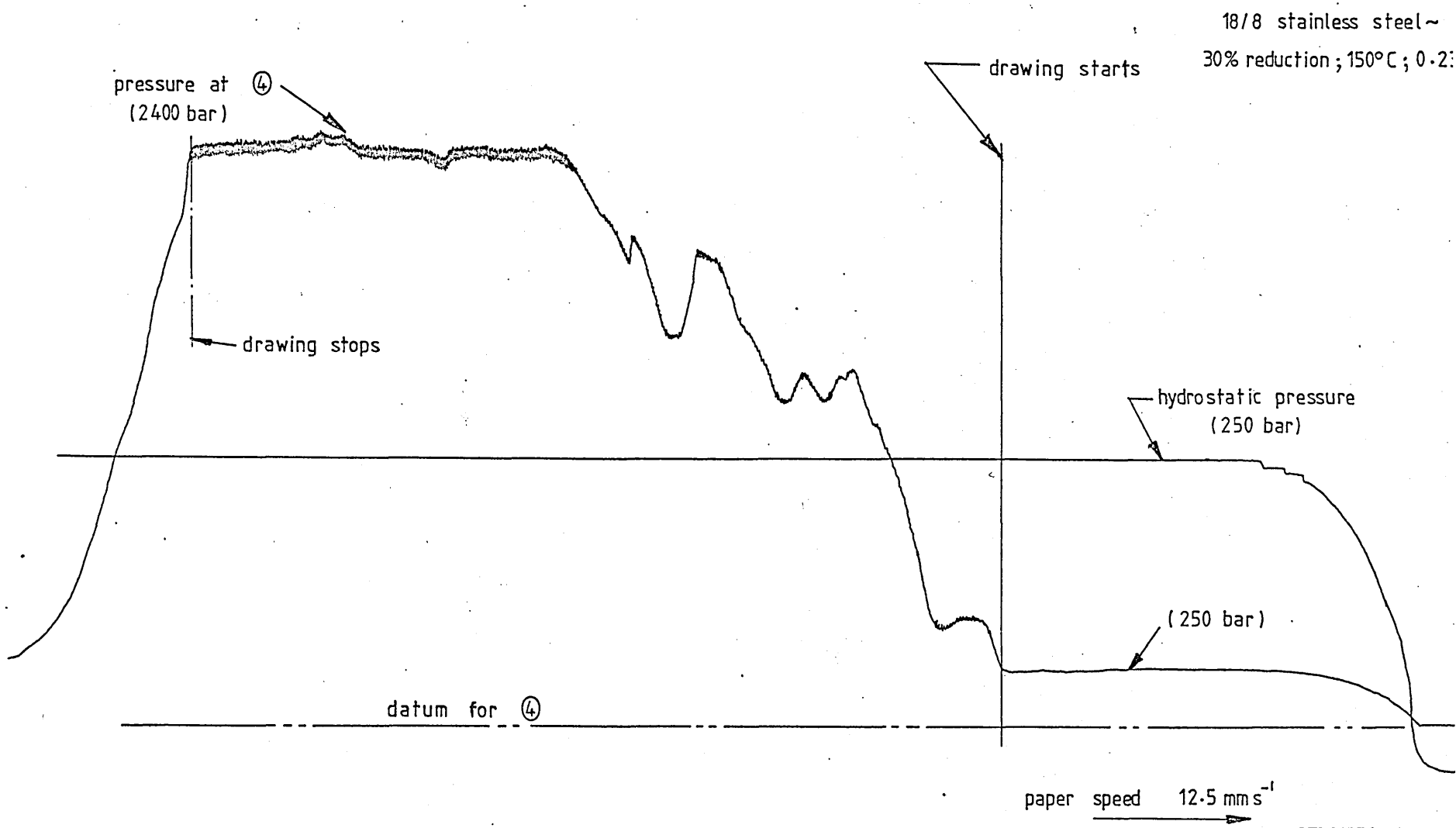

FIG 34d UV TRACE OF PRESSURE FOR INITIAL RUN WITH HYDROSTATIC PRESSURE

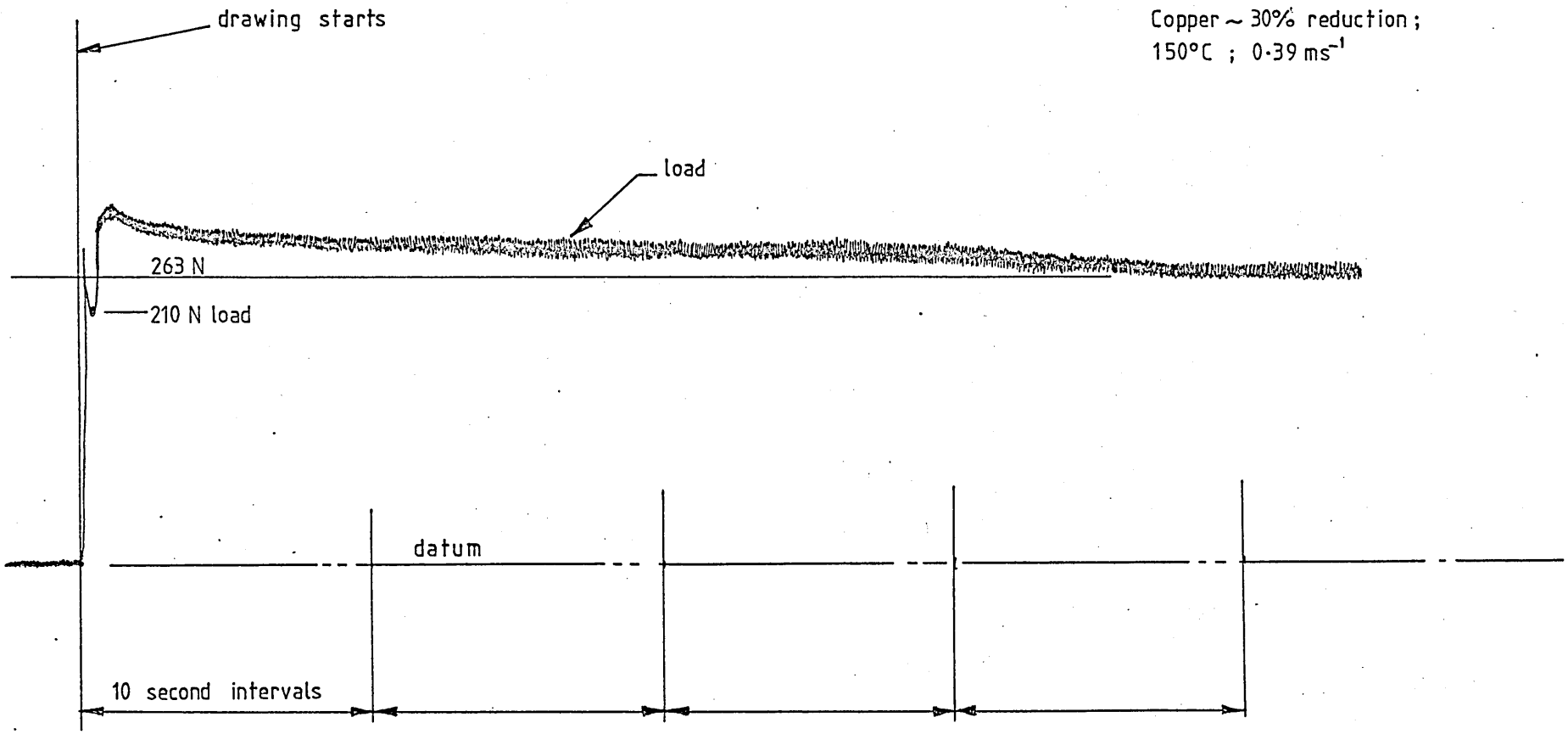

FIG 35a UV TRACE OF LOAD

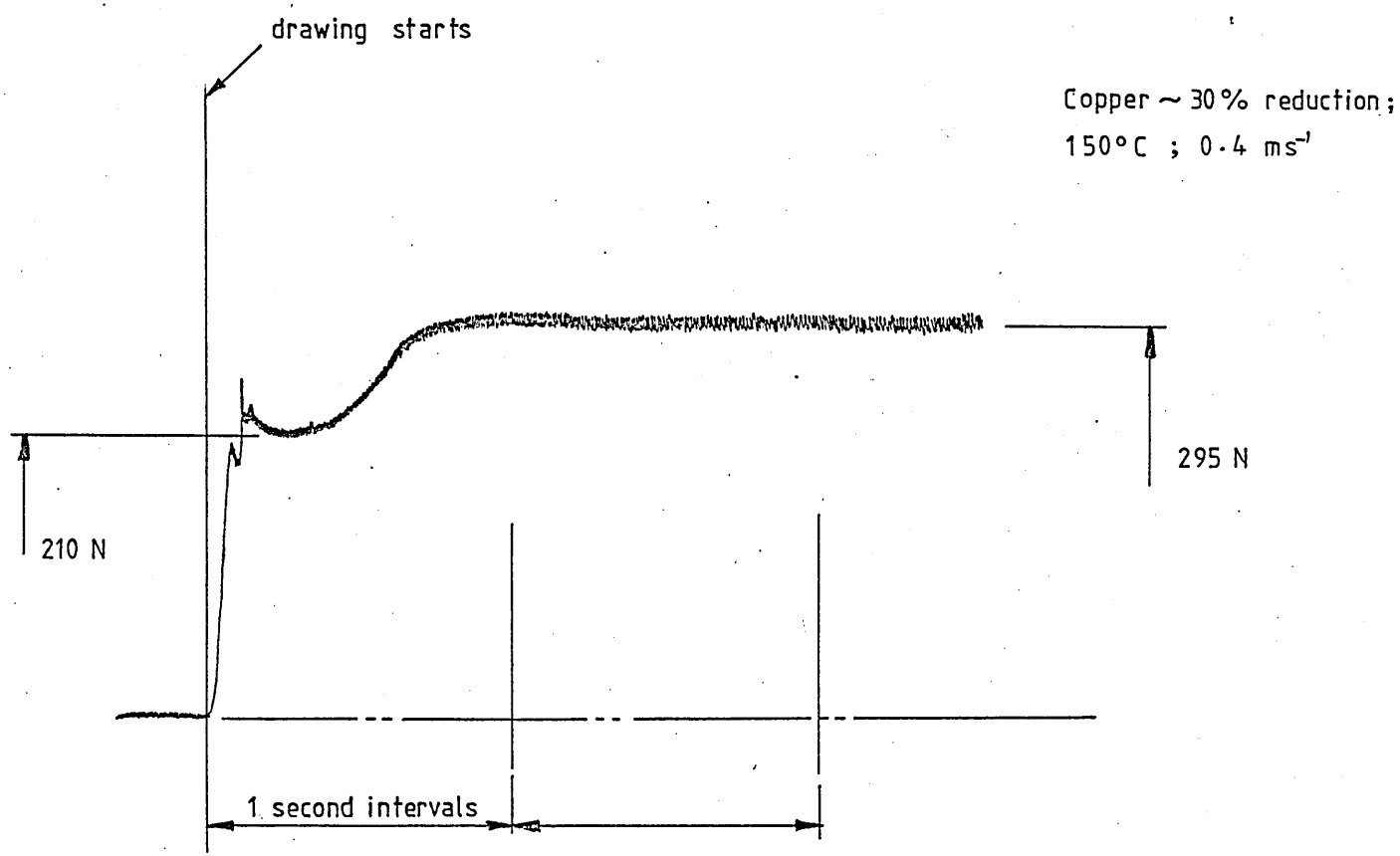

FIG 35b UV TRACE OF LOAD AT START UP

CHAPTER 5. ANALYSIS OF THE PROCESS.

This chapter examines previous theories as applied to the Christopherson tube/die unit with regards to their shortcomings and advantages. A critical survey is also made of the small amount of work which has previously been carried out on polymer melt lubrication.

The present study utilises an empirical expression relating shear stress and rate of shear with an experimentally derived pressure coefficient of viscosity, in determining the coating thickness possible on the wire. The theory contains the effect of a limiting value to the shear stress which exhibits itself as slip in the polymer. On the basis of experimental evidence, it is apparent that deformation commences before the wire reaches the die, in the Christopherson tube itself, with the die effectively acting only as a seal. Under these conditions, the die geometry becomes of secondary importance and the deformation actually takes place as if an effective die of continuously changing die angle is being used. To take this aspect of the process into account, a mathematically described effective die shape is used in the present analysis. The plastic strain hardening properties and strain rate sensitivity of the wire material are also incorporated.

5.1 Critical Review of Previous Analyses.

The Christopherson tube was introduced by Christopherson and Naylor[3] in 1955. In their analysis they could obtain the expressions for the drag and pressure in the tube in terms of the geometrical constants of the tube, provided that the flow rate of lubricant was known. They used in their analysis a parameter which described the eccentricity of the wire in the tube, the validity of which has been questioned[26, 27]. The familiar Reynolds equation was used as a basis of this work. Later work carried out by Tattersall[26] improved upon Christopherson and Naylor's work by examining the tube in three zones; (i) the parallel portion of the tube, (ii) the entry to the die and (iii) the deformation area. His work also used Reynolds equation as a basis and assumed that the viscosity of oil increased in an exponential manner with increasing pressure. His work also included the use of soap as a lubricant. He noted that the rheology of soap at high shear rates and at high pressures was little known, and used his experimental results to obtain a graph of viscosity versus wire speed.

The next work to be published (although it appears to have preceded Tattersall's work) was that of Osterle and Dixon[27]. Their work included the effects of temperature variation in the tube, but assumed that the wire deformation followed the shape of the die, which does not occur for hydrodynamic lubrication. Chu[28] used Tattersall's equations and solved them using computer techniques to develop design graphs for nozzles.

More recently, Dowson et al[29] published a more comprehensive analysis for plane strain drawing which could be applied to wire drawing (although the work did not refer to inlet tubes). They defined four regions, namely; (i) Elasto-hydrodynamic inlet region, (ii) Plasto-hydrodynamic inlet region (iii) Plasto-hydrodynamic region in the land and (iv) Elasto-hydrodynamic outlet region. Their work showed that a simple rigid-plastic analysis was quite accurate, ie. the elasto-hydrodynamic inlet region need not be considered.

All of the above analyses used either oil or soap as the lubricant, defining the viscosity either as a constant or by using an empirical pressure-viscosity relationship. All of the above assumed that the fluid was Newtonian in respect to shear stress and strain rates.

The use of a polymer melt as a lubricant in wire drawing was introduced in 1977 by Thompson and Symmons[30]. Their analysis included the effects of temperature variation in the thickness direction but assumed that the melt viscosity was a function of the temperature only and could be treated as a Newtonian fluid using the concept of apparent viscosity. Later work by Symmons, Stevens and Thompson[31] again used the apparent viscosity, but introduced the effect of a critical shear stress and substantiated the theory with a limited amount of experimental results. The most recent addition to these polymer melt analyses is the theory proposed by Stevens[11]. His work also assumed an apparent viscosity determined from the rheological data for the polymer used. The effect of a critical shear stress was included which gave a two stage flow curve - one for sub-critical flow and another

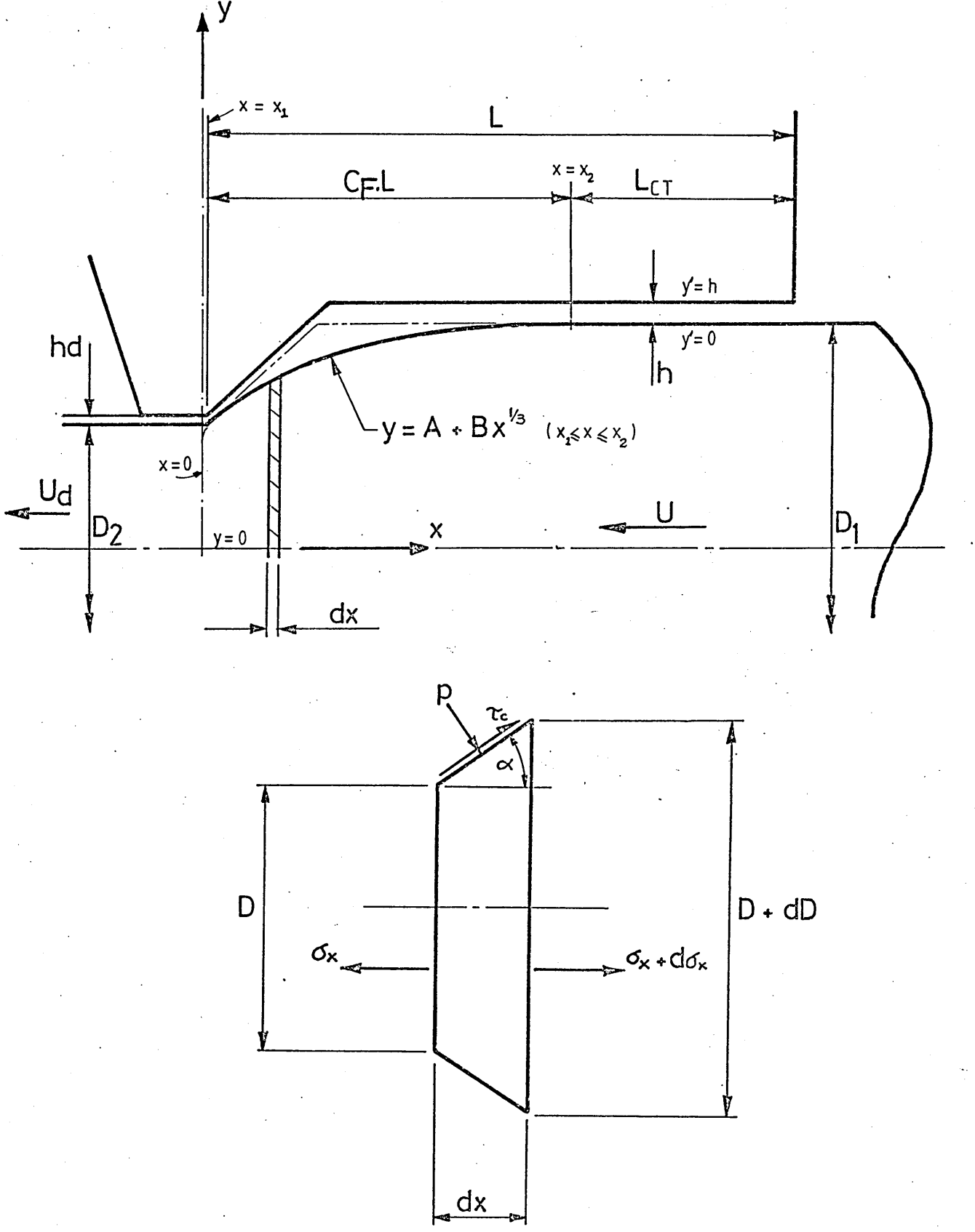

FIG 36 GEOMETRY USED IN THE ANALYSIS

one for critical flow. Stevens produced a computer aided solution and showed the effects of altering the geometric and rheological variables.

The present analysis aims to overcome the shortcomings of the previous analyses by including shear stress and rate of shear components and pressure coefficient of viscosity, together with the effects of a limiting shear stress. The strain hardening and strain rate sensitivity of the wire material are also incorporated into the analysis.

5.2 Analysis.

Fig 36 shows the principal geometric features of the die assembly considered in the following analysis.

The following assumptions are made:-

a) Flow of the polymer melt is laminar
b) Flow of the polymer melt is axial
c) The thickness of the polymer melt layer is small compared with the dimensions of the Christopherson tube
d) Pressure in the polymer melt is uniform in the thickness direction
e) Deformation occurs isothermally

Referring to Fig 36 and equating stresses in the x direction:-

$$-\frac{\sigma_x \pi D^2}{4} + (\sigma_x + d\sigma_x)\frac{\pi}{4}(D+dD)^2 + p\left(\frac{\pi D dx}{\cos\alpha}\right)\sin\alpha + \tau_c\left(\frac{\pi D dx}{\sin\alpha}\right)\cos\alpha = 0$$

Rearranging and ignoring powers of dD leads to,

$$\frac{\pi}{2}\sigma_x dD + \frac{\pi}{4}Dd\sigma_x + p\pi\tan\alpha dx + \tau_c \pi dx = 0$$

But $dD = 2dx\tan\alpha$, hence,

$$\sigma_x dD + \frac{D}{2}d\sigma_x + pdD + 2\tau_c dx = 0 \quad .$$

Also, $2dx = \frac{dD}{\tan\alpha} = dD\cot\alpha$, therefore,

$$\sigma_x dD + \frac{D}{2}d\sigma_x + pdD + \tau_c dD\cot\alpha = 0 \quad .$$

Hence,

$$Dd\sigma_x + 2dD(\sigma_x + p + \tau_c\cot\alpha) = 0 \qquad \ldots\ldots (1)$$

Radial equilibrium gives;

$$\sigma_r(\pi Ddx) = -p(\frac{\pi Ddx}{\cos\alpha})\cos\alpha + \tau_c(\frac{\pi Ddx}{\cos\alpha})\sin\alpha \quad ,$$

hence,

$$\sigma_r = -p + \tau_c\tan\alpha = -p(1 - \frac{\tau_c\tan\alpha}{p}) \quad .$$

The value of $\frac{\tau_c}{p}$ has been shown to be of the order of 10^{-2} and since $\tan\alpha$ is very small, $\frac{\tau_c}{p}\tan\alpha$ is of the order 10^{-4}. The term $\frac{\tau_c}{p}\tan\alpha$ is therefore ignored and the state of stress is cylindrical, the principal stresses being;

$\sigma_1 = \sigma_x$, $\sigma_2 = \sigma_3 = \sigma_r = -p$

Hence by using Tresca or von Mises, the yield criterion becomes;

$\sigma_x + p = Y$ and substitution in equation (1) gives:-

$$D d\sigma_x + 2dD(Y + \tau_c \cot\alpha) = 0 \qquad \ldots\ldots (2)$$

Equation (2) is the basic differential equation governing the deformation process. The experimental results show that deformation commences before the wire reaches the die. Under these conditions, the angle α is not constant, but the wire profile measured from the experimental results (Fig 33) may be given by:

$y = A + Bx^{1/3}$ $\quad (x_1 \leqslant x \leqslant x_2)$

where, from the geometry of the system;

$$A = \frac{D_2}{2}$$

$$B = \frac{(\frac{D_1}{2} - A)}{(C_F . L)^{1/3}}$$

Hence,

$$\frac{dy}{dx} = \frac{B}{3} x^{-2/3}$$

therefore,

$$\cot\alpha = \frac{3}{Bx^{-2/3}} \qquad \ldots\ldots (3)$$

Substitution of equation (3) into (2) gives;

$$d\sigma_x = -2Y\frac{dD}{D} - \frac{6\tau_c}{B}\frac{dD}{Dx^{-2/3}} \qquad \ldots\ldots (4)$$

but x is a function of D ie;

$$y = \frac{D}{2} = A + Bx^{1/3}$$

therefore,

$$x = \left(\left(\frac{D}{2} - A\right)\frac{1}{B}\right)^3 \qquad \ldots\ldots (5)$$

Substitution of equation (5) into equation (4) gives;

$$d\sigma_x = -2Y\frac{dD}{D} - \frac{6\tau_c}{B^3}\frac{dD}{D}\left(\frac{D^2}{4} - DA + A^2\right) \qquad \ldots\ldots (6)$$

The strain hardening characteristics of the wire are assumed to take the form:-

$$Y = Yo + K\varepsilon^n \qquad \text{where} \quad \varepsilon = \ln\left[\frac{D_1}{D}\right]$$

as shown in Figs 20 - 22

therefore, $Y = Yo + K\left(\ln\frac{D_1}{D}\right)^n$

ie. Y is a function of D and must be included into equation (6) before the integration is carried out.

Hence equation (6) becomes:-

$$d\sigma_x = -2Yo\frac{dD}{D} - 2K\left(\ln\frac{D_1}{D}\right)^n\frac{dD}{D} - \frac{6\tau_c}{B^3}\left(\frac{D^2}{4} - DA + A^2\right)\frac{dD}{D}$$

Integration gives;

$$\sigma_x = -2Yo\ln D + \frac{2K}{(n+1)}\left(\ln\frac{D_1}{D}\right)^{n+1} - \frac{6\tau_c}{B^3}\left(\frac{D^2}{8} - AD + A^2\ln D\right) + \text{constant}$$

In order to arrive at suitable boundary conditions, the equilibrium of the wire in the tube must be considered. This leads to,

$$\sigma_x = \frac{4\tau_c L_{CT}}{D} \qquad \text{where} \quad L_{CT} = (1 - C_F)L \quad .$$

the boundary condition then becomes;

$$\text{at} \quad D = D_1 \; ; \quad \sigma_x = \frac{4\tau_c L_{CT}}{D_1}$$

hence,

$$\text{constant} = \frac{4\tau_c L}{D_1} + 2Y_o \ln D_1 + \frac{6\tau_c}{B^3}\left(\frac{D_1^2}{8} - AD_1 + A^2 \ln D_1\right)$$

giving,

$$\sigma_x = 2Y_o \ln\left[\frac{D_1}{D}\right] + \frac{2K}{(n+1)}\left(\ln \frac{D_1}{D}\right)^{n+1} + \frac{6\tau_c}{B^3}\left(\frac{(D_1^2 - D^2)}{8} + A(D - D_1) + A^2 \ln\left[\frac{D_1}{D}\right]\right) + \frac{4\tau_c L}{D_1} C_T \qquad \ldots\ldots (7)$$

and since $p = Y - \sigma_x$,

$$p = Y_o\left(1 - \ln\left[\frac{D_1}{D}\right]^2\right) + K\left(\ln \frac{D_1}{D}\right)^n \left(1 - \frac{2}{(n+1)}\left(\ln \frac{D_1}{D}\right)\right) - \frac{6\tau_c}{B^3}\left(\frac{(D_1 - D^2)}{8} + A(D - D_1) + A^2 \ln \frac{D_1}{D}\right) - \frac{4\tau_c L}{D_1} C_T$$

$$\text{where} \quad D = 2(A + B(x)^{1/3})$$

For a complete solution, the strain rate sensitivity of the wire material may also be taken into account. A general solution was attempted, but proved impossible to integrate. The mean strain rate will therefore be included.

$$\bar{\dot{\varepsilon}} = (-2\,\frac{dD}{D})\frac{1}{dt}$$

$$\bar{\dot{\varepsilon}}_m = \frac{1}{x_2 - x_1}\int_{x_1}^{x_2} \bar{\dot{\varepsilon}}\, dx$$

therefore;

$$\bar{\dot{\varepsilon}}_m = \frac{-2}{x_2 - x_1}\int_{x_1}^{x_2} \frac{dD}{D}\,\frac{dx}{dt}$$

but $\frac{dx}{dt} = U(\frac{D_1}{D})^2$ (from volume continuity),

hence,

$$\bar{\dot{\varepsilon}}_m = \frac{-2UD_1^2}{x_2 - x_1}\int_{x_1}^{x_2} \frac{dD}{D^3}$$

$$= + \frac{UD_1^2}{x_2 - x_1}\left[\frac{1}{D^2}\right]_{x_1}^{x_2}$$

When $x_1 = 0$; $D = D_2$

$x_2 = C_F.L$; $D = D_1$

therefore,

$$\bar{\dot{\varepsilon}}_m = \frac{UD_1^2}{C_F.L}\left[\frac{1}{D_2^2} - \frac{1}{D_1^2}\right]$$

A flow rule of the form;

$$S = \frac{Yd}{Ys} = \left(1 + \left(\frac{\bar{\varepsilon}_m}{N}\right)^{1/T}\right)$$

where Yd = dynamic yield stress

Ys = static yield stress

has been proposed[32].

Combining this with equation (7) gives:-

$$\sigma_x = 2SYo.\ln\left(\frac{D_1}{D}\right) + \frac{2KS}{n+1}\left(\ln\frac{D_1}{D}\right)^{n+1} +$$

$$+ \frac{6\tau_c}{B^3}\left(\left(\frac{D_1^2-D^2}{8}\right) + A(D-D_1) + A^2.\ln\left(\frac{D_1}{D}\right)\right) + \frac{4\tau_c L}{D_1}CT \quad \ldots (8)$$

It is now necessary to determine some function for τ_c in terms of known parameters. This may be found by considering the polymer melt flow in the Christopherson tube.

As the thickness of the polymer melt layer contained in the Christopherson tube is small compared with the dimensions of the tube, the analysis of flow is carried out in rectangular rather than cylindrical coordinates.

An empirical expression relating shear stress and rate of shear can be:-

$$\tau + k\tau^3 = \eta_o \frac{\partial v}{\partial y}, \quad \ldots\ldots (9)$$

This equation was first suggested by Rabinowitsch[33] and was used by Rotem and Shinnar[34] and Swamy et al[35] to investigate flow of non-Newtonian fluids. This equation has been shown

to be applicable to polymer melts as shown in Fig 7.

Equilibrium of the melt in the tube gives:-

$$\frac{\partial p}{\partial x} = \frac{\partial \tau}{\partial y'} \qquad (x_2 \leqslant x \leqslant (L + x_1)) \qquad \ldots\ldots (10)$$

Integrating equation (10) gives;

$$\tau = p' y' + \tau_c \qquad \ldots\ldots (11)$$

where $p' = \frac{\partial p}{\partial x}$

τ_c = shear stress at $y' = 0$

Substituting equation (11) into (9) gives:-

$$\frac{\partial v}{\partial y'} = \frac{p' y'}{\eta_o} + \frac{\tau_c}{\eta_o} + \frac{k}{\eta_o}(p'^3 y'^3 + 3p'^2 y'^2 \tau_c + 3p' y' \tau_c^2 + \tau_c^3)$$

Integration gives:-

$$v = \frac{p' y'^2}{2\eta_o} + \frac{\tau_c y'}{\eta_o} + \frac{k}{\eta_o}\left(\frac{p'^3 y'^4}{4} + p'^2 y'^3 \tau_c + \frac{3p' y'^2 \tau_c^2}{2} + \tau_c^3 y'\right) + \text{constant} \quad \ldots (12)$$

Considering the boundary conditions.

Two regimes may be considered; at slow drawing speeds when slip is not present and at higher speeds when the effect of slip must be included.

For conditions of no slip:-

When $y' = 0$; $v = U$ ..... (a)

$y' = h$; $v = 0$ ..... (b)

Applying boundary condition (a) to equation (12); constant=U

therefore,

$$v = \frac{p'y'^2}{2\eta_o} + \frac{\tau_c y'}{\eta_o} + \frac{k}{\eta_o}\left(\frac{p'^3 y'^4}{4} + p'^2 y'^3 \tau_c + \frac{3p}{2} y'^2 \tau_c^2 + \tau_c^3 y'\right) + U \quad \ldots\ldots (13)$$

The rate of flow of polymer melt through the die may be obtained by integrating equation (13) thus,

$$Q = \int_o^h v \, dy'$$

hence,

$$Q = \frac{p'h^3}{6\eta_o} + \frac{\tau_c h^2}{2\eta_o} + \frac{k}{\eta_o}\left(\frac{p'^3 h^5}{20} + \frac{p'^2 h^4 \tau_c}{4} + \frac{p' h^3 \tau_c^2}{2} + \frac{\tau_c^3 h^2}{2}\right) + Uh \quad \ldots\ldots (14)$$

Applying boundary condition (b) to equation (13) gives;

$$0 = \frac{p'h^2}{2\eta_o} + \frac{\tau_c h}{\eta_o} + \frac{k}{\eta_o}\left(\frac{p'^3 h^4}{4} + p'^2 h^3 \tau_c + \frac{3p' h^2 \tau_c^2}{2} + \tau_c^3 h\right) + U \quad \ldots\ldots (15)$$

This equation may be used to find τ_c provided p' can be found in terms of the other parameters. The Tresca or von Mises yield criterion for the wire in the tube gives;

$$Y = p + \sigma_x \qquad \text{as before,} \qquad \ldots\ldots (16)$$

and equilibrium of stresses in the wire in the Christopherson tube gives;

$$\sigma_x = \frac{4\tau_c L_c}{D_1} CT \qquad \text{as before.} \qquad \ldots\ldots (17)$$

Combining equations (16) and (1() gives;

$$Y = P + k!cLCT \qquad (18)$$
$$Di$$

Assuming a linear axial pressure gradient in the Christopherson tube, (the validity of this assumption will be discussed in Chapter 8) ie;

$$p' = p \qquad \text{(pressure p at x = x2)}$$
$$LCT \qquad (x24 \times 4 (L + xx))$$

hence ,

$$P = P \qquad - \qquad ...0.(19)$$

Substituting equation (19) into (18) gives;

$$Y = v' + 4xc$$
$$LCT$$

or $$p7 = Y \quad klc. \qquad ..... (20)$$
$$LCT \quad hi$$

Substituting equation (20) into- (15) and rearranging leads to;

$$0 = Ci \text{ TO } TCw + C2\ T|0Tc2 + 83\ T0xc + C^Tjo + U \qquad ..o..(21)$$

v/here $$Ci = kh(1 - 6h + 16h2 - 16h3)$$
$$' dt \quad W$$

Equation (21) above does not include the effect of pressure on viscosity. It is known that an increase in hydrostatic pressure increases viscosity for most fluids. For low density polyethylene, this may be represented by;

$$\eta_o = \eta_a + ap \quad \ldots\ldots \quad 0 \leqslant p \leqslant 190 \text{ MNm}^{-2}$$
$$\eta_o = \eta_a + ap - bp^2 - c \quad \ldots \quad p > 190 \text{ MNm}^{-2} \qquad \ldots\ldots (22)$$

(see Fig 10)

where η_a is the viscosity at ambient pressure and a, b, c are constants.

It will be assumed that shear stresses and their effects remain independant of pressure (Fig 11 gives some support to this assumption) and that the pressure alters only the initial value of viscosity, η_o , with respect to shear. Since pressure is assumed to be constant in the thickness direction, it is independant of v and therefore may be considered separately.

Rewriting equation (20);

$$p = Y - \frac{4\tau_c L_{CT}}{D_1} \quad , \text{ since } \quad p = p' L_{CT} \quad ,$$

therefore, from equation (22);

$$\eta_o = \eta_a + \tau_c\left(\frac{8bL_{CT}}{D_1}Y - \frac{4aL_{CT}}{D_1}\right) - \frac{16bL_{CT}^2}{D_1^2}\tau_c^2 + Y(a-bY) - c$$

or

$$\eta_o = C_5\tau_c^2 + C_6\tau_c + C_7 \qquad \ldots\ldots (23)$$

where $C_5 = -\frac{16bL^2}{D_1^2}CT$

$C_6 = \frac{8bL}{D_1}CT^Y - \frac{4aL}{D_1}CT$

$C_7 = \eta_a + Y(a-bY) - c$

Combining equations (21) and (23) gives;

$$0 = \frac{C_1\tau_c^3 + C_2\tau_c^2 + C_3\tau_c + C_4}{C_5\tau_c^2 + C_6\tau_c + C_7} + U \qquad \ldots\ldots (24)$$

where $C_1 - C_7$ have been previously defined.

The inclusion of the strain hardening and strain rate sensitivity of the wire material may be taken into account by rewriting Y as;

$S(Yo + K(\ln\frac{D_1}{D})^n)$ as before.

But since no deformation occurs in this part of the tube;

$$Y = YoS \ .$$

Equation (24) may now be solved since all of the constants are known physical parameters. The equation was solved by digital computer, the program for which is included in Appendix I.

Having solved the above equation for τ_c, this may be then substituted into equation (7) giving the stress in the wire and also into equation (20) which gives p' and then substitution of τ_c into equation (23) gives η_o. Finally substitution of τ_c, η_o and p' into equation (14) will give the polymer flow rate, for conditions of no slip between

the polymer melt and the wire. The coat thickness may be calculated from the flow rate since;

$$Q = h_d . U_d \quad , \text{ hence } \quad h_d = \frac{Q}{U_d} \qquad \ldots\ldots (25)$$

where h_d is the coat thickness and U_d is the wire velocity after drawing.

Critical Melt Flow

The conditions in the foregoing analysis assumed that slip did not occur. It is known that polymers have a maximum shear stress value, after which catastrophic slip occurs, as discussed in Chapter 2.. The boundary conditions for slip (for equation (12)) are;

when $y' = 0$; τ_c = constant = τ_a ; $v = U_s$
$y' = h$; $v = 0$ as before

where U_s is the velocity of the wire at commencement of slip.

(These conditions assume that slip occurs at the wire-polymer interface only and not at the polymer tube interface)

Equation (14) then becomes;

$$Q = \frac{p'h^3}{6\eta_o} + \frac{\tau_a h^2}{2\eta_o} + \frac{k}{\eta_o}\left(\frac{p'^3h^5}{20} + \frac{p'^2h^4\tau_a}{4} + \frac{p'h^3\tau_a^2}{2} + \frac{\tau_a^3h^2}{2}\right) + U_s h \qquad \ldots (26)$$

U_s may be determined from the no-slip conditions if τ_a is known (Lupton and Regester[17] have quoted examples of τ_a being in the region of 10^6 Nm^{-2}). This equation shows that when

slip occurs, the flow rate becomes constant. The thickness must then progressively reduce as the speed is increased, since;

$$h_d = \frac{Q}{U_d}$$

The relevant equations were used as a basis for a computer program to give the theoretical results which are presented in Chapter 6.

6.1 Introduction.

The theoretical results obtained using the equations deduced in Chapter 5 are presented here. Computer programs were written to solve the equations simultaneously and express the results either in tabular or graphical form on a visual display unit. The development and listing of the programs are given in Appendix I. The equations used for the theoretical results are summarised in the order that they require to be solved.

$$0 = \frac{C_1 \tau_c^3 + C_2 \tau_c^2 + C_3 \tau_c + C_4}{C_5 \tau_c^2 + C_6 \tau_c + C_7} + U \qquad \text{.....(24)}$$

where $C_1 - C_7$ are defined

$$L_{CT} = (1 - C_F)L$$

$$p' = \frac{Yo}{L_{CT}} - \frac{4\tau_c}{D_1} \qquad \text{..... (20)}$$

$$\eta_o = C_5 \tau_c^2 + C_6 \tau_c + C_7 \qquad \text{..... (23)}$$

$$Q = \frac{p' h^3}{6\eta_o} + \frac{\tau_c h^2}{2\eta_o} + \frac{k}{\eta_o}\left(\frac{p'^3 h^5}{20} + \frac{p'^2 h^4 \tau_c}{4} + \frac{p' h^3 \tau_c^2}{2} + \frac{\tau_c^2 h^2}{2}\right) + Uh \qquad \text{.... (14)}$$

$$U_d = U\left(\frac{D_1}{D_2}\right)^2 \quad ; \quad h_d = \frac{Q}{U_d} \qquad \text{..... (25)}$$

$$A = \frac{D_2}{2} \quad ; \quad B = \frac{1}{(C_F.L)^{1/3}}\left(\frac{D_1}{2} - A\right) \quad ; \quad D = 2(A + B(x)^{1/3})$$

$$\bar{\dot{\varepsilon}}_m = \frac{UD_1^2}{C_F.L}\left(\frac{1}{D_2^2} - \frac{1}{D_1^2}\right) \quad ; \quad S = 1 + \left(\frac{\bar{\dot{\varepsilon}}}{N}_m\right)^{1/T}$$

$$\sigma_x = 2Y_oS.\ln\left(\frac{D_1}{D}\right) + \frac{2KS}{n+1}\left(\ln\frac{D_1}{D}\right)^{n+1} + \frac{6\tau_c}{B^3}\left(\left(\frac{D_1^2-D^2}{8}\right) +\right.$$

$$\left. + A(D-D_1) + A^2.\ln\left(\frac{D_1}{D}\right)\right) + \frac{4\tau_c L}{D_1}CT \qquad \ldots\ldots (7)$$

$$p = S\left(Y_o + K\left(\ln\frac{D_1}{D}\right)^n\right) - \sigma_x$$

$$Q = \frac{p'h^3}{6\eta_o} + \frac{\tau_a h^2}{2\eta_o} + \frac{k}{\eta_o}\left(\frac{p'^3h^5}{20} + \frac{p'^2h^4\tau_a}{4} + \frac{p'h^3\tau_a^2}{2} + \frac{\tau_a^3h^2}{2}\right) + U_{sh} \qquad (26)$$

Since τ_c is dependant upon the wire speed (U), all of the above equations require to be solved for each wire speed. The computer programs were arranged such that wire speeds of 0.1 ms^{-1} to 2.5 ms^{-1} were solved in steps of 0.1 ms^{-1}. The stress and pressure equations were solved at each speed for values of x between x = 0 and x = $C_F.L$ in ten equal increments.

The results from the analysis are given in graphical form for convenience.

Input data. The following physical parameters were taken as a basis from which to work and were varied in the program as shown on the respective graphs.

η_o	$= 70\ Nsm^{-2}$	Data for Alkathene WVG 23 at 150°C
k	$= 8.07 \times 10^{-11}\ m^2N^{-2}$	
τ_a	$= 1 \times 10^{6}\ Nm^{-2}$	
a	$= 1.1 \times 10^{-5}\ s$	
b	$= 1.0575 \times 10^{-14}\ msN^{-1}$	
c	$= -381.76\ Nsm^{-2}$	
Yo	$= 1 \times 10^{8}\ Nm^{-2}$	Data for copper wire
K	$= 3.41 \times 10^{8}\ Nm^{-2}$	
n	$= 0.25$	
N	$= 55000$	
T	$= 3.8$	
D_1	$= 1.62 \times 10^{-3}\ m$	
L	$= 0.08\ m$	Data for Christopherson tube
h	$= 1.8 \times 10^{-4}\ m$	
C_F	$= 0.5$	
D_2	$= 1.37 \times 10^{-3}\ m$	30% reduction die.

6.2 Theoretical Coat Thickness.

Figs 37 to 46 show the theoretical effects of changing the various parameters on the coat thickness at different wire speeds. The results obtained using the standard set of data shown above gives curves which have three well defined zones:-

a) At very low drawing speeds (below 0.12 ms^{-1}) a lack of coat is predicted. The wire under these circumstances would be subjected to boundary lubrication.

b) At higher drawing speeds (between 0.12 and 2.4 ms^{-1}) the coat thickness is increased as the speed is increased.

c) Above 2.4 ms^{-1} the coat thickness is reduced as the drawing speed is increased. The cause of this reduction is the limiting value of shear stress - since the shear stress cannot increase, no further polymer can be dragged into the Christopherson tube, hence an increase in speed causes a decrease in coat thickness. These trends are typical of the computed results with the speeds at which the zones change and the corresponding coat thickness altering for the different input parameters.

Fig 37 shows the effect of changing the initial yield stress of the wire material. The higher the yield stress, the smaller the coat thickness possible. The yield stress also alters the speed at which the shear stress in the polymer becomes critical - the greater the yield stress, the lower the drawing speed necessary to cause critical flow. Note also that the greater the yield stress of the wire, the higher the speed at which coating first occurs.

Figs 38a and 38b show the effects of changing the gap between the wire and the Christopherson tube. For very small gaps the coat thickness is approximately constant and very small in magnitude. As gap increases, the maximum thickness increases until a stage is reached where the maximum thickness actually reduces for increasing gap. There is, evidently, an optimum gap for each set of conditions considered. The optimum gap for the parameters used here is 0.18mm (which was in fact the gap used in the experiments).

Fig 39a shows the effect of changing the length of the Christopherson tube. The longer the Christopherson tube, the greater the maximum thickness possible. The longer tubes give essentially constant coat thickness for the speed range shown. Little advantage is gained by using longer tubes than necessary as fig 39b shows. Increases in length above 0.3m produce only very small increases in coat thickness.

Fig 40 shows the theoretical effect of changing the critical shear stress of the polymer. The effect is simply to change the speed at which the maximum thickness is reached.

Fig 41 shows the theoretical effects of changing wire radius (whilst the reduction is maintained at the same value). An increase in wire size;

a) brings about an increase in coat thickness
b) increases the speed at which the shear stress becomes critical
c) causes flow to start at a lower drawing speed.

Fig 42 shows the theoretical effects of changing the initial viscosity (this is equivalent to changing the temperature of the polymer). The major effect is to change the speed at which the flow becomes critical. The coat thickness at critical speed is the same for all values of initial viscosity.

Fig 43a shows the theoretical effects of changing the pressure coefficient of viscosity. Increasing the value of "a" has the effect of lowering the speed at which the flow becomes critical although the coat thickness at critical speed remains constant. Fig 43b shows the effects of changing

the shear component of viscosity. A reduction in the value of k increases the maximum coat thickness but decreases the speed at which the critical shear stress in the polymer is reached. The general effect is, therefore, to reduce the coat thickness as the polymer becomes more Newtonian in nature.

Fig 44 shows the theoretical effects of die size on coat thickness. The smaller wire reductions give greater thicknesses and also reduce the speed at which the critical shear stress in the polymer is reached.

Fig 45 shows the theoretical effects on coat thickness of including the strain rate sensitivity of the wire material. If the strain rate sensitivity of the wire is not included, the coat is marginally thicker and the speed for critical flow is increased.

Fig 46a shows the theoretical effects of changing the value of C_F on coat thickness. The effect appears to be rather unclear in that the maximum thickness for $C_F = 0.1$ is higher than that for $C_F = 0.25$ but the thickness for $C_F = 0.0001$ is less than that for $C_F = 0.25$. Fig 46b clarifies the situation. There is an optimum value for C_F at which the maximum coat thickness is greatest. The speed at which the critical stress is reached is changed likewise.

FIG 37 THEORETICAL VARIATION IN COAT THICKNESS DUE TO CHANGING INITIAL YIELD STRESS OF WIRE

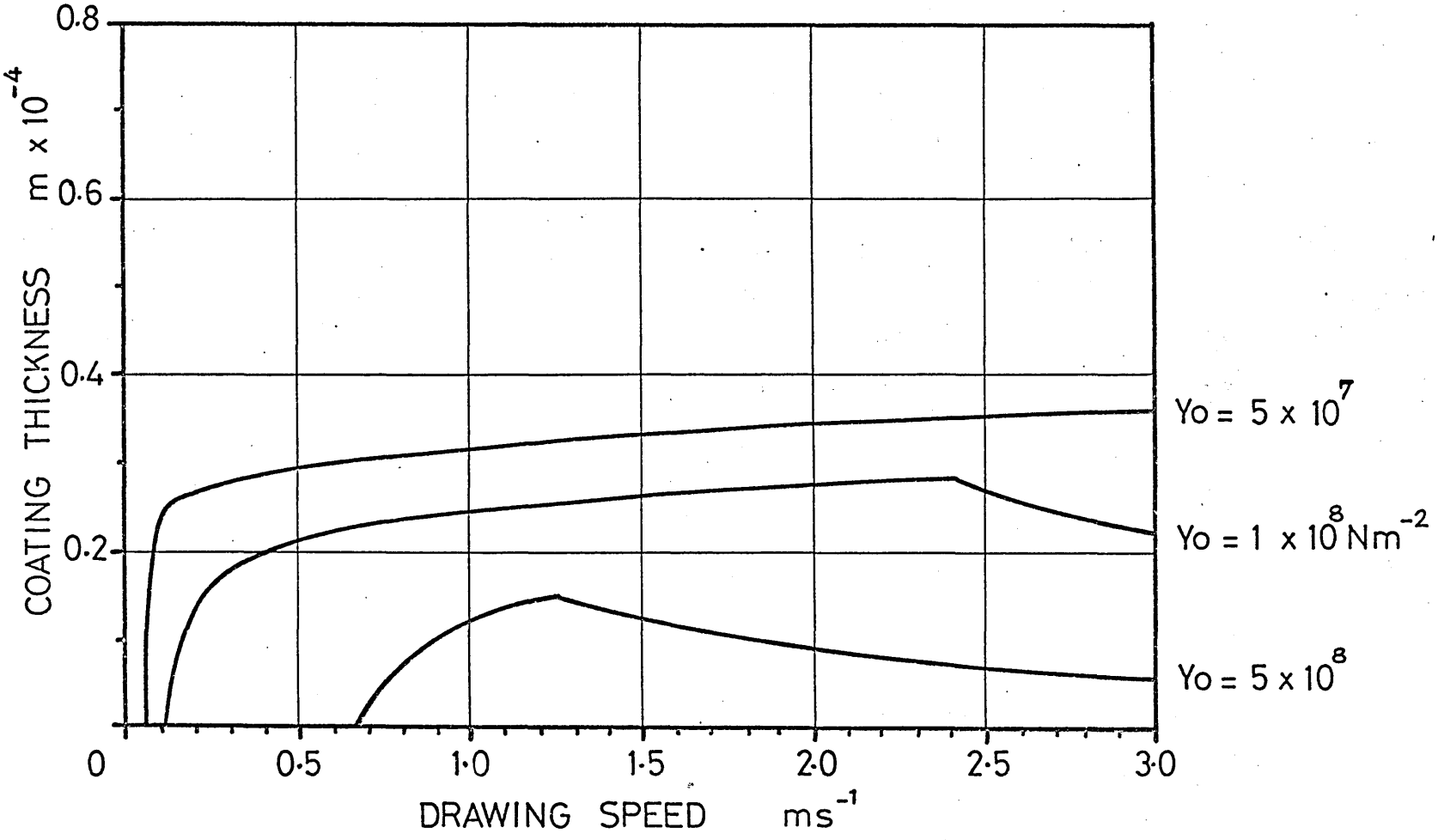

FIG 38a THEORETICAL VARIATION IN COAT THICKNESS DUE TO CHANGING GAP

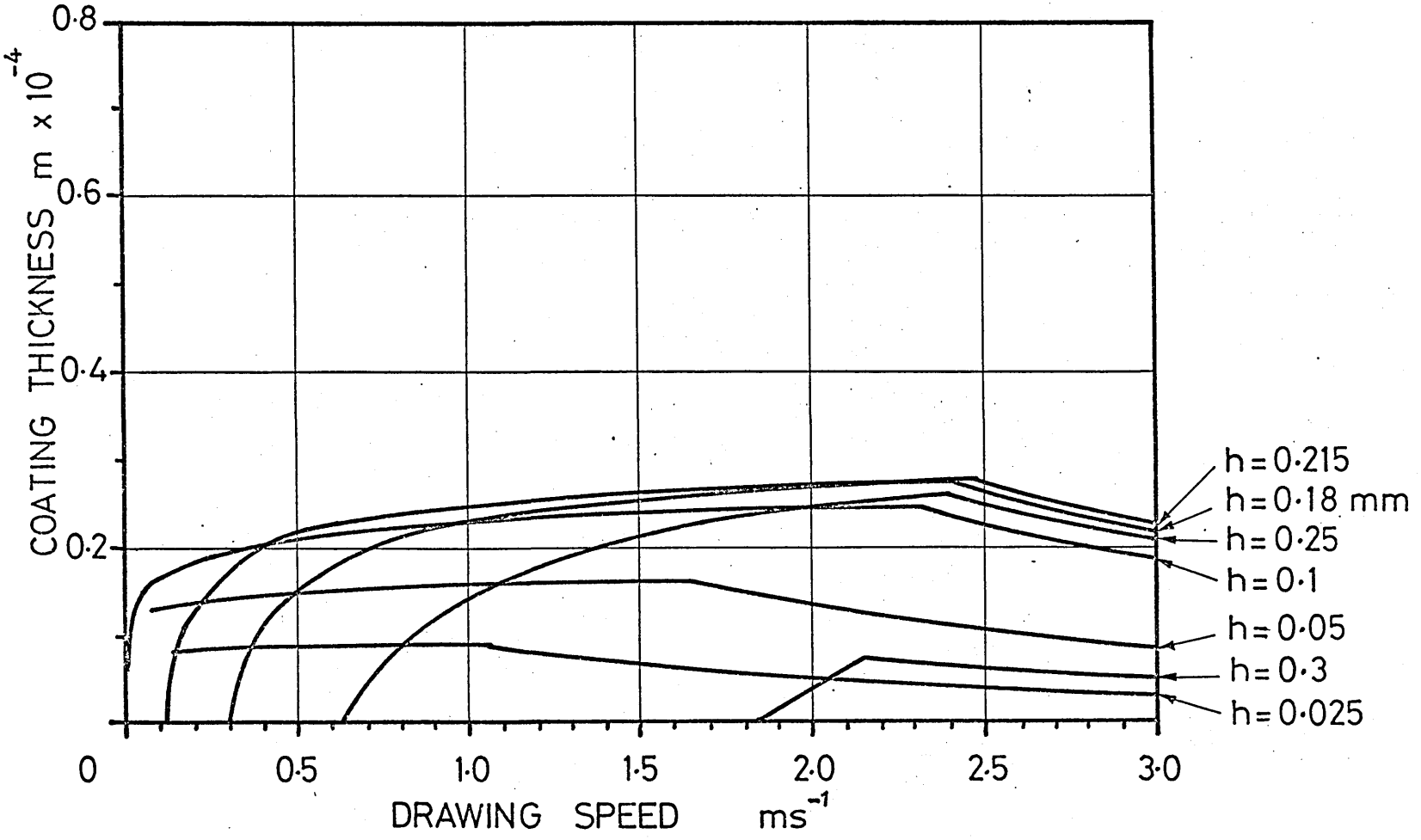

FIG 38b THEORETICAL VARIATION IN MAX. THICKNESS AND CRITICAL SPEED DUE TO CHANGING GAP

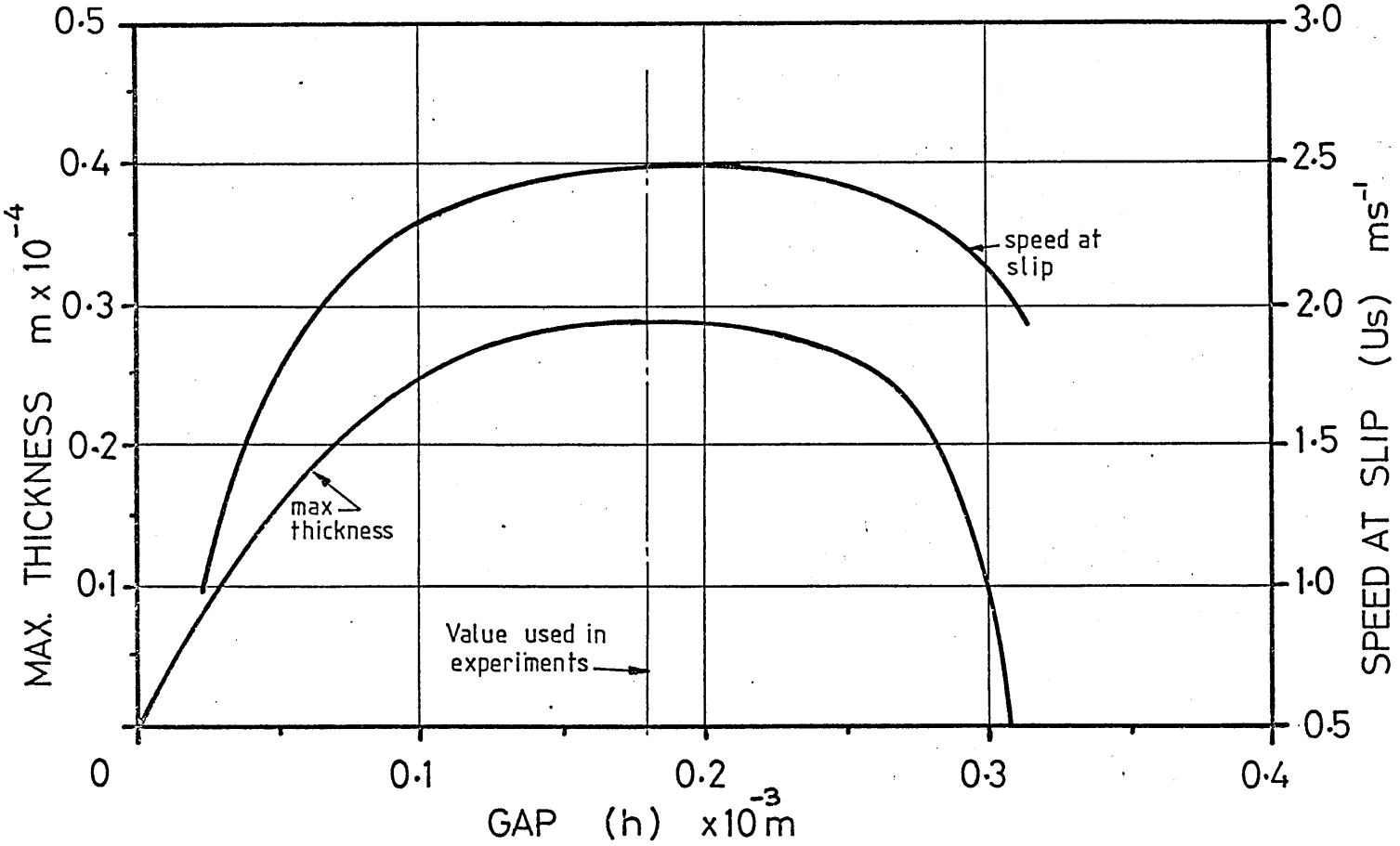

FIG 39a THEORETICAL VARIATION IN COAT THICKNESS DUE TO CHANGING CHRISTOPHERSON TUBE LENGTH

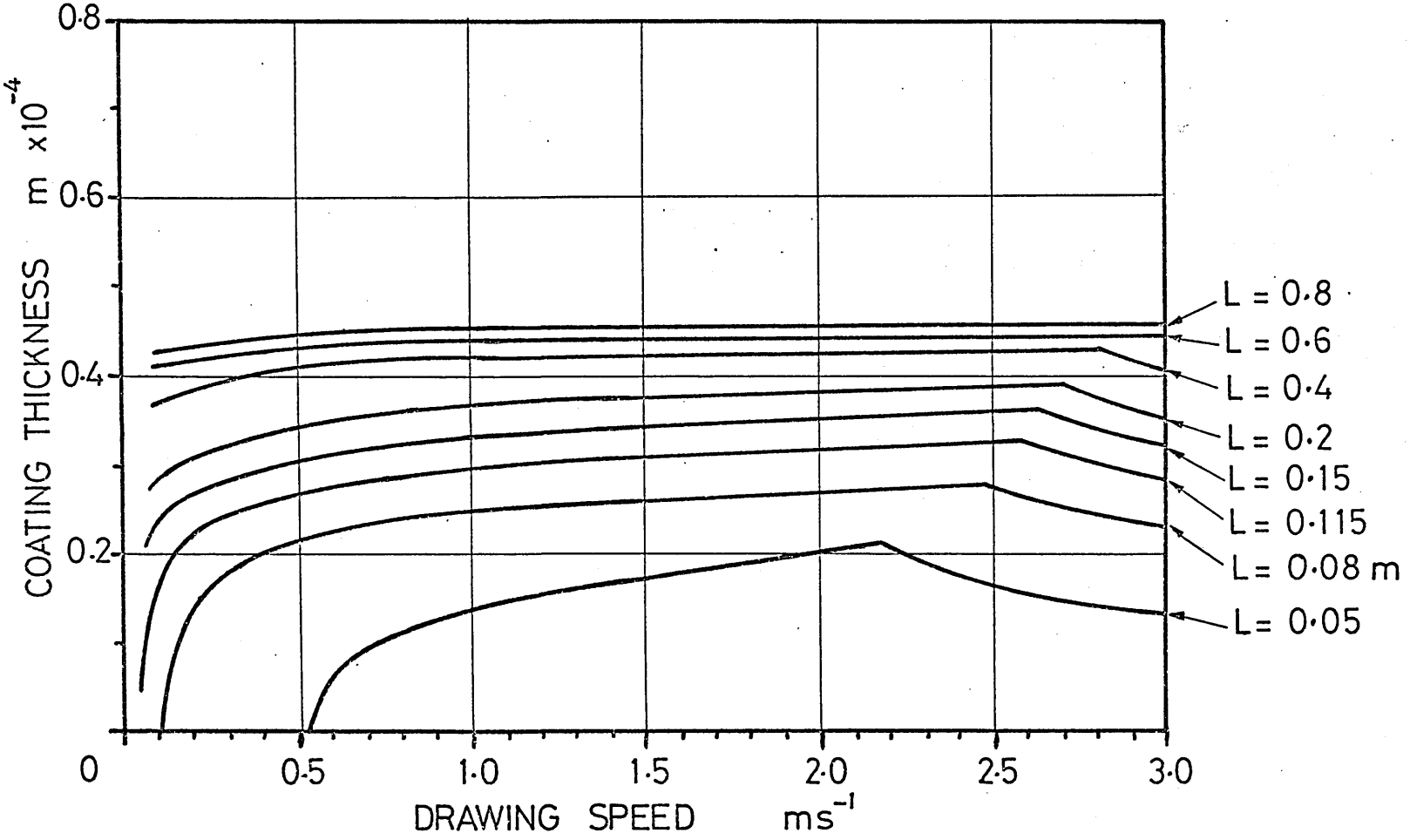

FIG 39b THEORETICAL VARIATION IN MAX. THICKNESS DUE TO CHANGING CHRISTOPHERSON TUBE LENGTH

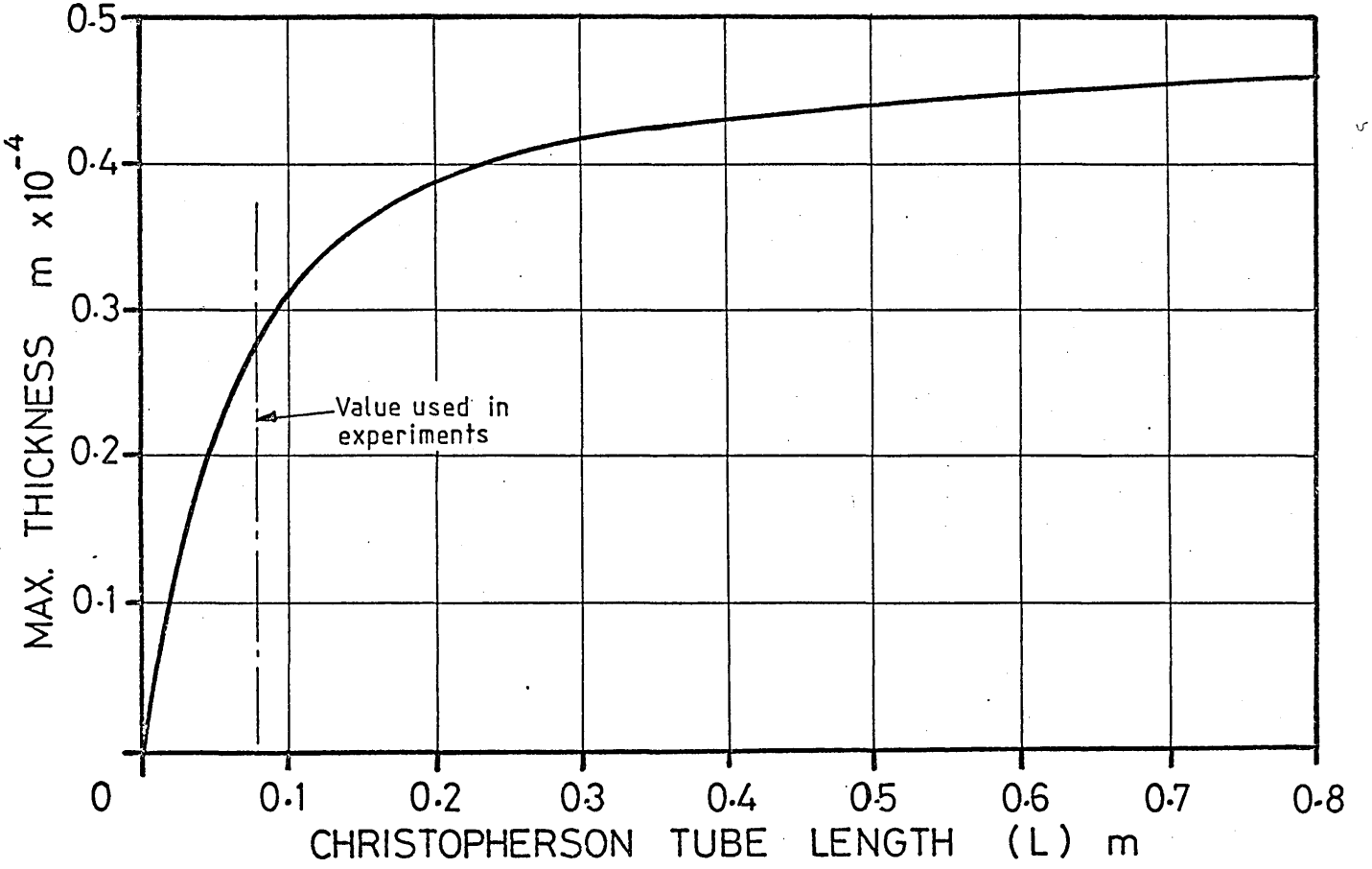

FIG 4.0 THEORETICAL VARIATION IN COAT THICKNESS DUE TO CHANGING CRITICAL SHEAR STRESS

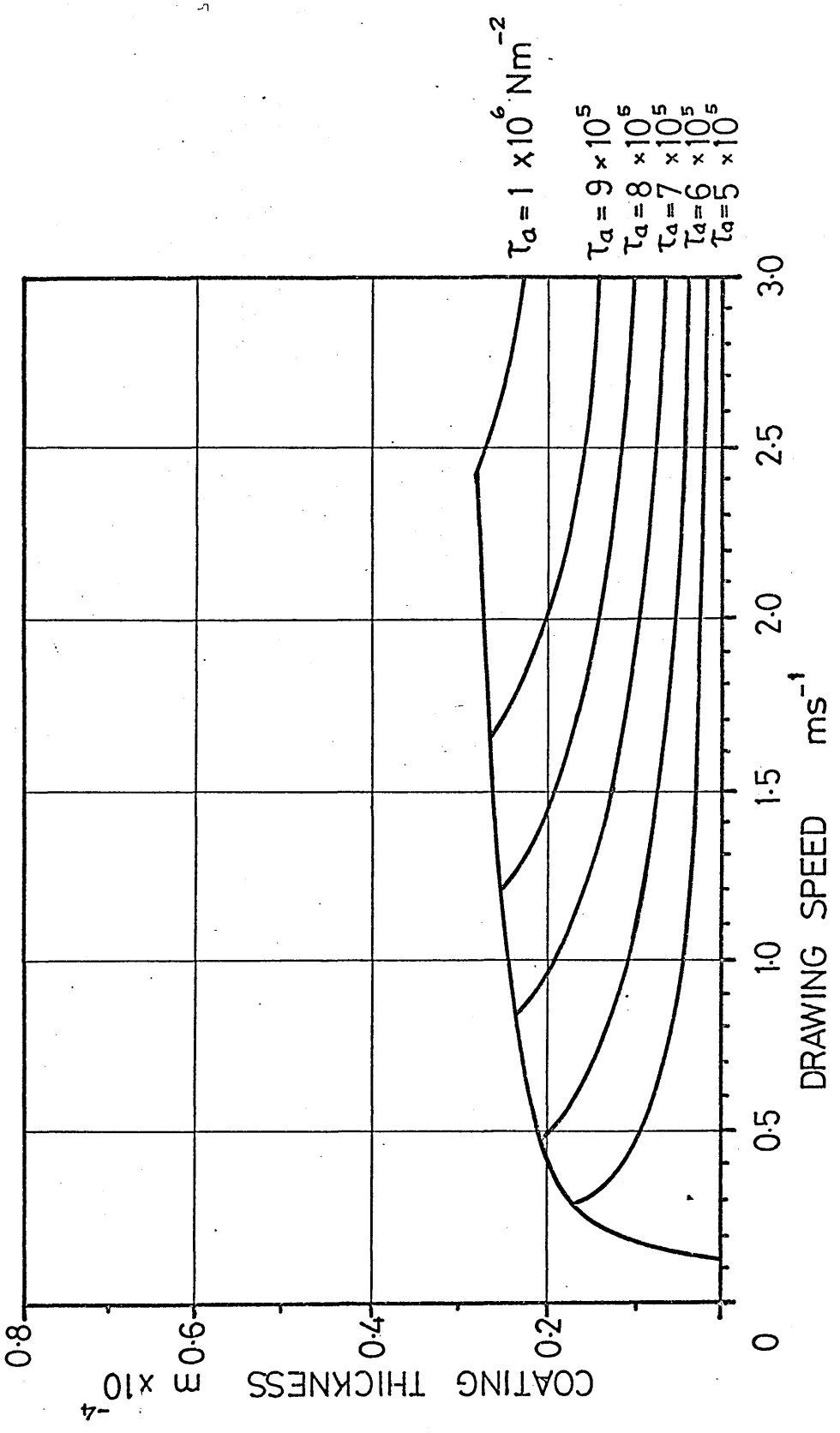

FIG 4.1 THEORETICAL VARIATION IN COAT THICKNESS DUE TO CHANGING WIRE RADIUS

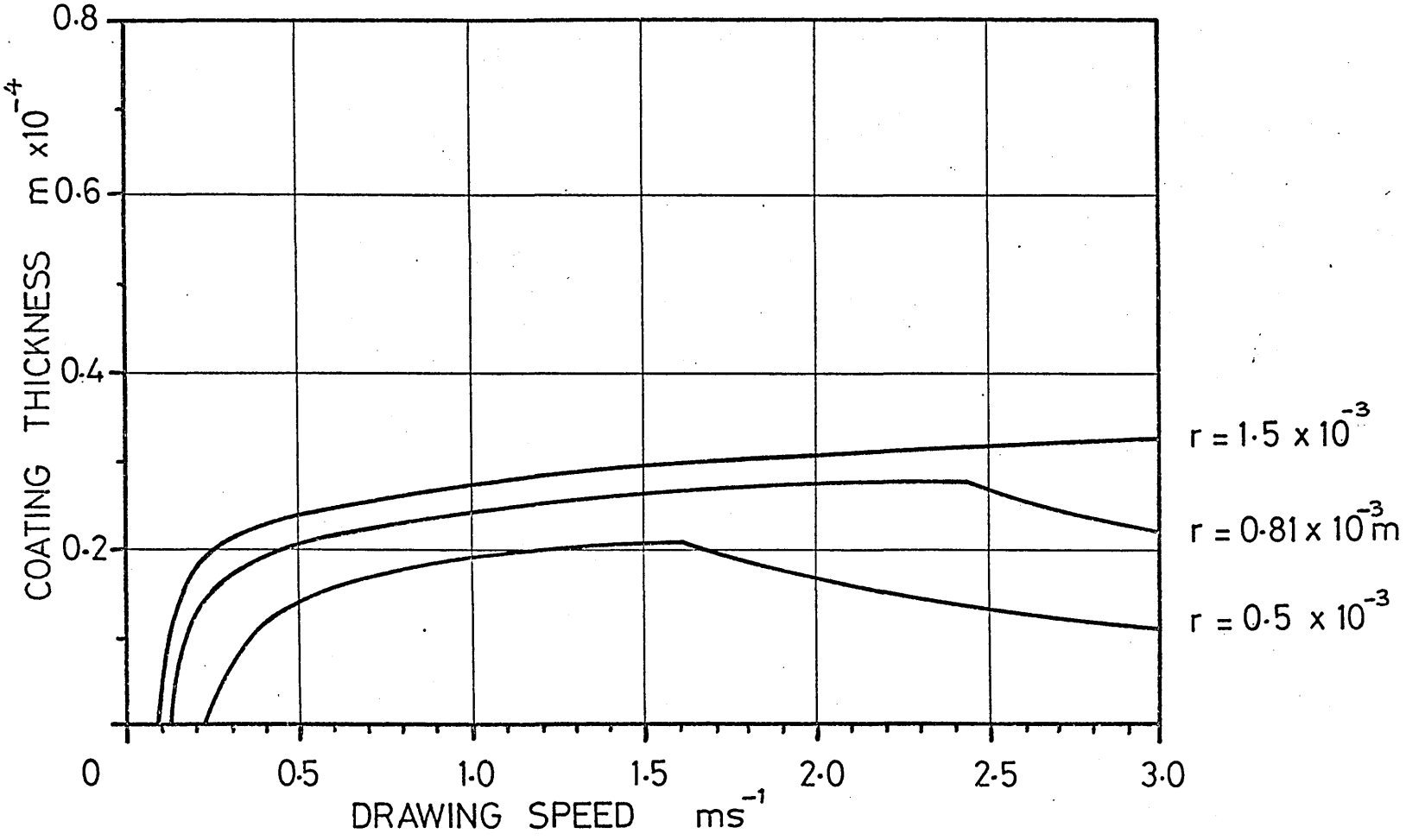

FIG 42 THEORETICAL VARIATION IN COAT THICKNESS DUE TO CHANGING INITIAL VISCOSITY

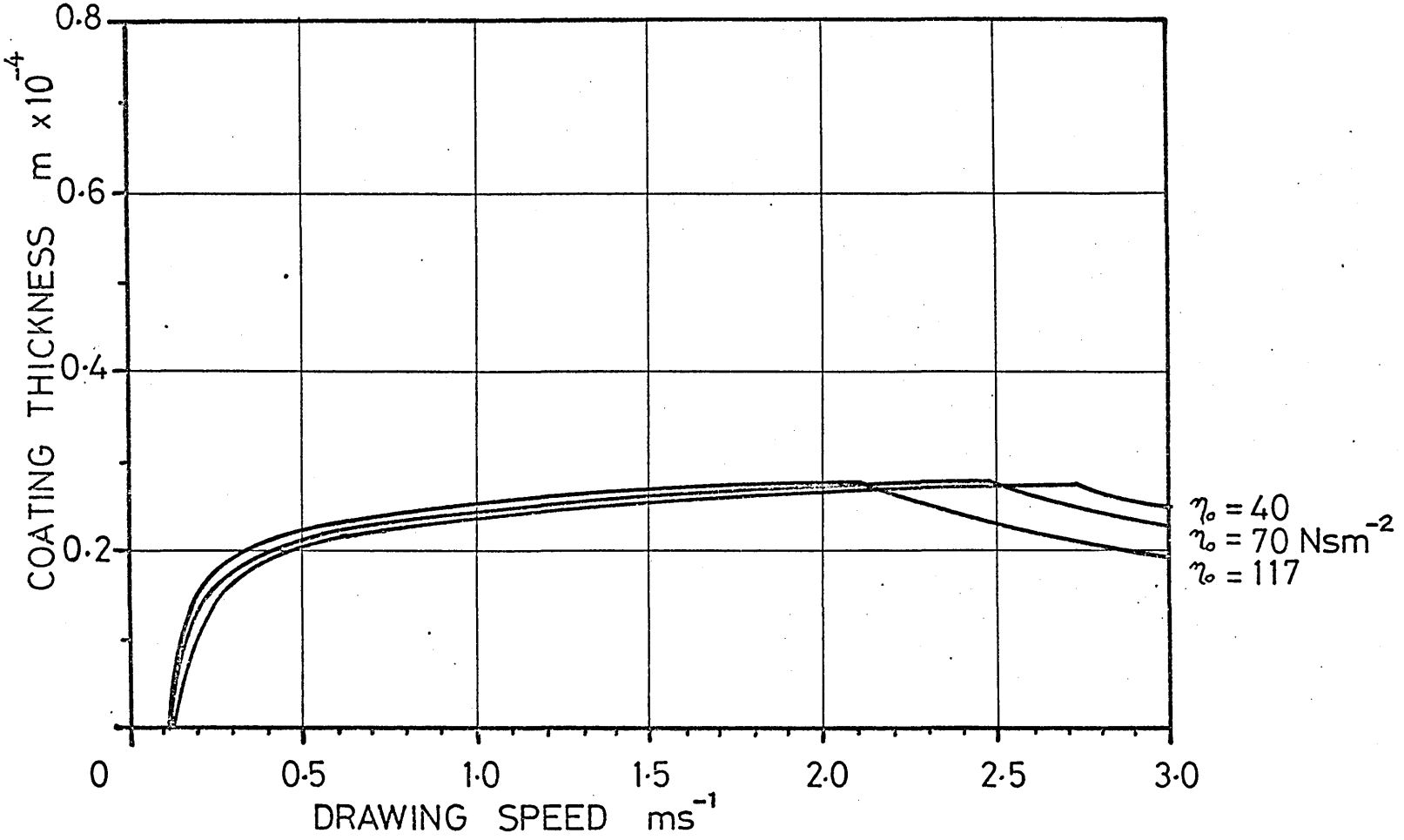

FIG 43a THEORETICAL VARIATION IN COAT THICKNESS DUE TO CHANGING PRESSURE COEFFICIENT OF VISCOSITY

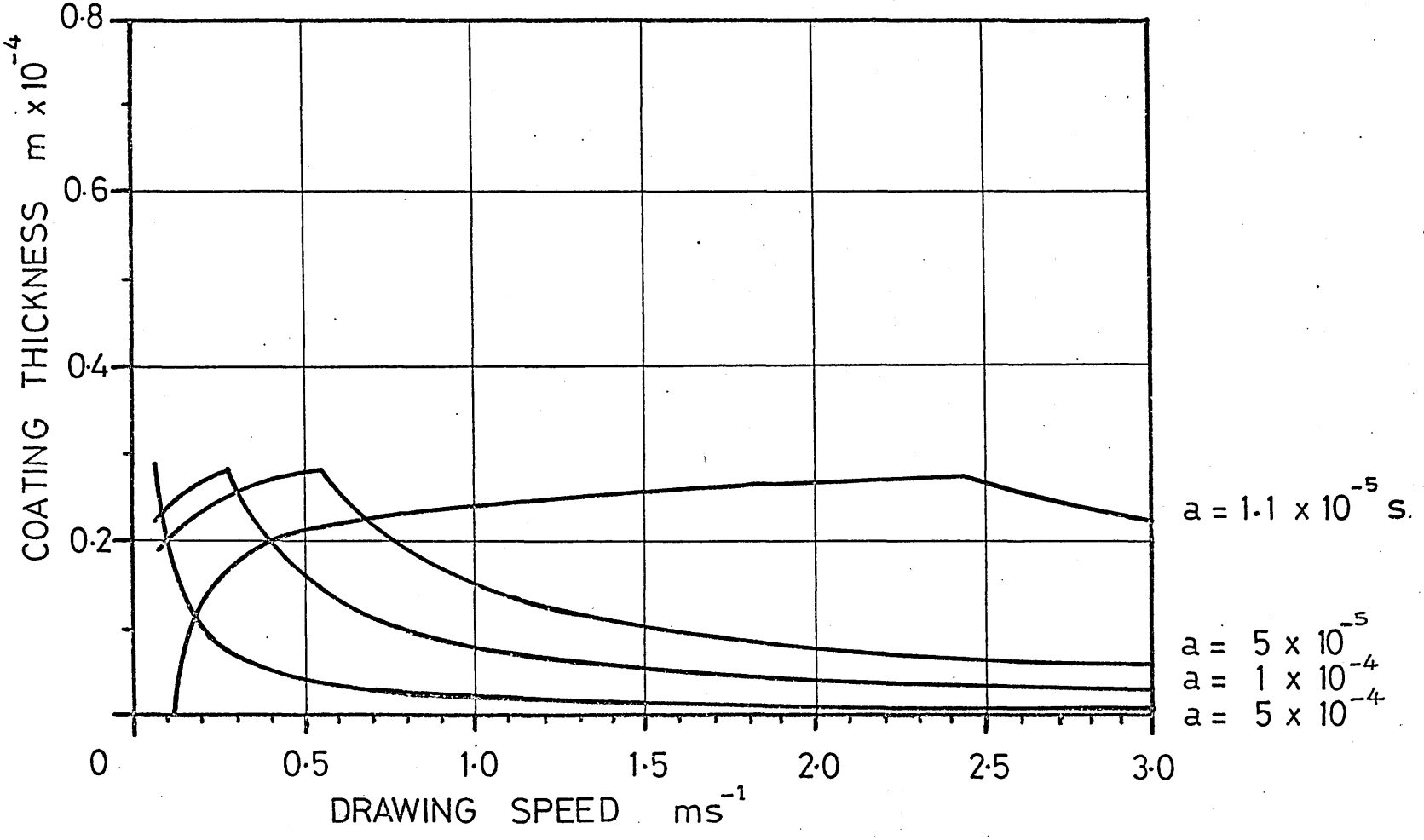

FIG 43b THEORETICAL VARIATION IN COAT THICKNESS DUE TO CHANGING SHEAR COEFFICIENT OF VISCOSITY

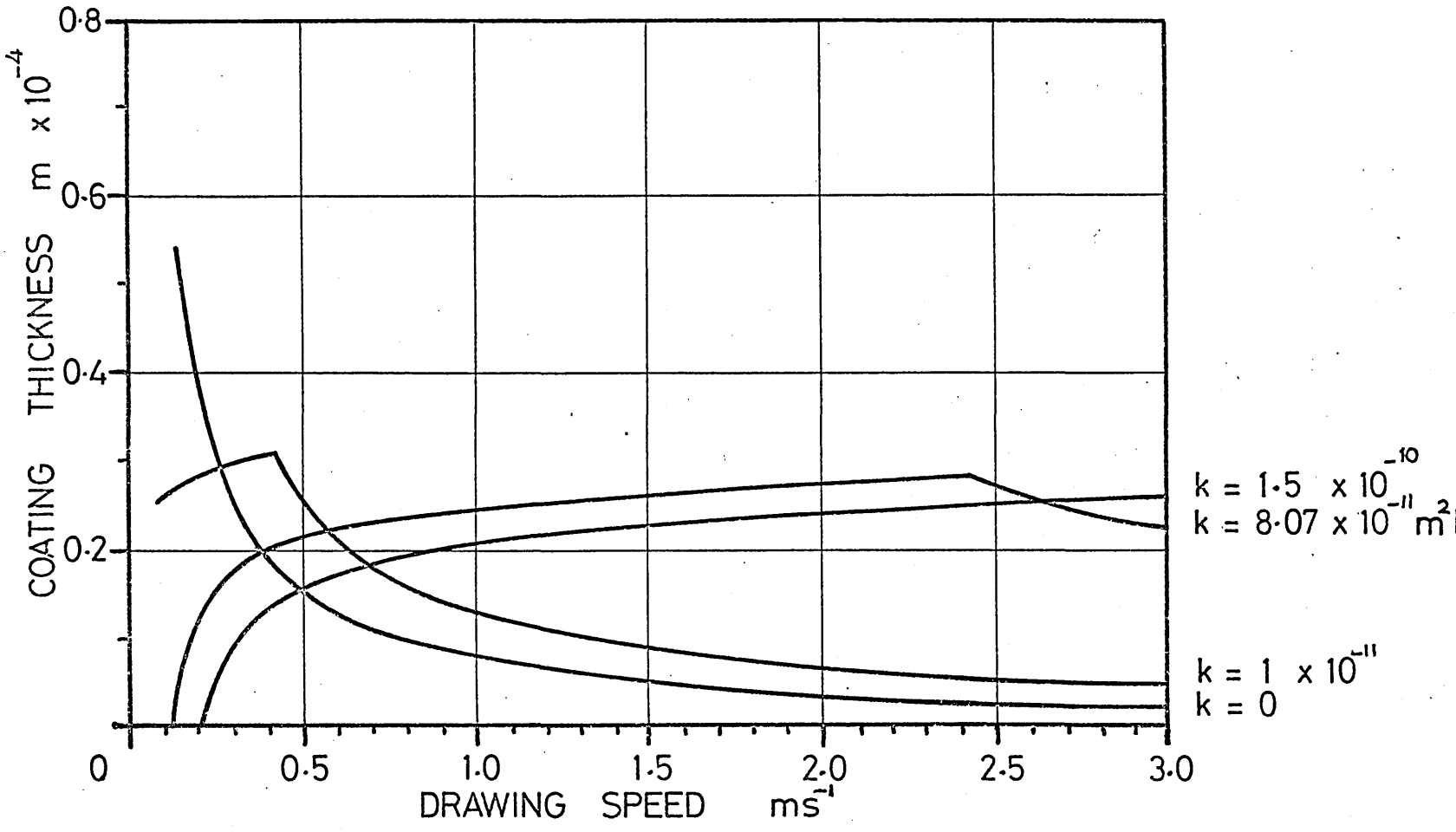

FIG 44 THEORETICAL VARIATION IN COAT THICKNESS DUE TO CHANGING DIE SIZE

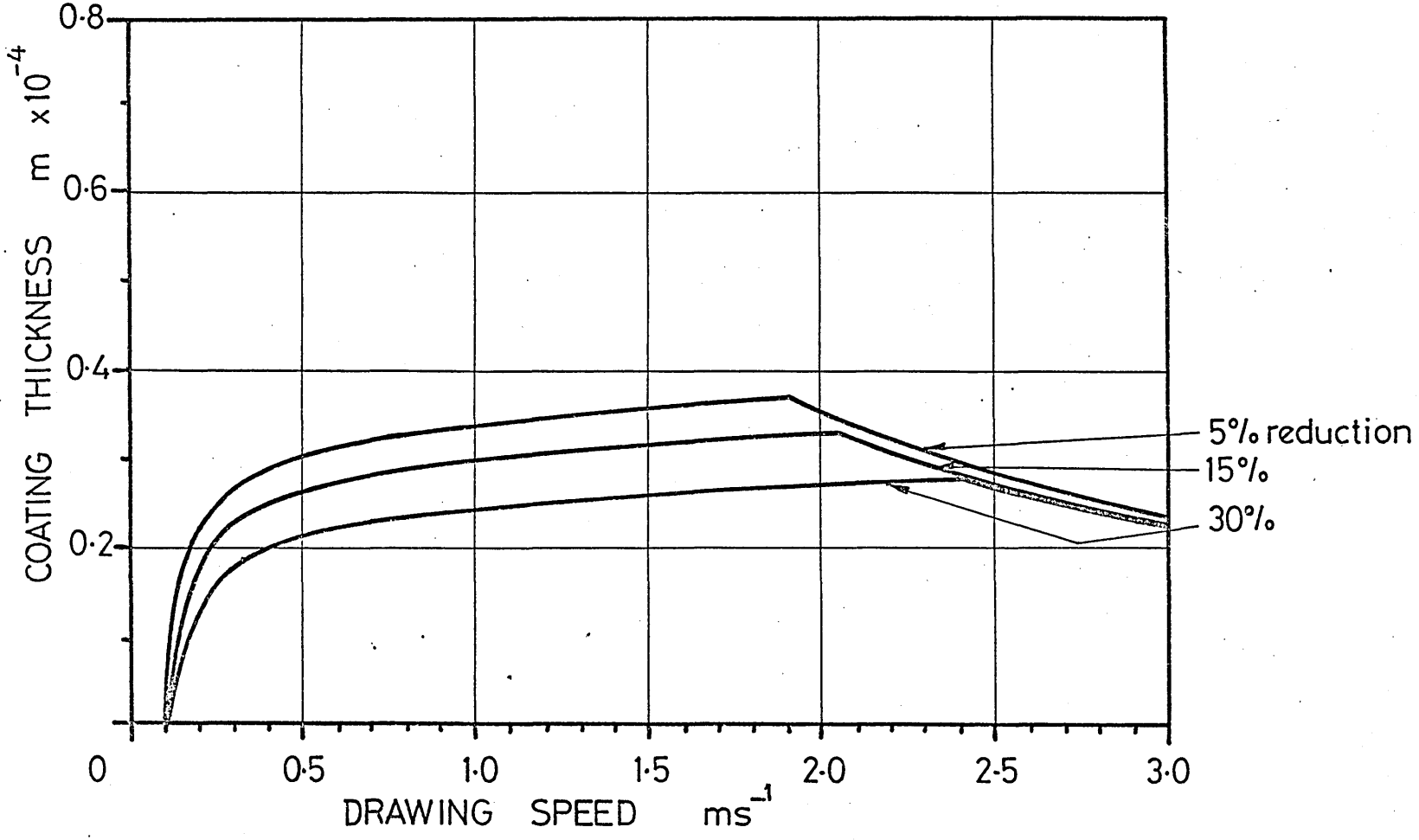

FIG 45 THEORETICAL VARIATION IN COAT THICKNESS DUE TO OMITTING STRAIN RATE SENSITIVITY

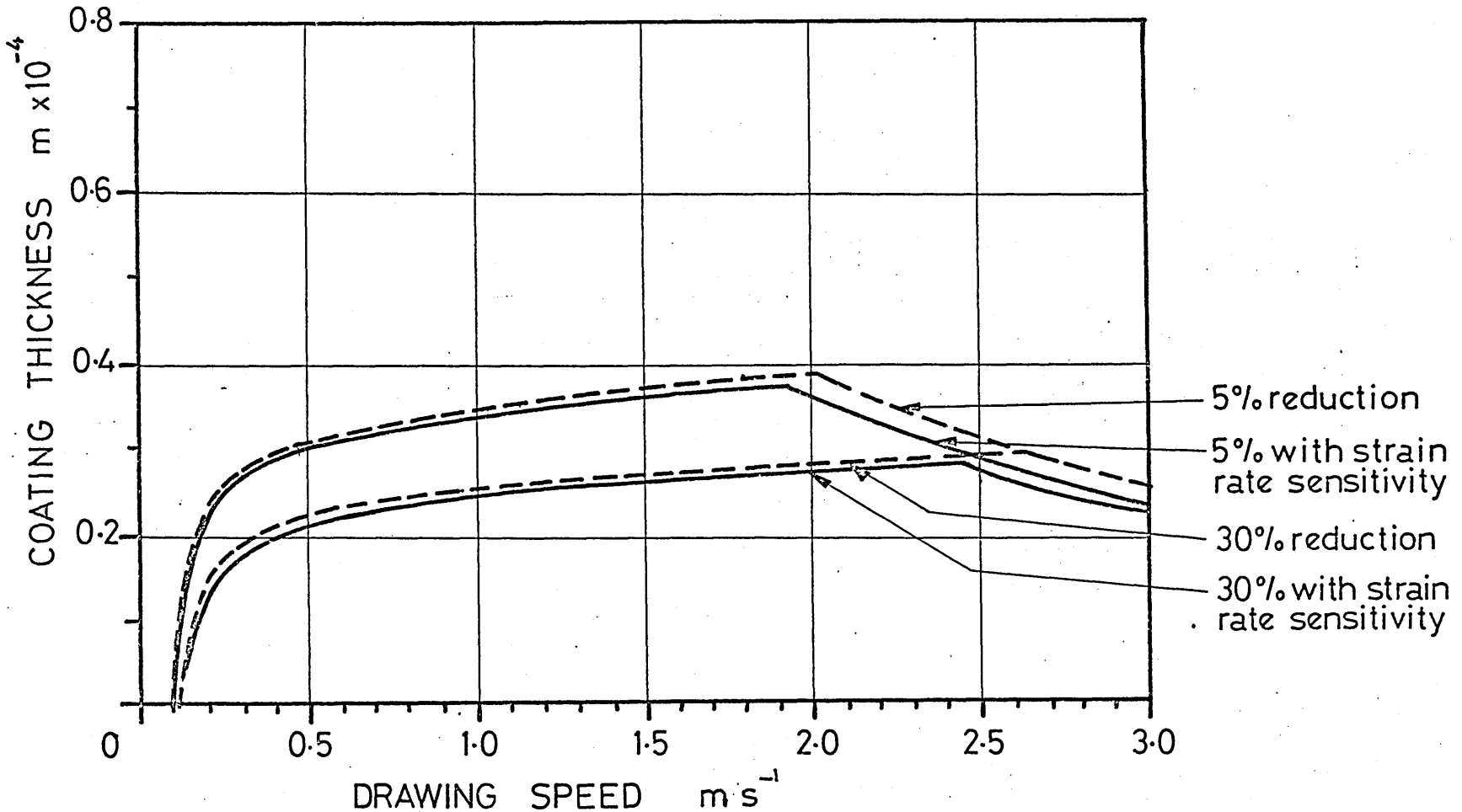

FIG 46a THEORETICAL VARIATION IN COAT THICKNESS DUE TO CHANGING THE DEFORMATION LENGTH

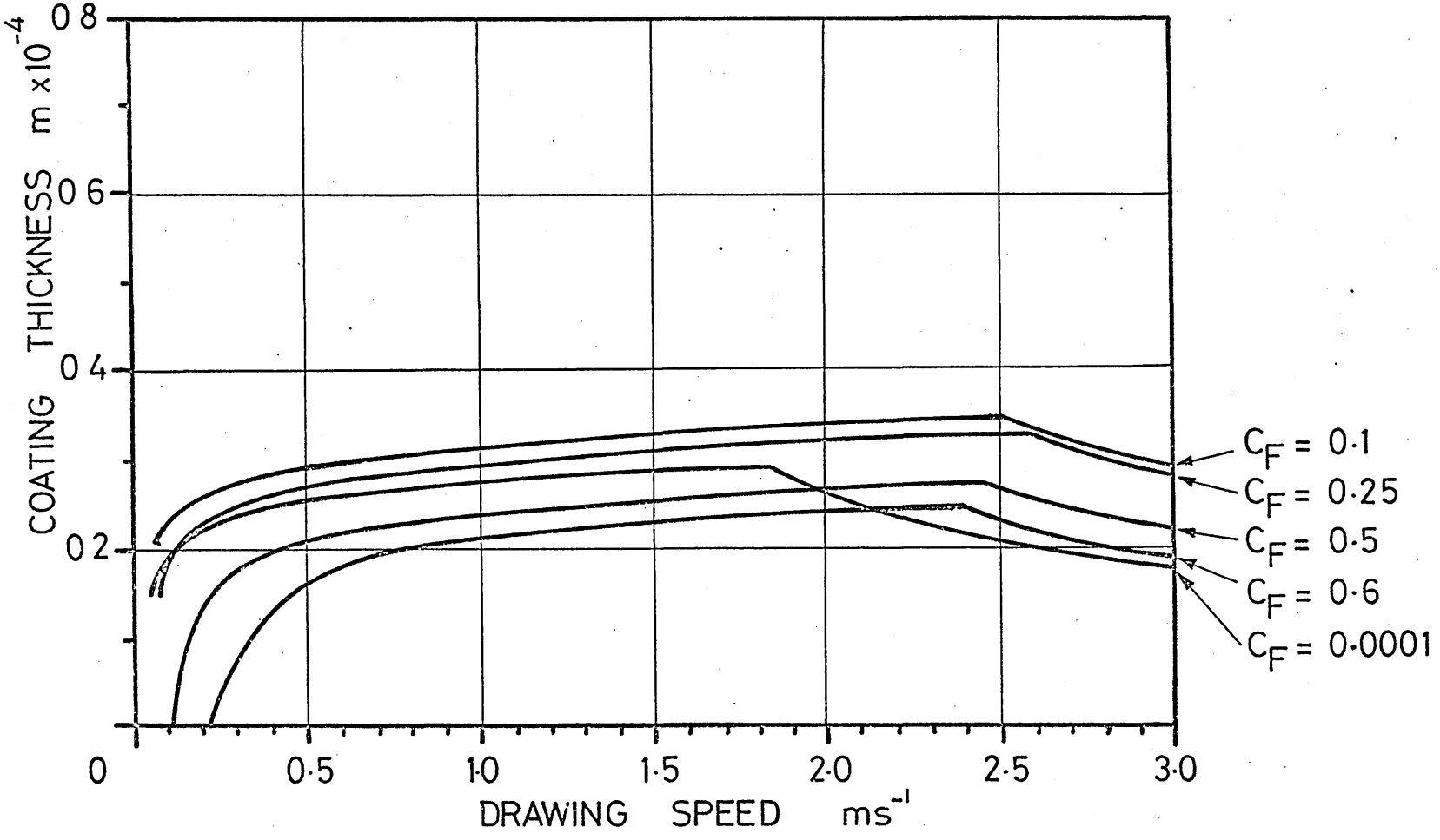

FIG 46b THEORETICAL VARIATION IN MAX. THICKNESS AND CRITICAL SPEED DUE TO CHANGING C_F

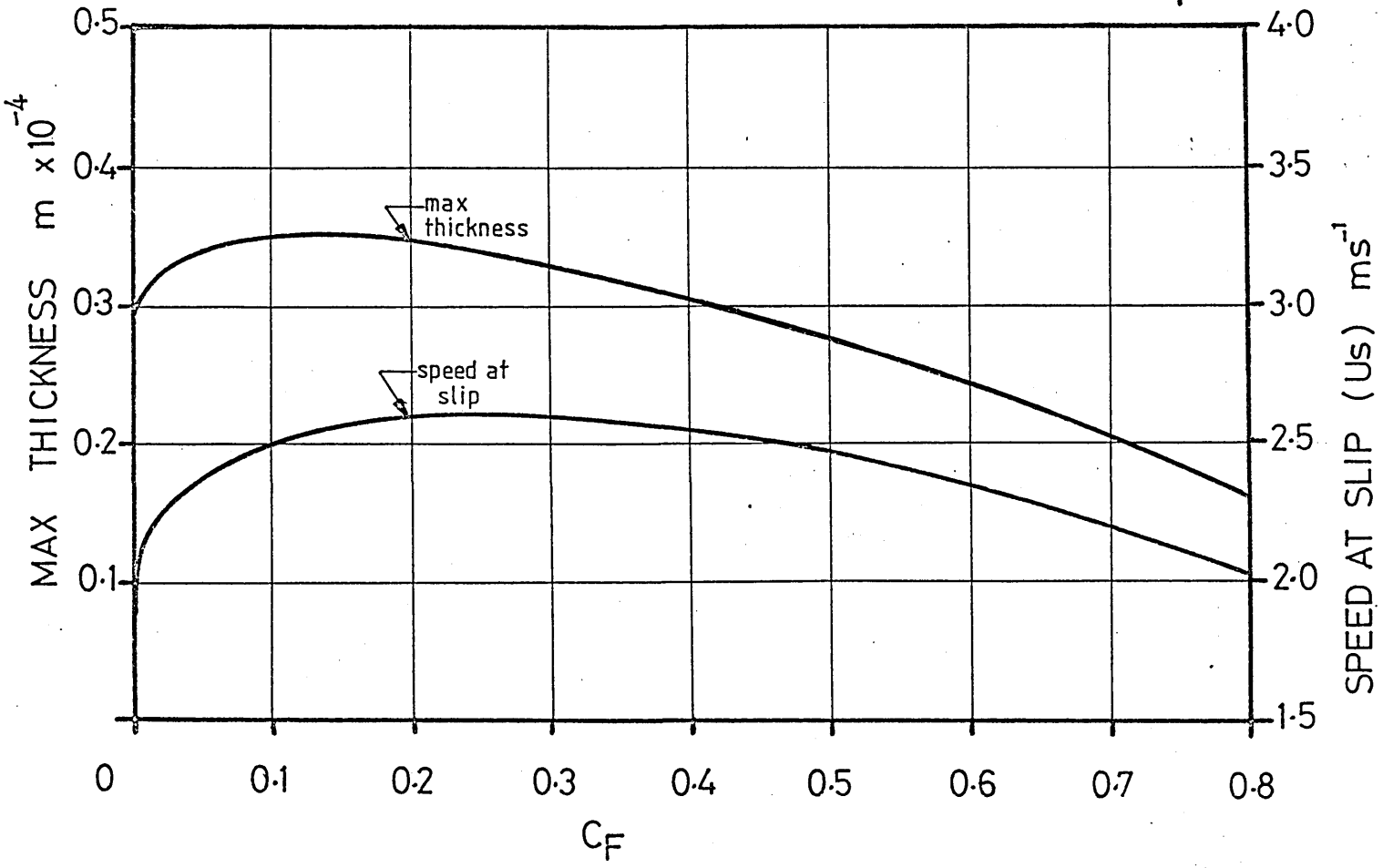

6.3 Theoretical Pressure Distributions.

The analysis enabled the pressure distributions of the polymer in the deformation zone to be determined. The distributions were computed for different parameters.

Fig 47a shows the distribution along the Christopherson tube when using a 30% reduction die for two speeds when:-

a) Assuming constant yield stress for the wire
b) Strain hardening of the wire is included
c) Strain rate sensitivity and strain hardening are included.

The deformation zone is between 0mm and 40mm along the Christopherson tube for $C_F = 0.5$ and $L = 0.08m$. A linear pressure distribution is assumed in the undeformed region of the Christopherson tube.

The curves show that pressure reduces as speed increases and that the strain rate sensitivity has more effect at high speeds (which is expected). The distribution at 2.5 ms^{-1} suggests that the pressure gradient in the undeformed region of the Christopherson tube is very small. The effects of speed on the pressure are more clearly seen by reference to Fig 47b which shows the pressure at specific points along the tube as drawing speed is altered. The points chosen coincide with those used in the experimental apparatus. The curves show that pressure reduces as speed is increased until critical speed is reached when the pressure remains constant. The effect of including the strain rate sensitivity of the wire is shown; the higher the speed, the further apart are the relevant curves.

The curves for 5% reduction (Figs 48a and 48b) show the same trends as 30% reduction but the pressures reached are proportionately lower and the pressure distribution has a slightly different shape.

6.4 Theoretical Stress Distributions in the Wire.

Figs 49a and 50a show the stress distributions in the wire along the Christopherson tube at two speeds, for 30% and 5% reductions respectively. The curves should be of interest and very useful for obtaining some estimate of the stress distribution since measurements of this parameter would be difficult to obtain in practice.

The stress in the undeformed region of the Christopherson tube is linear since it is directly related to the shear stress on the polymer. In the deformation region, the stress increases in an exponential manner as the wire approaches the die. The effect of including the strain rate sensitivity of the wire is to raise the stress slightly. Figs 49b and 50b show how the stress varies as speed is changed at a distance of 20mm from the die. The stress increases with speed until the critical shear stress of the polymer is reached when the stress remains constant. The effect of including the strain rate sensitivity of the wire is to increase stress and has more effect at the higher speeds.

It must be remembered that the curves in the preceding sections (6.2 -6.4) were computed assuming the wire deformed

within an effective die shape given by the equation:-

$$y = A + B(x)^{1/3}$$

at all times and that the length of deformed wire remained constant at $(C_F.L) = (0.5 \times 0.08)$ ie. 40mm from the die. It is appreciated that this may not be the case and that the deformed length would probably increase as speed increased. To this end, some method of determining the deformed length $(C_F.L)$ was investigated. A separate theory was postulated and is included in Chapter 7.

FIG 47a THEORETICAL PRESSURE DISTRIBUTION IN THE CHRISTOPHERSON TUBE ~30% REDUCTION

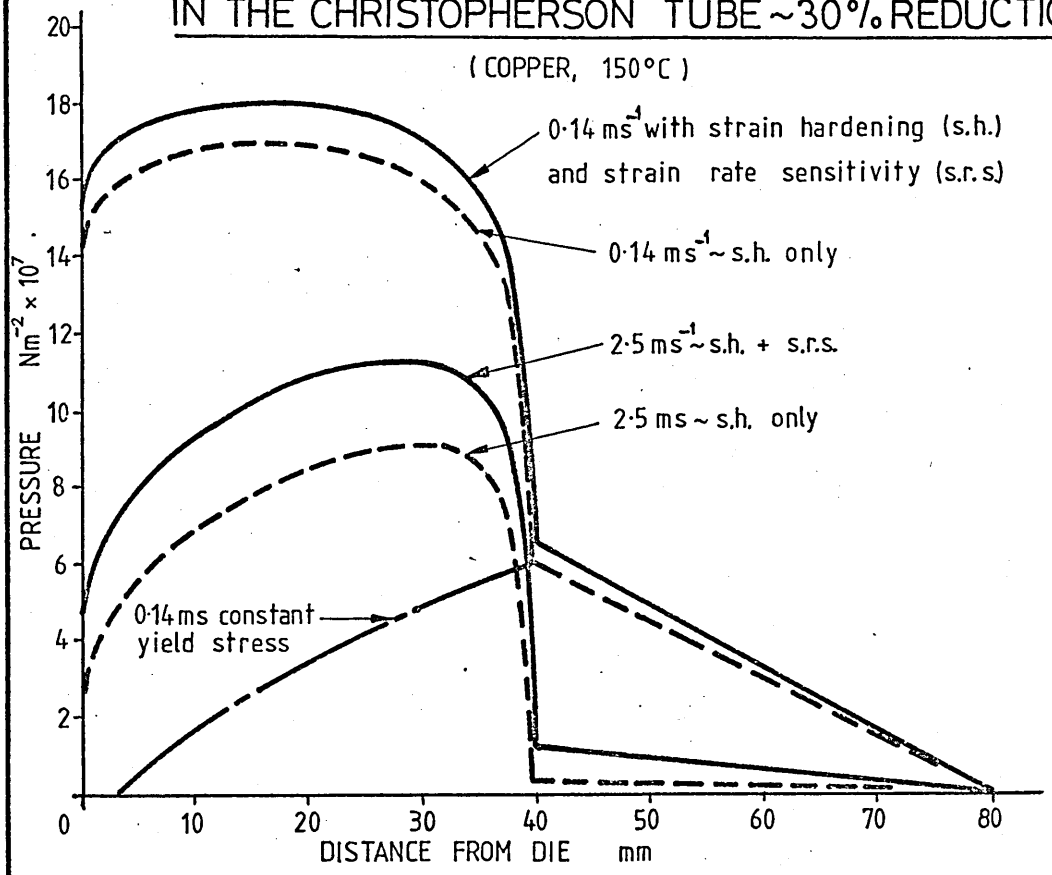

FIG 47b THEORETICAL PRESSURE DISTRIBUTION WHEN VARYING DRAWING SPEED ~30% REDUCTION

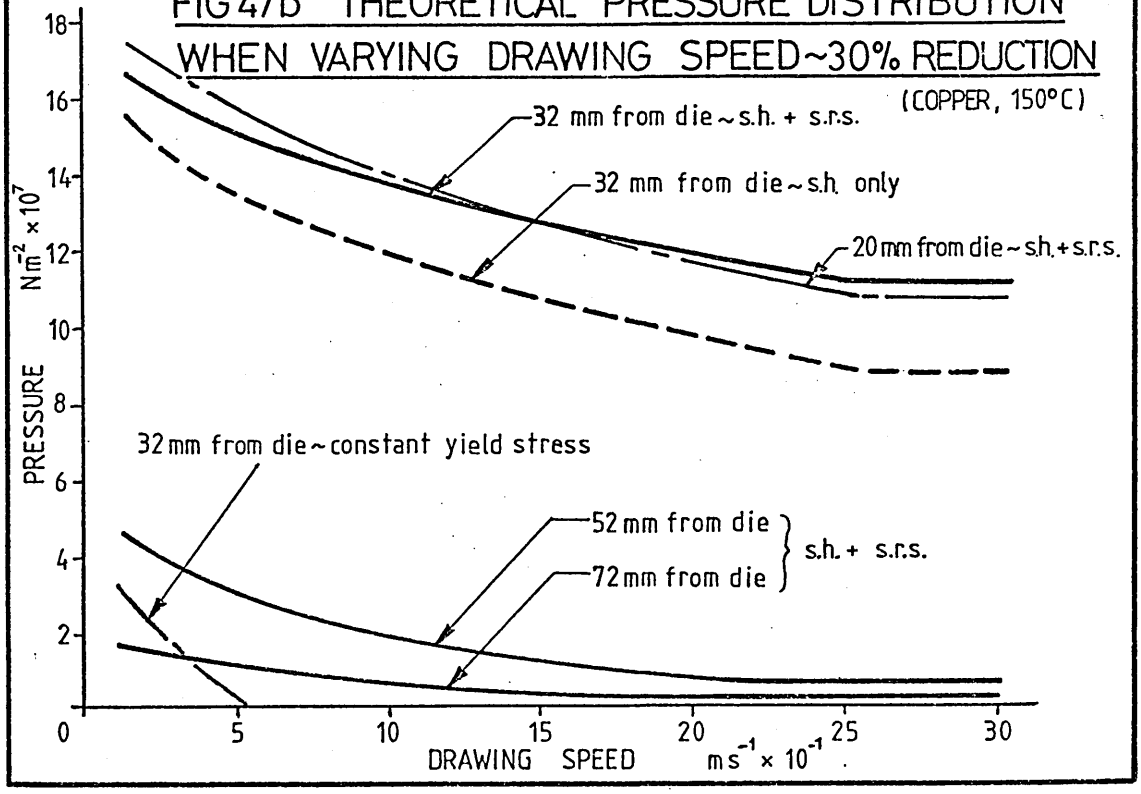

FIG 48a THEORETICAL PRESSURE DISTRIBUTION IN THE CHRISTOPHERSON TUBE ~ 5% REDUCTION

(COPPER, 150°C)

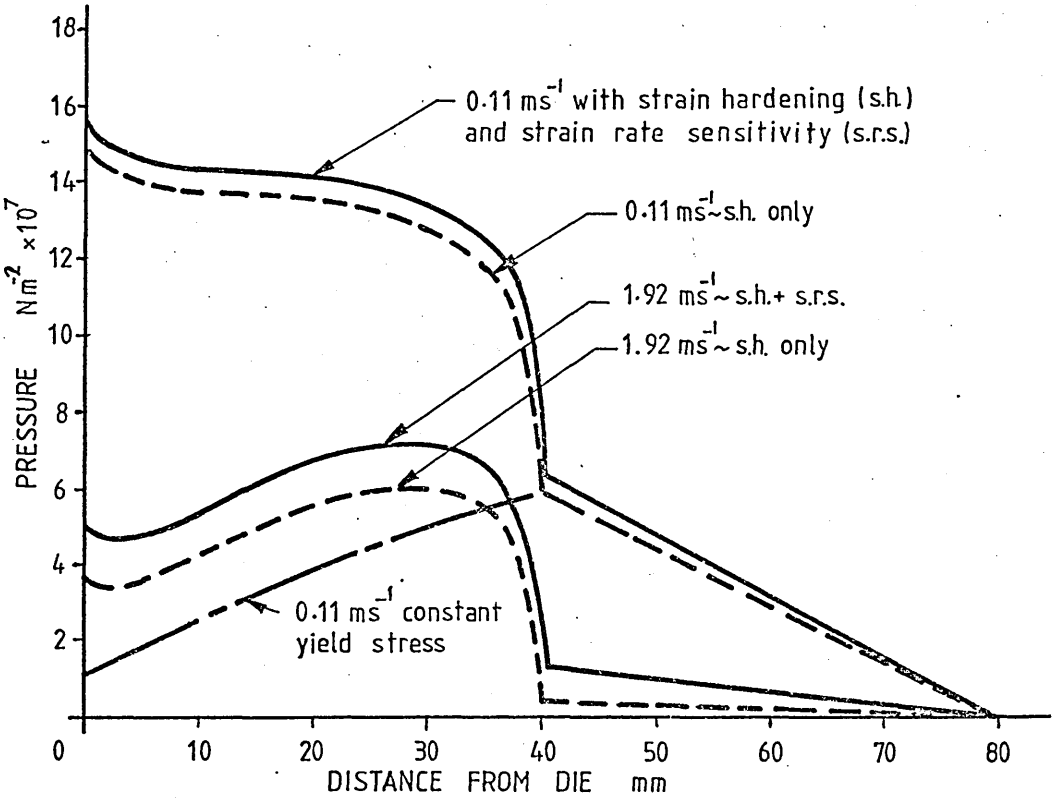

FIG 48b THEORETICAL PRESSURE DISTRIBUTION WHEN VARYING DRAWING SPEED ~ 5% REDUCTION

(COPPER, 150°C)

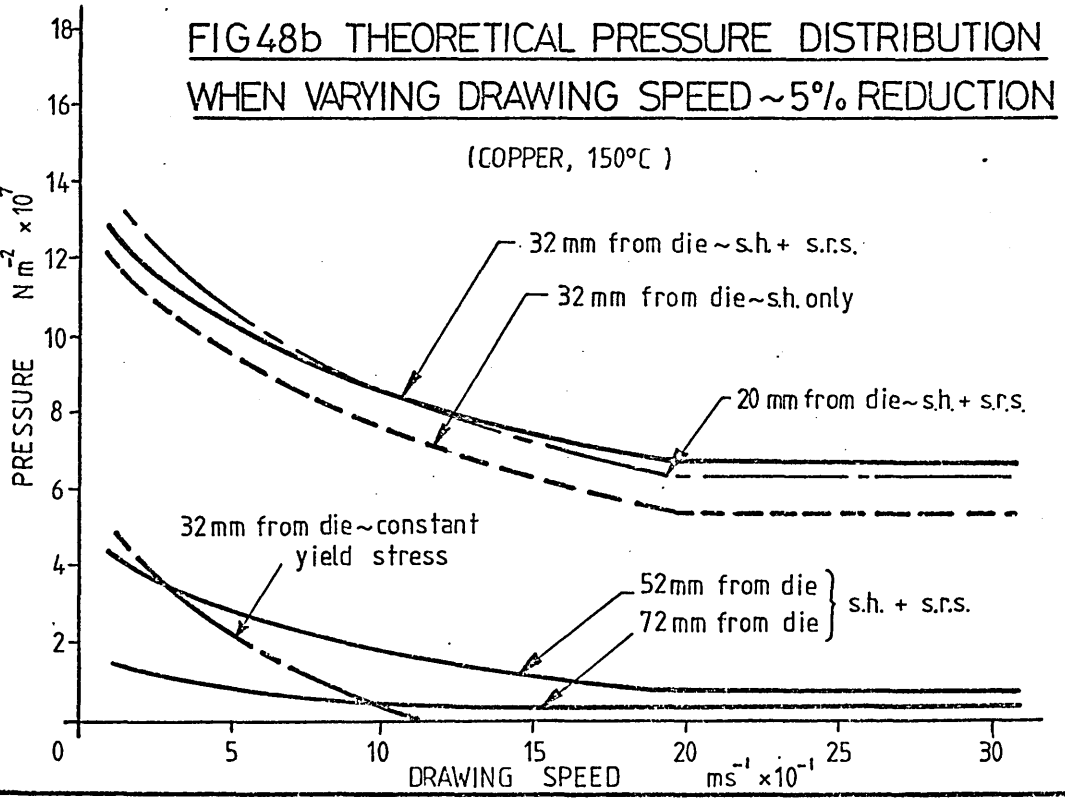

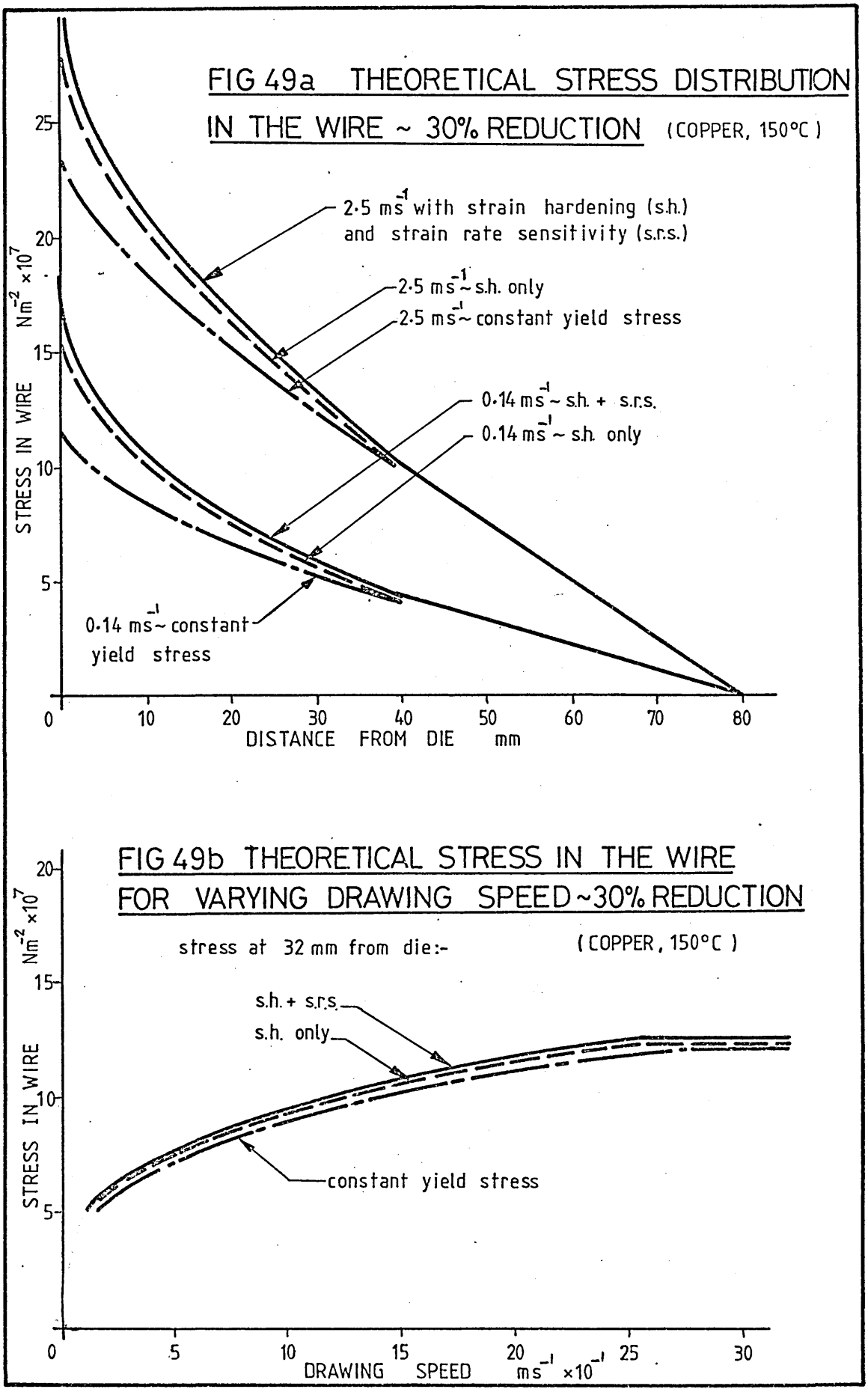
FIG 49a THEORETICAL STRESS DISTRIBUTION IN THE WIRE ~ 30% REDUCTION (COPPER, 150°C)
2·5 ms⁻¹ with strain hardening (s.h.) and strain rate sensitivity (s.r.s.)
2·5 ms⁻¹ ~ s.h. only
2·5 ms⁻¹ ~ constant yield stress
0·14 ms⁻¹ ~ s.h. + s.r.s.
0·14 ms⁻¹ ~ s.h. only
0·14 ms⁻¹ ~ constant yield stress
STRESS IN WIRE Nm⁻² ×10⁷
DISTANCE FROM DIE mm
FIG 49b THEORETICAL STRESS IN THE WIRE FOR VARYING DRAWING SPEED ~30% REDUCTION
stress at 32 mm from die:-
(COPPER, 150°C)
s.h. + s.r.s.
s.h. only
constant yield stress
STRESS IN WIRE Nm⁻² ×10⁷
DRAWING SPEED ms⁻¹ ×10⁻¹

FIG 50a THEORETICAL STRESS DISTRIBUTION IN THE WIRE ~ 5% REDUCTION (COPPER, 150°C)

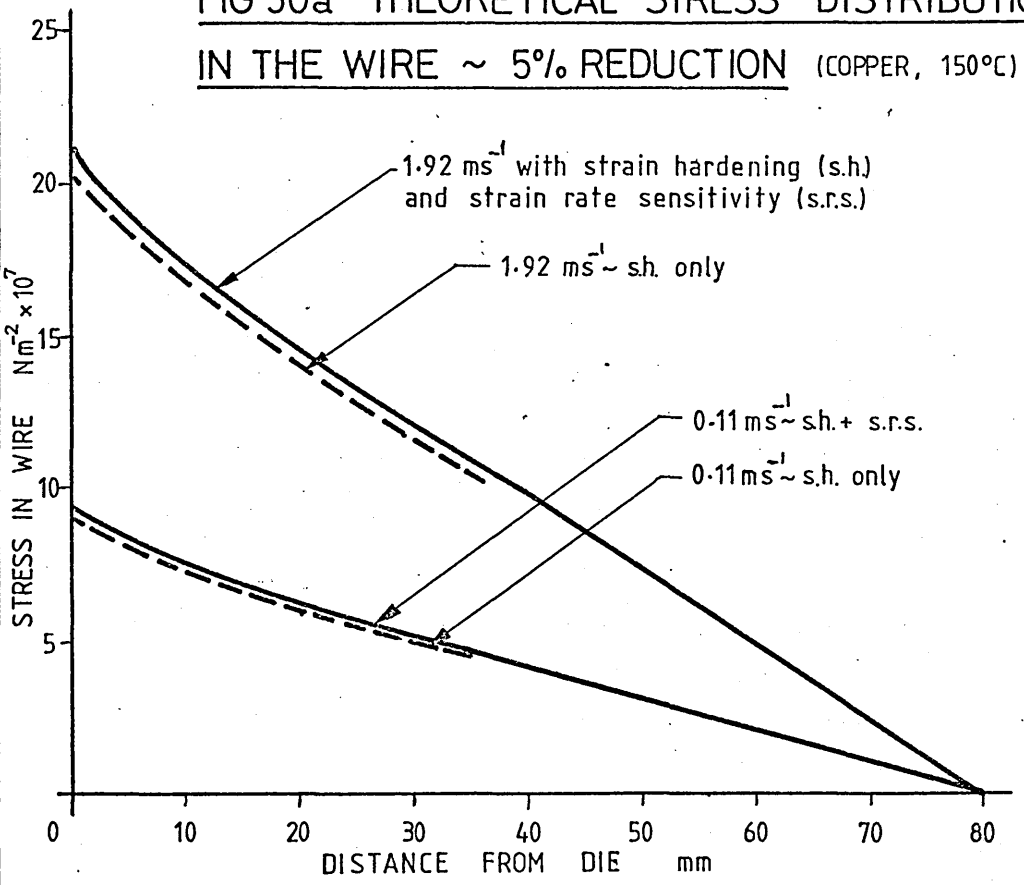

FIG 50b THEORETICAL STRESS IN THE WIRE FOR VARYING DRAWING SPEED ~ 5% REDUCTION

(COPPER, 150°C)

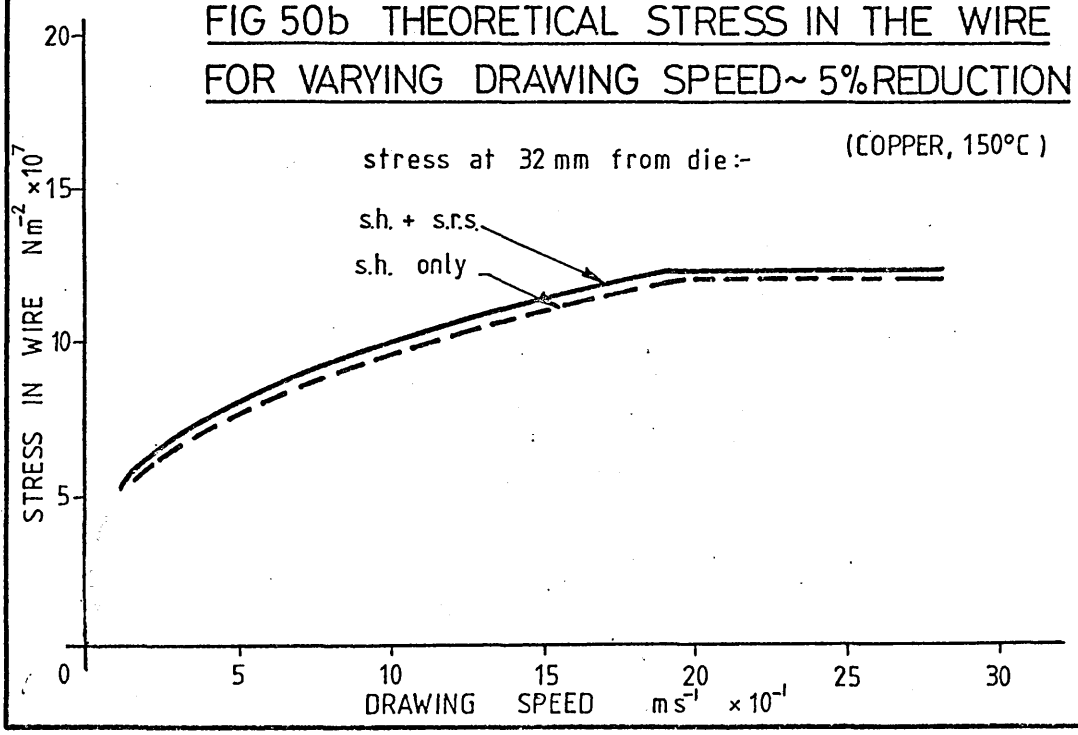

7.1 Introduction.

In Chapter 6 the results obtained from the theory outlined in Chapter 5 have been presented. One shortcoming of this theory was in the determination of the deformed length of wire, $C_F.L$. Common sense suggests that this length may vary with wire speed, but in the foregoing analysis, it was not possible to take this aspect into account. It was realised that if the boundary condition; $\tau = 0$ at $y' = h$ is applicable then a much simpler solution would be possible. It is known that for most fluids and processes, this boundary condition is not valid, however, solutions to equation (13) have shown that for the process considered here, this boundary condition is approximately true for almost all conditions. Fig 51 shows the solution to equation (13) in graphical form and compares them with those for a Newtonian fluid. The analysis for a Newtonian fluid is presented in Appendix II. Note that the curves for the present analysis show very small velocity gradients at $y' = h$ compared to those for a Newtonian analysis.

In this chapter an alternative solution developed using the above boundary condition is presented. This solution enables the length of the deformation zone within the Christopherson tube to be calculated.

FIG 51 THEORETICAL VELOCITY GRADIENTS IN THE GAP

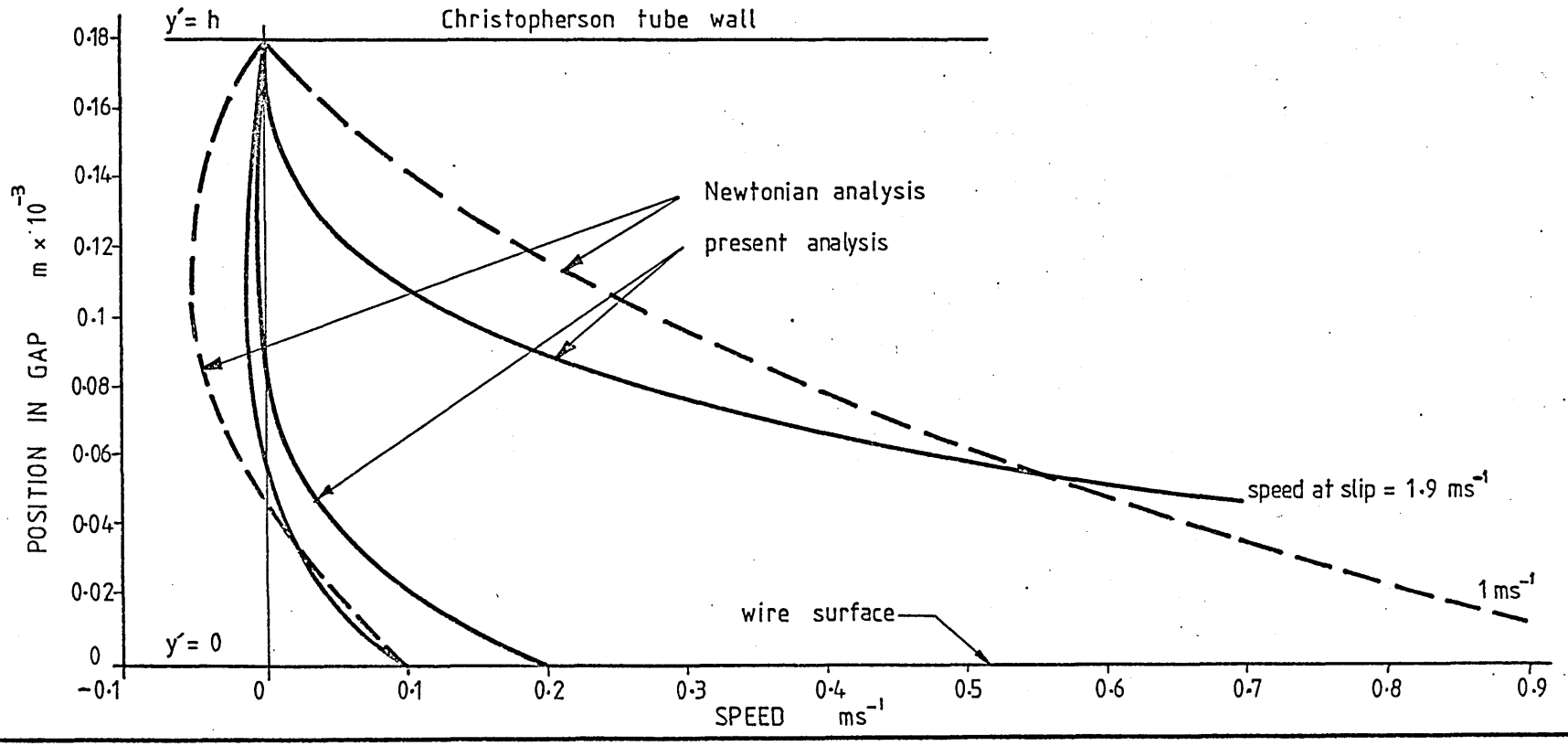

7.2 Analysis.

As before it is assumed that the fluid follows the equation;

$$\tau + k\tau^3 = \eta_o \frac{\partial v}{\partial y'} \qquad \ldots\ldots (9)$$

and equilibrium of the polymer melt in the tube gives:-

$$\frac{\partial p}{\partial x} = \frac{\partial \tau}{\partial y'} \qquad \ldots\ldots (10)$$

From equation (10);

$$\tau = p'y' + c \qquad \ldots\ldots (27)$$

where $p' = \frac{\partial p}{\partial x}$

Boundary conditions

at $y' = 0$; $\tau = \tau_c$, $v = U$ .... (a)

at $y' = h$; $\tau = 0$, $v = 0$ .... (b)

Note- for τ to be equal to zero, $\frac{\partial v}{\partial y'}$ must be equal to zero ie. there must be zero slope on the velocity profile at $y' = h$.

This is shown to be the case in Fig 51, the curves in which are drawn from solutions to equation (13).

From boundary condition (b):- $c = -p'h$

therefore,

$$\tau = p'(y' - h) \qquad \ldots\ldots (28)$$

Substituting for τ from equation (28) into equation (9) gives;

$$\frac{\partial v}{\partial y'} = \frac{p'(y'-h)}{\eta_o} + \frac{kp'^3(y'^3 - 3hy'^2 + 3h^2y' - h^3)}{\eta_o} .$$

Hence,

$$v = \frac{p'}{\eta_o}\left(\frac{y'^2}{2} + hy'\right) + \frac{kp'^3}{\eta_o}\left(\frac{y'^4}{4} - hy'^3 + \frac{3}{2}h^2y'^2 - h^3y'\right) + \text{constant}$$

but; at $y' = 0$, $v = U$ therefore constant $= U$.

Hence,

$$v = \frac{p'}{\eta_o}\left(\frac{y'^2}{2}+hy'\right) + \frac{kp'^3}{\eta_o}\left(\frac{y'^4}{4}-hy'^3+\frac{3}{2}h^2y'^2-h^3y'\right) + U \qquad \ldots\ldots (29)$$

Also at $y' = h$, $v = 0$ hence from equation (29):-

$$0 = \frac{p'}{\eta_o}\left(\frac{h^2}{2}-h^2\right) + \frac{kp'^3}{\eta_o}\left(\frac{h^4}{4} - h^4 + \frac{3h^4}{2} - h^4\right) + U$$

Therefore;

$$0 = U - \frac{p'h^2}{2\eta_o} - \frac{kp'^3h^4}{4\eta_o} \qquad \ldots\ldots (30)$$

Flow rate $Q = \int_o^h v\, dy'$; hence :-

$$Q = \frac{p'}{\eta_o}\left(\frac{h^3}{6}-\frac{h^3}{2}\right) + \frac{kp'^3}{\eta_o}\left(\frac{h^5}{20}-\frac{h^5}{4}+\frac{h^5}{2}-\frac{h^5}{2}\right) + Uh$$

therefore;

$$Q = Uh - \frac{p'h^3}{3\eta_o} - \frac{kp'^3h^5}{5\eta_o} \qquad \ldots\ldots (31)$$

As before, the dependance of viscosity on pressure may now be included;

$$\eta_o = \eta_a + ap - bp^2 - c$$

but, $p = p' L_{CT}$

therefore,

$$\eta_o = \eta_a + aL_{CT}p' - bL_{CT}^2 p'^2 - c$$

Hence equation (30) becomes;

$$0 = U - \frac{p'h^2(1 + \frac{kp'^2h^2}{2})}{2(\eta_a + aL_{CT}p' - bL_{CT}^2p'^2 - c)} \qquad \ldots\ldots (32)$$

Tresca or von Mises yield criteria give;

$$Y = p + \sigma_x \qquad \text{(as before)}$$

and equilibrium of the wire in the tube gives;

$$\sigma_x = \frac{4\tau_c L_{CT}}{D_1} \qquad \text{(as before)}.$$

Hence;

$$Y = p + \frac{4\tau_c L_{CT}}{D_1}$$

Assuming a linear pressure gradient in the Christopherson tube; ie. $p' = \frac{p}{L_{CT}}$

gives;

$$\frac{Y}{L_{CT}} = \frac{4\tau_c}{D_1} + p' .$$

Therefore;

$$\tau_c = \left(\frac{Y}{L_{CT}} - p'\right)\frac{D_1}{4}$$

but $\tau_c = -p'h$ (from boundary condition (a) in equation (27)).

Hence, $p'h = -\left(\frac{Y}{L_{CT}} - p'\right)\frac{D_1}{4}$

therefore,

$$p' = \frac{YD_1}{L_{CT}(D_1 - 4h)}$$

Note; this is the pressure gradient required to give yield and is independant of U.

or $$L_{CT} = \frac{YD_1}{p'(D_1 - 4h)}$$

..... (33)

and $$C_F = \left(\frac{L - L_{CT}}{L}\right)$$

Equation (32) may be solved simultaneously with equations (33) to give p' and C_F for each wire speed. Equation (31) may then be solved to give coating thickness since $h_d = \frac{Q}{U_d}$ and τ_c may be found knowing $\tau_c = -p'h$ for solutions of stress equation (7) as before.

7.3 Results from the Analysis.

A computer program was written to solve equations (32) and (33) simultaneously giving the deformed length of wire $C_F.L$ for each wire speed. Equation (31) was then solved to give coat thickness and stress equation (8) was solved to give the stress and pressure distributions along the length of the Christopherson tube.

The equations are summarised below in the order that they require to be solved.

$$0 = U - \frac{p'h^2(1 + \frac{kp'^2h^2}{2})}{2} \qquad \ldots\ldots (32)$$
$$(\eta_a + aL_{CT}p' - bL_{CT}^2p'^2 - c)$$

$$L_{CT} = \frac{YD_1}{p'(D_1 - 4h)} \qquad \ldots\ldots (33)$$

$$S = 1 + \left(\frac{\bar{\varepsilon}_m}{N}\right)^{1/T} \quad \text{where} \quad \bar{\varepsilon}_m = \frac{UD_1^2}{(L-L_{CT})}\left(\frac{1}{D_2^2} - \frac{1}{D_1^2}\right)$$

these need to be solved simultaneously since p' and L_{CT} are unknown.

$$Q = Uh - \frac{p'h^3}{3\eta_o} - \frac{kp'^3h^5}{5\eta_o} \qquad \ldots\ldots (31)$$

$$h_d = \frac{Q}{U_d} \qquad \ldots\ldots (25)$$

$$\tau_c = -p'h$$

$$\sigma_x = 2Y_oS\left(\ln\frac{D_1}{D}\right) + \frac{2KS}{n+1}\left(\ln\frac{D_1}{D}\right)^{n+1} + \frac{6\tau_c}{B^3}\left(\left(\frac{D_1^2 - D^2}{8}\right) + A(D - D_1) + \right.$$

$$\left. + A^2.\ln\left(\frac{D_1}{D}\right)\right) + \frac{4\tau_c L_{CT}}{D_1} \qquad \ldots\ldots (7)$$

$p = Y - \sigma_x$ where $Y = (Yo + K(\ln\frac{D_1}{D})^n)S$

The development and listing of the computer program is given in Appendix I.

7.3.1 Theoretical Christopherson Tube Length.

The theoretical length of the Christopherson tube was computed, the results being shown in Figs 52a and 52b. Fig 52a shows the length of tube necessary for varying drawing speeds with 30% and 5% wire reductions and with and without the effects of strain rate sensitivity. It is evident that a 5% reduction would require a shorter tube length than 30% and the inclusion of strain rate sensitivity would increase the length required. Since, in practice, the Christopherson tube length is fixed, the length of the deformation region ($C_F.L$) is altered as the drawing speed is changed. Note that at very low drawing speeds the predicted tube length is greater than the actual tube length. The interpretation of this is that a coat cannot occur since the hydrodynamic pressure generated is insufficient to cause yielding before the die.

Fig 52b shows the tube length required when using an initial yield stress of 3.4×10^8 Nm^{-2} (18/8 stainless steel). The theory suggests that a coat is not possible at any speed with the tube length used, and that a minimum length of 110mm would be required.

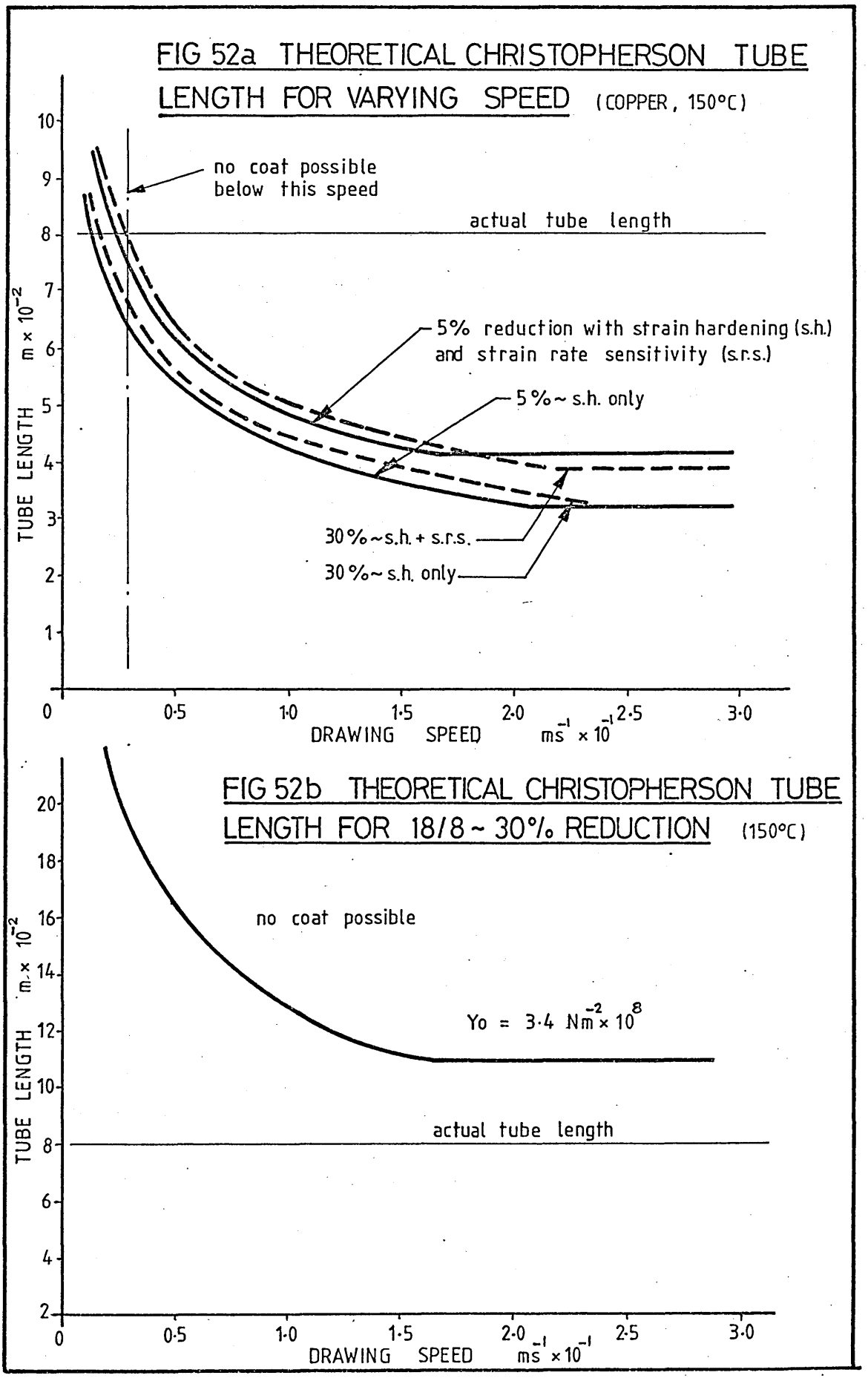
FIG 52a THEORETICAL CHRISTOPHERSON TUBE LENGTH FOR VARYING SPEED (COPPER, 150°C)
no coat possible below this speed
actual tube length
5% reduction with strain hardening (s.h.) and strain rate sensitivity (s.r.s.)
5% ~ s.h. only
30% ~ s.h. + s.r.s.
30% ~ s.h. only
TUBE LENGTH m × 10⁻²
DRAWING SPEED ms⁻¹ × 10⁻¹
FIG 52b THEORETICAL CHRISTOPHERSON TUBE LENGTH FOR 18/8 ~ 30% REDUCTION (150°C)
no coat possible
Yo = 3·4 Nm⁻² × 10⁸
actual tube length
TUBE LENGTH m × 10⁻²
DRAWING SPEED ms⁻¹ × 10⁻¹

7.3.2 Results for Coating Thickness.

Fig 53 shows the theoretical coat thickness possible on the wire as the speed is changed for wires of various strengths. The standard input values ($Yo = 1 \times 10^8$ Nm^{-2}) produce a curve with two zones. Firstly, below the critical shear stress of the polymer, the coat thickness remains essentially constant. This does not follow the previous theory, where the coat thickness was predicted to increase as the speed increased. The reason for this difference lies in the fact that the length of the deformation zone in this modified theory is allowed to vary and hence the pressure reached at the commencement of deformation will be constant. This is substantiated by other results (see Appendix I) which show that the viscosity of the polymer melt does not vary widely in this zone. The second zone follows the previous theory, whereby the coat thickness reduces for increasing speed above the critical shear stress value of the polymer.

The effect of changing the initial yield stress of the wire material is the same as before; ie. the greater the yield, the lower the speed at which critical flow is reached and the smaller the maximum thickness possible.

Fig 54 shows the effects of changing the gap between the wire and the Christopherson tube on coating thickness. The effects here do not appear to be the same as the previous theory. As gap increases, the maximum coat thickness also increases. In the previous theory, further increases in gap from that used in practice caused a decrease in coat thickness. In this modified theory, the length of the Christopherson

tube is seen to increase as the gap increase, maintaining a high length to diameter ratio. For large gaps, however, the length of the Christopherson tube required exceeds that used in practice, which means that the thickness would, in fact, reduce as the gap is increased.

Fig 55 shows the effects of changing the initial viscosity on the coating thickness. The effects are the same as in the previous theory; ie. for a greater initial viscosity the critical speed is lower and hence the coating thicknesses are also smaller. The effects of changing the shear constant and pressure coefficients were not investigated since a change in these parameters may cause the fluid to act in a Newtonian manner and the assumptions used for this analysis would then become invalid.

Fig 56 shows the effects of changing die size and neglecting the strain rate sensitivity of the wire on the coat thickness. The effects are the same as those predicted by the previous theory; ie. the greater the reduction, the smaller the coating thickness, and neglecting the strain rate sensitivity of the wire increases the coat thickness.

FIG 53 THEORETICAL VARIATION IN COAT THICKNESS DUE TO CHANGING INITIAL YIELD STRESS OF WIRE

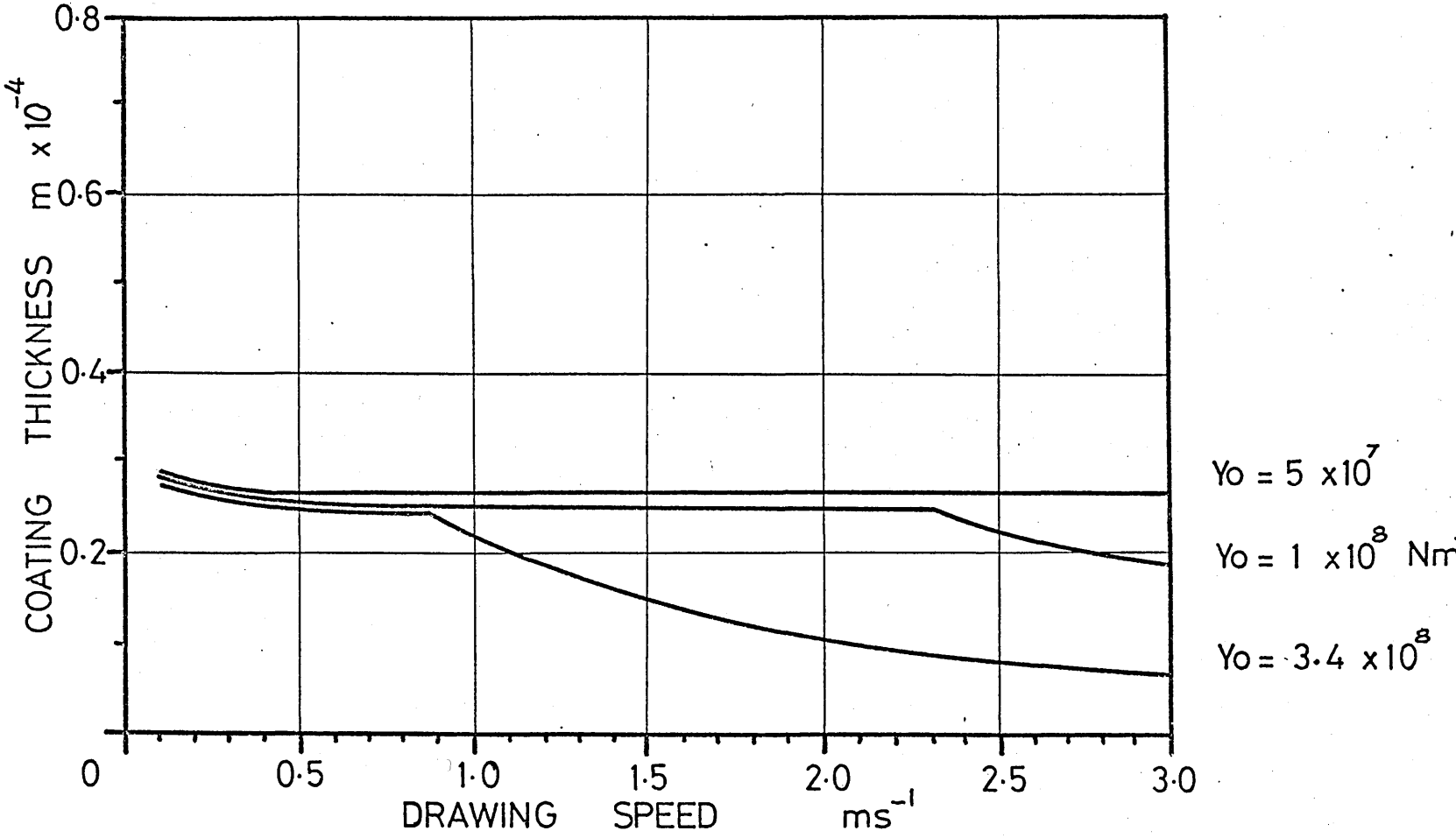

FIG 54 THEORETICAL VARIATION IN COAT THICKNESS DUE TO CHANGING GAP

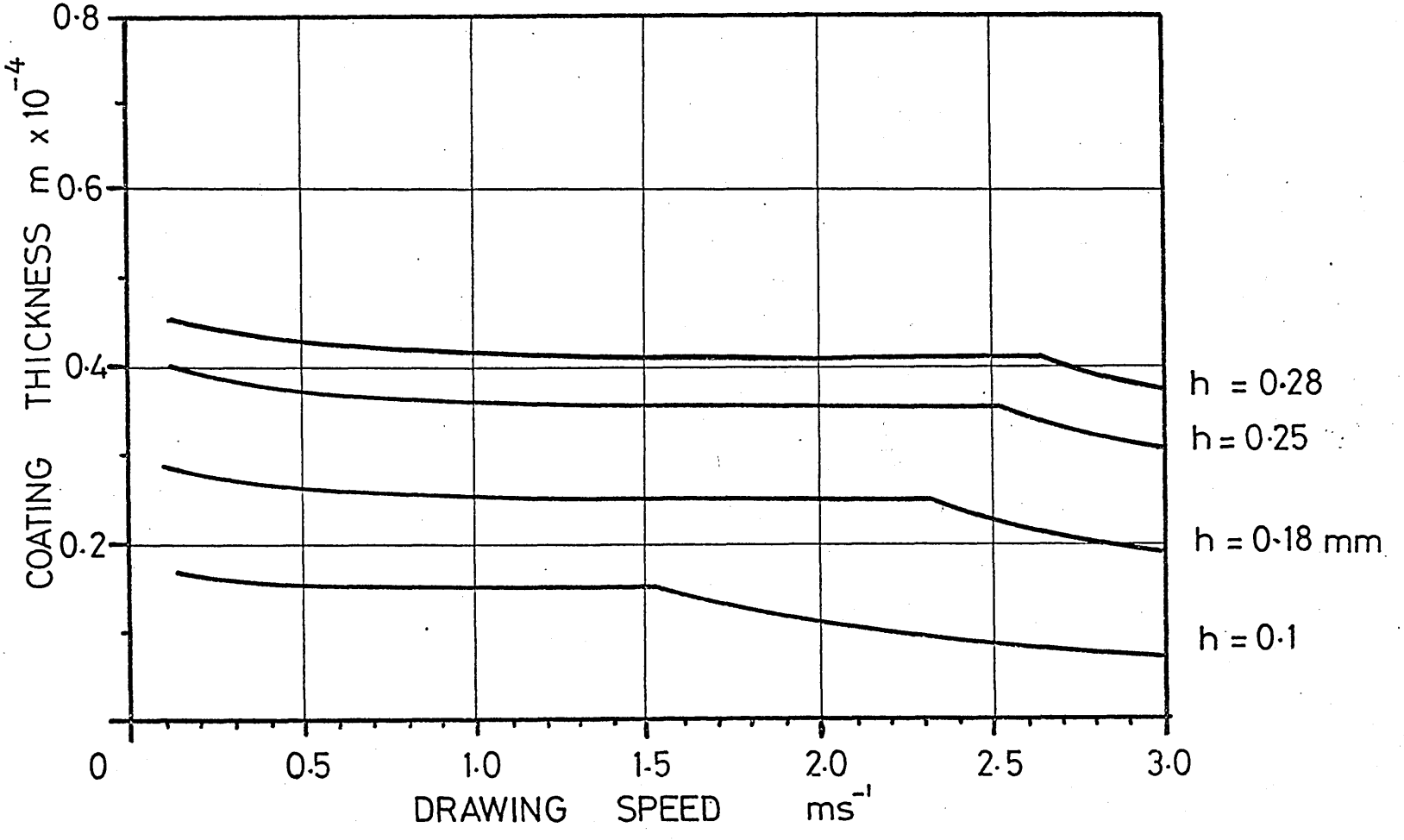

FIG 55 THEORETICAL VARIATION IN COAT THICKNESS DUE TO CHANGING INITIAL VISCOSITY

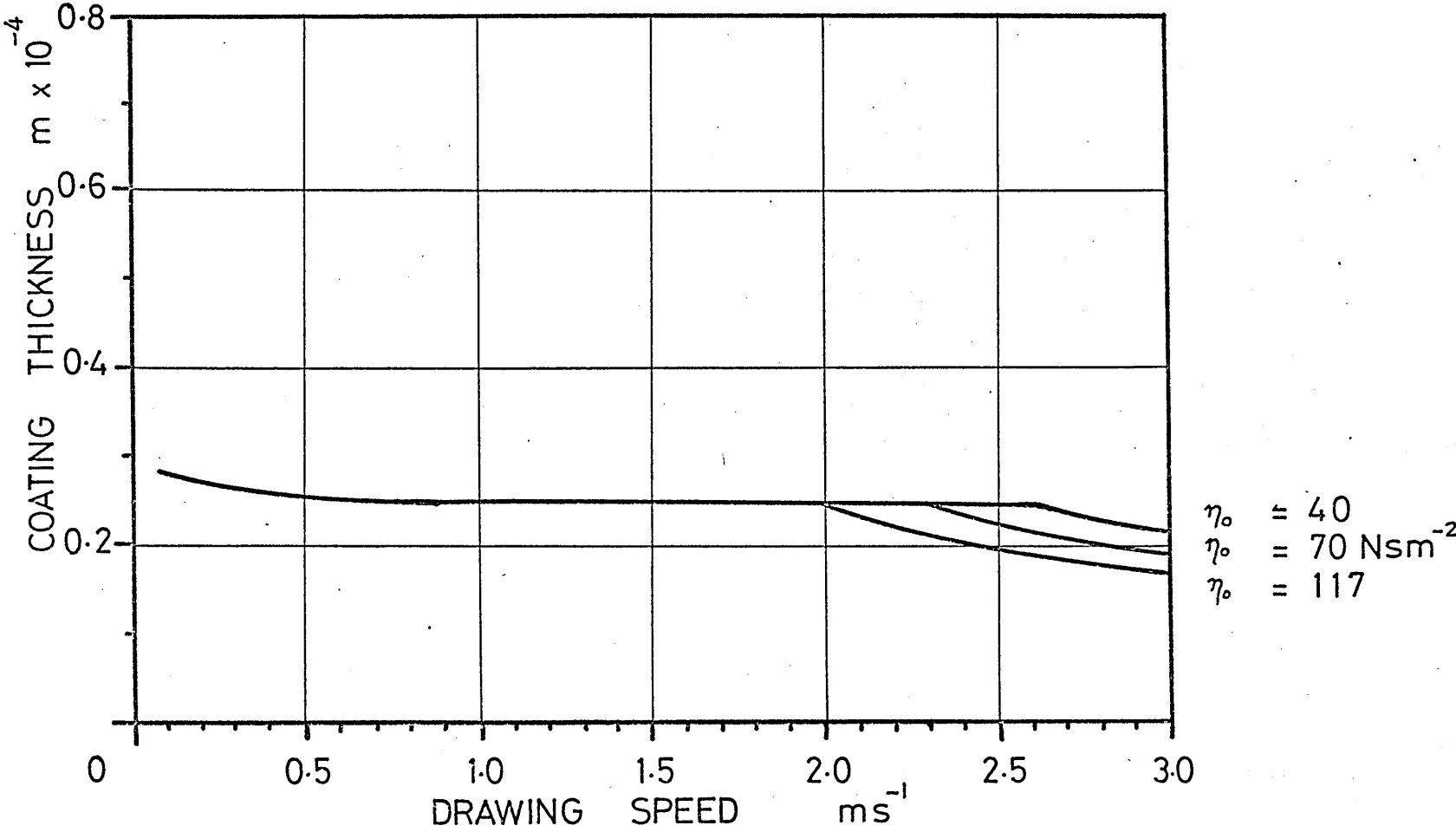

FIG 56 THEORETICAL VARIATION IN COAT THICKNESS DUE TO CHANGING DIE SIZE

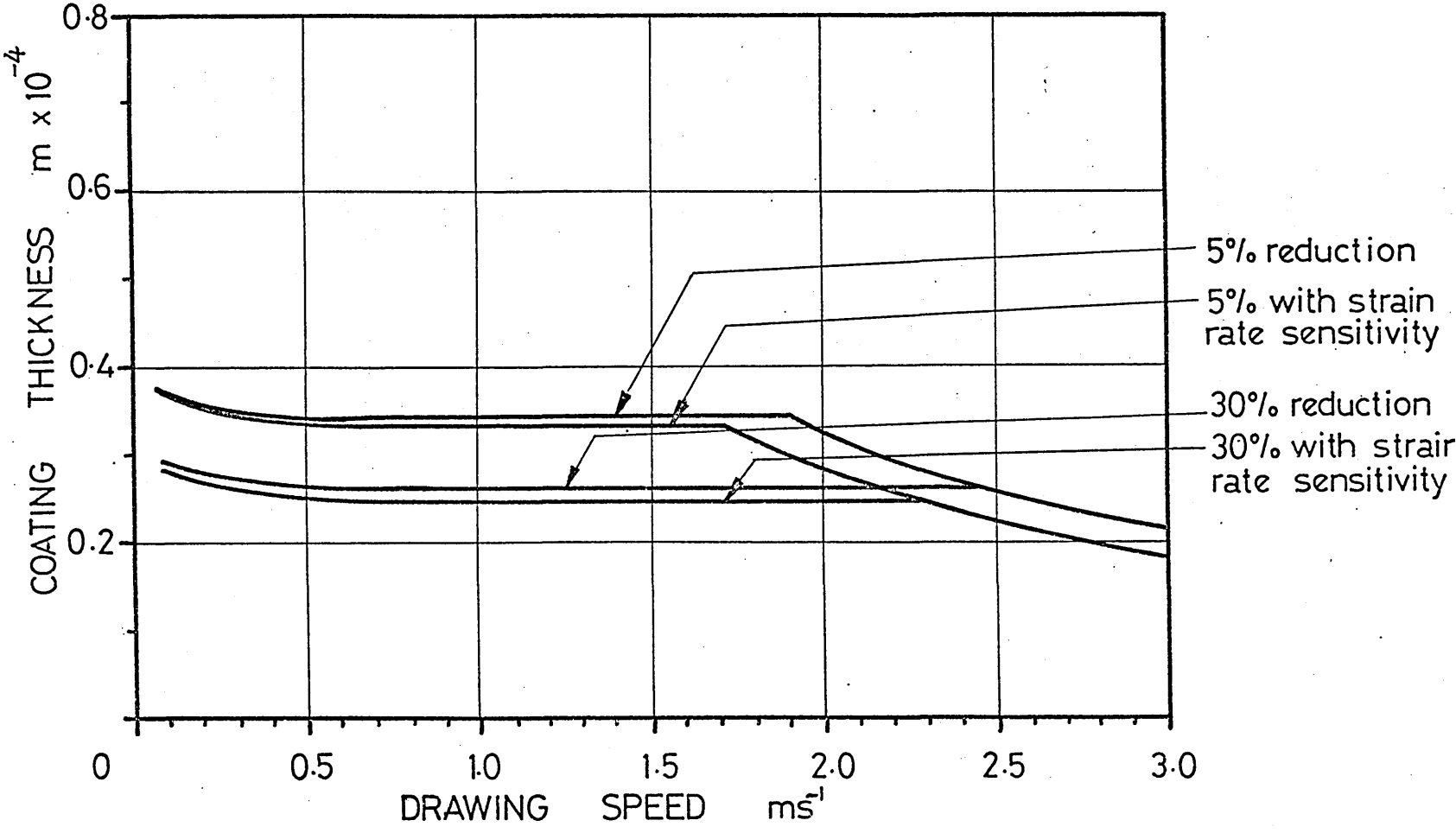

7.3.3 Results for Pressure Distributions.

Figs 57 and 58 show the pressure distributions in the Christopherson tube for 30% and 5% reductions respectively. These may be compared with Figs 47 and 48 from the previous analysis.

The most obvious difference between the two theories is the effect of the change in deformed length, $C_F.L$. The modified theory presented here gives pressure curves for which the position of commencement of deformation changes with drawing speed. This causes the position of transition between linear pressure in the Christopherson tube and deformation pressure to move away from the die as the speed is increased. These effects cause pressure at any point to increase as the speed is increased, whereas the previous theory showed a reduction in pressure as the speed was increased.

It must be noted that when the deformation length in this modified theory is the same as in the previous theory, the same results are obtained. This reinforces the validity of the assumptions made in the analysis.

7.3.4 Results of Stress Distributions.

Figs 59 and 60 show the stress distribution in the wire along the Christopherson tube as the drawing speed is varied. These may be compared with Figs 49 and 50 from the previous theory. Only very slight differences are noticeable.

FIG 57a THEORETICAL PRESSURE DISTRIBUTION IN THE CHRISTOPHERSON TUBE ~ 30% REDUCTION

(COPPER, 150°C)

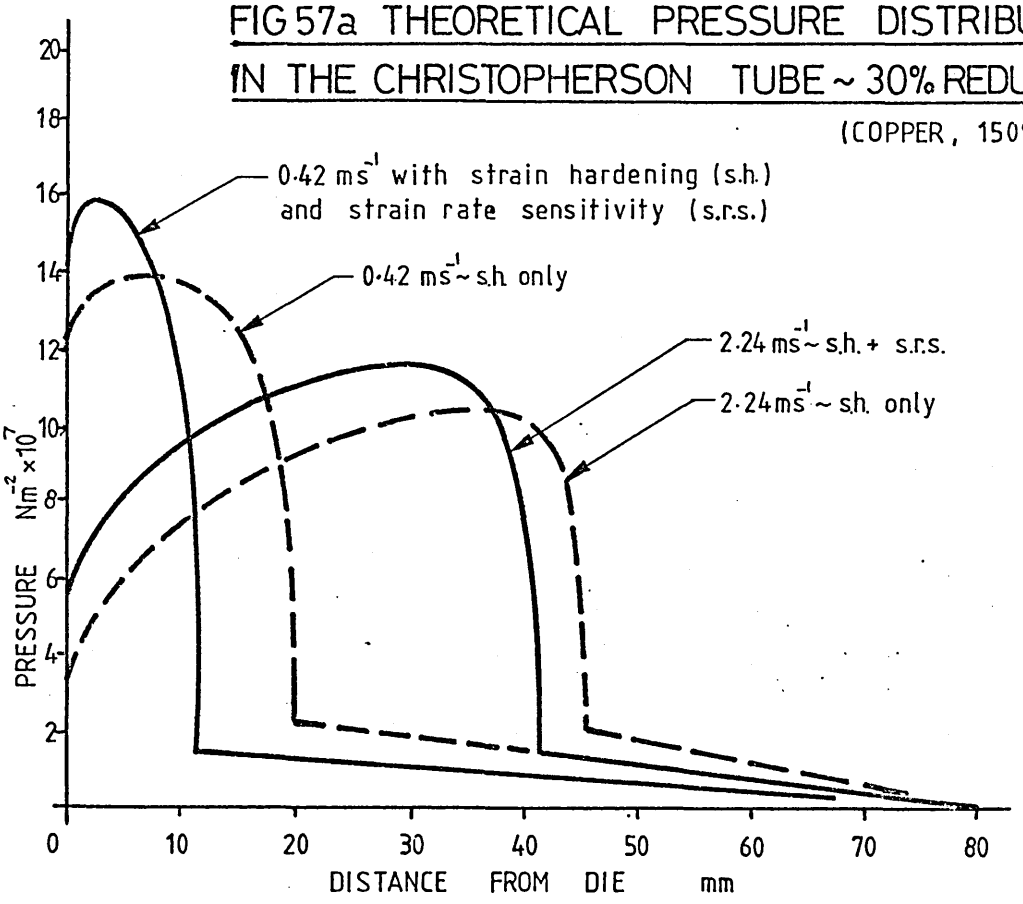

FIG 57b THEORETICAL PRESSURE DISTRIBUTION FOR VARYING DRAWING SPEED ~ 30% REDUCTION

(COPPER, 150°C)

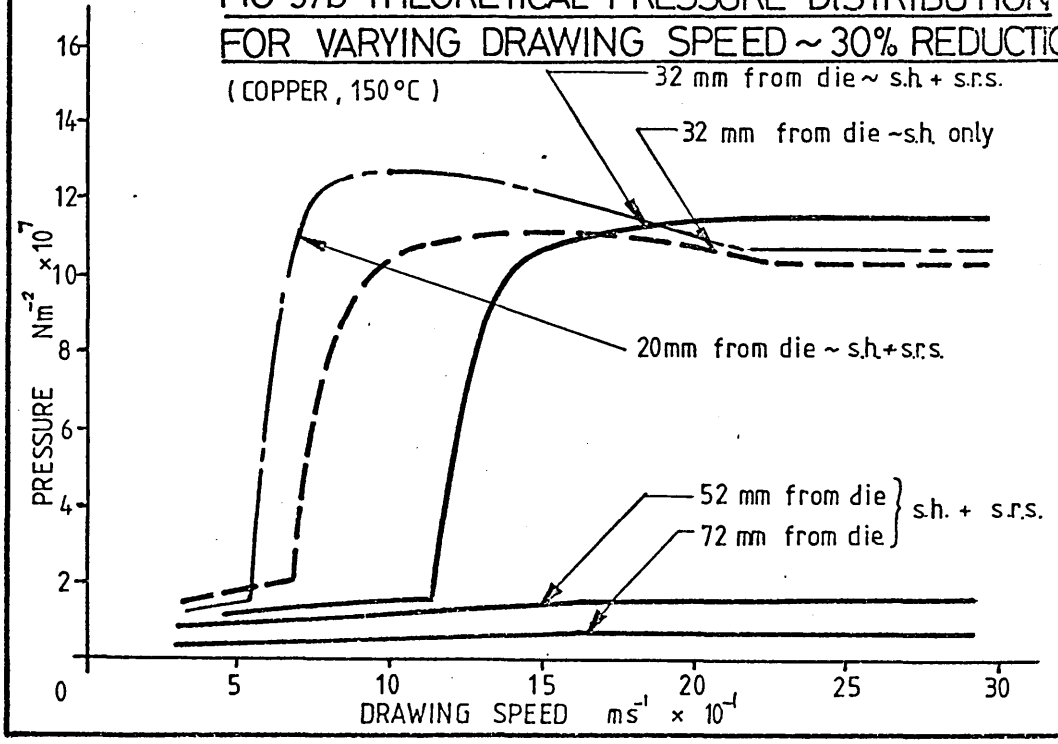

FIG 58a THEORETICAL PRESSURE DISTRIBUTION IN THE CHRISTOPHERSON TUBE ~ 5% REDUCTION

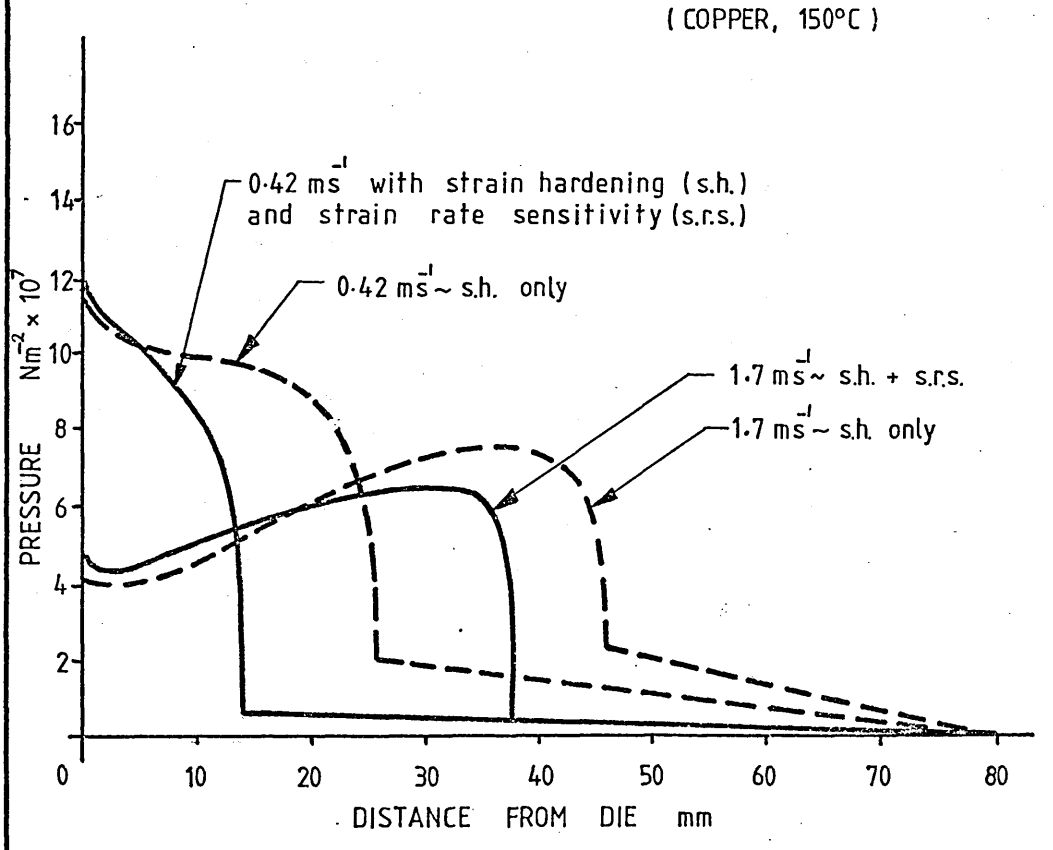

FIG 58b THEORETICAL PRESSURE DISTRIBUTION FOR VARYING DRAWING SPEED ~ 5% REDUCTION

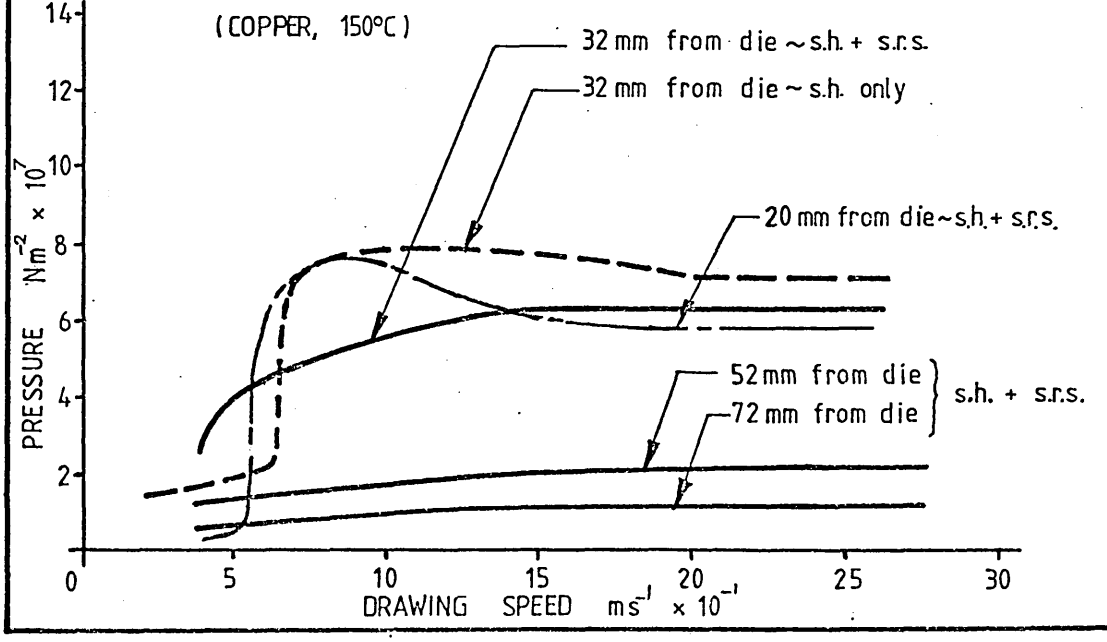

FIG 59a THEORETICAL STRESS DISTRIBUTION IN THE WIRE ~ 30% REDUCTION (COPPER, 150°C)

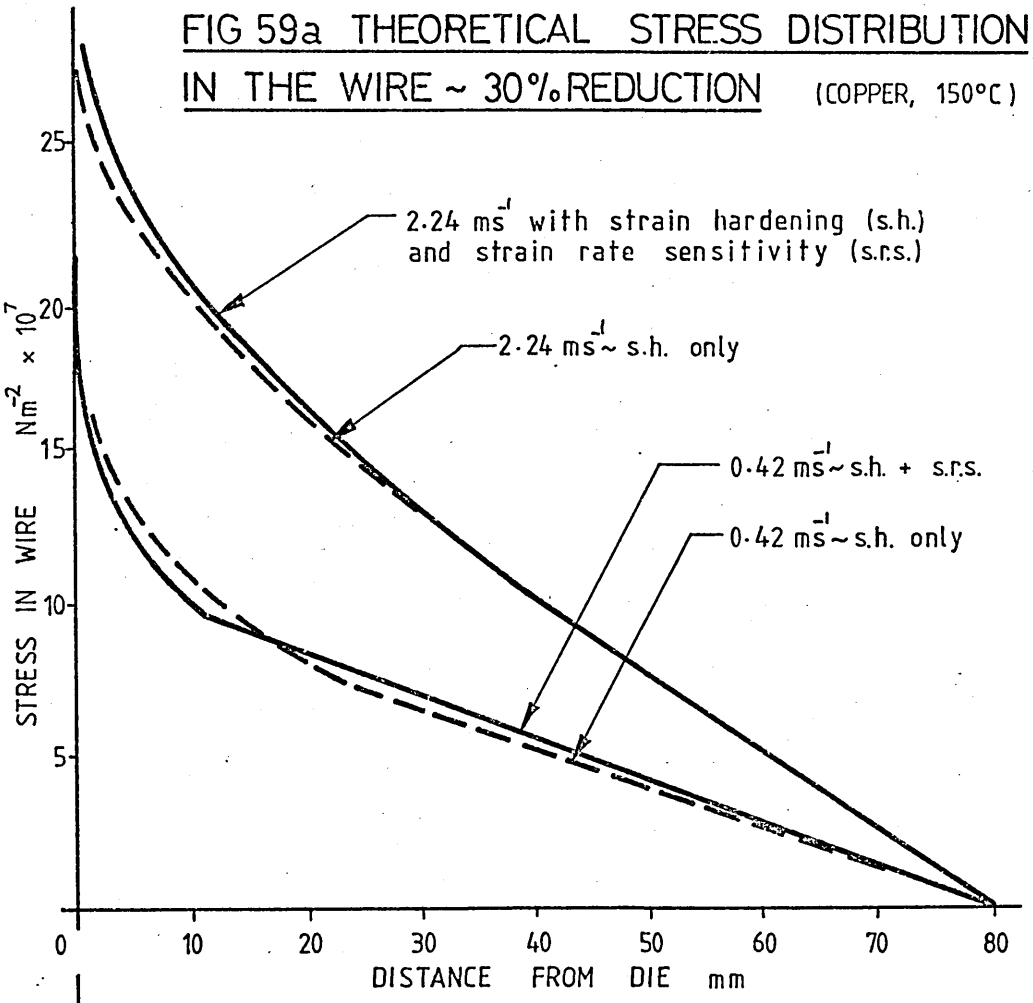

FIG 59b THEORETICAL STRESS IN THE WIRE FOR VARYING DRAWING SPEED ~ 30% REDUCTION

stress at 32 mm from die :- (COPPER, 150°C)

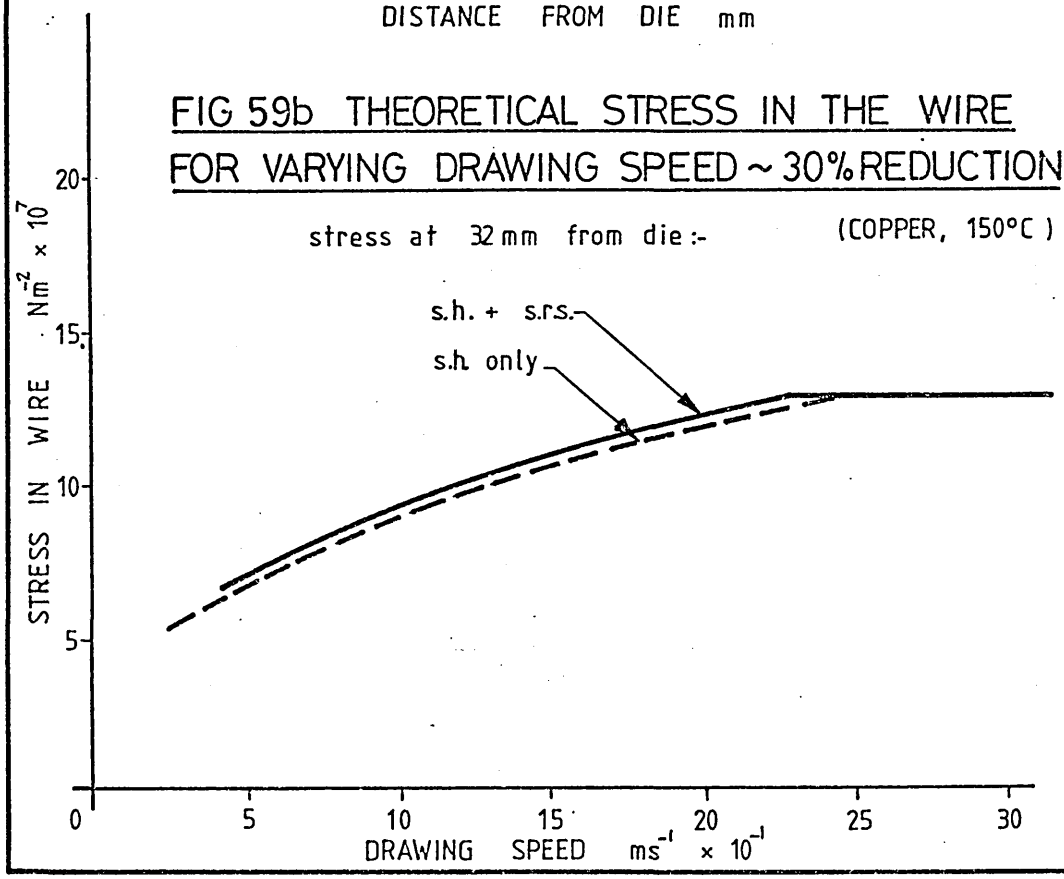

FIG 60a THEORETICAL STRESS DISTRIBUTION IN THE WIRE ~ 5% REDUCTION (COPPER, 150°C)

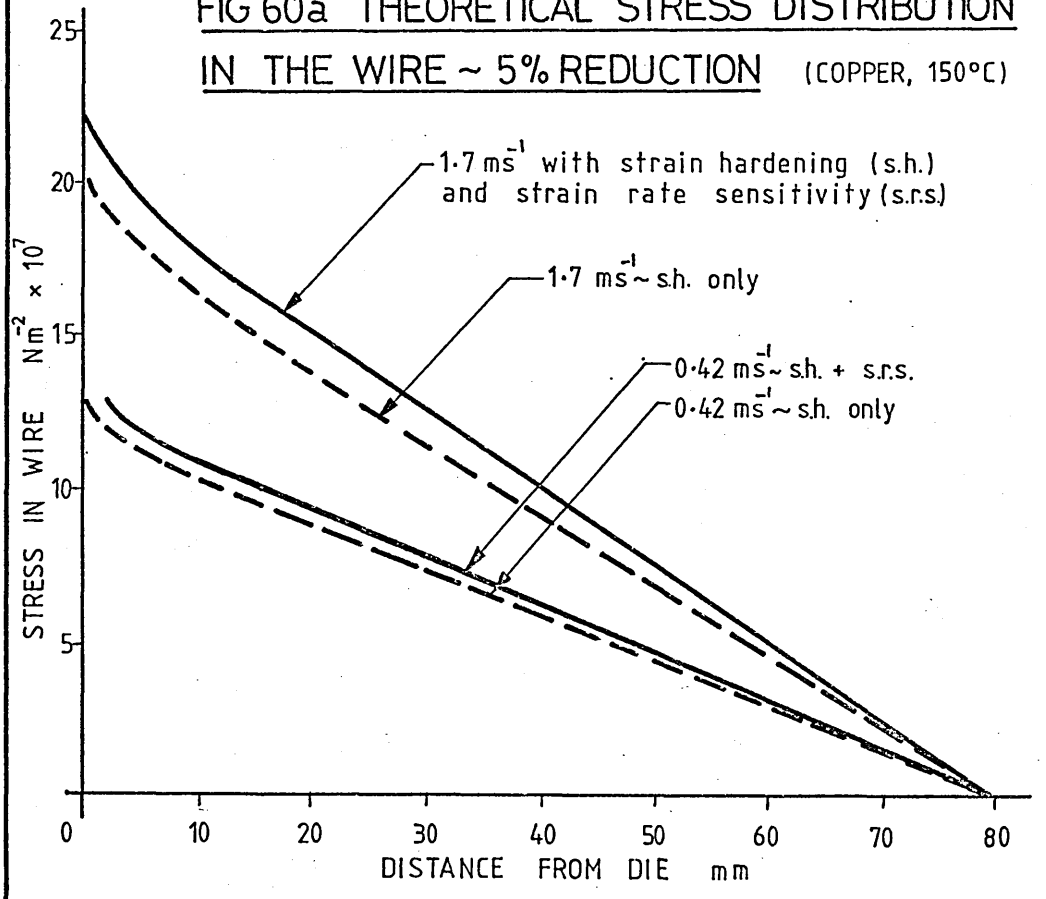

FIG 60b THEORETICAL STRESS IN THE WIRE FOR VARYING DRAWING SPEED ~ 5% REDUCTION

stress at 32 mm from die:- (COPPER, 150°C)

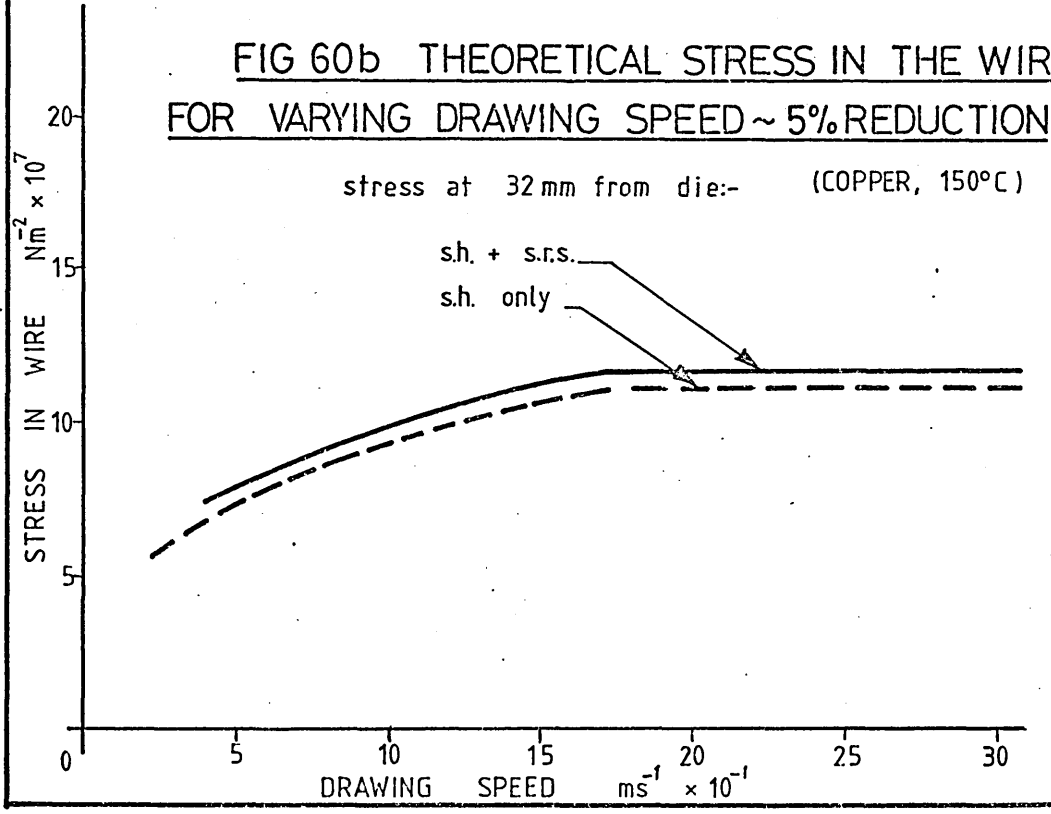

CHAPTER 8. DISCUSSION.

In this study many interesting results have emerged, both from the experimental tests and theoretical analyses. This chapter aims to highlight the more salient points from experiment and theory and to compare the results obtained thereby. The discussion is subdivided into five main section; estimation of errors, experimental procedure and results, analysis, comparison between theoretical and experimental results and recommendations for future work.

8.1 Estimation of Errors.

Errors always arise in any experiment from the slight inaccuracies in the variables upon which the final result depends. An appreciation of the magnitude of the errors is required so that the results may be considered with some degree of confidence. This section examines the probable uncertainty in the value of the coating thickness.

Theory.

If $A = fn(x, y, z, ...)$

then $\Delta A = \frac{\partial A}{\partial x}\Delta x + \frac{\partial A}{\partial y}\Delta y + \frac{\partial A}{\partial z}\Delta z + \ldots .$

where ΔA is the probable error in A

For multicomponent errors;

ie: $P = A + B + C + \ldots$ where A, B and C are mean values

Then the probable error in P is given by :-

$$\sqrt{(A \times \Delta A)^2 + (B \times \Delta B)^2 + (C \times \Delta C)^2 + \ldots}$$

In the present work, coat thickness is given by:-

$$h_d = \frac{p' h^3}{6\eta_o U} + \frac{\tau_c h^2}{2\eta_o U} + \frac{kp'^3 h^5}{20\eta_o U} + \frac{kp'^2 h^4 \tau_c}{4\eta_o U} + \frac{kp' h^3 \tau_c^2}{2\eta_o U} +$$

$$+ \frac{kh^2 \tau_c^3}{2\eta_o U} + h$$

and therefore the error in h_d is given by:-

$$\Delta h_d = \sqrt{\left(\frac{\partial h}{\partial h}_d \Delta h\right)^2 + \left(\frac{\partial h}{\partial p'}_d \Delta p'\right)^2 + \left(\frac{\partial h}{\partial \eta_o}_d \Delta \eta_o\right)^2 + \left(\frac{\partial h}{\partial k}_d \Delta k\right)^2 +}$$

$$\overline{+\left(\frac{\partial h}{\partial U}_d \Delta U\right)^2 + \left(\frac{\partial h}{\partial \tau_c}_d \Delta \tau_c\right)^2}$$

Before assessing the overall error in the calculated coat thickness, consideration must be made of the errors present from the determination of the individual variables in the analysis.

Shear stress:- not a true independant variable but will be treated as such here. Any error in τ_c is difficult to estimate but a $\pm 5\%$ error is assigned.

Pressure gradient:- again, not a true independant variable.

Errors are assumed to be ±2%.

Gap:- a true independant variable, where error is easily estimated. If the wire is assumed to run concentrically in the Christopherson tube, the error in the gap is dependant on the tolerance of the wire and tube. Any temperature effects must also be considered. The wire is assumed to have a tolerance of ±0.0127mm. The tube can be manufactured to a tolerance of ±0.01mm. Total radial tolerance is then 0.0114mm giving an error of ±6.3% for a nominal gap of 0.18mm. Temperature effects were investigated and were found to be negligibly low.

Initial viscosity at ambient pressure is easily determined and it is this that is present in the equations, however, when the melt is subjected to high shear forces and high pressures, the certainty of the value of viscosity is low. An error of ±2% is assumed for the initial viscosity.

Wire speed:- this was measured electronically with an estimated error of ±1%.

Shear constant (k) was determined experimentally with an estimated error of ±2%.

Estimation of errors;

$$\frac{\partial h}{\partial h}_d = \frac{p'h^2}{2\eta_o U} + \frac{\tau_c h}{\eta_o U} + \frac{kp'^3h^4}{4\eta_o U} + \frac{kp'^2h^3\tau_c}{\eta_o U} + \frac{3kp'h^2\tau_c^2}{2\eta_o U} + \frac{kh\tau_c^3}{\eta_o U} + 1$$

$$\frac{\partial h}{\partial p'}_d = \frac{h^3}{6\eta_o U} + \frac{3kp'^2h^5}{20\eta_o U} + \frac{kp'h^4\tau_c}{2\eta_o U} + \frac{kh^3\tau_c^2}{2\eta_o U}$$

$$\frac{\partial h}{\partial \eta_o}_d = \frac{-p'h^3}{6\eta_o^2 U} - \frac{\tau_c h^2}{2\eta_o^2 U} - \frac{kp'^3h^5}{20\eta_o^2 U} - \frac{kp'^2h^4\tau_c}{4\eta_o^2 U} - \frac{kp'h^3\tau_c^2}{2\eta_o^2 U} - \frac{kh^2\tau_c^3}{2\eta_o^2 U}$$

$$\frac{\partial h}{\partial k}_d = \frac{p'^3h^5}{20\eta_o U} + \frac{p'^2h^4\tau_c}{4\eta_o U} + \frac{p'h^3\tau_c^2}{2\eta_o U} + \frac{h^2\tau_c^3}{2\eta_o U}$$

$$\frac{\partial h}{\partial U}_d = \frac{-p'h^3}{6\eta_o U^2} - \frac{\tau_c h^2}{2\eta_o U^2} - \frac{kp'^3h^5}{20\eta_o U^2} - \frac{kp'^2h^4\tau_c}{4\eta_o U^2} - \frac{kp'h^3\tau_c^2}{2\eta_o U^2} - \frac{kh^2\tau_c^3}{2\eta_o U^2}$$

$$\frac{\partial h}{\partial \tau_c}_d = \frac{h^2}{2\eta_o U} + \frac{kp'^2h^4}{4\eta_o U} + \frac{kp'h^3\tau_c}{\eta_o U} + \frac{3kh^2\tau_c^2}{2\eta_o U}$$

Typical values:-

$\tau_c = -8.2073 \times 10^5$ and $\Delta\tau_c = 4.1 \times 10^4$

$p' = 4.5265 \times 10^9$ and $\Delta p' = 9.05 \times 10^7$

$h = 1.8 \times 10^{-4}$ and $\Delta h = 1.14 \times 10^{-5}$

$\eta_o = 2.0967 \times 10^3$ and $\Delta\eta_o = 4.193 \times 10^1$

$U = 1$ and $\Delta U = 1 \times 10^{-2}$

$k = 8.07 \times 10^{-11}$ and $\Delta k = 1.614 \times 10^{-12}$

These give;

$$\frac{\partial h}{\partial h}_d = 1.44 \times 10^{-3}$$

$$\frac{\partial h}{\partial p'}_d = 2.296 \times 10^{-14}$$

$$\frac{\partial h}{\partial \eta_o}_d = 6.815 \times 10^{-8}$$

$$\frac{\partial h}{\partial k}_d = -1.718 \times 10^6$$

$$\frac{\partial h}{\partial U}_d = 1.4288 \times 10^{-4}$$

$$\frac{\partial h}{\partial \tau_c}_d = 6.4075 \times 10^{-10}$$

Hence;

$$\Delta h_d^2 = (1.44 \times 10^{-3}\ \Delta h)^2 + (2.296 \times 10^{-14}\ \Delta p')^2$$

$$+ (6.815 \times 10^{-8}\ \Delta \eta_o)^2 + (1.718 \times 10^{6}\ \Delta k)^2$$

$$+ (1.429 \times 10^{-4}\ \Delta U)^2 + (6.41 \times 10^{-10} \Delta \tau_c)^2$$

Which leads to; $\Delta h_d = 2.95 \times 10^{-5}$

A typical value of h_d is 3.8×10^{-5}, hence an error of approximately 77% could occur.

Investigations of the error analysis show that the major errors occur due to the uncertainty in the determination of the values of h and τ_c. If τ_c and h could be estimated within a limit of (say) ±2%, then an error of 31% is predicted by the above analysis. Since the theoretical results are considerably different to those obtained experimentally, this seems to suggest that the values of τ_c and h used in the theoretical results were not correct. This is discussed in detail later.

8.2 Experimental Procedure and Results.

An extensive experimental programme was undertaken which produced considerable amounts of data. To rationalise

information received, it was decided to investigate three parameters (coating thickness, pressure in the Christopherson tube and drawing load) while varying as many physical conditions as possible - ie. drawing speed, polymer temperature die size, wire material and polymer material. Bamboo, coat quality and adhesion were also noted as drawing proceeded. The Christopherson tube length and diameter, wire initial diameter and die geometry were kept constant throughout the tests.

The coating thickness was measured using the weight loss method which gave very repeatable results considering the magnitude of thickness present. The results showed that thickness decreased as the speed was increased. An increase in polymer temperature gave a slight reduction in thickness at all speeds. The effect of die size on coat thickness is not certain. The results appear to show that a smaller reduction gave an increase in thickness at low speeds and a decrease at higher speeds. The higher tensile strength wires produced smaller coat thicknesses in most cases but 18/8 stainless steel at 5% reduction gave greater thicknesses than copper at the same reduction. Very high tensile strength wires (60/65 carbon steel) gave very small coat thicknesses - often no coat at all was observed, especially at the lower polymer temperatures (60/65 carbon steel at 135°C gave spasmodic coatings).

Alkathene WVG 23 was found to be the most promising polymer type. Most other types investigated gave very poor results for the test conditions used, the major faults being; the lack of coat due to the very high viscosities of the

polymer melts resisting flow through the tube, melt temperatures too high for the equipment, wire fracture because of viscous drag in the tube, polymer deterioration because of the high temperatures used and the nauseating smell associated with some of the deteriorating plastics.

A most interesting phenomenon was encountered throughout the tests, namely "bamboo". This effect was observed generally at low drawing speeds. The graphical presentation of the results show that a transition between bamboo and smooth wire coating exists. No trends to the transitions were apparent for changes in temperature, but changes in die size produced narrower transition ranges for smaller wire reductions. The cause of the bamboo is a matter of conjecture only, since direct proof is very difficult to obtain. In Chapter 2, discussions were made of possible causes of bamboo in relation to the properties of polymer melts. Certain polymer melts have been observed to give very unstable flow at high shear rates with subsequent characteristic distortion when the melt solidified. It is not clear whether the bamboo in this case is attributable to the same causes. It has been observed and mentioned in the results section that the multiple necking of the wire associated with the bamboo originates in the Christopherson tube itself - well before the wire reaches the die. The cause of this multiple necking is most probably the pulsation of pressure in the tube which hammers the wire into the distorted shape. This distorted wire on entry to the die possibly gives rise to variable shear stress in the polymer melt, causing bamboo of the polymer on the surface of the drawn wire. Why pulsation of pressure should occur in the first place is the matter for

conjecture. Once started it is easy to see that the necked shape of the wire would then cause a pulsation of pressure in the Christopherson tube as the polymer was released at the die through the reduced diameter of the wire. However, the origin of such a pulsation is not easy to envisage. It is possible that at low speeds the slip-stick phenomenon of the melt against the wire produced a discontinuity in pressure generation. As speed was increased, a critical shear stress value was surpassed which then caused slip to be continuous, producing a constant pressure (irrespective of speed) and hence the coat thicknesses would reduce and remain smooth. The effect of the high pressures on the polymer melt may also be a contributing factor. It has been reported that at very high pressures (above 140 MNm^{-2}) polymer melts tended to recrystallise[23]. Slightly lower pressures were encountered when drawing copper wire but it is possible that recrystallisation was occurring in parts of the Christopherson tube, giving rise to pressure (and velocity) discontinuities. The effect of the discontinuities could be to initiate the necking of the wire in the Christopherson tube. Since the results show mainly a decrease in thickness as the drawing speed increases, the assumption of a critical shear stress is justified. However, the drawing speed at which the polymer began to slip must have been very low. A transition between non-critical and critical flow was seen to exist for copper at 180°C and 30% reduction (Fig 23) and for 18/8 stainless steel at 150°C and 30% reduction (Fig 26), but all other temperatures and reductions failed to produce such a transition.

One problem encountered during drawing was the breakage of wire at low speeds. This happened mainly with

high tensile strength wires (60/65 carbon steel) but also with copper when a combination of high reduction and low temperature was used. The fracture occurred as a consequence of a severe necking of the wire as described above. It is interesting to note that a reduction ratio greater than 30% could not be achieved, probably because of the very high back stresses involved due to the viscous drag of the polymer melt.

It had been hoped that the resulting coat on the wire could have been used to lubricate the wire in subsequent manufacturing operations. The results indicate that the adhesion of the polymer to the wire was not sufficiently strong to achieve this. Careful storage of the wire after drawing showed that the coat could be used to prevent deterioration of the wire through corrosion.

The results obtained for pressure in the Christopherson tube partly confirmed the existence of slip. Pressure readings were taken from four locations in the tube and are shown in Figs 29-31. At very low speeds the pressure decreased as speed was increased at locations 1, 2 and 3 in the tube. A minimum pressure was reached at about 0.3 ms^{-1} and pressure then increased as speed was increased. The presence of this reversal was shown most clearly for 18/8 stainless steel (Figs 30 and 31). For a 30% reduction, the pressure dropped rapidly from 17 x 10^7 Nm^{-2} to 8 x 10^7 Nm^{-2} at location 3. Similar variations in pressure were observed at locations 4 and 2. For 5% reduction the effect was not as marked but was still apparent. The reason for the sudden drop in pressure was probably the transition from no-slip to slip in the polymer melt, ie. at very low drawing speeds (below 0.3 ms^{-1}) slip

did not occur and a high pressure was developed. As the speed was increased, a transition from no-slip to slip occurred and the polymer melt was unable to develop such high pressures since the velocity gradient became discontinuous. A critical speed was reached at approximately 0.3 ms^{-1} whereby slip was total around the wire. For increasing speed, therefore, no further change in pressure occurred. This is a simplified assessment of the situation since localised crystallisation could have occurred as discussed previously. For the copper wire, the pressure, once reduced to a minimum, increased with increasing speed. In all probability, the polymer melt was able to accomodate a further increase in shear stress even after slip had occurred. This would account for the increase in pressure.

Pressures at location 4 for the copper wire at both reductions did not follow the same trends. It is reasonable to assume that since location 4 is in the deformation zone, as shown in Fig 33, pressures at that point would be dictated by the deformed shaped of the wire. The pressures at position 4 for 18/8 stainless steel wire did not follow the same trends as those for copper wire. This seems to suggest that the deformation zone for 18/8 was not of the same length as that for copper, although this was not borne out by measurement of the deformed wire (see Fig 33).

Close inspection of the UV traces obtained from the pressure transducers revealed some interesting facts. When bamboo had occurred, the pressure traces showed a distinct oscillation, confirming that pulsating pressure actually existed in the Christopherson tube. Because of these

oscillations, it was possible to identify on the traces the point at which the coating had developed (measurements of the uncoated length of the drawn wire verified this).

It had been decided to attempt to externally pressurise the polymer melt and feed it into the Christopherson tube in order to reduce the time for the hydrodynamic pressure to build up and hence reduce the uncoated length of wire at start up. The pressure traces enabled the effectiveness of such a system to be examined. Figs 34a and 34b show the traces of pressure at location 4 when drawing copper wire with hydrostatic pressure and basic hydrodynamic pressure respectively. The hydrostatic pressure is seen to increase the start up pressure by an amount dependent upon the magnitude of the available hydrostatic pressure. It is clear that for the hydrostatic pressure used, little advantage was gained, although if this pressure could be doubled, then possibly much greater benefit would become available. A hydrostatic pressure of 250 bar (2.5×10^7 Nm^{-2}) was present although a designed pressure of 520 bar should have occurred. Large losses were presumably occurring in the injector, since the hydrostatic pressure was measured at the delivery end of the injector. These losses can only be accounted for by the frictional and compressive effects of the melt in the injector. Because only low shear stresses could be generated by the injector, pressure effects on the viscosity would be dominant. The melt, therefore, would have a very high viscosity in the injector. Any attempt to increase the pressure available to the Christopherson tube would be largely hindered by a further increase in viscosity, possibly even solidification of the melt. For a hydrostatic system to work effectively, a basic piston/cylinder type of

injector must be abandoned in favour of a screw type of injector which would exert shear forces on the polymer melt and so reduce its viscosity.

The hydrostatic system used here did have one notable advantage over the basic hydrodynamic system. Under initial start up conditions (ie, after cleaning out the system), hydrodynamic pressure was not developed until the wire had pulled in sufficient polymer to refill the cleaned out spaces. This is shown clearly by Fig 34c. The use of hydrostatic pressure before the run commenced filled these spaces and enabled the generation of hydrodynamic pressure to begin when drawing started. The practical effect of this was to reduce the uncoated length of wire (ie. unlubricated) from approximately 2m to 300mm, thus reducing the die wear at start up.

The drawing load followed the same trends as the pressure, ie. at very low speeds the loads were high and reduced as the speed was increased. This reinforces the arguments laid down previously about the existence of slip in the polymer melt. The high loads combined with the necking of the wire are the causes of the wire breakage at low speeds. The load did not remain constant throughout a test. Fig 35a shows the UV trace obtained for load whilst drawing copper wire over a fairly long period. At start up, the load rose quickly with a sudden drop before rising again to a peak. As time progressed, the load gradually reduced until a stable value was reached after about 35 seconds. This is interpreted as the time taken for the system to reach thermal stability. Closer inspection of the start up period reveals the hydrodynamic build up. Fig 35b shows the load over a short time

span at start up. After reaching an initial peak, the load reduced to 210 N before gradually rising to 295 N after a period of about one second. The 210 N load is assumed to be that required to draw the wire unlubricated with no back pull. As hydrodynamic pressure developed, a greater back pull was generated, which exceeded the reduction gained by reduced die friction by an amount shown in the figure. Oscillations of load due to the bamboo can also be seen.

8.3 Discussion of the Analyses and the Results Obtained from the Analyses.

Two complementary analyses have been presented which enabled coat thickness, fluid pressure and stress in the wire to be estimated. Various assumptions were made in order to simplify the mathematics and are now discussed:-

a) Flow of the polymer is laminar - A reasonable assumption since the gaps are small, velocities are low and the viscosity is high.

b) Flow of the polymer is axial - Once flow through the die has commenced, little or no back flow is expected. This assumption allowed one dimensional flow to be considered.

c) The thickness of the polymer layer is small compared to the dimensions of the Christopherson tube - Enabled the analysis to be done in rectangular rather than cylindrical coordinates.

d) Pressure in the polymer melt is uniform in the thickness direction - A reasonable assumption which enabled the pressure coefficient of viscosity to be considered

separately from the velocity.

e) Deformation occurs isothermally - A major simplification from which some errors could result, since the wire temperature is known to increase when drawing is conducted.

f) Deformation of the wire may be assumed to take place within an effective die shape which can be represented by:-

$$y = A + Bx^{1/3}, \qquad (x_1 \leqslant x \leqslant x_2).$$

Experimental tests have shown that an effective die shape exists which can be approximately described by the above equation. It is not certain whether the deformation follows this equation in all cases, since only a limited number of experimental tests were performed on die shape. The results from these, however, produced good correlation and any error is expected to arise from the assumed effective die length (ie. $C_F.L$) which could vary as the speed is changed.

g) The polymer flow may be represented by:-

$$\tau + k\tau^3 = \eta_o \frac{\partial v}{\partial y'}$$

where k is polymer shear constant ($m^2 N^{-2}$).

This is shown to be the case from the rheological tests on the polymer melt and is accurate within the no-slip range of the polymer used.

h) The pressure gradient in the undeformed region of the Christopherson tube is linear - Newtonian theory suggests that this is so, ie;

$$\frac{\partial p}{\partial x} = \frac{6\eta U}{h^2}$$

Since a non-Newtonian solution is presented, it is possible

that this assumption may be in error, however, some pressure gradient needed to be assumed in order to solve the equations, so the solutions may be regarded as a first approximation in this respect. Experimental measurements of pressure in the Christopherson tube were undertaken to check this assumption and largely confirm the existence of a linear distribution, and so it is believed that any errors from this source would be negligibly small.

i) The pressure coefficient of viscosity may be represented by;

$$\eta_b = \eta_a + ap - bp^2 - c$$

An equation derived from the graphical results of Westover[10] for polyethylene. The accuracy of the results is not known although the equation fits the graphs closely. The pressure coefficient of viscosity is normally represented exponentially, but this was found to overestimate the viscosity at high pressures. Westover's results show the combined effects of shear stress and pressure on polyethylene and indicate that pressure modifies the initial viscosity of the polymer as represented by Fig 11. Unfortunately, similar data was not available for Alkathene WVG 23, therefore small errors are possible from the determination of the constants a, b and c.

j) Polymer slip occurs at the wire-polymer interface only - A reasonable assumption since the highest shear stresses occur at the wire polymer interface.

k) After slip has occurred, the polymer cannot accomodate further increases in shear stress. This assumption simplifies the analysis after slip has occurred by assuming a constant flow rate irrespective of wire speed. It is

likely that further shear stress may be accomodated but a slip ratio would be difficult to determine. The presence of slip is justified since the experimental results show that the coat thickness reduced as the speed was increased.

1) The shear stress is zero at the polymer-tube interface - An alternative theory was derived based on this assumption. It is realised that this assumption is normally invalid, but solutions to the analysis already presented showed that the velocity gradients at the polymer-tube interface were zero for almost all conditions considered.

8.3.1 Basic Analysis.

The analysis was considered in two parts - the flow of the polymer in the undeformed region of the Christopherson tube and the deformation of the wire in the tube and die.

Considerations of the flow of the polymer melt in the tube enabled the theoretical coating thickness to be determined. The analysis of the deformation of the wire allowed pressure of the melt and the stress in the wire to be calculated.

The results for coat thickness showed three zones;

a) At low drawing speeds, no coat was possible
b) At higher speeds, coat thickness increased as the speed was increased
c) After a critical shear stress had occurred, the thickness reduced as the speed was increased further.

Various trends became apparent as the input parameters were altered;

a) An increase in the initial yield strength of the wire reduced the coat thickness.
b) The gap between the wire and the tube had an optimum value of 0.18mm for the geometry used.
c) Increases in the Christopherson tube length above 0.6m yielded only very small increases in coating thickness.
d) An increase in wire radius increased the coat thickness.
e) Increases in initial viscosity produced only very small changes in coating thickness.
f) An increase in the pressure coefficient of viscosity reduced the overall coat thickness by reducing the speed at which the polymer melt reached the critical shear stress. Reducing the value of k had similar effects.
g) Increasing the drawing reduction ratio reduced the coat thickness as did the inclusion of strain rate sensitivity.

The observations and results outlined above are important in many ways. The decreased coat thickness due to increased yield stress was expected as was the decrease due to increased wire reduction. The other results, however, were not fully expected. The existence of an optimum gap is interesting. For small gaps, only low polymer flow rates can exist even though shear stresses may be high. The coat thickness is therefore low. For large gaps, back flow could occur which would reduce pressure and therefore reduce the coat thickness. An optimum gap occurs when a balance is struck between these two effects, and is shown clearly by the analysis.

Increases in the length of the Christopherson tube above 0.6m for the given conditions appear to be unjustified. Indeed, above a length of about 0.35m, the increase in coat thickness is only marginal. A combination of the effects of the variation in the gap and the length of the Christopherson tube on the results shows that an optimum length/gap ratio would be 1944:1 and in this case would produce a maximum coat thickness of 0.43×10^{-4} m at 2.5 ms^{-1}.

Perhaps the most interesting results are those obtained by changing the initial viscosity and the pressure and shear coefficients of viscosity. It had been assumed that an increase in viscosity should increase the coating thickness. (This project was initiated with this assumption in mind). The theoretical results seem to contradict this assumption. An increase in the initial viscosity reduced the critical speed of the polymer melt whilst the coat thickness there remained constant. The pressure coefficient had a similar effect. A reduction in the shear coefficient of viscosity (ie, the fluid being more Newtonian) did increase the maximum coat thickness, but since it also reduced the speed at which the critical stress was reached, the overall coat thickness reduced. Evidently the interaction between the various equations in the analysis predicted a constant flow rate as viscosity was changed. Why this should be so is difficult to see from the analysis. However, a Newtonian solution gives similar results and the equations are more easily analysed. It is easily seen that $U.\eta$ is a constant in the equation for determining the value of τ_c (see Appendix II equation A2.7), hence any change in η simply changes the speed at which τ_c becomes critical. Since the coat thickness equation contains terms of $U.\eta$ throughout (equation A2.8),

any change in η will be ineffective, giving a constant coat thickness at the critical speed as shown by the results.

The theoretical results for the pressure distributions show that the pressure in the deformation zone is very much greater than that in the undeformed region, when the effects of strain hardening and strain rate sensitivity are considered. The distribution assuming a constant yield stress shows a reduction in pressure as the wire is deformed towards the die. Because of the assumed linear pressure distribution in the Christopherson tube, a sudden change in pressure becomes evident when deformation commences. An increase in drawing speed theoretically decreases the pressure in the tube. The inclusion of strain rate sensitivity is found to increase the pressure and is more prominent at higher drawing speeds. The theoretically derived results for the stress in the wire show that the stress increases linearly in the tube until deformation commences, at which point the stress increases more rapidly until the die is reached. The linear part of the curve was due solely to the viscous drag of the polymer melt on the wire. Since, in that portion of the tube, the pressure is linear and the wire is undeformed, a linear stress distribution is expected. After deformation commences, however, the pressure distribution is no longer expected to be linear, since the shear component no longer acts axially. An increase in drawing speed increases the stress. The effect of including strain rate sensitivity is to increase the stress and has a slightly greater effect at higher speeds. The assumption of a constant wire yield stress produces lower stress values. Since the wire material was assumed to obey either Tresca or von Mises yield criterion, ie. $Y = p + \sigma_x$ an increase in σ_x gave a reduction in the pressure required to cause flow. This

is why the pressure distribution for a material of constant yield stress reduced as the wire approached the die. For strain hardening and strain rate sensitive materials the value of Y is modified as deformation occurs and therefore $(p + \sigma_x)$ is no longer constant, giving the curves as shown (Figs 49 and 50).

8.3.2 Alternative Theory.

The analysis presented earlier needed the length of the deformation zone of the effective die profile given by the equation;

$$y = A + Bx^{1/3}, \quad (x_1 \leq x \leq x_2)$$

to be known beforehand. Some results were obtained by suddenly stopping the drawing process and carefully measuring the profile of the wire which remained inside the Christopherson tube. This procedure gave results as shown in Fig 33. A deformed length of 40mm is shown. Unfortunately, the equipment needed resetting after each test. This involved allowing the equipment to cool, dismantling and cleaning out the die and Christopherson tube, reassembling the equipment and setting up as described in Chapter 3. Only one test could be done each day and, consequently, only a limited number of tests were conducted. It was thought that the length would vary as the speed was altered and even though the results were inconclusive, in order to determine whether this was so, an alternative theory was proposed.

In the existing theory, τ_c was found by considering the deformation pressure. Determination of the deformed length required the solution of τ_c independant of the pressure. The boundary condition; $y = h$, $\tau = 0$ was proposed. Ordinarily this boundary condition would not be valid but solutions of the existing non-Newtonian theory showed that it was valid for all of the polymers investigated under all conditions other than for very small gaps. The use of this boundary condition enabled a greatly simplified analysis to be produced which did not require the deformation pressure to be included in order to determine τ_c . This meant that equation (20) could then be used to determine the deformed length necessary to satisfy Tresca or von Mises yield criteria.

Figs 52a and 52 b show the theoretical length of the Christopherson tube with changing drawing speed. The length reduced as the speed was increased until slip was reached, when the length remained constant. A greater wire reduction required a longer tube as did a wire of a higher initial yield stress. The results suggest that no coat would be possible for 18/8 stainless steel ($Yo = 3.4 \times 10^8$ Nm^{-2}) since the Christopherson tube was not long enough, and that a minimum length of 110mm would be required, although this was not substantiated by experiment.

Solutions for coat thickness and pressure and stress distributions were also determined for comparison with the existing analysis. The results for coat thickness are different in that a two stage curve is evident rather than the three stage one as predicted from the main analysis. For this modified theory, the coat thickness remains essentially constant

during the no-slip region and follows the previous theory when slip occurs. The previous theory showed an increase in coat thickness for increasing speed during the no-slip range. The reason for the difference may be that since the modified theory allowed the Christopherson tube length to vary, a constant pressure at the commencement of deformation occurred, giving essentially constant viscosity (since pressure effects were dominant over shear effects) and therefore constant flow rate. Changing the different parameters have similar effects to the previous theory although changing the gap produces a general increase in coat thickness, whereas in the existing theory, further increases in gap above that used in practice caused a decrease in coat thickness. The reason for this apparent difference lies in the fact that the Christopherson tube length changes as the speed is changed. An optimum gap to length ratio is maintained as the gap is altered. For large gaps, however, the length of the tube required exceeds that used in practice and therefore the actual coat thickness reduces as the gap is increased further.

The pressure and stress distributions are changed because of the variable deformation length. These changes cause the pressure to increase as speed increases, whereas the existing theory showed a decrease in pressure for increasing speed. It was noted that when the deformation length in the modified theory is the same as in the previous theory, the pressure and stress distributions are identical.

8.4 Comparison between Theory and Experiment.

In the previous two sections the experimental and theoretical results were discussed and in some cases discrepancies were apparent. In this section possible causes of these discrepancies will be discussed.

Fig 61 shows typical results obtained for coat thickness from experiment and compares them with the results obtained from the various theories under the same conditions. It is clear that at low speeds (below 2 ms^{-1}) all of the theories underestimate the thickness by large amounts. There are three possible explanations for these discrepancies.

a) Errors. The error analysis presented earlier shows that very large errors are probable due to the small size of the gap and the inability to determine accurate values of viscosity and shear stress.

b) The effect of bamboo. The theories do not take into account the increase in coat thickness caused by the presence of bamboo. The minimum diameter of the necked wire was much smaller than the die size. Reference to Fig 27 shows that the polymer coat was thickest where the wire diameter was smallest. A pulse ejection of polymer obviously occurred whilst the wire was being drawn, and it is clear that the average thickness in this case would be greater than if the wire had been smooth.

c) Determination of constants. Sixteen variables were required as input data before the analysis could be solved by computer. Of the sixteen variables, eleven were constants

derived from either experiment or from available data. These were:- η_o, k, τ_a, a, b, c, Yo, K, n, N, T

It is believed that η_o, k, N, and T were reasonably accurate but the accuracy of the other constants could not be ascertained. The critical shear stress (τ_a) was assumed to be 1 x 10^6 Nm^{-2}, since evidence from Reference 17 suggested that slip occurred with shear stresses of that order. Its precise value for the polymer used is not known since the equipment used to evaluate the rheological data of the polymer was unsuitable for reaching such high shear stresses. The experimental coat thickness curves seem to suggest that τ_a was lower than that assumed, but reference to Fig 40 shows that a lower value would not increase the theoretical coat thickness sufficiently to reach those of the experimental curves. It is thought that errors could have arisen from the pressure coefficients of viscosity (a, b, c) as previously discussed. The value of "a" was altered in the program and the results obtained are shown in Fig 43a. Again it is clear that a change in this parameter would not account for all of the error present at low speeds. The determination of the yield characteristics of the copper wire (Yo, K, n) presented some difficulty because of inconsistency and the final results were obtained by averaging results from a number of tests. A change in the initial yield stress in the computed results (Fig 37) shows that the coat thickness is relatively sensitive to this parameter and errors could have occurred here.

The alternative theory appeared to give more realistic results than the main theory in that no build up of thickness to a maximum was shown. Figs 62 and 63 show graphs of pressure

distribution for both theories and experiment for copper wire using reductions of 30% and 5% respectively. The pressure in the undeformed region of the Christopherson tube was underestimated at low speed and overestimated at high speed. The alternative theory gave much lower pressures in the undeformed region than either experiment or the main theory, but reference to parts (b) of the above figures show that the experimental results lie between the two theories, especially for a 5% reduction (Fig 63b).

8.5 Recommendations for Future Work.

It has been shown that a polymer coat could be applied successfully to the wire during drawing, demonstrating that a hydrodynamic film was present. However, several practical restrictions were noted:-

a) The adhesion of the polymer to the wire was not very good.
b) Wire fracture could occur at low drawing speeds.
c) A "bamboo" defect existed at low drawing speeds.
d) The addition of a pressurised feed (hydrostatic) was partially successful.
e) The coat thickness reduced as the drawing speed was increased.

The analysis attempted to take into account as many factors as possible, but further work on this topic may be usefully conducted in the following areas:-

8.5.1 Experimentally Some method of obtaining a better bond

between the polymer and the wire would be beneficial. This could be achieved by careful selection of polymer and possible pre-drawing treatment of the wire. It must be noted, however, that the system was very sensitive to changes in polymer type and that any further research in this area may require modifications to the Christopherson tube geometry.

The cause of the bamboo on the polymer coat requires further investigation. It may be possible to examine the bamboo directly by manufacturing a Christopherson tube from reinforced glass or quartz and by using high speed photographic techniques, the factors causing the bamboo may be seen. Although this area appears to be of rather academic interest, any advances here would be useful by increasing the knowledge of polymer technology and the wire drawing process, since bamboo is a problem common to both.

Further work to determine the deformed length of the wire in the Christopherson tube as the speed is changed is necessary. This would be easily accomplished and would verify, or otherwise, the validity of the alternative theory presented in this work. The process itself could benefit from the incorporation of a pressurised polymer feed using a screw injector. This modification would require only small changes to the existing experimental apparatus.

8.5.2 Theoretically An adiabatic analysis would be useful for comparison with the isothermal one presented here. This would require the effects of temperature variation on the polymer to be included into the analysis.

The addition of the effect of bamboo on coat thickness should improve the accuracy of the theoretical results.

FIG 61 COMPARISON OF COAT THICKNESSES AS PREDICTED BY THE VARIOUS ANALYSES AND EXPERIMENT

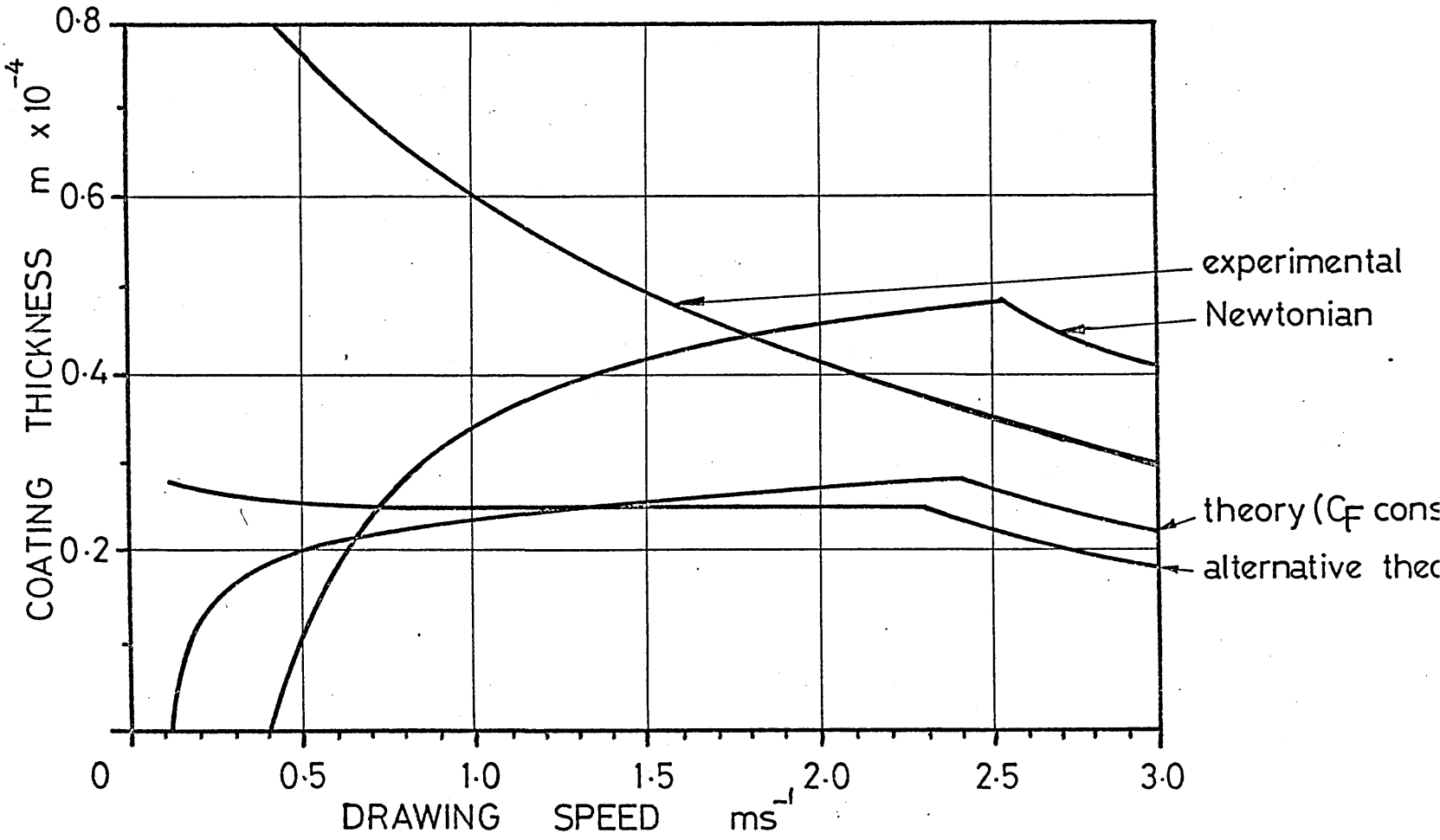

FIG 62a COMPARISON BETWEEN THEORY AND EXPERIMENT FOR PRESSURE DISTRIBUTIONS ~ 30% REDUCTION

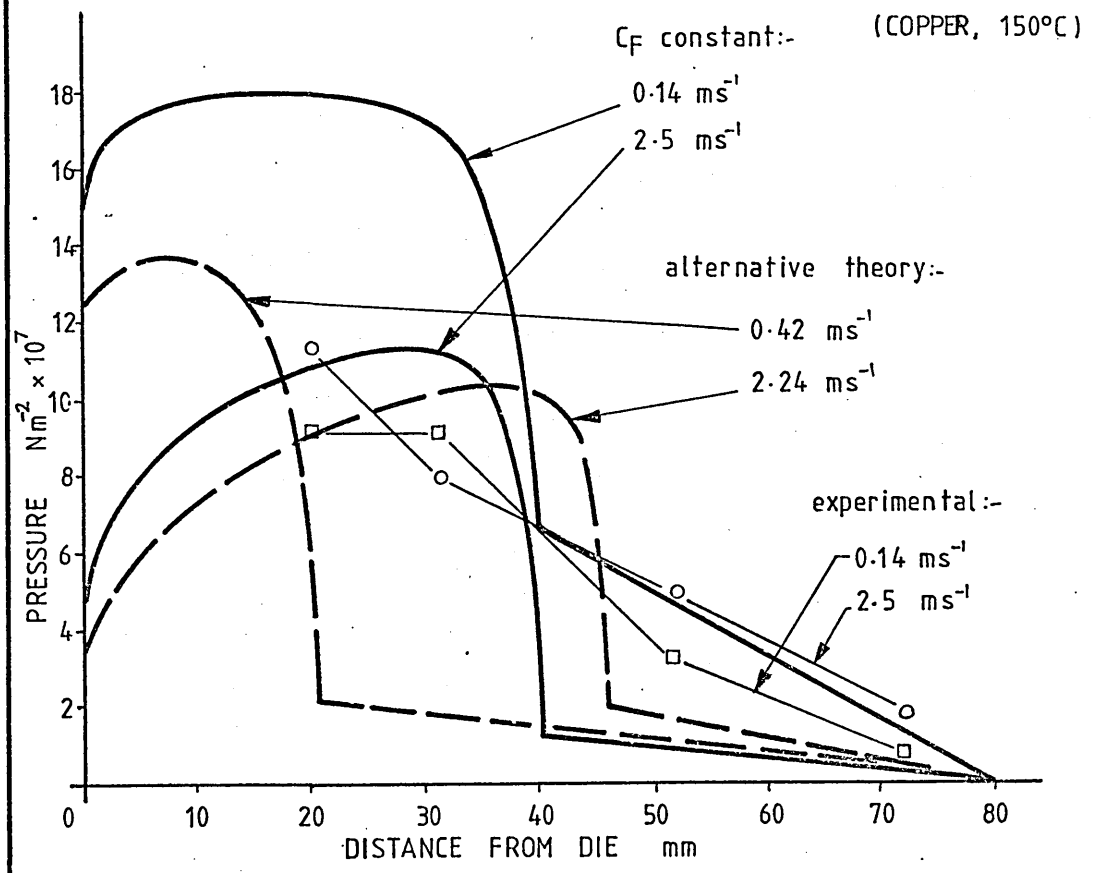

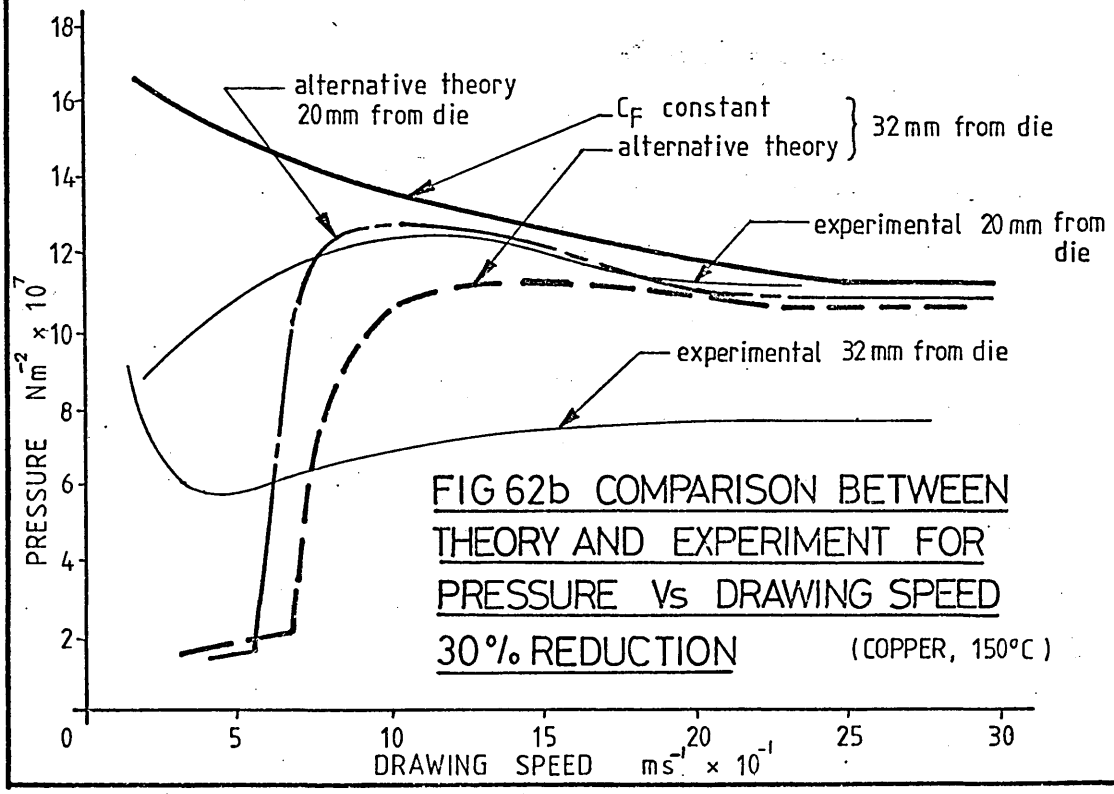

FIG 62b COMPARISON BETWEEN THEORY AND EXPERIMENT FOR PRESSURE Vs DRAWING SPEED 30% REDUCTION (COPPER, 150°C)

FIG 63a COMPARISON BETWEEN THEORY AND EXPERIMENT FOR PRESSURE DISTRIBUTIONS ~ 5% REDUCTION

(COPPER, 150°C)

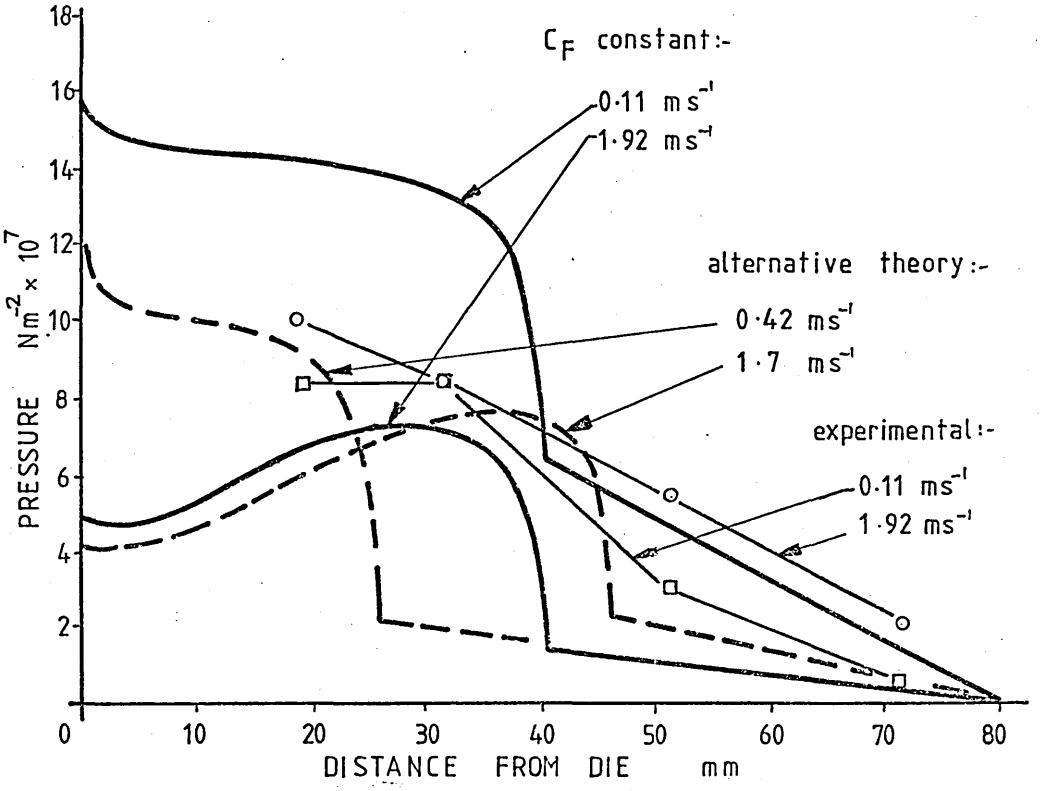

FIG 63b COMPARISON BETWEEN THEORY AND EXPERIMENT FOR PRESSURE Vs DRAWING SPEED ~ 5%

(COPPER, 150°C)

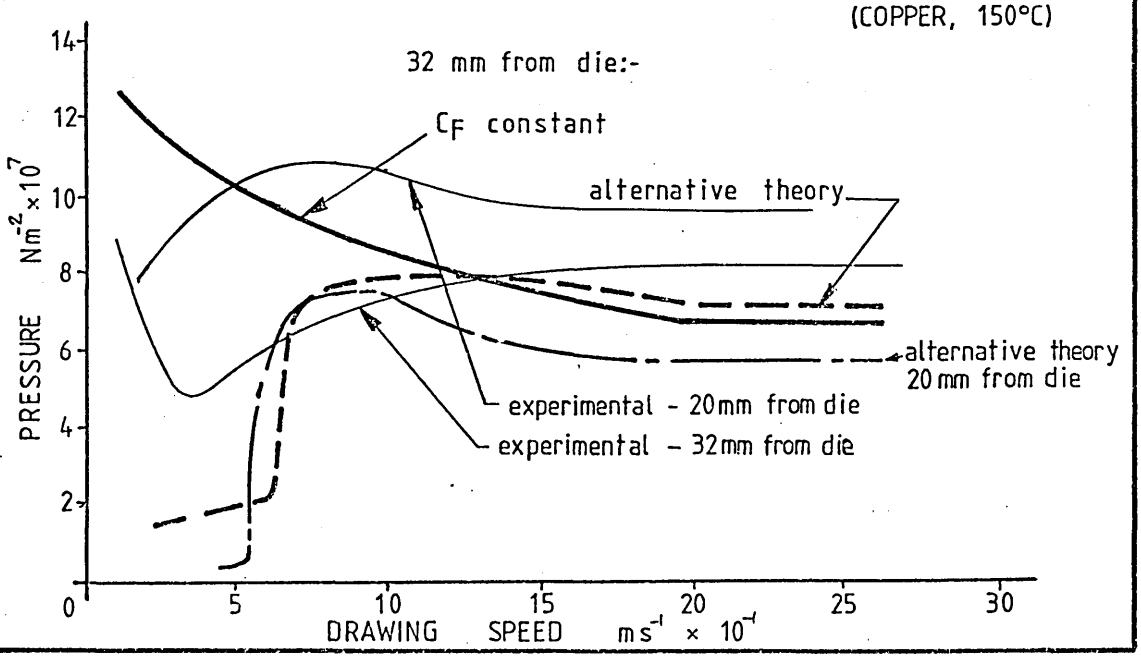

CHAPTER 9. CONCLUSIONS.

This work has presented many aspects of wire drawing when using a polymer melt as the lubricant. Certain limitations and disadvantages in the process became apparent during the tests, notably the bamboo defect and the lack of coat at start up. The experimental work has shown the extent of the bamboo such that it may be successfully avoided. The lack of coat at start up is the major drawback to full scale production since this could produce excessive die wear and even wire fracture. Attempts were made to improve start up by externally pressurising the polymer melt and feeding it into the Christopherson tube prior to drawing. This was partially successful and modifications to the equipment used in this work should give improved results.

The theoretical solutions tended to underestimate the recorded values, especially at low drawing speeds. It is probable that this was because of the bamboo effect which was not accounted for in the analysis.

It must be noted that in nearly all cases a coat was applied to the wire (albeit with varying degrees of adhesion) and in this respect the process is successful, but it is felt that further development is required before it could be used to advantage in full scale production.

10. REFERENCES.

1. WISTREICH, J.G. "The Fundamentals of Wire Drawing", Metallurgical Review, (1958), Vol 3, No 10, 97-142

2. WISTREICH, J.G. "ABC of Better Lubrication and Cooling in Steel Wire Drawing", (1959), Nov., Wire, pg 1486.

3. CHRISTOPHERSON, D.G.& NAYLOR, H. "Promotion of Fluid Lubrication in Wire Drawing". Proc. Inst. Mech. Eng., (1955), 169, 643

4. MACLELLAN, G.D.S.& CAMERON, A. 1943 British Patent Specification

5. STURGEON, G.M.& TATTERSALL, G.H. "Thick Film Lubrication in Wire Drawing". Wire Industry, (1959), Vol 26, 1183.

6. MIDDLEMISS, A. "Hydrodynamic Lubrication for Drawing Steel Wire". Tribology in Iron and Steel Works, ISI Publication 125

7. KOLMOGOROV, V.L., ORLOV, S.I.& SELISHCHEV, K.P. Translation of Russian Book, Published by National Lending Library, England (1968).

8. ORLOV, S.I., KOLMOGOROV, V.L. URAL SKII, STUKALOV, V.T. "Integrated Development and Introduction of New High-speed Mills and Hydrodynamic Lubrication Systems for Drawing Wire". Steel in the USSR, (1974), Oct, 844.

9. METZNER, A.B. "Fracture of non-Newtonian Fluids at High Shear Stresses". Industrial and Eng. Chemistry, (1958) Vol 50, No 10, pg 1577.

10. WESTOVER, R.F. "Effect of Hydrostatic Pressure on polyethylene Melt Rheology". S.P.E. Technical Papers, (1960), 6, 80-1.

11. STEVENS, A.J. "A Plasto-Hydrodynamic Investigation of the Lubrication and Coating of Wire using a Polymer Melt During Drawing". M.Phil Thesis, Sheffield City Polytechnic, (1979).

12. DIENES, G.J. Journal Applied Physics, (1953), 24, 779

13. CLEGG, P.L. "Elastic Effects in the Extrusion of Polythene" Rheology of Elastomers, Pergammon Press, London, (1957)

14. SPENCER, R.S.,& DILLON, R.E, "The Viscous Flow of Molten Polystyrene". J. Colloid Sci. (1948), Vol 3, pg 163.

15. TORDELLA, J.P. Trans. Soc. Rheology, (1957), 1, 203.

16. BENBOW, J.J.,& LAMB, P. "New Aspects of Melt Fracture". S.P.E. Transactions (Jan 1963), pg 7.

17. LUPTON, J.M.,& REGESTER, J.W. "Melt Flow of Polyethylene at High Rates". Polymer Eng. & Sci., (Oct 1965), pg 235.

18. WESTOVER, R.F. "The Significance of Slip in Polymer Melt Flow". Polymer Eng. & Sci., (Jan 1966), pg 83.

19. NASON, H.K. "A High Temperature, High Pressure Rheometer for Plastics". J. Applied Physics, (1949), 16, 338.

20. WESTOVER, R.F.,& MAXWELL, B. S.P.E. Journal, (1957), 13 (18), 27.

21. BAGLEY, E.B.,& BIRKS, A.M. "Flow of Polyethylene into a Capillary". J. Applied Physics, (1960), Vol 31, 3, 556.

22. BRYDSON, J.A. "Flow Properties of Polymer Melts". Published by Plastics Institute, London, Illiffe Books (1970).

23. MAXWELL, B.,& JUNG, A. "Hydrostatic Pressure Effect on Polymer Melt Viscosity". Modern Plastics, (Nov 1957) pg 174.

24. CHOI, S.Y. "Determination of Melt Viscosity as a Function of Hydrostatic Pressure in an Extrusion Rheometer". J. Polymer Sci. Part A2, Vol 6, pg 2043, (1968).

25. COGSWELL, F.N. "The Influence of Pressure on the Viscosity of Polymer Melts". Plastics and Polymers, (Feb 1973), 39.

26. TATTERSALL, G.H. "Hydrodynamic Lubrication in Wire Drawing" J. Mech. Eng. Sci. (1961), Vol 3, No 4, pg 378.

27. OSTERLE, J.F.,& DIXON, J.R. "Viscous Lubrication in Wire Drawing". ASLE Trans., (1962), 5, pg 233.

28. CHU, P.S.Y. "Theory of Lubrication Applied to Pressure Nozzle Design in Wire Drawing". Proc. Inst. Mech. Eng. (1966-67), Vol 181, P3, pg 104.

29. BLOOR, M., DOWSON, D.,& PARSONS, B. "An Elasto-Plasto-Hydrodynamic Lubrication Analysis of the Plane Strain Drawing Process", J. Mech. Eng. Sci., (1970), Vol 12, No 3, pg 178.

30. THOMPSON, P.J.,& SYMMONS, G.R. "A Plasto-Hydrodynamic Analysis of the Lubrication and Coating of Wire using a Polymer Melt during Drawing". Proc. Inst. Mech. Eng. (1977), Vol 191, 13, pg 115.

31. SYMMONS, G.R., STEVENS, A.J.,& THOMPSON, P.J. "Hydrodynamic Lubrication and Coating of Wire using a Polymer Melt during the Drawing Operation". Wire Industry, June 1978, pg 469.

32. HASHMI, M.S.J. "Strain Rate Sensitivity of Commercially Pure Copper at Room Temperature and Strain Rates of up to 10^6 per second". Sheffield City Polytechnic Technical Report No SCP/MPE/R106 (Oct 1978).

33. RABINOWITSCH, B. "Uber die Viskostat und Elastizitat von Solen". Z. Phys. Chem. (1929), A145, pg 141.

34. ROTEM, Z.,& SHINNAR, R. "Non-Newtonian Flow between Parallel Boundaries in Linear Movement". Chem. Eng. Sci. (1961), Vol 15, pg 130.

35. SWAMY, S.T.N., PRABHU, B.S.,& RAO, B.V.A. "Calculated load Capacity of Non-Newtonian Lubricants in Finite Width Bearings". Wear, (1975), 277.

APPENDIX I.

Development and Listing of the Computer Programs.

Three independant programs were written which were able to solve the various equations simultaneously. Program 1 was developed to give a graphical display of coating thickness against wire speed. Program 2 used the equations developed for program 1 to determine τ_c which could then be used to solve for wire stress and fluid pressure in the deformation zone. Program 3 used the alternative theory to calculate the length of the deformation zone and used this to predict the pressure and stress distributions in the same way as program 2.

I.1 Development of Program 1.

The equations to be solved are summarised:-

$$0 = \frac{C_1 \tau_c^3 + C_1 \tau_c^2 + C_3 \tau_c + C_4}{C_5 \tau_c^2 + C_6 \tau_c + C_7} + U \qquad \ldots\ldots (24)$$

where;

$$C_1 = kh\left(1-\frac{6h}{D_1}+\frac{16h^2}{D_1^2}-\frac{16h^3}{D_1^3}\right)$$

$$C_2 = \frac{kh^2 Yo}{L_{CT}}\left(\frac{12h^2}{D_1^2}-\frac{8h}{D_1}+\frac{3}{2}\right)$$

$$C_3 = h\left(1-\frac{2h}{D_1}-\frac{3kh^3 Yo^2}{D_1 L_{CT}^2}+\frac{kh^2 Yo^2}{L_{CT}^2}\right)$$

$$C_4 = \frac{h^2 Yo}{2L_{CT}} + \frac{kh^4 Yo^3}{4L_{CT}^3}$$

$$C_5 = -\frac{16bL_{CT}^2}{D_1^2}$$

$$C_6 = \frac{8bL_{CT} Yo}{D_1^2} - \frac{4aL_{CT}}{D_1}$$

$$C_7 = \eta_a + Yo(a-bYo) - c$$

$$L_{CT} = (1-C_F)L$$

$$p' = \frac{Yo}{L_{CT}} - \frac{4\tau_c}{D_1} \quad \ldots\ldots (20)$$

$$= C_5 \tau_c^2 + C_6\tau_c + C_7 \quad \ldots\ldots (23)$$

$$Q = \frac{p'h^3}{6\eta_o} + \frac{\tau_c h^2}{2\eta_o} + \frac{k}{\eta_o}\left(\frac{p'^3h^5}{20} + \frac{p'^2h^4\tau_c}{4} + \frac{p'h^3\tau_c^2}{2} + \frac{\tau_c^3h^2}{2}\right) + Uh \quad \ldots\ldots (14)$$

$$Q = \frac{p'h^3}{6\eta_o} + \frac{\tau_a h^2}{2\eta_o} + \frac{k}{\eta_o}\left(\frac{p'^3h^5}{20} + \frac{p'^2h^4\tau_a}{4} + \frac{p'h^3\tau_a^2}{2} + \frac{\tau_a^3h^2}{2}\right) + U_s h \quad \ldots\ldots (26)$$

$$h_d = \frac{Q}{U_d} \quad \ldots\ldots (25)$$

The cubic equation in τ_c (equation 24) was arranged to be solved by iteration using a starting value for τ_c and terminating when the left hand side of the equation approached a defined limit close to zero. Having solved for τ_c for a a particular wire speed the remaining equations were solved and the values stored in an array. The computations were then repeated for all values of wire speed between 0.1 and 2.5 ms^{-1} at intervals of 0.1 ms^{-1}.

Advanced graphing facilities were used to present the stored data in graphical form on a Tektronix graphics terminal. This was particularly useful since changes in the input parameters could be easily achieved and the corresponding variations in coat thickness could be easily identified.

The flowchart for program 1 is shown in Fig A1 and the program listing is shown in Fig A2.

I.2 Development of Program 2.

Program 2 used the same equations as program 1 but also included the stress and pressure equations:-

$$A = \frac{D_2}{2} \quad ; \quad B = \frac{(\frac{D_1}{2} - A)}{C_F . L^{1/3}} \quad ; \quad D = 2(A + B(x)^{1/3})$$

$$\sigma_x = 2YoS.\ln(\frac{D_1}{D}) + \frac{2KS}{n+1}(\ln\frac{D_1}{D})^{n+1} + \frac{6\tau_c}{B^3}((\frac{D_1^2 - D^2}{8}) + A(D-D_1) + A^2.\ln(\frac{D_1}{D})) + \frac{4\tau_c L}{D_1}CT \quad \ldots\ldots (7)$$

$$p = Y - \sigma_x$$

$$Y = S(Yo + K(\ln\frac{D_1}{D})^n)$$

$$S = 1 + (\frac{\dot{\bar{\varepsilon}}}{N}_m)^{1/T} \qquad \text{where} \qquad \dot{\bar{\varepsilon}}_m = \frac{UD_1^2}{C_F L}(\frac{1}{D_2^2} - \frac{1}{D_1^2})$$

Having solved for τ_c as before the values of σ_x and p were computed for values of x between 0 and $x = C_F.L$. Each change in wire drawing speed required a set of σ_x and p to be calculated and stored. The results were printed in tabular form on a standard terminal.

A flowchart for program 2 is shown in Fig A3 and the program listing is shown as Fig A4. A typical set of printed results is shown as Fig A5.

I.3 Development of Program 3.

Program 3 was used to solve the equations from the alternative theory in order to calculate the length of the deformation zone. The equations to be solved are:-

$$0 = U - \frac{p'h^2(1 + \frac{kp'^2h^2}{2})}{2(\eta_a + aL_{CT}p' - bL_{CT}^2p'^2 - c)} \quad \ldots\ldots (32)$$

$$L_{CT} = \frac{YD_1}{p'(D_1-4h)} \quad \ldots\ldots (33)$$

$$Q = Uh - \frac{p'h^3}{3\eta_o} - \frac{kp'^3h^5}{5\eta_o} \quad \ldots\ldots (31)$$

$$h_d = \frac{Q}{U_d} \quad \ldots\ldots (25) \quad ; \quad \tau_c = -p'h \quad ; \quad B = \frac{(\frac{D_1}{2}-A)}{(C_F.L)^{1/3}}$$

$$D = 2(A+B(\dot{x})^{1/3})$$

$$\sigma_x = 2YoS(\ln\frac{D_1}{D}) + \frac{2KS}{(n+1)}(\ln\frac{D_1}{D})^{n+1} + \frac{6\tau_c}{B^3}((\frac{D_1^2-D^2}{8}) + A(D-D_1) + A^2.\ln(\frac{D_1}{D})) + \frac{4\tau_c L_{CT}}{D_1}$$

$$p = Y - \sigma_x \quad \text{where} \quad Y = S(Yo + K(\ln\frac{D_1}{D})^n)$$

$$S = 1 + (\frac{\dot{\bar{\varepsilon}}}{N}m)^{1/T} \quad \text{where} \quad \dot{\bar{\varepsilon}}_m = \frac{UD_1^2}{C_F.L}(\frac{1}{D_2^2} - \frac{1}{D_1^2})$$

The cubic equation in p' (equation 32) was solved by iteration for a specific speed assuming a starting value for both p' and L_{CT}. Computations terminated when the left hand side of the equation reached a specified value close to zero. Equation 33 was then solved using the calculated value of p' to compute a new value for L_{CT}. Initial and new values of L_{CT} were then subtracted and the resulting error compared with a specified maximum error. If the error was greater than that specified, equation (32) was solved again using the newly calculated starting values. If the error was less than that specified, the values of p' and L_{CT} were stored and used to calculate the remaining parameters in the same way as program 2. A change in speed changed the values of p' and L_{CT}.

The flow chart for program 3 is shown in Fig A6 and the program listing is shown as Fig A7. A typical set of printed results is shown as Fig A8.

FIG A1 FLOWCHART FOR PROGRAM 1

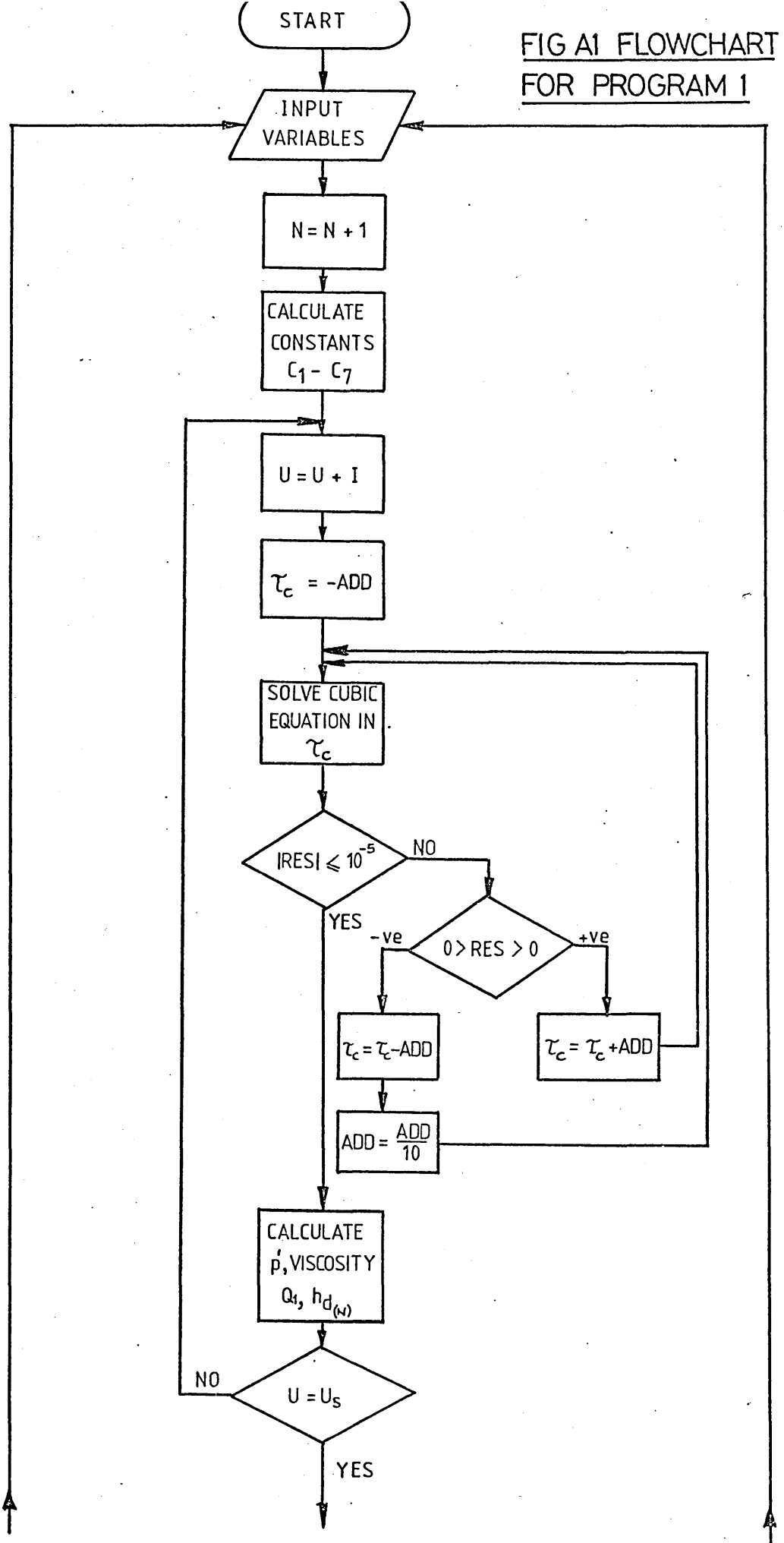

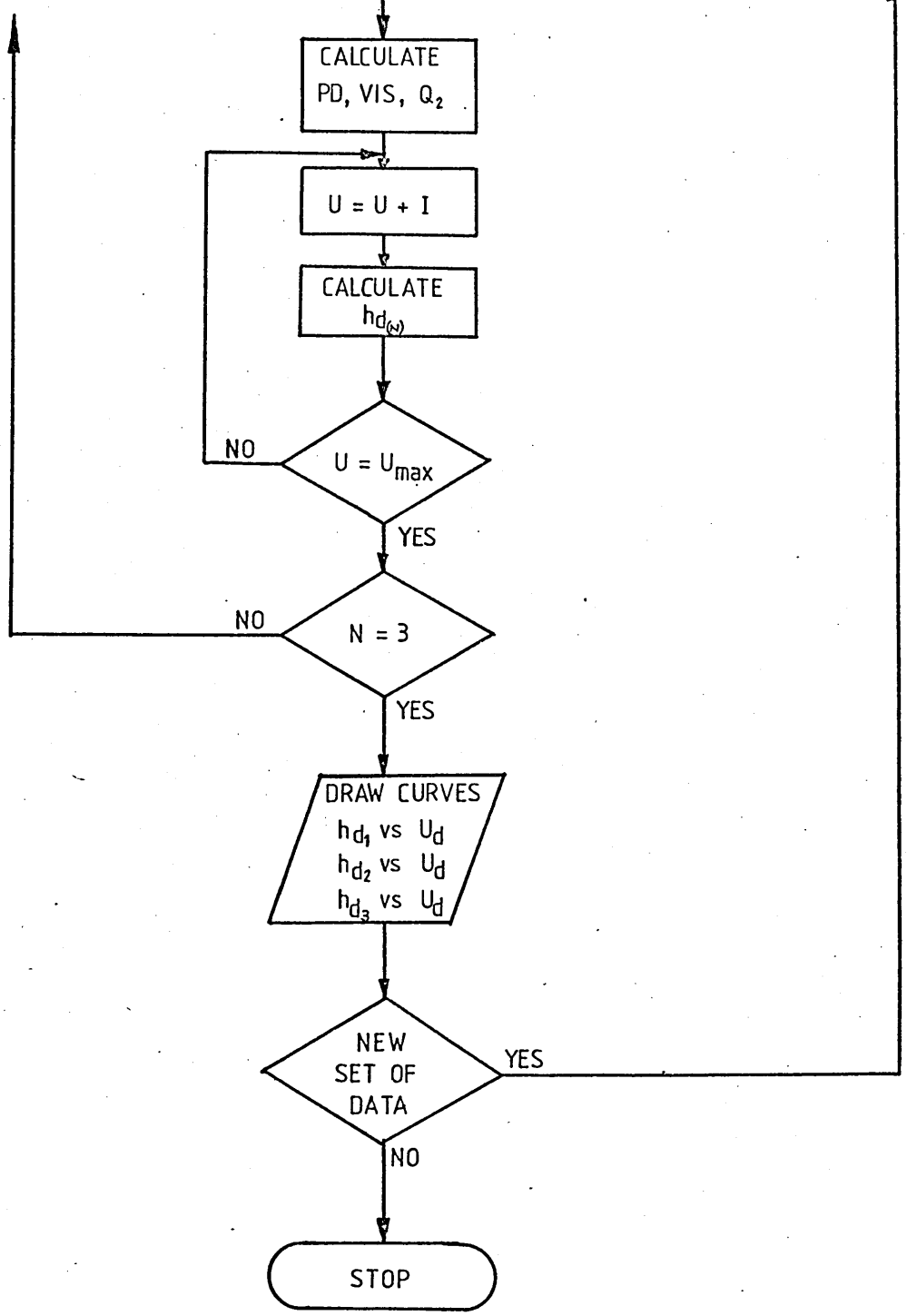

FIG A1 CONTINUED

FIG A2 LISTING OF PROGRAM 1

```
/SYS TIME=4K
LOAD FORTG1
/JOB XESD=40
      DIMENSION U(51),U2(3,51),HI(3,51)
      COMMON HA(51),HB(51),HC(51),UA(51),UB(51),UC(51)
      DIMENSION LABL1(12), LABL3(3)
      DATA LABL1/33,30,69,69,63,32,32,40,77,47,33,41/
      DATA LABL3/40,77,41/
      WRITE(6,200)
  200 FORMAT('1THIS PROGRAM WILL GIVE THE COATING THICKNESS ON'/
     C'+THE WIRE WHEN USING A POLYMER MELT AS THE LUBRICANT'/
     C'+INCORPORATING A CHRISTOPHERSON TUBE'//
     C'+THE FOLLOWING PARAMETERS MUST BE INPUTTED'/
     C'+FOR THE POLYMER- INITIAL VISCOSITY'/
     C13X,'CONSTANTS A, B AND C OF PRESSURE COEFFT.'/
     C13X,'CONSTANT K, FOR SHEAR EQUATION'/
     C13X,'CRITICAL SHEAR STRESS'/
     C'+FOR THE WIRE-     RADIUS'/13X,'INITIAL YIELD STRESS'/
     C'FOR THE C. TUBE- LENGTH'/13X,'GAP'/
     C13X,'FRACTION OF C.T. THAT DEFN STARTS'/
     C'+ALSO TYPE IN DIE SIZE'//
     C'+UP TO THREE SETS OF DATA MAY BE INPUTTED'/
     C'+TYPE IN THE NUMBER OF SETS REQUIRED')
      READ(9,*) II
      WRITE(6,201)
  201 FORMAT(' INPUT THE VALUES IN THE ABOVE ORDER, IN FREE FORMAT'//)
  202 DO 199 I=1,II
  133 WRITE(6,132)
  132 FORMAT('1INPUT VALUES!')
      READ(9,*) VIS,CA,CB,CC,CK,TA,R,YO,CTL,H,AL,D2
      CL=CTL*(1-AL)
      WRITE(6,300)
  300 FORMAT('THE PROGRAM ALSO INCLUDES STRAIN RATE SENSITIVITY'/
     C'+   INPUT CONSTANTS OF THE EQUATION:-'//
     C5X,'S = (1 + (EPS/N) ** (1/P))'//
     C'+IE CONSTANTS N AND P')
      READ(9,*)HEN,PEE
      DO 192 J=2,51
      U(J)=(J-1)*0.05
      EPS=U(J)*4*R*R*(1/(D2*D2)-1./(4*R*R))/(CTL*AL)
      S=(1+((EPS/HEN)**(1/PEE)))
      Y=YO*S
      A=CK*H*(1.-3.*H/R+4.*H*H/(R*R)
     C-2.*H**3/(R**3))
      B=(CK*H*H*Y/CL)*(3.*H*H/(R*R)
     C-4.*H/R+3./2.)
      C=H*(1-H/R-3.*CK*H**3*Y*Y/(2.*R*CL*CL)
     C+CK*H*H*Y*Y/(CL*CL))
      D=H*H*Y/(2.*CL)+CK*H**4*Y**3/(4.*CL**3)
      E=-4.*CB*CL*CL/(R*R)
      F=4.*CB*CL*Y/R-2.*CA*CL/R
      G=VIS+Y*(CA-Y*CB)-CC
```

FIG A2 CONTINUED

```
      ADD=-100000.
      TC=ADD
  198 RES=(A*TC**3+B*TC*TC+C*TC+D)/(E*TC*TC
     C+F*TC+G)+U(J)
      IF(ABS(RES).LT.0.00001) GO TO 195
      IF(RES)197,195,196
  197 TC=TC-ADD
      ADD=ADD/10.
      GO TO 198
  196 TC=TC+ADD
      GO TO 198
  195 CONTINUE
      IF(TA+TC)193,193,194
  194 VISCO=E*TC*TC+F*TC+G
      PD=Y/CL-2.*TC/R
      Q1=PD*H**3/(6.*VISCO)+TC*H*H/(2.*VISCO)+(CK/VISCO
     C)*(PD**3*H**5/20.+PD*PD*H**4*TC/4.+PD*H**3*TC
     C*TC/2.+TC**3*H*H/2.)+U(J)*H
      U2(I,J)=U(J)*4.*B*R/(D2*D2)
      HI(I,J)=Q1/U2(I,J)
      GO TO 192
  193 J=J
      TO=TC
      GO TO 191
  192 CONTINUE
  191 CONTINUE
      VS=(J-1)*0.05
      VISCA=E*TO*TO+F*TO+G
      PD2=Y/CL-2.*TO/R
      Q2=PD2*H**3/(6.*VISCA)+TO*H*H/(2.*VISCA)+(CK/VISCA)*
     C(PD2**3*H**5/20.+PD2*PD2*H**4*TO/4.+PD2*H**3*TO*TO/2.
     C+TO**3*H*H/2.)+VS*H
      DO 190 L=N,51
      U(L)=(L-1)*0.05
      U2(I,L)=U(L)*4.*B*R/(D2*D2)
      HI(I,L)=Q2/U2(I,L)
  190 CONTINUE
  199 CONTINUE
      U(1)=50
      U2(1,1)=50
      U2(2,1)=50
      U2(3,1)=50
      HI(1,1)=50
      HI(2,1)=50
      HI(3,1)=50
      DO 100 J=1,51
      HA(J)=HI(1,J)
      HB(J)=HI(2,J)
      HC(J)=HI(3,J)
      UA(J)=U2(1,J)
      UB(J)=U2(2,J)
      UC(J)=U2(3,J)
  100 CONTINUE
```

FIG A2 CONTINUED

```
      CALL INITT(120)
      CALL BINITT
      CALL DLIMX(0.0,3.0)
      CALL DLIMY(0.0,3.0E-05)
      CALL CHECK(UB,HI)
      CALL DSPLAY(UA,HA)
      CALL CPLOT(UB,HB)
      CALL CPLOT(UC,HC)
      CALL NOTATE(450,10,12,LABL1)
      CALL NOTATE(1,100,3,LABL3)
      CALL MOVABS(14,620)
      CALL ANMODE
      WRITE(6,175)
  175 FORMAT('C'/2X,'O'/2X,'A'/2X,'T'/2X,'I'/2X,'N'/2X,'G'//
     C2X,'T'/2X,'H'/2X,'I'/2X,'C'/2X,'K'/2X,'N'/2X,'E'/2X,'S'/2X,'S')
      CALL TINPUT(I)
      CALL PROMPT
      CALL NEWPAG
      WRITE(6,135)
  135 FORMAT('1IF ANOTHER SET OF DATA IS REQUIRED, TYPE 1'/
     C'+IF NOT, TYPE 0.')
      READ(9,*) X
      IF(X.EQ.0.0) GO TO 134
      IF(X.EQ.1.0) GO TO 202
  134 CONTINUE
      CALL FINITT(0,700)
      CALL EXIT
      END
/INC AG
```

FOR PROGRAM 2

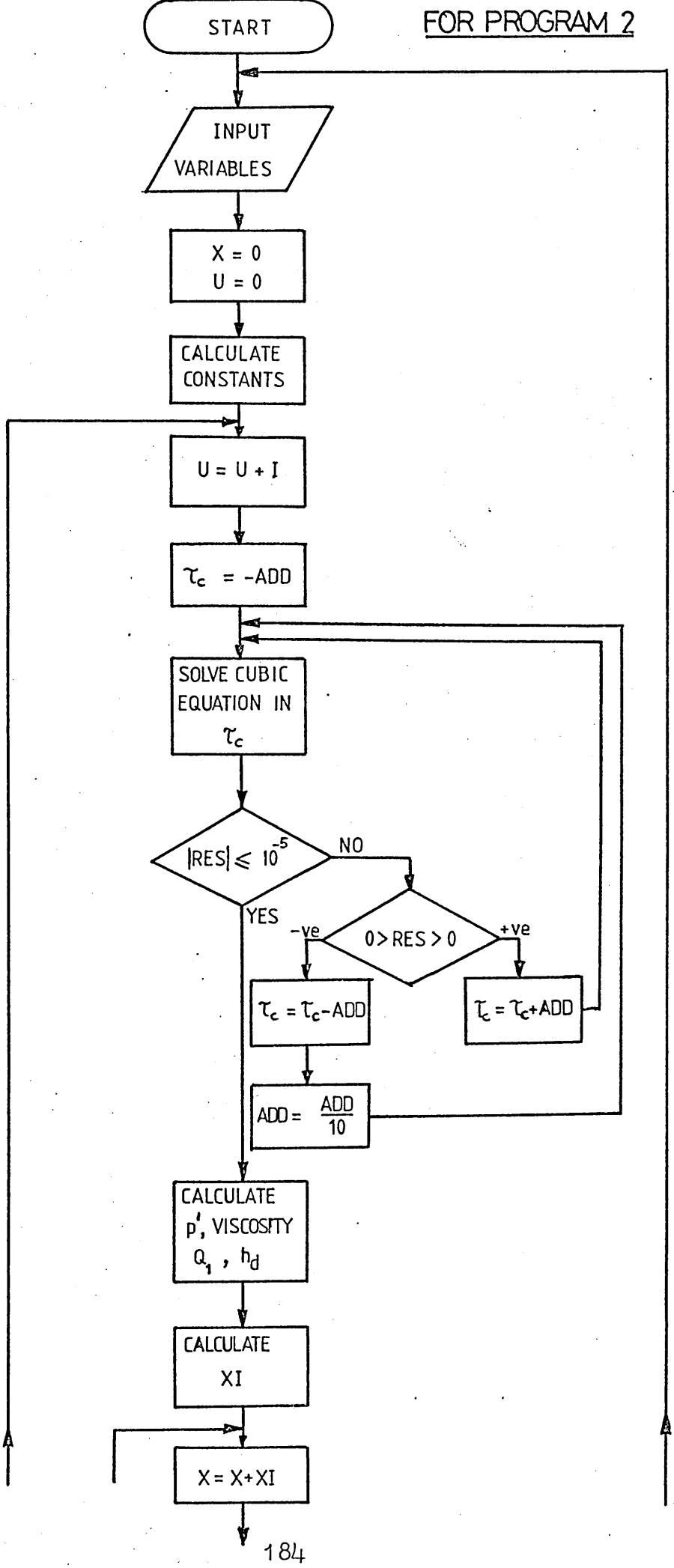

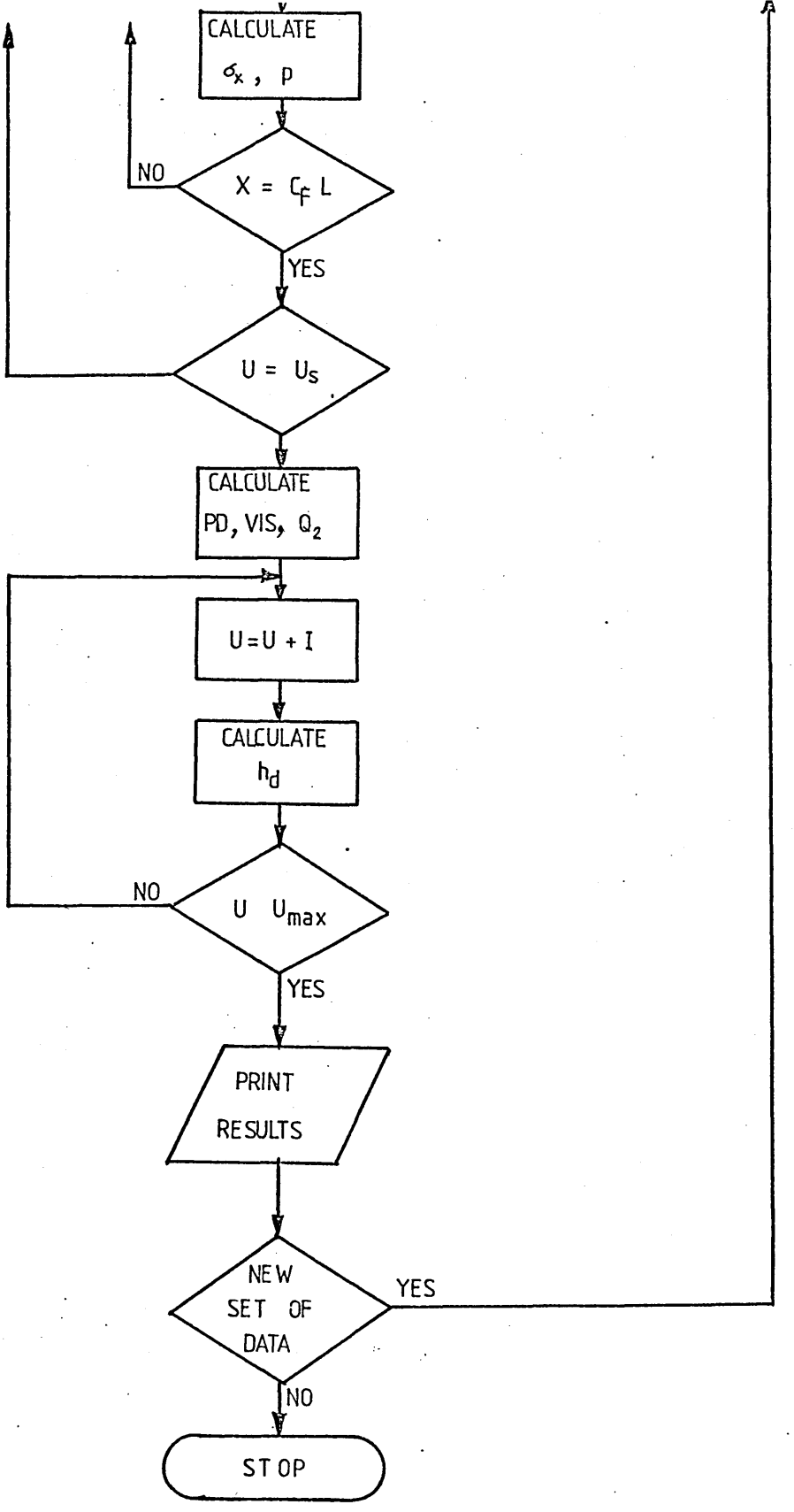

FIGA3 CONTINUED

FIG A4 LISTING OF PROGRAM 2

```
/SYS TIME=MAX
/LOAD FORTG1
      DIMENSION VISCO(25),PD(25),TC(25),Q1(25)
      DIMENSION U(25),U2(25),HI(25),K(21),P(25,11),SIG(25,11)
      WRITE(6,100)
100   FORMAT('1PROGRAM 2.  IF INSTRUCTIONS ARE REQUIRED,'/
     C'+TYPE 1.  IF NOT TYPE 0 TO INPUT DATA'/)
      READ(9,*) KI
      IF(KI.EQ.1.0) GO TO 101
      IF(KI.EQ.0.0) GO TO 105
101   WRITE(6,102)
102   FORMAT('1THIS PROGRAM WILL GIVE THE COATING THICKNESS ON'/
     C'+THE WIRE WHEN USING A POLYMER MELT AS THE LUBRICANT'/
     C'+INCORPORATING A CHRISTOPHERSON TUBE'//
     C'+THE THEORY INCLUDES STRAIN HARDENING OF THE FORM:-'//
     C'+   Y=YO + C(LOG(D1/D))**T     WHERE  T IS THE STRAIN COEFF.'/
     C'+                                    C IS THE STRAIN CONSTANT'//
     C'+THE FLUID IS ASSUMED NON-NEWTONIAN OF THE FORM:-'//
     C'     TAU +  K(TAU**3)= NO*DV/DY  WHERE TAU IS SHEAR STRESS'/
     C'                                 K IS A CONSTANT'/
     C'                                 NO IS VISCOSITY AT ZERO SHEAR'/)
      WRITE(6,103)
103   FORMAT('+THE VISCOSITY IS ASSUMED TO FOLLOW THE LAW:-'//
     C'        NO = NA + AP - BP**2 - C   WHERE P IS PRESSURE'/
     C'                                   NA IS VISCOSITY AT P= ATMOS'/
     C'                                   A, B, AND C ARE CONSTANTS'//
     C'+SLIP IS ASSUMED AT SOME CRITICAL VALUE OF TAU'//
     C'+THE FOLLOWING PARAMETERS MUST BE INPUTTED'//
     C'+FOR THE POLYMER- INITIAL VISCOSITY'/
     C13X,'CONSTANTS A, B, AND C OF THE PRESSURE COEFFT.'/
     C13X,'CONSTANT K, FOR SHEAR EQUATION'/
     C13X,'CRITICAL SHEAR STRESS'/)
      WRITE(6,104)
104   FORMAT('+FOR THE WIRE-    RADIUS'/13X,'INITIAL YIELD STRESS'/
     C13X,'STRAIN COEFFICIENT'/13X,'STRAIN CONSTANT'/
     C'+FOR THE C. TUBE- LENGTH'/13X,'GAP'//
     C'+THE THEORY ASSUMES DEFORMATION BEFORE THE DIE, IN THE '/
     C'+CHRISTOPHERSON TUBE. TYPE IN THE FRACTION OF THE C.T. THAT'/
     C'+DEFORMATION TAKES PLACE. IE. LAST QUARTER = 0.25 '/
     C'+ALSO TYPE IN THE DIE SIZE.'//
     C'+INPUT THESE VALUES IN THE ABOVE ORDER, IN FREE FORMAT')
105   WRITE(6,106)
106   FORMAT('1INPUT VALUES!')
      READ(9,*)  VIS,CA,CB,CC,CK,TA,R,YO,T,CO,CTL,H,AL,D2
      WRITE(6,107)
107   FORMAT('1PROGRAM ALSO INCLUDES STRAIN RATE SENSITIVITY'/
     C'+  INPUT CONSTANTS OF EQUATION:-'//
     C5X,'S = (1 + (EPS/H)**(1/P))'//
     C'+IE  CONSTANTS  H  AND  P')
      READ(9,*)HEN,PEE
```

FIG A4 CONTINUED

```
C  *  *  *  *  *  *  *  *  *  *  *  *  *  *  *  *  *  *  *  *  *  *  *
C  *                                                                    *
C  *     C A L C U L A T E   C O N S T A N T S                          *
C  *                                                                    *
C  *  *  *  *  *  *  *  *  *  *  *  *  *  *  *  *  *  *  *  *  *  *  *
      CL=CTL*(1-AL)
      M=0
      XI=AL*CTL/10.
      DO 115 J=1,25
      M=M+1
      U(J)=J*0.1
      EPS=U(J)*4*R*R*(1/(D2*D2)-1./(4*R*R))/(XI*10.)
      S=(1+((EPS/HEN)**(1/PEE)))
      YA=Y0*S
      A=CK*H*(1.-3.*H/R+4.*H*H/(R*R)-2.*H**3/(R**3))
      B=(CK*H*H*YA/CL)*(3.*H*H/(R*R)-4.*H/R+3./2.)
      C=H*(1.-H/R-3.*CK*H**3*YA*YA/(2.*R*CL*CL)+CK*H*H*YA*YA/(CL*CL))
      D=H*H*YA/(2.*CL)+CK*H**4*YA**3/(4.*CL**3)
      E=-4.*CB*CL*CL/(R*R)
      F=4.*CB*CL*YA/R-2.*CA*CL/R
      G=VIS+YA*(CA-YA*CB)-CC
      AA=D2/2.
      BB=(R-AA)/((XI*10.)**0.33333)
C  *  *  *  *  *  *  *  *  *  *  *  *  *  *  *  *  *  *  *  *  *  *  *
C  *                                                                    *
C  *     S O L V E   C U B I C   I N   T C                              *
C  *                                                                    *
C  *  *  *  *  *  *  *  *  *  *  *  *  *  *  *  *  *  *  *  *  *  *  *
      ADD=-100000.
      TC(J)=ADD
  103 RES=(A*TC(J)**3+B*TC(J)*TC(J)+C*TC(J)+D)/(E*TC(J)*TC(J)
     C+F*TC(J)+G)+U(J)
      IF(ABS(RES).LT.0.00001) GO TO 111
      IF(RES)109,111,110
  109 TC(J)=TC(J)-ADD
      ADD=ADD/10.
      GO TO 103
  110 TC(J)=TC(J)+ADD
      GO TO 103
  111 CONTINUE
C  *  *  *  *  *  *  *  *  *  *  *  *  *  *  *  *  *  *  *  *  *  *  *
C  *                                                                    *
C  *  D E T E R M I N E   V I S C O S I T Y ,  P R E S S U R E          *
C  *                                                                    *
C  *        A N D   T H I C K N E S S                                   *
C  *                                                                    *
C  *  *  *  *  *  *  *  *  *  *  *  *  *  *  *  *  *  *  *  *  *  *  *
  112 VISCO(J)=E*TC(J)*TC(J)+F*TC(J)+G
      PD(J)=YA/CL-2.*TC(J)/R
      Q1(J)=PD(J)*H**3/(6.*VISCO(J))+TC(J)*H*H/(2.*VISCO(J))+(CK/VISCO
     C(J))*(PD(J)**3*H**5/20.+PD(J)*PD(J)*H**4*TC(J)/4.+PD(J)*H**3*TC(J)
     C*TC(J)/2.+TC(J)**3*H**4/2.)+U(J)*H
      U2(J)=U(J)*4.*R*R/(D2*D2)
      HI(J)=Q1(J)/U2(J)
      TB=-TC(J)
      DO 113 NN=1,11
      X(NN)=XI*(NN-1)
      DI=2.*(AA+BB*(X(NN)**0.33333))
```

FIG A4 CONTINUED

```
C  *  *  *  *  *  *  *  *  *  *  *  *  *  *  *  *  *  *  *  *  *
C  *                                                             *
C  *     C A L C U L A T E   S T R E S S   A N D   P R E S S .   *
C  *                                                             *
C  *           D I S T R I B U T I O N                           *
C  *                                                             *
C  *  *  *  *  *  *  *  *  *  *  *  *  *  *  *  *  *  *  *  *  *
      YSH=2.*YO*S*ALOG(2.*R/DI)+(2.*CO*S*(ALOG(2.*R/DI))**(T+1))/(T+1)
      Y=(Y0+CO*(ALOG(2.*R/DI))**T)*S
      SIG(J,NN)=YSH+6.*TB/(BB**3)*(((2.*R)**2-DI**2)
     C/3.+AA*(DI-(2.*R))+AA*AA*ALOG(2.*R/DI))+4*TB*(1-AL)*CTL/(2.*R)
      P(J,NN)=Y-SIG(J,NN)
  113 CONTINUE
C  *  *  *  *  *  *  *  *  *  *  *  *  *  *  *  *  *  *  *  *  *
C  *                                                             *
C  *  L O G I C   S T E P   F O R   S L I P   C O N D I T I O N  *
C  *                                                             *
C  *  *  *  *  *  *  *  *  *  *  *  *  *  *  *  *  *  *  *  *  *
      IF(TA+TC(J))116,116,115
  115 CONTINUE
  116 N=J
      DO 117 J=J,25
      TC(J)=TC(N)
      VISCO(J)=VISCO(N)
  117 CONTINUE
      TO=TC(N)
      VS=N*0.1
      VISCA=E*TO*TO+F*TO+G
      PD2=YA/CL-2.*TO/R
      Q2=PD2*H**3/(6.*VISCA)+TO*H*H/(2.*VISCA)+(CK/VISCA)*(PD2**3*
     CH**5/20.+PD2*PD2*H**4*TO/4.+PD2*H**3*TO*TO/2.+TO**3*H*H/2.)+VS*H
      DO 113 L=N,25
      U(L)=L*0.1
      U2(L)=U(L)*4.*R*R/(D2*D2)
      HI(L)=Q2/U2(L)
  113 CONTINUE
C  *  *  *  *  *  *  *  *  *  *  *  *  *  *  *  *  *  *  *  *  *
C  *                                                             *
C  *   P R I N T   O U T   R E S U L T S                         *
C  *                                                             *
C  *  *  *  *  *  *  *  *  *  *  *  *  *  *  *  *  *  *  *  *  *
      WRITE(6,119)
  119 FORMAT('1THE COATING THICKNESS IS AS FOLLOWS-'///
     C5X,'SPEED',15X,'THICKNESS',9X,'VISCOSITY',7X,'SHEAR STRESS'//
     C,6X,'M/S',20X,'M.',13X,'NS/SQ.M',10X,'N/SQ.M'//)
      DO 121 J=1,25
      WRITE(6,120) U2(J),HI(J),VISCO(J),TC(J)
  120 FORMAT(1PE12.4,10X,1PE12.4,3X,1PE10.4,6X,1PE12.4)
  121 CONTINUE
```

FIG A4 CONTINUED

```
      WRITE(6,122)
122   FORMAT('1IF PRESSURE AND STRESS DISTRIBUTIONS ARE REQUIRED,'/
     C'+TYPE 1 - IF NOT THEN TYPE 0'/)
      READ(9,*) KK
      IF(KK.EQ.0.0) GO TO 129
      IF(KK.EQ.1.0) GO TO 123
123   DO 127 J=1,M
      WRITE(6,124) U2(J)
124   FORMAT(//'1AT SPEED =',1X,F4.2,1K,'M/S:-'///,2K,'DISTANCE FROM DIE
     C ',7K,'PRESSURE',13K,'STRESS'//,3K,'(M)',17K,'N/SQ.M',
     C14K,'N/SQ.M'//)
      DO 126 NN=1,11
      WRITE(6,125) X(NN),P(J,NN),SIG(J,NN)
125   FORMAT(4K,1PE12.4,3K,1PE12.4,3K,1PE12.4)
126   CONTINUE
127   CONTINUE
      WRITE(6,128)
128   FORMAT(//,'SHEAR STRESS (TC) IS NOW CONSTANT GIVING CONSTANT'/
     C'1PRESSURE AND STRESS DISTRIBUTIONS AS ABOVE')
129   WRITE(6,130)
130   FORMAT('1IF ANOTHER SET OF DATA IS REQUIRED, TYPE 1'/
     C'+IF NOT, TYPE 0')
      READ(9,*) K
      IF(K.EQ.0.0) GO TO 131
      IF(K.EQ.1.0) GO TO 105
131   CONTINUE
      CALL EXIT
      END
```

FIG A5 TYPICAL PRINTOUT FROM PROGRAM 2

```
PROGRAM 2.  IF INSTRUCTIONS ARE REQUIRED,
TYPE 1.  IF NOT TYPE 0 TO INPUT DATA

?
0

INPUT VALUES!
?
70,1.1E-05,1.0575E-14,-331.76,3.07E-11,1E06,.31E-03,1E03,.25
?
3.41E03,.03,.13E-03,.5,1.37E-03

PROGRAM ALSO INCLUDES STRAIN RATE SENSITIVITY
  INPUT CONSTANTS OF EQUATION:-

    S = (1 + (EPS/N)**(1/P))

IE  CONSTANTS  N  AND  P
?
55000,3.8

THE COATING THICKNESS IS AS FOLLOWS-
```

SPEED	THICKNESS	VISCOSITY	SHEAR STRES
M/S	M.	NS/SQ.M	N/SQ.M
1.3933E-01	4.5053E-06	1.3433E+03	-4.2906E+05
2.7965E-01	1.6672E-05	1.9239E+03	-5.1611E+05
4.1943E-01	1.9993E-05	1.9736E+03	-5.3142E+05
5.5931E-01	2.1624E-05	2.0220E+03	-6.3439E+05
6.9913E-01	2.2667E-05	2.0533E+03	-6.7945E+05
8.3896E-01	2.3444E-05	2.0796E+03	-7.1397E+05
9.7878E-01	2.4070E-05	2.1173E+03	-7.5433E+05
1.1186E+00	2.4603E-05	2.1422E+03	-7.3659E+05
1.2584E+00	2.5067E-05	2.1643E+03	-8.1625E+05
1.3983E+00	2.5481E-05	2.1857E+03	-8.4331E+05
1.5381E+00	2.5854E-05	2.2050E+03	-8.6961E+05
1.6779E+00	2.6197E-05	2.2230E+03	-8.9391E+05
1.8177E+00	2.6511E-05	2.2399E+03	-9.1600E+05
1.9576E+00	2.6802E-05	2.2559E+03	-9.3377E+05
2.0974E+00	2.7075E-05	2.2710E+03	-9.5963E+05
2.2372E+00	2.7331E-05	2.2853E+03	-9.7959E+05
2.3770E+00	2.7571E-05	2.2990E+03	-9.9376E+05
2.5169E+00	2.7798E-05	2.3121E+03	-1.0172E+06
2.6567E+00	2.8335E-05	2.3121E+03	-1.0172E+06
2.7965E+00	2.5013E-05	2.3121E+03	-1.0172E+06
2.9364E+00	2.3327E-05	2.3121E+03	-1.0172E+06
3.0762E+00	2.2744E-05	2.3121E+03	-1.0172E+06
3.2160E+00	2.1755E-05	2.3121E+03	-1.0172E+06
3.3558E+00	2.0843E-05	2.3121E+03	-1.0172E+06
3.4957E+00	2.0015E-05	2.3121E+03	-1.0172E+06

FIGA6 FLOWCHART FOR PROGRAM 3

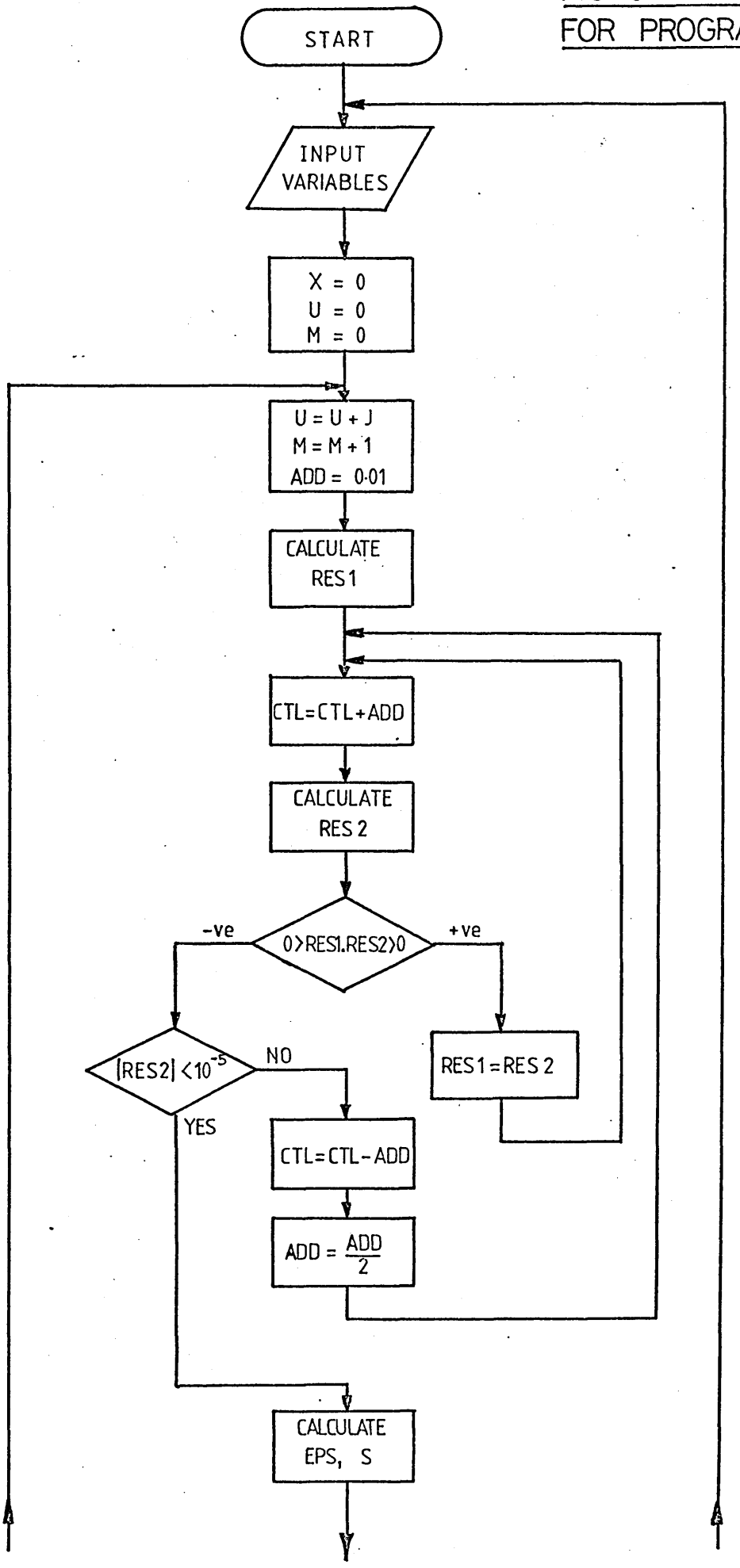

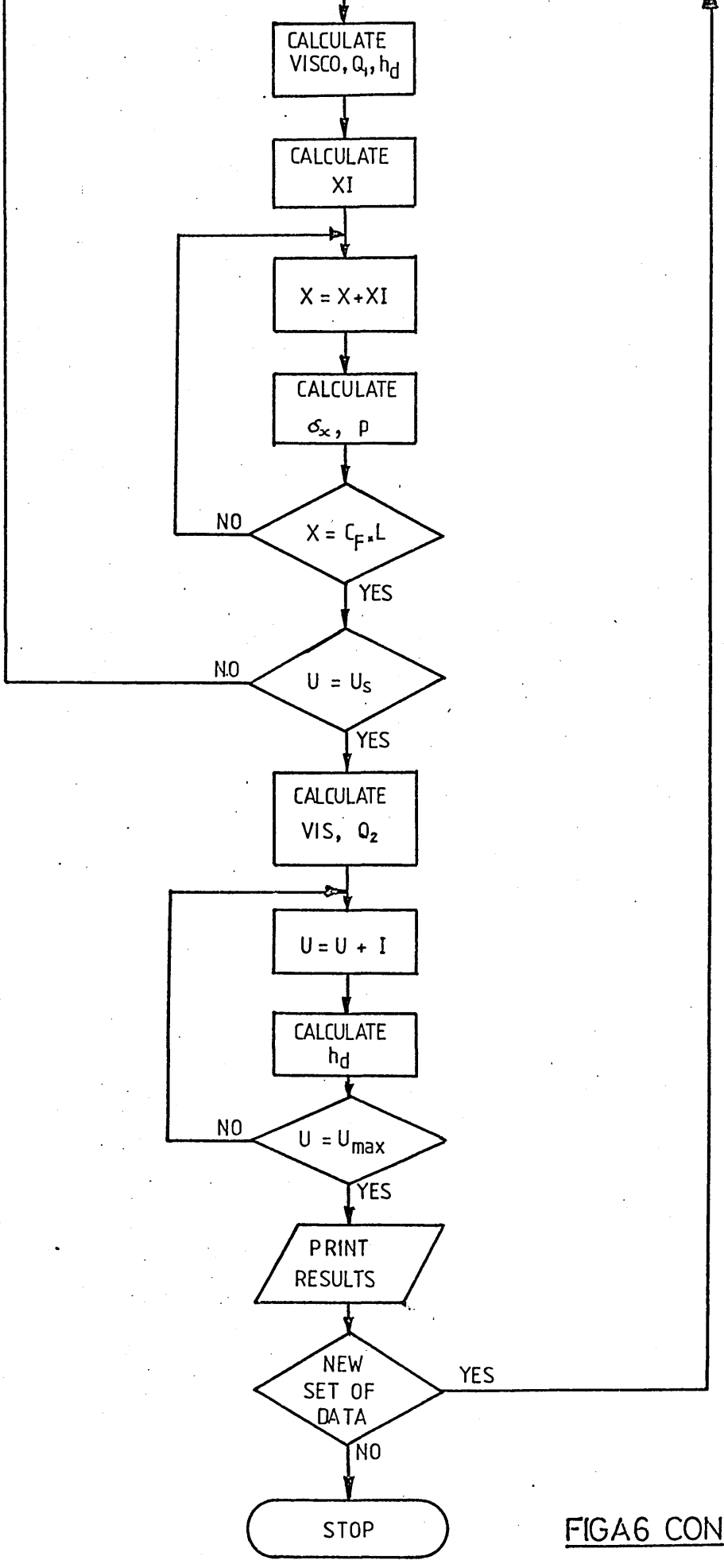

FIGA6 CONTINUED

FIGA7 LISTING OF PROGRAM 3

```
/SYS TIME=MAX
/LOAD FORTG1
      DIMENSION PD(25),U(25),CL(25),VISCO(25),HI(25),Q(25),TC(25)
      DIMENSION SIG(25,11),U2(25),P(25,11),X(25,11)
  100 WRITE(6,101)
  101 FORMAT('1PROGRAM 3.  THIS PROGRAM ASSUMES DV/DY = 0 AT Y = H.'/
     C'+INPUT THE FOLLOWING VARIABLES:-'/
     C3X,'GAP',/3X,'INITIAL VISCOSITY',/3X,'CONSTANTS A,B AND C',/
     C3X,'CONSTANT K',/3X'WIRE DIAMETER',/3X,'INITIAL YIELD',/
     C3X,'TUBE LENGTH',/3X,'CRITICAL SHEAR STRESS'/
     C3X,'DIE SIZE',/3X,'STRAIN HARDENING COEFFT.',/
     C3X,'STRAIN HARDENING CONSTANT',//'INPUT IN ABOVE ORDER'/
     C'IN FREE FORMAT')
      READ(5,*) H,VIS,A,B,C,CK,D1,YO,FL,TA,D2,T,CO
      WRITE(6,102)
  102 FORMAT('1THIS PROGRAM ALSO INCLUDES THE EFFECT OF STRAIN'/
     C'+RATE SENSITIVITY - INPUT CONSTANTS OF EQUATION:-'//
     C3X,'S = (1+(EPS/N)**(1/P))'//
     C'+IE. CONSTANTS N AND P')
      READ(5,*)HEN,PEE
      M=0
      DO 116 J=1,25
      M=M+1
      U(J)=J*0.1
      ADD=0.01
      CTL=0.00001
      FLX1=ABS(FL-CTL)
      PA=YO*D1/(CTL*(D1-4.*H))*(1.+(U(J)*D1*D1/(HEN*FLX1*(D1*D1
     C-D2*D2)))**(1./PEE))
      RES1=U(J)-(PA*H*H/2.*(1.+CK*PA*PA*H*H/2.)/(VIS+A*CTL
     C*PA-B*CTL*CTL*PA*PA-C))
  103 CTL=CTL+ADD
      FLX2=ABS(FL-CTL)
      PD(J)=YO*D1/(CTL*(D1-4.*H))*(1.+(U(J)*D1*D1/(HEN*FLX2*(D1*D1
     C-D2*D2)))**(1./PEE))
      RES2=U(J)-(PD(J)*H*H/2.*(1.+CK*PD(J)*PD(J)*H*H/2.)/(VIS
     C+A*CTL*PD(J)-B*CTL*CTL*PD(J)*PD(J)-C))
      IF(RES1*RES2) 105,106,104
  104 RES1=RES2
      GO TO 103
  105 IF(ABS(RES1).LT.0.00001) GO TO 106
      CTL=CTL-ADD
      ADD=ADD/2.
      GO TO 103
  106 EPS=U(J)*D1*D1*(1./(D2*D2)-1./(D1*D1))/FLX2
      S=(1.+((EPS/HEN)**(1./PEE)))
      CL(J)=CTL
      VISCO(J)=VIS+A*CL(J)*PD(J)-B*CL(J)**2*PD(J)**2-C
      Q(J)=U(J)*H-PD(J)*H**3/(3.*VISCO(J))-CK*PD(J)**3
     C*H**5/(5.*VISCO(J))
      U2(J)=U(J)*D1*D1/(D2*D2)
      HI(J)=Q(J)/U2(J)
      TC(J)=-PD(J)*H
```

```
      XI=(EL-CL(J))/10.
      IF(XI) 113,113,111
  111 AA=D2/2.
      BB=(D1/2-AA)/((XI*10.)**0.33333)
      TB=-TC(J)
      DO 112 NN=1,11
      X(J,NN)=XI*(NN-1)
      DI=2.*(AA+BB*(X(J,NN)**0.33333))
      YSH=2.*YO*S*ALOG(D1/DI)+(2.*CO*S*(ALOG(D1/DI))**(T+1))/(T+1)
      Y=(YO+CO*(ALOG(D1/DI))**T)*S
      SIG(J,NN)=YSH+.6*TB/(BB**3)*((D1**2-DI**2)/3.+AA
     C*(DI-D1)+AA*AA*ALOG(D1/DI))+4.*TB*CL(J)/D1
      P(J,NN)=Y-SIG(J,NN)
  112 CONTINUE
      GO TO 115
  113 DO 114 NN=1,11
      SIG(J,NN)=0
      P(J,NN)=0
  114 CONTINUE
  115 IF(TA+TC(J)) 117,117,116
  116 CONTINUE
  117 DO 118 N=J,25
      CL(N)=CL(J)
      U(N)=N*.1
      PD(N)=PD(J)
      VISCO(N)=VISCO(J)
      Q(N)=Q(J)
      U2(N)=U(N)*D1*D1/(D2*D2)
      HI(N)=Q(N)/U2(N)
  118 CONTINUE
      WRITE(6,119)
  119 FORMAT('1THE COATING THICKNESS IS AS FOLLOWS:-'///
     C3X,'SPEED',5X,'THICKNESS',4X,'VISCOSITY',4X,'P-DASH',5X,
     C'LENGTH'//4X,'M/S',11X,'M',9X,'NS/SQ.M',21X,'M'//)
      DO 121 J=1,25
      WRITE(6,120) U2(J),HI(J),VISCO(J),PD(J),CL(J)
  120 FORMAT(1PE11.4,1X,1PE12.4,3X,1PE10.4,1X,1PE11.4,3X,1PE10.4)
  121 CONTINUE
      WRITE(6,122)
  122 FORMAT('1IF PRESSURE AND STRESS DISTRIBUTIONS ARE REQUIRED,'/
     C'+TYPE 1 - IF NOT THEN TYPE 0'/)
      READ(9,*) KK
      IF(KK.EQ.0.0) GO TO 123
      IF(KK.EQ.1.0) GO TO 123
  123 DO 126 J=1,4
      WRITE(6,124) U2(J)
  124 FORMAT(//'1AT SPEED=',1X,F4.2,1X,'M/S:-'///,2X,'DISTANCE FROM DIE
     C',7X,'PRESSURE',13X,'STRESS'//9X,'M',18X,'N/SQ.M',14X,'N/SQ.M'//)
      DO 126 NN=1,11
      WRITE(6,125) X(J,NN),P(J,NN),SIG(J,NN)
  125 FORMAT(4X,1PE12.4,8X,1PE12.4,3X,1PE12.4)
  126 CONTINUE
      WRITE(6,127)
  127 FORMAT(//,'SHEAR STRESS (TC) IS NOW CONSTANT GIVING CONSTANT'/
     C'1PRESSURE AND STRESS DISTRIBUTIONS AS ABOVE')
  128 WRITE(6,129)
  129 FORMAT('1IF ANOTHER SET OF DATA IS REQUIRED TYPE 1'/
     C'+IF NOT THEN TYPE 0')
      READ(9,*) K
      IF(K.EQ.1.0) GO TO 100
      IF(K.EQ.0.0) GO TO 130
  130 CONTINUE
      CALL EXIT
      END
```

```
PROGRAM 3.  THIS PROGRAM ASSUMES DV/DY = 0 AT Y = H.
INPUT THE FOLLOWING VARIABLES:-
  GAP
  INITIAL VISCOSITY
  CONSTANTS A, B AND C
  CONSTANT K
  WIRE DIAMETER
  INITIAL YIELD
  TUBE LENGTH
  CRITICAL SHEAR STRESS
  DIE SIZE
  STRAIN HARDENING COEFFT.
  STRAIN HARDENING CONSTANT

INPUT IN ABOVE ORDER
IN FREE FORMAT
?
.13E-03,70,1.1E-05,1.0575E-14,-2-381.76,3.07E-11,1.62E-03,1E03
?
.03,1E06,1.37E-03,.25,3.41E03

THE PROGRAM ALSO INCLUDES THE EFFECT OF STRAIN
RATE SENSITIVITY - INPUT CONSTANTS OF EQUATION:-

  S = (1+(EPS/N)**(1/P))

IE. CONSTANTS N AND P
?
55000,3.3

THE COATING THICKNESS IS AS FOLLOWS:-
```

SPEED M/S	THICKNESS M	VISCOSITY NS/SQ.M	P-DASH	LENGTH M
1.3933E-01	2.3333E-05	2.2455E+03	2.0303E+09	9.7309E-02
2.7965E-01	2.7502E-05	2.3940E+03	2.7359E+09	8.2392E-02
4.1943E-01	2.6999E-05	2.3169E+03	3.1220E+09	6.3313E-02
5.5931E-01	2.6733E-05	2.3071E+03	3.4464E+09	6.1453E-02
6.9913E-01	2.6644E-05	2.3073E+03	3.7235E+09	5.6337E-02
8.3896E-01	2.6545E-05	2.3093E+03	3.9664E+09	5.3500E-02
9.7873E-01	2.6466E-05	2.3130E+03	4.1341E+09	5.0836E-02
1.1136E+00	2.6404E-05	2.3165E+03	4.3321E+09	4.8660E-02
1.2534E+00	2.6355E-05	2.3200E+03	4.5645E+09	4.6835E-02
1.3933E+00	2.6313E-05	2.3234E+03	4.7339E+09	4.5271E-02
1.5331E+00	2.6273E-05	2.3263E+03	4.8925E+09	4.3909E-02
1.6779E+00	2.6249E-05	2.3300EX03	5.0413E+09	4.2703E-02
1.8177E+00	2.6222E-05	2.3331E+03	5.1832E+09	4.1636E-02
1.9576E+00	2.6199E-05	2.3361E+03	5.3175E+09	4.0672E-02
2.0974E+00	2.6196E-05	2.3390E+03	5.4454E+09	3.9300E-02
2.2372E+00	2.6159E-05	2.3413E+03	5.5634E+09	3.8999E-02
2.3770E+00	2.4621E-05	2.3413E+03	5.5634E+09	3.8999E-02
2.5169E+00	2.3253E-05	2.3413E+03	5.5634E+09	3.8999E-02
2.6567E+00	2.2029E-05	2.3413E+03	5.5634E+09	3.8999E-02
2.7965E+00	2.0927E-05	2.3413E+03	5.5634E+09	3.8999E-02
2.9364E+00	1.9931E-05	2.3413E+03	5.5634E+09	3.8999E-02
3.0762E+00	1.9025E-05	2.3413E+03	5.5634E+09	3.8999E-02
3.2160E+00	1.8198E-05	2.3413E+03	5.5634E+09	3.8999E-02
3.3558E+00	1.7440E-05	2.3413E+03	5.5634E+09	3.8999E-02
3.4957E+00	1.6742E-05	2.3413E+03	5.5634E+09	3.8999E-02

APPENDIX II

Newtonian Solution.

For comparison purposes, a Newtonian theory was derived assuming constant viscosity with respect to both shear stress and pressure. The analysis is given below.

Equilibrium of the melt in the tube gives:-

$$\frac{\partial p}{\partial x} = \frac{\partial \tau}{\partial y'}$$

Integrating;

$$\tau = p' y' + \tau_c \qquad \ldots\ldots \text{(A2.1)}$$

where $p' = \frac{\partial p}{\partial x}$

τ_c = shear stress at $y' = 0$

Also $\tau = \eta \frac{\partial v}{\partial y'}$

Hence;

$$\frac{\partial v}{\partial y'} = \frac{p' y'}{\eta} + \frac{\tau_c}{\eta}$$

Integrating:-

$$v = \frac{p' y'^2}{2\eta} + \frac{\tau_c y'}{\eta} + c \qquad \ldots\ldots \text{(A2.2)}$$

Boundary conditions; at $y' = 0$, $v = U$ .... (a)

$y' = h$, $v = 0$ .... (b)

Using boundary condition (a), gives $c = U$

Therefore;

$$v = \frac{p'y^2}{2\eta} + \frac{\tau_c y'}{\eta} + U \qquad \ldots\ldots (A2.3)$$

Flow rate $Q = \int_o^h v\, dy'$ therefore;

$$Q = \frac{p'h^3}{6\eta} + \frac{\tau_c h^2}{2\eta} + Uh \qquad \ldots\ldots (A2.4)$$

Applying boundary condition (b) to equation (A2.3) gives:-

$$0 = \frac{p'h^2}{2\eta} + \frac{\tau_c h}{\eta} + U \qquad \ldots\ldots (A2.5)$$

Yield criteria give:-

$$p' = \frac{Y}{L} - \frac{2\tau_c}{r} \qquad \ldots\ldots (A2.6)$$

Therefore:-

$$0 = \frac{h^2}{2\eta}\left(\frac{Y}{L} - \frac{2\tau_c}{r}\right) + \frac{\tau_c h}{\eta} + U$$

Hence:-

$$\tau_c = -\frac{\left(\frac{h^2Y}{2L} + U\eta\right)}{h\left(1 - \frac{h}{r}\right)} \qquad \ldots\ldots (A2.7)$$

Substitution for τ_c and p' into equation (A2.4) gives:-

$$Q = \frac{h^3}{6\eta}\left(\frac{Y}{L} - \frac{2\tau_c}{r}\right) - \frac{h^2}{2\eta}\frac{\left(\frac{h^2Y}{2L} + U\eta\right)}{h\left(1-\frac{h}{r}\right)} + Uh$$

Which leads to :-

$$h_d\left(\frac{D_2}{D_1}\right)^2 = \frac{h^3 Y}{6\eta UL} + h + \frac{h(h^2Y + 2LU\eta)}{2\eta UL(r-h)}\left(\frac{h}{3} - \frac{r}{2}\right) \quad \ldots\ldots \text{(A2.8)}$$

Velocity profiles were required for comparison with the non-Newtonian theory presented in the main text. Solutions of equations A2.6, A2.7 and A2.3 gave the following results:-

y (mm)	U=0.1 ms^{-1}	U=1 ms^{-1}
0	0.1	1
0.02	4.9×10^{-2}	8.2×10^{-1}
0.04	8.57×10^{-3}	6.6×10^{-1}
0.06	-2.2×10^{-2}	5.2×10^{-1}
0.08	-4.3×10^{-2}	3.9×10^{-1}
0.1	-5.4×10^{-2}	2.8×10^{-1}
0.12	-5.5×10^{-2}	1.9×10^{-1}
0.14	-4.7×10^{-2}	1.1×10^{-1}
0.16	-2.8×10^{-2}	4.6×10^{-1}
0.18	0	0
τ_c	-1.946×10^{5}	-6.446×10^{5}
p'	1.731×10^{9}	2.842×10^{9}

Coat thicknesses were also calculated as shown in the table below.

U ms^{-1}	U_d ms^{-1}	Q $m^3 s^{-1}$	h_d m	τ_c Nm^{-2}
0.1	0.14	-ve	-ve	-1.9464×10^5
0.2	0.28	-ve	-ve	-2.4×10^5
0.3	0.42	2.11×10^{-6}	5.05×10^{-6}	
0.4	0.56	1.03×10^{-5}	1.84×10^{-5}	
0.5	0.7	1.84 "	2.63 "	
0.6	0.84	2.65 "	3.16 "	
0.7	0.98	3.47 "	3.54 "	
0.8	1.12	4.28 "	3.83 "	
0.9	1.26	5.09 "	4.05 "	
1.0	1.4	5.91 "	4.23 "	-6.447×10^5
1.1	1.54	6.73 "	4.38 "	
1.2	1.68	7.54 "	4.49 "	
1.3	1.82	8.35 "	4.6 "	
1.4	1.96	9.17 "	4.69 "	
1.5	2.1	9.98 "	4.76 "	
1.6	2.24	1.08×10^{-4}	4.83 "	
1.7	2.38	1.16 "	4.88 "	-9.946×10^5
1.8	2.52	1.24 "	4.94 "	-1.044×10^6
1.9	2.66	1.24 "	4.66 "	"
2.0	2.8	1.24 "	4.43 "	"

The coat thickness (h_d) versus drawing speed (U_d) were drawn in Fig 61 for comparison with the non-Newtonian theories.

APPENDIX III.

The following appendix contains a catalogue of the most important results in tabular form:-

Copper, 30% reduction, 135°C, WVG 23
" 5% " 150°C "
" 15% " " "
" 30% " " "
" 30% " 180°C "

18/8 Stainless steel, 5% reduction, 150°C, WVG 23
" " " 15% " " "
" " " 30% " " "

60/65 carbon steel, 30% reduction, 135°C, WVG 23
" " " " " 150°C "
" " " " " 180°C "

Copper, 30% reduction, 250°C, Polypropylene

Material - Copper, 30% reduction, 135°C, WVG 23

Speed (ms^{-1})	Thickness (mm)	Load (N)	Adhesion	Coat	Bamboo	Pressure (Nm^{-2}) 1	2	3
0.389	0.073	-	good	fair	yes			
0.445	0.074	-	good	fair	yes			
0.58	0.066	-	good	fair	yes			
0.58	0.071	-	good	poor	yes			
0.47	0.074	-	good	poor	yes			
0.38	0.076	-	excelt.	good	yes			
0.635	0.065	-	poor	good	just			
0.84	0.075	230	fair	good	yes			
0.93	0.070	230	fair	good	yes			
1.05	0.069	230	fair	good	yes			
1.24	0.057	230	fair	good	just			
1.41	0.061	230	poor	good	yes			
1.62	0.047	230	poor	good	yes			
1.79	0.046	240	poor	poor	just			
2.00	0.042	230	poor	fair	just			
2.27	0.037	230	poor	fair	just			
2.66	0.037	230	poor	fair	no			
3.02	0.034	230	poor	p/f	no			
2.85	0.041	230	poor	poor	no			
2.47	0.041	230	poor	fair	no			
2.06	0.044	225	poor	good	yes			
1.76	0.039	225	poor	poor	yes			
1.02	0.066	-	poor	poor	just			
0.95	0.051	-	fair	poor	just			
0.84	0.068	-	good	poor	just			
0.76	0.072	-	good	poor	yes			
0.64	0.065	-	poor	good	just			
0.25	-	-	-- wire snapped --					
0.37	0.079	-	good	good	yes			
0.41	0.082	-	fair	good	yes			

Material - Copper, 5% reduction, 150°C, WVG 23

Speed (ms^{-1})	Thickness (mm)	Load (N)	Adhesion	Coat	Bamboo	Pressure (Nm^{-2})		
						1	2	3
0.30	0.096	221	fair	v.good	yes			
0.25	0.094	221	f/g	v.good	partly			
0.26	0.098	210	fair	v.good	slight			
0.33	0.093	200	fair	good	yes			
0.43	0.087	195	f/p	good	yes			
0.47	0.084	195	poor	f/g	just			
0.40	0.088	190	fair	good	partly			
0.25	0.098	-	fair	v.good	yes			
0.26	0.093	-	fair	v.good	yes			
0.30	0.095	-	fair	v.good	yes			
0.33	0.097	-	fair	v.good	yes			
0.36	0.090	-	fair	v.good	yes			
0.40	0.090	-	fair	good	partly			
0.45	0.074	-	fair	good	partly			
0.47	0.066	-	fair	good	partly			
0.54	0.086	-	fair	good	partly			
0.64	0.087	-	fair	good	no			
0.72	0.070	-	fair	good	no			
0.76	0.033	-	fair	good	no			
0.82	0.040	-	fair	good	no			
0.64	0.084	174	fair	good	no			
0.57	0.090	200	f/p	g/f	just			
0.50	0.092	200	f/p	good	just			
0.81	0.080	200	poor	fair	no			
0.89	0.076	200	poor	fair	no			
0.98	0.071	190	f/p	fair	no			
1.08	0.064	190	poor	f/g	no			
1.03	0.064	200	f/p	good	no			
1.17	0.061	190	f/p	good	no			
0.96	0.068	242	poor	good	no	170	470	775
1.09	0.052	266	poor	v.good	no	195	540	850
1.34	0.042	260	poor	v.good	no	200	550	850

Continued on the next page.

Copper, 5% continued.

1.62	0.032	-	poor	v.good	no	-	-	-
1.88	0.034	266	poor	good	no	205	520	875
2.11	0.031	260	poor	good	no	203	510	875
2.37	0.028	260	f/p	good	no	190	525	825
2.59	0.021	260	poor	good	no	-	-	-
3.00	0.026	277	poor	good	no	210	570	875
0.13	0.110	311	fair	v.good	yes	45	190	650
0.18	0.107	289	v.good	v.good	yes	65	265	700
0.19	0.108	228	fair	good	just	65	275	750
0.21	0.104	245	fair	good	just	70	270	800
0.23	0.104	245	fair	good	yes	45	260	725
0.13	0.111	290	fair	good	yes	60	260	725
0.35	0.095	290	fair	good	yes	60	250	625

Material - Copper, 15% reduction, 150°C, WVG 23

Speed (ms^{-1})	Thickness (mm)	Load (N)	Adhesion	Coat	Bamboo	Pressure (Nm^{-2})		
						1	2	3
0.79	0.066	309	fair	good	just	-	450	800
1.11	0.043	310	poor	fair	no	115	320	725
1.24	0.039	305	fair	v.good	no	125	325	650
1.44	0.034	-	poor	good	no	-	-	-
1.68	0.035	309	poor	good	no	195	375	850
1.89	0.029	309	poor	good	no	200	430	875
2.19	0.029	309	poor	f/g	no	205	590	900
1.75	0.035	305	fair	good	no	205	565	900
1.51	0.039	305	fair	good	no	203	555	875
1.43	0.039	309	fair	good	no	200	540	875
0.94	0.054	305	fair	good	no	170	390	775
0.65	-	317	-	-	-	118	410	675
0.78	-	285	-	-	-	159	495	700
0.27	-	297	-	-	yes	45	179	450
0.91	-	273	-	-	no	164	505	700
1.04	-	269	-	-	-	184	579	800
0.79	-	277	-	-	-	154	505	750
0.65	0.077	231	fair	good	yes			
0.27	0.088	265	fair	good	yes			
0.29	0.088	265	poor	good	yes			
0.34	0.084	265	poor	fair	yes			
0.37	0.085	264	fair	good	yes			
0.42	0.086	274	fair	good	yes			
0.48	0.083	274	poor	good	yes			
0.53	0.082	264	poor	good	yes			
0.59	0.079	253	p/f	good	yes			
0.64	0.074	253	fair	good	yes			
0.70	0.070	253	poor	good	yes			
0.78	0.074	264	poor	good	yes			
1.17	0.057	221	poor	poor	no			
1.86	0.029	221	f/p	f/g	no			
2.32	0.029	-	f/p	good	no			
2.68	0.022	-	f/p	good	no			
3.10	0.020	-	poor	fair	no			

Material - Copper, 30% reduction, 150°C, WVG 23.

Speed (ms^{-1})	Thickness (mm)	Load (N)	Adhesion	Coat	Bamboo	Pressure (Nm^{-2})		
						1	2	3
1.02	0.045	-	fair	good	just			
0.98	0.046	-	poor	good	just			
0.92	0.052	-	poor	fair	just			
0.87	0.054	-	poor	good	just			
0.84	0.056	-	poor	good	yes			
0.78	0.056	-	fair	good	yes			
0.74	0.057	-	fair	good	yes			
0.69	0.056	-	poor	good	yes			
0.51	0.064	-	fair	good	yes			
0.48	0.061	-	fair	good	yes			
0.45	0.083	-	poor	good	yes			
0.13	0.081	267	fair	good	yes	90	290	800
0.13	0.074	262	fair	good	yes	82	290	810
0.18	0.081	323	f/g	good	yes	85	320	850
0.205	0.086	347	good	good	yes	82	300	800
0.27	0.082	345	good	good	yes	85	320	675
0.33	0.082	356	good	good	yes	85	300	650
0.13	0.08	294	good	good	yes	75	280	700
0.37	0.082	356	fair	good	yes			
0.26	0.069	-	fair	good	yes			
0.24	0.095	278	fair	good	yes	55	260	700
0.28	0.090	289	good	good	yes	85	300	750
0.32	0.089	323	good	good	yes	95	320	800
0.25	0.090	300	fair	good	yes	100	330	775
0.76	0.077	232	fair	good	yes			
0.89	0.072	230	fair	good	yes			
0.98	0.069	228	fair	good	yes			
1.15	0.062	225	fair	good	just			
1.34	0.061	242	fair	fair	just			
1.51	0.057	230	fair	fair	just			
1.73	0.043	220	fair	fair	just			
1.90	0.047	230	f/p	fair	just			
2.14	0.040	228	f/p	fair	partly			
2.36	0.040	228	f/p	fair	partly			

Continued on the next page

Copper, 30% continued

2.52	0.037	228	poor	fair	partly			
2.72	0.029	221	poor	poor	no			
2.93	0.029	221	poor	fair	no			
2.78	0.028	221	v.poor	fair	no			
0.19	0.091	289	good	good	yes	80	300	770
0.14	-	178	-- no coat		--	90	300	375
0.17	0.038	178	v.good	good	yes	105	300	400
0.20	-	178	-- no coat		--	125	380	475
0.23	0.025	207	v.good	fair	yes	145	410	600
0.23	0.022	225	v.good	v.good	yes	160	440	550
0.27	0.047	225	excell.	v.good	yes	140	440	625
0.14	-	178	-- no coat		--	100	320	350
0.13	-	-	-- wire snapped		--			
0.54	-	369	-	-	-	80	260	550
0.48	-	369	-	-	-	70	300	700
0.68	-	361	-	-	-	103	340	700
0.75	-	369	-	-	-	100	320	650
0.83	-	369	-	-	-	108	320	650
0.99	-	360	-	-	-	130	280	780
1.22	-	369	-	-	-	165	445	730
1.48	-	369	-	-	-	165	420	650
2.67	-	370	-	-	-	190	450	800
1.90	-	370	-	-	-	205	550	875

Material - Copper, 30% reduction, 180°C, WWG 23

Speed (ms^{-1})	Thickness (mm)	Load (N)	Adhesion	Coat	Bamboo	Pressure (Nm^{-2})		
						1	2	3
1.02	0.049	-	poor	good	just			
0.95	0.054	-	poor	good	just			
0.90	0.052	-	poor	good	just			
0.85	0.052	-	poor	good	just			
0.77	0.055	-	poor	fair	just			
0.72	0.053	-	fair	good	yes			
0.65	0.059	-	fair	good	yes			
0.61	0.062	-	fair	good	yes			
0.55	0.065	-	fair	good	yes			
0.51	0.069	-	poor	good	yes			
0.48	0.066	-	fair	good	yes			
0.45	0.070	-	fair	good	yes			
0.42	0.067	-	fair	good	yes			
0.39	0.064	-	fair	good	yes			
0.36	0.064	-	fair	good	yes			
0.33	0.069	-	fair	good	yes			
0.30	0.067	-	fair	good	yes			
0.22	0.07	-	fair	good	yes			
0.23	0.068	-	fair	good	just			
0.76	0.063	221	fair	good	just			
0.86	0.057	221	fair	good	just			
0.87	0.055	219	fair	good	just			
1.02	0.051	217	fair	good	just			
1.15	0.048	219	fair	good	partly			
1.31	0.047	221	f/p	good	partly			
1.43	0.043	196	f/p	good	no			
1.60	0.038	196	fair	good	no			
1.72	0.037	193	poor	good	no			
1.95	0.033	198	poor	good	no			
2.18	0.032	198	poor	good	no			
2.44	0.030	198	poor	good	no			
2.66	0.029	198	poor	good	no			
2.82	0.027	198	poor	fair	no			
3.00	0.022	219	poor	fair	no			

Material - 18/8 Stainless steel, 5% reduction, 150 C, WG 23.

Speed (ms^{-1})	Thickness (mm)	Load (N)	Adhesion	Coat	Bamboo	Pressure (Nm^{-2})		
						1	2	3
0.37	0.094	389	fair	good	yes			
0.43	0.073	368	f/p	good	yes			
0.50	0.079	368	f/p	f/g	yes			
0.55	0.062	358	f/p	good	yes			
0.68	0.049	337	poor	f/g	just			
0.73	0.044	347	poor	fair	yes			
0.82	0.057	337	poor	fair	yes			
0.96	0.054	337	fair	f/g	partly			
0.97	0.047	316	fair	fair	just			
1.04	0.024	316	poor	poor	no			
1.10	0.039	316	poor	poor	no			
1.17	0.047	316	poor	fair	partly			
0.25	0.103	421	f/p	f/g	yes			
1.13	0.029	-	poor	good	no	180	510	875
0.80	0.033	332	poor	good	partly	150	410	700
1.04	0.027	332	poor	good	partly	155	440	850
1.05	0.038	332	poor	good	yes	155	440	850
1.43	0.023	332	poor	fair	no	200	540	900
1.76	0.020	350	poor	fair	no	200	520	900
2.11	0.021	335	poor	fair	no	185	500	875
2.57	0.018	332	poor	fair	no	185	500	850
2.92	0.017	332	poor	fair	no	175	480	800
0.93	0.036	332	poor	fair	partly	135	420	730
0.19	0.100	512	poor	fair	yes	70	370	-
0.155	0.111	400	fair	f/g	yes	55	270	-
0.13	0.114	490	poor	f/p	yes	-	-	-
0.29	0.100	445	poor	fair	yes	60	270	625
0.22	0.121	445	poor	f/p	yes	40	190	825
0.45	0.097	440	poor	f/p	yes	-	-	-
0.13	0.118	445	poor	v.p	yes	75	300	1275
0.16	0.112	467	poor	poor	yes	65	320	1150
0.177	0.116	478	fair	fair	yes	55	500	-
0.27	0.096	400	fair	fair	yes	65	230	600
0.33	0.093	440	fair	g/f	yes	60	260	600
0.52	0.064	400	fair	poor	partly	135	390	1100
0.62	-	365	poor	poor	partly	155	380	1075

Material - 18/8 Stainless steel, 15% reduction, 150°C, WVG 23.

Speed (ms^{-1})	Thickness (mm)	Load (N)	Adhesion	Coat	Bamboo	Pressure (Nm^{-2})		
						1	2	3
0.42	0.068	474	v.p	fair	yes			
0.50	0.068	453	v.p	fair	yes			
0.56	0.061	452	v.p	p/f	partly			
0.62	0.065	432	v.p	p/f	partly			
0.72	0.038	421	v.p	p/f	no			
0.76	0.04	421	v.p	p/f	partly			
0.84	0.052	411	v.p	fair	partly			
0.92	0.038	400	v.p	p/f	partly			
1.03	0.035	389	v.p	p/f	partly			
1.17	0.025	369	v.p	fair	no			
0.25	0.079	500	poor	fair	yes			
0.14	0.076	623	fair	f/g	yes	105	410	1075
0.17	0.072	601	poor	f/g	yes	85	300	1025
0.21	0.081	579	poor	good	yes	70	270	850
0.27	0.076	490	poor	fair	yes	70	260	850
0.33	0.061	500	v.p	p/f	yes	105	290	775
0.35	0.065	556	poor	g/f	yes	60	170	575
0.13	0.097	645	fair	good	yes	90	340	1125
0.87	0.028	-	fair	good	no			
1.09	0.026	-	poor	g/f	no			
1.34	0.026	-	poor	fair	no			
1.66	0.021	-	poor	fair	no			
2.11	0.018	-	poor	fair	no			
2.49	0.021	-	poor	fair	no			
2.8	0.019	-	poor	fair	no			
0.86	0.036	-	fair	fair	no			

Material - 18/8 Stainless steel, 30% reduction, 150°C, WVG 23

Speed (ms^{-1})	Thickness (mm)	Load (N)	Adhesion	Coat	Bamboo	Pressure (Nm^{-2})		
						1	2	3
0.37	0.062	611	fair	g/f	yes			
0.41	0.066	600	good	good	yes			
0.47	0.063	611	good	good	yes			
0.55	0.056	600	fair	good	yes			
0.62	0.054	600	fair	good	yes			
0.74	0.048	548	fair	fair	yes			
0.81	0.036	558	fair	fair	yes			
0.89	0.038	548	fair	fair	yes			
0.97	0.040	548	fair	fair	yes			
1.06	0.030	537	f/p	f/p	yes			
1.12	0.029	527	fair	fair	just			
1.17	0.043	527	fair	good	yes			
0.25	0.070	579	fair	good	yes			
0.77	0.019	615	fair	f/p	partly	130	380	700
0.87	0.035	615	f/p	fair	yes	145	420	600
1.30	0.016	615	fair	poor	no	135	390	-
1.61	0.022	-	fair	f/g	partly	180	490	850
1.89	0.02	615	fair	fair	partly	180	380	750
2.07	0.015	600	fair	f/p	just	175	330	675
2.49	0.016	615	fair	fair	no	190	400	850
2.45	0.015	615	fair	fair	no	210	530	875
2.85	0.015	615	f/g	fair	no	195	510	875
0.79	0.03	615	fair	f/g	yes	160	480	750
1.13	0.022	-	fair	fair	partly	140	420	725
0.245	0.02	743	f/p	f/p	yes	33	230	825
0.22	0.023	730	fair	f/p	yes	50	230	1100
0.20	0.02	757	fair	fair	partly	65	250	1000
0.17	0.01	757	fair	poor	partly	65	250	900
0.14	-	767	-	-	-	90	320	1000
0.21	-	712	-	-	-	80	250	950
0.23	-	712	-	-	-	70	260	850
0.13	-	780	-	-	-	95	400	1700
0.16	0.023	800	good	poor	yes	80	370	1600
0.14	0.068	890	poor	good	yes	115	680	1600
0.21	0.075	734	good	fair	yes	140	460	1525

Material - 60/65 carbon steel, 30% reduction 135°C. WVG 23

Speed (ms^{-1})	Thickness (mm)	Load (N)	Adhesion	Coat	Bamboo	Pressure (Nm^{-2}) 1	2	3
0.79	-	-	-- wire snapped --					
1.48	0.042	589	v.p	poor	yes			
2.63	0.033	632	poor	poor	yes			
1.82	0.019	632	poor	f/p	yes			
2.05	-	653	-- burst seal --					
2.06	0.029	632	poor	f/p	yes			
1.65	0.050	611	poor	poor	yes			
1.50	0.035	632	poor	poor	yes			
2.95	-	632	-- no coat --					
1.14	0.047	579	fair	fair	yes			
1.28	0.048	-	good	fair	yes			
1.64	0.043	-	good	fair	yes			
1.55	0.017	579	fair	fair	partly			
2.14	0.018	579	poor	fair	partly			
2.59	0.007	579	fair	poor	partly			
2.82	0.003	579	fair	fair	no			
2.37	0.009	568	fair	poor	partly			
2.06	0.031	558	poor	fair	partly			
1.75	0.011	565	fair	fair	partly			
1.59	0.018	579	fair	fair	partly			
1.31	0.018	600	poor	fair	yes			
1.22	0.012	589	fair	fair	partly			
0.92	0.018	589	fair	fair	yes			
1.17	0.006	610	fair	fair	no			
1.07	0.018	632	fair	fair	yes			
0.91	0.017	632	fair	f/g	yes			
0.76	0.028	632	fair	fair	yes			
0.84	0.042	632	fair	good	yes			
0.74	0.034	684	f/g	good	yes			
1.12	-	663	-- no coat --					
0.99	0.021	674	fair	fair	partly			
0.91	0.011	663	f/p	fair	partly			
0.88	0.013	663	f/p	fair	partly			
0.79	0.039	684	fair	fair	yes			

Material - 60/65 carbon steel, 30% reduction, 150°C, WVG 23

Speed (ms^{-1})	Thickness (mm)	Load (N)	Adhesion	Coat	Bamboo	Pressure (Nm^{-2}) 1	2	3
1.66	0.012	600	v.p	v.p	just			
0.84	-	684	- Wire snapped ——					
1.31	0.039	621	fair	poor	just			
1.72	-	632	-- no coat --					
1.91	0.004	631	fair	poor	no			
2.36	0.004	631	fair	poor	no			
2.88	0.002	610	fair	poor	no			
3.51	0.004	642	fair	poor	no			
2.00	0.003	631	fair	poor	no			
1.66	0.003	631	fair	fair	no			
1.41	0.004	631	fair	poor	no			
1.22	0.007	684	fair	poor	no			
2.87	0.003	589	fair	poor	no			
1.6	0.005	610	fair	poor	no			
1.36	0.006	610	fair	fair	no			
1.22	0.009	610	fair	fair	partly			
1.13	0.013	610	fair	fair	partly			
1.03	0.013	610	fair	f/g	yes			
0.92	0.015	610	fair	fair	partly			
0.85	0.019	600	fair	fair	partly			
0.92	0.022	632	fair	fair	yes			
1.00	0.008	653	fair	fair	no			
0.84	0.008	642	fair	f/g	no			
0.76	0.011	642	fair	fair	partly			
0.66	0.044	674	fair	fair	yes			
1.17	0.023	674	fair	fair	partly			
0.53	0.037	737	fair	fair	yes			
0.26	-	758	-- Wire snapped --					
0.77	0.057	-	fair	f/g	yes			
0.66	0.048	684	fair	good	yes			

Material - 60/65 carbon steel, 30% reduction, 180°C, WVG 23

Speed (ms^{-1})	Thickness (mm)	Load (N)	Adhesion	Coat	Bamboo	Pressure (Nm^{-2}) 1	2	3
2.75	0.002	568	poor	poor	no			
2.50	0.003	568	poor	poor	no			
2.17	0.004	568	fair	poor	no			
1.85	0.006	568	poor	poor	no			
1.60	0.005	568	fair	poor	no			
1.46	0.006	568	fair	poor	no			
1.28	0.006	568	fair	poor	no			
1.14	0.007	579	fair	fair	no			
1.11	0.007	579	fair	fair	no			
0.99	0.008	579	fair	fair	no			
0.85	0.012	589	fair	fair	just			
1.17	0.006	600	fair	poor	no			
1.05	0.008	610	f/p	poor	no			
0.96	0.009	620	poor	poor	no			
0.88	0.007	621	fair	p/f	no			
0.77	0.007	621	poor	poor	no			
0.65	0.017	642	fair	fair	yes			
0.53	0.010	632	fair	fair	yes			
0.43	-	652	-- no coat		--			
0.36	0.050	680	fair	fair	yes			
0.72	0.011	653	p/f	fair	just			
0.83	0.010	663	fair	f/g	just			
0.64	0.010	663	fair	fair	yes			
0.52	-	674	-- no coat		--			
0.46	0.037	674	f/p	fair	yes			
0.46	0.022	674	fair	fair	yes			

Material - Copper., 30% reduction, 250°C, Polypropylene

Speed (ms^{-1})	Thickness (mm)	Load (N)	Adhesion	Coat	Bamboo	Comments
0.61	0.056	358	poor	v.good	no	coat removed in one piece
0.81	0.013	421	fair	poor	no	flaky coat
0.53	0.010	316	fair	poor	no	
0.47	0.035	295	fair	poor	no	wire snapped
0.56	0.047	316	poor	fair	just	
0.76	0.010	421	fair	fair	no	wire snapped
0.69	0.042	263	poor	good	no	
0.86	0.029	263	poor	fair	no	
0.91	0.046	369	poor	good	no	wire snapped
1.07	0.041	316	poor	good	yes	
0.55	0.059	253	poor	poor	rough	wire necked at 10mm intervals
0.91	0.008	253	poor	v.poor	no	
1.13	0.051	263	poor	good	no	
0.80	0.032	316	poor	fair	no	
0.66	0.052	262	poor	fair	no	
0.91	0.057	263	poor	fair	no	
1.09	-	284	-- no coat		--	
1.17	-	274	-- no coat		--	
0.99	-	263	-- no coat		--	
0.47	0.069	369	fair	fair	yes	wire snapped
0.44	0.055	316	fair	good	yes	wire snapped
0.52	0.072	210	poor	good	yes	wire snapped

List of Courses attended, Visits and Papers Published.

Courses:-

1) Tribology Module of the Post Graduate Diploma, Sheffield City Polytechnic, 30 Jan - 24 April 1978.

2) Basic Lubrication Theory and A pplication, Imperial College, London, 12 - 16 June 1978.

Visits:-

1) Tinsley Wire Industries Ltd., Sheffield.

2) Arthur Lee and Sons Ltd., Sheffield.

3) Swinden Laboratories (BSC), Rotherham.

Papers:-

1) A Non-Newtonian, Plasto-Hydrodynamic Analysis of the Lubrication and Coating of Wire using a Polymer Melt during Drawing - International Symposium on Metalworking Lubrication, ASME Centenary Conference, San Francisco, North America, Aug 1980.